



SPACETIME MESHING FOR DISCONTINUOUS GALERKIN METHODS

BY

SHRIPAD VIDYADHAR THITE

B.E., University of Poona, 1997

M.S., University of Illinois at Urbana-Champaign, 2001

DISSERTATION

Submitted in partial fulfillment of the requirements  
for the degree of Doctor of Philosophy in Computer Science  
in the Graduate College of the  
University of Illinois at Urbana-Champaign, 2005

Urbana, Illinois

# Abstract

Important applications in science and engineering, such as modeling traffic flow, seismic waves, electromagnetics, and the simulation of mechanical stresses in materials, require the high-fidelity numerical solution of hyperbolic partial differential equations (PDEs) in space and time variables. Many interesting physical problems involve nonlinear and anisotropic behavior, and the PDEs modeling them exhibit discontinuities in their solutions. Spacetime discontinuous Galerkin (SDG) finite element methods are used to solve such PDEs arising from wave propagation phenomena.

To support an accurate and efficient solution procedure using SDG methods and to exploit the flexibility of these methods, we give a meshing algorithm to construct an unstructured simplicial spacetime mesh over an arbitrary simplicial space domain. Our algorithm is the first spacetime meshing algorithm suitable for efficient solution of nonlinear phenomena in anisotropic media using novel discontinuous Galerkin finite element methods for implicit solutions directly in spacetime. Given a triangulated  $d$ -dimensional Euclidean space domain  $M$  (a simplicial complex) and initial conditions of the underlying hyperbolic spacetime PDE, we construct an unstructured simplicial mesh of the  $(d + 1)$ -dimensional spacetime domain  $M \times [0, \infty)$ . Our algorithm uses a near-optimal number of spacetime elements, each with bounded temporal aspect ratio for any finite prefix  $M \times [0, T]$  of spacetime. Unlike Delaunay meshes, the facets of our mesh satisfy gradient constraints that allow interleaving the construction of the mesh by adding new spacetime elements, and computing the solution within the new elements immediately and in parallel. Our algorithm is an advancing front procedure that constructs the spacetime mesh incrementally, in a fashion similar to the Tent Pitcher algorithm of Üngör and Sheffer (ÜS00), later extended by Erickson *et al.* (EGSÜ02). We extend previous work which was limited by conservative assumptions; in doing so, we solve the algorithmic problem of predicting discontinuous changes in the geometric constraints that must be satisfied by the mesh.

In  $2D \times \text{Time}$ , our algorithm simultaneously adapts the size and shape of spacetime tetrahedra to a spacetime error indicator. We build on and extend the mesh adaptivity technique (ACE<sup>+</sup>04) of Abedi and others including this author. We are able to incorporate more general front modification operations, such as edge flips and limited mesh smoothing. Our new algorithm is the first to simultaneously adapt to nonlinear and anisotropic response of the underlying medium, thus unifying mesh adaptivity with earlier work by the author. The key insight of our unified algorithm is to exploit the geometric structure of the so-called *cone constraints* that impose gradient constraints on certain facets of the mesh. We present our algorithm as a two-parameter optimization problem where the objective is to maximize the *height* of spacetime tetrahedra. The parameters that guide the algorithm can be chosen adaptively by the algorithm at each step. Our unified algorithm can choose to refine the mesh to increase the *temporal aspect ratio* of spacetime elements, independently of the numerical error indicator. Our new adaptive algorithm can better optimize the shape of spacetime elements and is therefore promising to produce better quality meshes.

The front is coarsened by merging adjacent facets, whether or not they were created by a previous refinement. We show how to make tent pitching less greedy about maximizing the progress at each step so that a subset of the front

can be made coplanar for coarsening in the next step. This algorithm can be used in arbitrary dimensions to make the entire front conform to a target time  $T \geq 0$ . The main contribution of this extension is to retain the progress guarantee of earlier algorithms up to a constant factor.

In higher spatial dimensions  $d \geq 3$ , we are able to guarantee limited mesh smoothing to improve in practice the quality of the mesh. Though we are unable to extend our adaptive algorithm to spatial dimensions  $d \geq 3$ , we state the major open problem that remains.

Empirical evidence confirms that improving the quality of the spatial projection of each front leads to better quality spacetime elements. We give an algorithm in arbitrary dimensions to smooth the front as by pitching inclined tentpoles, and by performing edge flips and edge contractions in  $2D \times \text{Time}$ , so that the quality of future spacetime elements can be improved in practice. We strengthen the progress constraints to anticipate future changes in the front geometry. This algorithm represents recent progress towards a meshing algorithm in  $2D \times \text{Time}$  to track moving domain boundaries and other singular surfaces such as shock fronts.

Additionally, we are able to prove theoretical bounds on the worst-case *temporal aspect ratio* of spacetime elements, while at the same time providing parameters to the algorithm that improve either the number or the aspect ratio of elements in practice. The number of elements in our mesh is provably close to that in a size optimal mesh that also satisfies certain constraints required of any mesh suitable for solution by SDG methods.

*To all my friends and co-travellers, who have made this journey almost more fun than the destination.*

# Acknowledgments

Thanks to the other members of the CPSD spacetime group with whom I have collaborated directly—Reza Abedi, Jonathan Booth, Shuo-Heng Chung, Jeff Erickson, Yong Fan, Michael Garland, Damrong Guoy, Robert Haber, Morgan Hawker, Mark Hills, Sanjay Kale, Jayandran Palaniappan, John Sullivan, and Yuan Zhou—especially Jeff Erickson and Robert Haber. I thank Prof. Haber for driving the whole group to solve more and more interesting problems, and for giving me the freedom to pursue my own interests within the larger project. Alper Üngör has been a great source of encouragement and has renewed my enthusiasm every time we met. Thanks, Alper!

I have been enormously fortunate to have Professors Michael Loui and Jeff Erickson as my M.S. and Ph.D. advisors respectively. I thank them for their time and effort, and for holding me up to such high standards of research and professional service. I cannot thank Prof. Loui enough for many substantial discussions on ethics in research and teaching. I hope to carry those ideals with me throughout my professional career. I thank Jeff for his continuous financial support and the several conference trips (especially where I did *not* have a paper!) for which he paid. One day, I hope to write a paper written as clearly as, with figures drawn as well as, his “worst” paper.

Sariel Har-Peled and Edgar Ramos, together with Jeff who started it all, made computational geometry a happening thing at UIUC. Thank you all very much for your wonderful talks in the theory and computational geometry seminars and in classes, and for attracting so many excellent visitors to the middle of the cornfields.

Thanks to Mitch Harris and Ari Trachtenberg for being such great friends, colleagues, and role models. I couldn’t have asked for better people to look up to. David Bunde and Erin Wolf Chambers were a great help—you guys were always there to give me feedback when I asked. Thank you for the time and effort you spared for me. Thanks to Afra Zomorodian for being around (if only briefly) and for being so cool. Lenny Pitt and Cinda Heeren let me participate in MathManiacs occasionally—I had never done anything like it before and it was an awesome experience. Professors West and Kostochka were the reason I liked the Math department so much. The combinatorics group is the friendliest group of researchers I have known (and that includes you, Radhika and André!). Thanks!

Thanks also to the anonymous referees for the 20th ACM Symposium on Computational Geometry (SoCG) and the 13th International Meshing Roundtable (IMR 2004), where papers related to this thesis appeared, for their valuable feedback. I also gave a talk about the results in this thesis at the 21st European Workshop on Computational Geometry (EuroCG) at TU-Eindhoven, the Netherlands, in March 2005; I would like to thank the students and faculty at Eindhoven for their hospitality. I completed the final revision of this thesis at TU-Eindhoven during the first few weeks of my postdoc position. I would like to especially thank Mark de Berg for giving me the time and freedom to do so.

I gratefully acknowledge funding from the Center for Process Simulation and Design (CPSD) at the University of Illinois at Urbana-Champaign. CPSD is funded primarily by the National Science Foundation under the ITR initiative, with joint sponsorship by the Division of Materials Research, and the Directorate for Computer and Information Science and Engineering. My research was supported in part by NSF ITR grant DMR 01-21695.

# Table of Contents

<b>List of Figures</b> . . . . .	<b>ix</b>
<b>Chapter 1 Introduction</b> . . . . .	<b>1</b>
1.1 Background . . . . .	1
1.1.1 Numerical methods . . . . .	3
1.1.2 Mesh generation . . . . .	5
1.1.3 Causality . . . . .	7
1.2 Spacetime meshing . . . . .	10
1.2.1 Terminology and notation . . . . .	11
1.2.2 Meshing objectives . . . . .	13
1.2.3 Meshing challenges . . . . .	16
1.2.4 Summary of results . . . . .	17
1.2.5 Previous work . . . . .	17
<b>Chapter 2 Basic advancing front meshing algorithm</b> . . . . .	<b>20</b>
2.1 Problem statement . . . . .	20
2.2 Meshing in $1D \times \text{Time}$ . . . . .	21
2.2.1 Progress guarantee . . . . .	22
2.3 Meshing in $2D \times \text{Time}$ . . . . .	24
2.3.1 Need for progress constraints . . . . .	24
2.3.2 Progressive fronts in $2D \times \text{Time}$ . . . . .	26
2.4 Meshing in arbitrary dimensions $dD \times \text{Time}$ . . . . .	33
2.4.1 Progress constraint for a $k$ -dimensional simplex . . . . .	36
2.4.2 Combining constraints for all dimensions . . . . .	38
2.5 Element quality . . . . .	38
2.6 Size optimality . . . . .	39
2.7 Geometric primitives . . . . .	40
<b>Chapter 3 Meshing with nonlocal cone constraints</b> . . . . .	<b>43</b>
3.1 Problem statement . . . . .	43
3.2 Nonlocal cone constraints in $1D \times \text{Time}$ . . . . .	44
3.3 Nonlocal cone constraints in $2D \times \text{Time}$ . . . . .	47
3.3.1 Looking ahead . . . . .	47
3.3.2 Greedily maximizing progress . . . . .	49
3.4 Nonlocal cone constraints in arbitrary dimensions $dD \times \text{Time}$ . . . . .	51
3.5 Estimating future slope . . . . .	52

<b>Chapter 4 Adaptive refinement and coarsening</b>	<b>55</b>
4.1 Problem statement	55
4.2 Meshing in $2D \times \text{Time}$	57
4.2.1 Hierarchical front refinement	58
4.2.2 Coarsening	63
4.2.3 Adaptive meshing in $2D \times \text{Time}$	63
4.2.4 Causality and Progress Constraints	66
4.2.5 Changing the apex	75
4.2.6 Another look at the adaptive progress constraint	76
4.3 Mesh adaptivity in higher dimensions	77
<b>Chapter 5 Adaptive Meshing with Nonlocal Cone Constraints</b>	<b>79</b>
5.1 Adaptive meshing in $1D \times \text{Time}$ with nonlocal cone constraints	80
5.2 Adapting the progress constraint to the level of refinement in $2D \times \text{Time}$	81
5.2.1 A unified adaptive algorithm in $2D \times \text{Time}$	83
5.2.2 A simpler algorithm in $2D \times \text{Time}$	83
<b>Chapter 6 Target time conformity</b>	<b>85</b>
6.1 Conforming to a target time	85
6.2 Conforming to a target time: a simpler heuristic	88
6.3 Smoothing out large variations in tentpole heights	89
6.4 Coarsening	89
6.4.1 New algorithm	90
6.4.2 Proof of correctness	92
<b>Chapter 7 Extensions</b>	<b>94</b>
7.1 Extensions and heuristics	94
7.1.1 Asymmetric cone constraints	94
7.1.2 Non-manifold domains	95
7.1.3 Front smoothing	96
7.1.4 Heuristics	101
7.2 Tracking moving boundaries	102
7.2.1 Tracking boundaries in $1D \times \text{Time}$	103
7.2.2 Tracking boundaries in $2D \times \text{Time}$	105
7.3 Practical issues	107
<b>Chapter 8 Conclusion and open problems</b>	<b>111</b>
8.1 Open problems	111
<b>References</b>	<b>114</b>
<b>Curriculum Vitæ</b>	<b>119</b>



# List of Figures

1.1	Points $A$ and $B$ are independent because $B$ lies outside the cone of influence of $A$ and $A$ lies outside the cone of dependence of $B$ . . . . .	8
1.2	No-focusing means that the wavespeed at a point in the future can be estimated from the wavespeeds of points on the current front. . . . .	9
1.3	Temporal aspect ratio of a spacetime element . . . . .	13
1.4	A causal triangle separates the cones of influence and dependence at every point on the face. . . . .	15
1.5	Cross-section of a patch of tetrahedra; the inflow and outflow faces are causal. Time increases up the page. . . . .	16
1.6	An unstructured tetrahedral spacetime mesh over a triangulated 2D grid . . . . .	18
1.7	The first few tents pitched by Tent Pitcher (EGSÜ02). . . . .	19
2.1	Advancing front algorithm in $1D \times \text{Time}$ . . . . .	22
2.2	Vector diagram . . . . .	25
2.3	Triangle $pqr$ of the front $\tau$ where $\tau(p) \leq \tau(q) \leq \tau(r)$ . . . . .	27
2.4	Triangle $pqr$ with (a) $\angle pqr$ obtuse; (b) $\angle pqr$ and $\angle prq$ acute; and (c) $\angle prq$ obtuse . . . . .	29
2.5	Advancing front algorithm in $2D \times \text{Time}$ . . . . .	30
2.6	An obtuse tetrahedron with $\bar{p}_0 \notin p_1 p_2 \dots p_k$ . . . . .	34
3.1	A sequence of tent pitching steps in $1D \times \text{Time}$ . Maximizing the height of each tentpole while staying below every cone of influence may require examining remote cones arbitrarily far away. . . . .	45
3.2	Algorithm in $2D \times \text{Time}$ with nonlocal cone constraints. . . . .	49
3.3	Algorithm to maximize height of tentpole $PP'$ subject to $h$ -progressive constraints . . . . .	50
3.4	Constructing and traversing a bounding cone hierarchy . . . . .	54
4.1	Adaptive meshing algorithm in $1D \times \text{Time}$ . . . . .	57
4.2	Newest vertex refinement (ACE <sup>+</sup> 04). Newest vertices of each triangle are marked. . . . .	59
4.3	Refining $\triangle abc$ propagates to neighboring triangles: (a) before and (b) after refinement. . . . .	60
4.4	Refinement propagation path terminates when it revisits a triangle. . . . .	60
4.5	Bisecting an edge and the two triangles incident on it . . . . .	61
4.6	Algorithm BISECTTRIANGLE . . . . .	61
4.7	Edge flip . . . . .	62
4.8	Refinement with earnest propagation. . . . .	63
4.9	Refinement with lazy propagation. . . . .	64
4.10	Operation of CLEANUP1 . . . . .	65
4.11	Operation of lazy CLEANUP2 . . . . .	65
4.12	Earnest propagation (top path) vs. lazy propagation (bottom path) . . . . .	66
4.13	Algorithm to de-refine . . . . .	67
4.14	De-refining a loop in the refinement propagation path requires edge flips to create degree-4 vertices . . . . .	67
4.15	Adaptive Tent Pitcher algorithm with refinement and coarsening . . . . .	68
4.16	A sequence of 5 tents pitched by the adaptive algorithm . . . . .	68

4.17	$\triangle abc$ where $a$ is the apex. . . . .	69
4.18	Merging eight progress constraints into one adaptive progress constraint . . . . .	69
4.19	Triangle $pqr$ with $\angle pqr \leq \pi/2$ with apex at $p, q,$ and $r$ respectively. . . . .	71
4.20	Triangle $pqr$ with $\angle pqr > \pi/2$ with apex at $p, q,$ and $r$ respectively. . . . .	72
5.1	Unified adaptive algorithm in $2D \times \text{Time}$ . . . . .	84
6.1	Coarsening a set of four triangles in one step. . . . .	92
6.2	Coarsening a set of several triangles in one step. . . . .	93
7.1	The length of an inclined tentpole is limited so that new front triangles are causal. . . . .	97
7.2	Moving a vertex can introduce or increase an obtuse angle on the front. . . . .	97
7.3	The allowed region for $p'$ is the shaded region in the top: $p'$ is restricted to the allowed region to ensure that $\min\{\sin \angle p'qr, \sin \angle p'rq, \sin \angle rp'q\} \geq \phi_{\min}$ . . . . .	99
7.4	An edge is flipped by inserting a single tetrahedron. . . . .	100

# Chapter 1

## Introduction

In this thesis, we study spacetime meshing to support fast and accurate simulation of certain physical phenomena by Spacetime Discontinuous Galerkin (SDG) finite element methods. We give algorithms to construct spacetime meshes. We prove guarantees on the performance of the algorithm. We prove worst-case bounds on the size and quality of the individual elements in our meshes. We want our meshes to be efficient and lead to accurate solutions in practice. Our meshes support an efficient solution strategy by SDG methods because they satisfy certain geometric constraints. Our meshing algorithms exploit the flexibility of novel SDG methods.

Mesh generation is an important problem in computational geometry. Delaunay meshes (dBSvKO00) are widely used in engineering applications. Solving engineering problems using a mesh imposes geometric requirements on the shape and size of mesh elements (She02). The efficiency of the solution technique depends on the number and distribution of elements in the mesh. Delaunay meshes are known to nicely satisfy many such requirements in practice and have very good theoretical properties such as size optimality. Our spacetime meshes are not Delaunay meshes but our spacetime meshing problem is motivated by similar geometric requirements and by a similar desire for efficiency. We confront and solve many challenges unique to meshing a non-Euclidean spacetime domain. We do so by building on previous research (ÜS00; Ü02; EGSÜ02; EGSÜ05) and insight due to several researchers. The research in this thesis is part of a larger project at the Center for Process Simulation and Design (CPSD) at the University of Illinois at Urbana-Champaign.

The algorithms in this thesis are being implemented by members of CPSD, including the author, and tested with actual DG solvers on practical simulation problems to illustrate the usefulness and applicability of the research. The reader is referred to other publications (ACE<sup>+</sup>04; ACF<sup>+</sup>04; AHTE05) for empirical results.

### 1.1 Background

In this section, we will review basic concepts about hyperbolic partial differential equations (PDEs) and physical phenomena modeled by hyperbolic PDEs, to motivate the application of this research to solving simulation problems in science and engineering. The reader is referred to classical textbooks (Str86; Hea02; Fol95; Whi74) for a review of the theory of PDEs, hyperbolic problems, and the finite element method. There are also several online resources. Jim Herod of Georgia Tech has notes and Maple worksheets online (Her04). See also MathWorld (Wei99b) and links therein. Introductory texts on PDEs include those by Tveito and Winther (TW98), Folland (Fol95), Cooper (Coo98), and Thomas (Tho99).

Simulation problems in mechanics consider the behavior of an object or region of space over time. Scientists and engineers use conservation laws and hyperbolic partial differential equations (PDEs) to model transient, wave-like phenomena propagating over time through the domain of interest. PDEs are mathematical models of physical

phenomena, often derived by applying a fundamental principle such as conservation of mass, momentum, or energy. Example applications are numerous, including, for instance, the equations of elastodynamics in seismic analysis and the Euler equations for compressible gas dynamics. Computational mechanics is concerned with the accurate computer simulation of physical phenomena.

An example of a hyperbolic PDE is the one-dimensional wave equation

$$\frac{\partial^2 u}{\partial t^2} = \omega^2 \frac{\partial^2 u}{\partial x^2} \quad \text{for } 0 \leq x \leq L \text{ and } t \geq 0$$

with boundary conditions

$$u(0, t) = u_0 \quad u(L, t) = u_L$$

and initial conditions

$$u(x, 0) = f(x) \quad \left. \frac{\partial u}{\partial t} \right|_{t=0} = g(x)$$

This PDE describes, for instance, the vibration of a taut string when it is plucked. Here,  $u(x, t)$  is the displacement of point  $x$  at time  $t$  and  $\omega$ , a constant, is the *wavespeed*, i.e., the speed at which the wave travels along the string.

A PDE is *homogeneous* if the trivial function  $u \equiv 0$  is a solution.

A PDE is *linear* if the PDE and the initial or boundary conditions do not include any product of the dependent variable  $u$  or its partial derivatives. A PDE that is not linear is *nonlinear*. For example,

- First-order linear PDE:  $u_t + cu_x = 0$
- Second-order linear PDE:  $u_{xx} + u_{yy} = \phi(x, y)$  for an arbitrary function  $\phi$  of the independent variables only.

A linear PDE has the property that if  $u_1$  and  $u_2$  both satisfy the PDE, then so does every linear combination  $\alpha u_1 + \beta u_2$ . This property is called the *principle of superposition*.

A nonlinear equation is *semi-linear* if the coefficients of the highest-order derivatives are functions of the independent variables  $x_1, x_2, \dots, x_n$  only. Examples of semi-linear PDEs are the following:

- $(x+3)u_x + xy^2u_y = u^3$
- $xu_{xx} + (xy + y^2)u_{yy} + uu_x + u^2u_y = u^4$

A nonlinear PDE of order  $m$  that is not semi-linear is *quasi-linear* if the coefficients of the derivatives of order  $m$  depend only on the independent variables and on derivatives of order less than  $m$ , e.g.,

$$(1 + u_y^2)u_{xx} - 2u_xu_yu_{xy} + (1 + u_x^2)u_{yy} = 0$$

A nonlinear PDE of order  $m$  is *fully nonlinear* if the highest-order derivatives of  $u$  appear nonlinearly in the equation.

The following examples illustrate the distinction between the different types of PDEs:

- $u_t + u_x = 0$  is homogeneous linear
- $u_t + xu_x = 0$  is homogeneous linear
- $u_{xx} + u_{yy} = 0$  is homogeneous linear

- $u_t + x^2 u_x = 0$  is homogeneous linear
- $u_t + u_{xxx} + uu_x = 0$  is homogeneous semi-linear
- $u_t + u_x + u^2 = 0$  is homogeneous semi-linear
- $u_{xx} + u_{yy} = x^2 + y^2$  is inhomogeneous linear
- $u_t + uu_x = 0$  is not semi-linear, but it is quasi-linear
- $u_x^2 + u_y^2 = 1$  is inhomogeneous fully nonlinear

Many interesting physical problems are modeled by second-order PDEs. The general form of a linear second-order PDE is

$$au_{xx} + bu_{xt} + cu_{tt} + du_x + eu_t + fu + g(x,t) = 0$$

This PDE is classified as (i) parabolic if  $b^2 - 4ac = 0$ , (ii) hyperbolic if  $b^2 - 4ac > 0$ , and (iii) elliptic if  $b^2 - 4ac < 0$ .

### 1.1.1 Numerical methods

It is very difficult and often impossible to obtain analytical solutions of PDEs arising in practical problems. Therefore, approximate solutions are obtained by numerical techniques. The choice of numerical method depends on the physical behavior of the system, i.e., on the type of PDE that models the system.

Several numerical techniques can be used for numerical solutions of partial differential equations. They are classified on the basis of the discretization method by which the continuum mathematical model is approximated. These include the finite difference method, finite volume method (FVM), meshfree methods, and finite element method (FEM).

The finite element (FEM) method is a vastly popular numerical technique for solving PDEs. The FEM method requires a mesh of the domain. There is a vast body of literature on mesh generation. In Section 1.1.2, we will briefly mention the results most relevant to our problem to place our meshing algorithms in context.

Discrepancies can arise between the actual physics and the approximate numerical solution of the PDE modeling the physics. The sources of such discrepancies include errors in modeling physical phenomena as well as errors due to computation such as discretization error and numerical roundoff error.

Some errors are caused because of the discretization of the domain. Errors are also caused by truncation and rounding due to finite precision of the computations. The *order of accuracy* of a numerical method is the exponent of the largest order term in the Taylor series expansion of the difference between the analytical solution and the approximate solution. Numerical instability occurs when the error term grows so fast that it dominates the actual solution. Both accuracy and stability affect the computational time required to converge (if at all) to the approximate solution. Therefore, it is important to minimize error and maximize stability. Since there is always a tradeoff between accuracy and efficiency of any numerical method, the most desirable methods are those for which the running time increases slowly as the acceptable error decreases.

### Galerkin method

The Galerkin method (Wei99a) provides a unifying basis from which several numerical methods, like finite element and finite difference methods, can be derived. The Galerkin approximation to the analytical solution of a PDE is an

approximate numerical solution that is the unique best approximation in a certain sense to the exact solution. We refer the reader to other resources, for instance the online lecture notes by the Chalmers Finite Element Center (Cen03), for a detailed discussion of the Galerkin method.

### **Discontinuous Galerkin method**

The discontinuous Galerkin (DG) method, originally developed by Reed and Hill in 1973 for neutron transport problems and first analyzed by Le Saint and Raviart in 1975, is used to solve ordinary differential equations and hyperbolic, parabolic, and elliptic partial differential equations.

The DG method is a technique that uses discontinuous basis functions to formulate a Galerkin approximation. Given a mesh of the analysis domain, the DG method approximates the solution within each element by a function from a low-dimensional vector space of functions, e.g., as a linear combination of basis functions like polynomials. For a pair of adjacent mesh elements, the approximate solution computed in the interior of the elements does not have to agree on their common boundary.

The DG method has many desirable properties that have made it popular. For example (i) it can sharply capture solution discontinuities relative to a computational mesh; (ii) it simplifies adaptation since inter-element continuity is neither required for mesh refinement and coarsening, nor for  $p$ -adaptivity; (iii) it conserves the appropriate physical quantities (e.g., mass, momentum, and energy) on an element-by-element basis; (iv) it can handle problems in complex geometries to high order; (v) regardless of order, it has a simple communication pattern to elements sharing a common face that simplifies parallel computation. If the solution field has a discontinuity in the form of a *shock*, SDG methods can exactly capture this discontinuity if the mesh facets are perfectly aligned with the shock surface. On the other hand, with a discontinuous basis, the DG method produces more unknowns for a given order of accuracy than traditional finite element or finite volume methods, which may lead to some inefficiency. The DG method is harder when applied to unstructured meshes; in particular, it is harder to formulate limiting strategies to reduce spurious oscillations when high-order methods are used.

For a thorough discussion of DG methods and a review of the state of the art, we refer the reader to the book by Cockburn, Karniadakis, and Shu (CKS00).

### **Spacetime discontinuous Galerkin methods**

The first discontinuous Galerkin formulation for spacetime problems, introduced by Reed and Le Saint *et al.*, was discontinuous in time only. The spacetime domain was divided into slabs by constant-time planes. The solution was assumed to be continuous within a slab and jump conditions at the inter-slab boundaries were used to enforce the appropriate level of continuity between adjacent slabs. The spacetime basis functions of this so-called *time-discontinuous Galerkin method* were continuous in spacetime except across the constant-time planes that separated two consecutive slabs. The spacetime mesh was, therefore, required to conform to the inter-slab boundaries.

Richter (Ric94) introduced the first spacetime-discontinuous Galerkin finite element method, which permitted basis functions to be discontinuous in spacetime across all element boundaries, for the wave equation. Yin *et al.* (YAS<sup>+</sup>99; YAS<sup>+</sup>00; Yin02) proposed the first spacetime-discontinuous Galerkin method for linear elastodynamics. Abedi *et al.* (ACF<sup>+</sup>04; AHP05; AHTE05) give an improved formulation. Since the SDG method allows every pair of adjacent elements to have basis functions that are discontinuous across their common boundary, the SDG method can solve fully unstructured and even nonconforming meshes. The flexibility of SDG methods, in terms of the types of mesh that are solvable, is exploited by the meshing algorithms in this thesis.

### 1.1.2 Mesh generation

Given a domain of interest, the mesh generation problem is to decompose the domain into simple cells, called *elements*, each of constant complexity. Such a decomposition is called a *mesh*. Elements consist of vertices, edges, ridges, and facets of appropriate dimensions. Linear, bilinear, or trilinear elements are often used; convex cells (e.g., simplices) are sometimes preferred. A *triangulation* is a decomposition into simplices (Zie95). In general, a mesh may contain hexahedra, prisms, pyramids, and other simple shapes, possibly in the same (hybrid) mesh.

If the domain is bounded, the mesh must conform to the boundary, i.e., the domain boundary must be contained in the union of a subset of the mesh faces. A curved domain boundary cannot be captured exactly by a mesh consisting of linear elements; in this case, the mesh must conform to the boundary approximately in a piecewise linear fashion.

An important question is whether a domain can be meshed at all and, if so, with how many elements. It is well-known that every simple polygon in the plane can be triangulated (GJPT78), in fact in linear time (Cha91; AGR00). In dimensions three and higher, additional vertices, called *Steiner points*, may be required; in general, it is NP-complete to determine if one or more Steiner points are required and to compute the minimum number of Steiner points (RS92).

The accuracy and stability of numerical methods are affected by the geometric shape of mesh elements. Therefore, it is important to generate a mesh with only good quality elements. The notion of element quality depends on the numerical method (She02).

When the domain is Euclidean, several popular metrics are used to define the quality of the mesh elements and of the mesh as a whole. Popular objectives are to optimize at least one of the following quality measures for every element in the mesh: minimize ratio of circumradius to length of shortest edge, maximize smallest angle, minimize largest angle, etc. Different metrics appear to work better than others depending on the application. See Shewchuk (She02) for a comprehensive study of quality metrics. In 2D, all these metrics are equivalent to each other up to constant factors; this is not true in higher dimensions. In 2D, Delaunay triangulations (dBSvKO00) have guaranteed quality (CDE<sup>+</sup>00; CD03).

For anisotropic problems, quality metrics should also be anisotropic. Typically, the local anisotropic nature of the problem is used to define a local quality measure at each point in the domain. The problem now is to generate a mesh such that for every point in the domain, the quality of the element that contains the point is at least as good as the desired quality metric at that point. Labelle and Shewchuk (LS03) propose a definition of an anisotropic Delaunay triangulation and an algorithm to construct such a triangulation of guaranteed quality.

Bern, Eppstein, Gilbert (BEG94) use quadtrees to construct triangulations with extra Steiner vertices added to the original input. They present the first algorithm to triangulate a planar point set and polygons, with all angles bounded away from zero, using a number of triangles within a constant of optimal. In higher dimensions, they are able to triangulate point sets such that the resulting triangulation has no small solid angles and the number of its simplices is within a constant factor of the optimal number. The result of Bern *et al.* was generalized to higher dimensions by Mitchell and Vavasis (MV00).

A  $d$ -dimensional *structured mesh*, also known as a (structured) *grid*, is a cubical complex (Zie95) with the property that every  $k$ -dimensional cell belongs to exactly  $2^{d-k}$   $d$ -dimensional cells; only cells on the boundary of the complex are excepted from this rule. Thus, all interior nodes are incident on the same number of elements. For example, a structured quadrilateral grid in 2D has each interior node incident on four quads; a structured hexahedral grid in 3D has each interior node incident on eight hexahedra. Because the combinatorial structure of such a grid is so regular, simple data structures suffice to store and manipulate the grid. Unstructured meshes relax the uniformity requirement on the node degree.

Mesh smoothing and mesh refinement are commonly used to improve the quality of a given mesh, for instance, a Delaunay triangulation of a given domain.

Mesh smoothing, also called  $r$ -refinement, adjusts the locations of the vertices of the mesh while keeping the combinatorics of the mesh unchanged. Smoothing serves to improve the quality of the elements at least locally (ABE99) but global convergence to some optimum quality is not guaranteed. Mesh smoothing can be applied to both structured and unstructured meshes.

Mesh refinement, also called  $h$ -refinement, is the operation of introducing additional Steiner points to alter the mesh and improve its quality. Delaunay refinement (Che89; Rup95), is used when the objective is to obtain a Delaunay triangulation (dBSvKO00) of the domain where each element has some guaranteed quality. Delaunay refinement proceeds by destroying bad quality elements by inserting their circumcenters and updating the Delaunay triangulation. The refinement process eventually terminates but in 3D does not eliminate so-called *slivers*. Weighted Delaunay refinement (CD03) attempts to remove slivers in the next step. If the mesh is required to conform to a piecewise linear boundary and if the boundary contains an acute dihedral angle, it is not known whether weighted Delaunay refinement can produce a good-quality triangulation without slivers.

Delaunay refinement is an incremental algorithm to improve the quality of a simplicial mesh, for instance by inserting circumcenters of bad-quality simplices, and updating the mesh to maintain the Delaunay property. See the seminal papers by Chew (Che89) and by Ruppert (Rup95) on the quality and optimality of the triangulations resulting from Delaunay refinement by circumcenter insertion. For Delaunay refinement using alternatives to circumcenter insertion, see Rivara's longest edge bisection (Riv97), sink insertion by Edelsbrunner and Guoy (EG01), and Üngör's Off-Center insertion algorithm (Üng04).

Another popular technique to mesh a domain is to begin with a surface mesh of the boundary of the domain and extend it incrementally into the interior of the domain to get a volume mesh. Such an approach is called an *advancing front* method. Advancing front techniques are popular due to their simplicity, but suffer from a lack of provable guarantees; for instance, an advancing front algorithm may create degenerate or inverted elements (Sev97), it may create non-triangulable volumes and fail (fPCS99), or it may require resorting to ad-hoc techniques and heuristics where different parts of the front collide.

Meshes of complicated domains frequently consist of millions or billions of elements. Representing and storing large meshes in memory is complicated because memory in real-world computers is organized in a hierarchy ranging from fast online storage to slow offline devices, and the amount of fastest memory is limited. Exploiting the spatial and temporal locality exhibited by most algorithm to compactly store a large mesh in a way that supports efficient access is an active and exciting area of research (CRMS03; YLPM05). Minimizing memory usage is of concern to us too. Our algorithms minimize memory requirements by storing in main memory only a small subset of the mesh, i.e., the elements adjacent to the advancing front, instead of the entire spacetime mesh.

Multiprocessor computers and computer networks are available to solve large-scale problems. Parallel algorithms for mesh generation (STÜ04) and parallel numerical methods take advantage of such computer systems by sophisticated techniques. Our meshing algorithms are highly parallelizable and the discontinuous nature of the SDG method makes it possible to compute the solution in unrelated subdomains simultaneously in parallel.

Automatic generation of good quality finite element meshes—with at most minimal user interaction—remains a topic of active research interest (Owe99). In the spacetime domain, we have only begun addressing the many challenges with many exciting avenues to explore in the future.



### 1.1.3 Causality

The phenomenon that characterizes hyperbolic problems is causality, the fairly intuitive notion of cause and effect, stimulus and response, commonly observed in daily life. When a pebble is dropped into a pond, the disturbance radiates outwards in expanding circles from the point of origin. The result is waves traveling on the surface of the water, traveling with a bounded wavespeed. An example in one-dimensional space is the vibration of a taut string fixed at both ends when it is plucked. Let  $L$  be the length of the string. The displacement  $u(x,t)$  of the point of the string at coordinate  $x$  about its mean position at time  $t$  is described by a second-order hyperbolic PDE, the wave equation  $u_{tt} - \omega^2 u_{xx} = 0$  with the initial conditions  $u(x,0) = 0$  for every  $x \in [0,L]$  and  $u(0,t) = u(L,t) = 0$  for every  $t \geq 0$ . The wavespeed  $\omega$  is the rate at which the initial stimulus travels to other points of the string. The propagation of influence with a bounded wavespeed within a spatial domain, a subset of  $\mathbb{E}^d$ , can be visualized as a relation between points in the spacetime domain one dimension higher, i.e.,  $\mathbb{E}^d \times \mathbb{R}$ .

#### Influence and dependence

Points in spacetime are partially ordered by *causality*—a point  $P$  *influences* another point  $Q$ , written as  $P \prec Q$  if and only if changing the physical parameters at  $P$  could possibly change the result at  $Q$ . A point  $Q$  *depends* on  $P$ , written as  $Q \succ P$ , if and only if  $P$  influences  $Q$ , i.e.,  $P \prec Q \Leftrightarrow Q \succ P$ . The *domain of influence* of  $P$  is the set of points  $Q$  such that  $P \prec Q$ . Symmetrically, the *domain of dependence* of a point  $P$  is the set of points  $R$  such that  $P \succ R$ . We say that two distinct points  $P$  and  $Q$  are *independent* if and only if neither  $P \prec Q$  nor  $Q \prec P$ .

A *characteristic* of a PDE through a given point  $\mathbf{x}$  is the iso-surface along which  $u$  satisfies an ordinary differential equation (ODE). Thus, characteristics are curves or surfaces or hypersurfaces, of dimension  $n - 1$  or less, in the space spanned by the  $n$  independent variables. Each characteristic corresponds to a *characteristic equation* which is an ordinary differential equation (ODE) or a system of ODEs. The *slope* of a characteristic at  $P$  is the slope of the tangent to the characteristic at  $P$ . The method of characteristics for solving a given PDE changes coordinates from  $(x,t)$  to a new coordinate system  $(x(s),s)$  in which the PDE becomes an ordinary differential equation (ODE) in the independent variable  $s$ . The variable  $s$  is a parameter that varies along the characteristic hypersurface.

For a hyperbolic spacetime PDE, a characteristic hypersurface through a point  $P$  represents the flow of information through the space domain with time. For hyperbolic PDEs such as the wave equation  $u_{tt} - \omega^2 u_{xx} = 0$  the solution at  $p = (x_p, t_p)$  influences the solution at every future point in the wedge bounded by the characteristic lines through  $p$  with slope  $\pm\omega$ . The information at  $p$  propagates into the future with a uniform bounded speed  $\omega$  in every direction.

A curve  $\Gamma = (x,y(x))$  is *characteristic* for the second-order PDE

$$au_{xx} + bu_{xy} + cu_{yy} + du_x + eu_y + fu + g(x,y) = 0$$

if

$$\frac{dy}{dx} = \frac{b \pm \sqrt{b^2 - 4ac}}{2a} \tag{1.1}$$

along  $\Gamma$ . The three different classes of second-order PDEs have three different types of characteristics. Hyperbolic PDEs have  $b^2 - 4ac > 0$ , so Equation 1.1 has two real solutions and there are two characteristic curves through every point  $(x,y)$ . For example, the wave equation  $u_{xx} - u_{yy} = 0$  is hyperbolic and has two characteristic lines given by  $y = \pm x$ .

The solution to a PDE can have discontinuities. If two characteristics intersect at a point  $\mathbf{x}$ , the two values for the

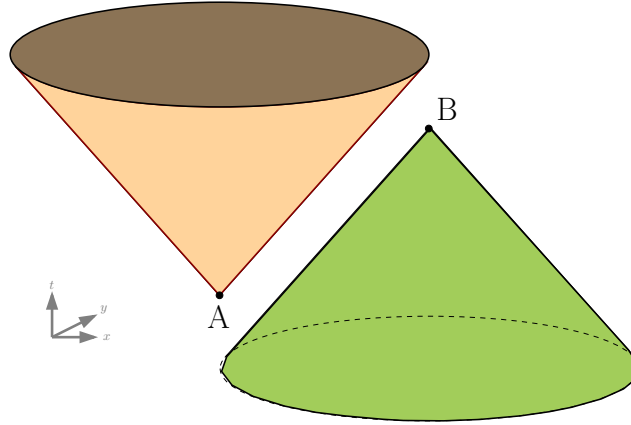


Figure 1.1: Points  $A$  and  $B$  are independent because  $B$  lies outside the cone of influence of  $A$  and  $A$  lies outside the cone of dependence of  $B$

solution  $u$  at  $\mathbf{x}$  obtained by back-tracing the characteristics can be different. Such discontinuities are called *shocks*. Shocks can occur even when the initial conditions are smooth.

For spacetime hyperbolic PDEs, the wavespeed everywhere is finite, i.e., information propagates through the space domain with a bounded wavespeed.

### **Cones of influence and dependence**

The *slope*  $\sigma(P)$  at a point  $P$  is a quantity computed by the numerical solver to bound from above the speed at which any change in the parameters at  $P$  propagates through the spacetime domain. For instance,  $\sigma(P)$  can be computed as the maximum slope of every characteristic through  $P$ . The *wavespeed* at  $P$ , denoted by  $\omega(P)$ , is the reciprocal of the slope, i.e.,

$$\omega(P) = \frac{1}{\sigma(P)}$$

Thus, the slope (or wavespeed) at every point in the domain defines a scalar field over the domain.

The *cone of influence* of  $P$ , denoted by  $\text{cone}^+(P)$ , is a circular cone with apex at  $P$ , axis in the positive time direction, and slope equal to  $\sigma(P)$ . The cone  $\text{cone}^+(P)$  is a closed full-dimensional subset of the spacetime domain. Symmetrically, the *cone of dependence* of  $P$ , denoted by  $\text{cone}^-(P)$ , is a circular cone with apex at  $P$ , axis in the negative time direction, and slope equal to  $\sigma(P)$ . See Figure 1.1.

When the underlying medium is anisotropic, due to nonlinear response, waves propagate faster in some spatial directions than in others. In such cases, cones of influence need not have circular cross-sections. We will postpone a discussion of this anisotropic situation until later in this section.

### **No-focusing assumption**

We make the following assumption about how well the cone of influence  $\text{cone}^+(P)$  at a point  $P$  approximates the domain of influence of  $P$ . We assume that the slope of the cone of influence at a point  $P$  in the future can be estimated from the slopes of the cones of influence of all points  $Q$  such that  $P \in \text{cone}^+Q$ . In other words, we assume that  $P$  is influenced only by points  $Q$  such that  $P \in \text{cone}^+Q$ . This property is formally stated as Axiom 1.1.

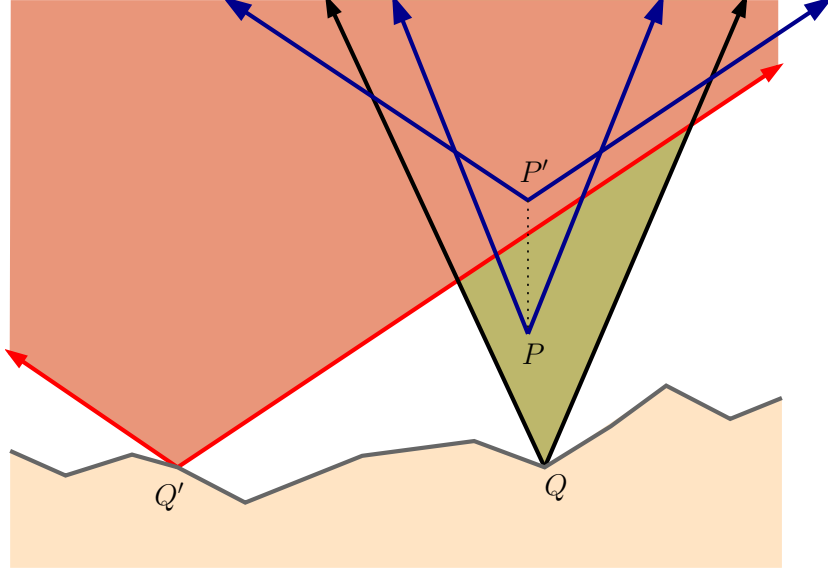


Figure 1.2: No-focusing means that the wavespeed at a point in the future can be estimated from the wavespeeds of points on the current front.

**Axiom 1.1** (No focusing). *For every point  $P$  in the spacetime domain, the slope  $\sigma(P)$  is bounded by the minimum and maximum slope of every cone of influence containing  $P$ . Thus,*

$$\min_{P \in \text{cone}^+(Q)} \{\sigma(Q)\} \leq \sigma(P) \leq \max_{P \in \text{cone}^+(Q)} \{\sigma(Q)\}$$

In Figure 1.2, point  $P$  is influenced by point  $Q$ , hence  $\sigma(P) = \sigma(Q)$  is possible. Suppose  $P$  is advanced in time to  $P'$ . The point  $P'$  is influence by both  $Q$  and  $Q'$ . Hence,  $\sigma(P') = \min\{\sigma(Q), \sigma(Q')\}$  is possible.

If a point  $P = (p, t)$  is in a cone of influence  $C$ , then every point  $P' = (p, t')$  where  $t' > t$  is also in  $C$ . See Figure 1.2. Together with Axiom 1.1, we obtain the following monotonicity lemma.

**Lemma 1.2.** *For an arbitrary fixed point  $p \in \mathbb{E}^d$ , let  $P = (p, t)$  and  $P' = (p, t')$  be two points in spacetime with the same spatial projection  $p$  and time coordinates  $t$  and  $t'$  respectively. If  $t' \geq t$ , then  $\sigma(P') \leq \sigma(P)$ .*

**EXPLANATION OF THE NO-FOCUSING ASSUMPTION: AXIOM 1.1** The causal slope  $\sigma(P)$  is a first-order approximation to the slope of the characteristic curves/surfaces through  $P$ ; the slope of the cone of influence at  $P$  in every direction is less than or equal to the slope of all the characteristics through  $P$  in that direction. Axiom 1.1, which holds in the absence of focusing, allows us to conservatively estimate the causal slope at every point in spacetime where the solution has not been computed by our algorithm yet. Cones of influence are locally conservative approximations to the domains of influence. A sufficiently conservative cone can be chosen that is a valid approximation of the actual domain of influence for the finite step size chosen by our algorithm to advance the solution. Thus, in Figure 1.1, points  $A$  and  $B$  are independent because neither influences the other.

We assume only that the no-focusing assumption of Axiom 1.1 holds everywhere in the spacetime domain  $\Omega$ . Our algorithms guarantee correctness of the solution only in the absence of focusing.

**ASYMMETRIC CONES** Due to nonlinear response and anisotropy of the underlying medium, waves can propagate with different speeds in different directions. Therefore, in general, the wavespeed at a point  $P$  is a function of the spatial direction  $\mathbf{n}$ , and hence, cones of influence and dependence have non-circular cross-sections. Our assumption of no-focusing in this anisotropic context can be stated as the following axiom.

**Axiom 1.3** (Anisotropic no-focusing). *For every point  $P$  in the spacetime domain, the slope at  $P$  in an arbitrary spatial direction  $\mathbf{n}$ , denoted by  $\sigma_{\mathbf{n}}(P)$ , is bounded by the minimum and maximum slope in the same spatial direction  $\mathbf{n}$  of every cone of influence containing  $P$ . Thus, for every spatial direction  $\mathbf{n}$ , we have*

$$\min_{P \in \text{cone}^+(Q)} \{\sigma_{\mathbf{n}}(Q)\} \leq \sigma_{\mathbf{n}}(P) \leq \max_{P \in \text{cone}^+(Q)} \{\sigma_{\mathbf{n}}(Q)\}$$

## 1.2 Spacetime meshing

We saw in Section 1.1 that wave propagation is modeled by hyperbolic partial differential equations (PDEs) in both space and time variables, for instance, the wave equation  $u_{tt} - \omega^2 u_{xx} = 0$  in 1D space  $\times$  time. The *wavespeed*  $\omega$ , the speed at which changes in physical parameters at a point  $(x, t)$  propagate to other points in the domain, may be a function of  $x$  and  $t$  as well as of  $u$  and its derivatives. The spacetime discontinuous Galerkin (SDG) method approximates the solution within each spacetime element of a mesh of the spacetime domain as a linear combination of simple basis functions such as polynomials. The SDG method allows basis functions to be discontinuous across element boundaries—adjacent elements need not agree on the solution along their common boundary.

The spacetime DG method motivates our meshing problem. In this chapter, we will give an overview of the goal of this thesis—to give provably correct algorithms for generating efficient spacetime meshes suitable for DG solvers. We will describe the challenges that are encountered. We will enumerate the assumptions under which our algorithms and the meshes they produce satisfy the stated goal. We conclude this chapter with a summary of our results and of previous research on spacetime meshing.

This section defines the basic notions and vocabulary used throughout the rest of the thesis. We will remind the reader of our assumptions and refer back to this section whenever necessary.

### Patches

The notions of influence and dependence extend naturally to arbitrary subsets of spacetime. For arbitrary elements  $A$  and  $B$ , not necessarily distinct, of a spacetime mesh, we say that  $A$  *influences*  $B$ , written as  $A \preceq B$  if and only if some point  $a \in A$  influences some point  $b \in B$ . If  $A \preceq B$ , then  $A$  must be solved no later than  $B$ , otherwise the solution in  $B$  is not valid. Elements  $A$  and  $B$  are *coupled* if and only if both  $A \preceq B$  and  $B \preceq A$ . A pair of coupled elements must be solved together, i.e., as a simultaneous system of equations. If neither  $A \preceq B$  nor  $B \preceq A$ , then we say  $A$  and  $B$  are *independent*.

A *patch*  $\Pi$  in a spacetime mesh  $\Omega$  is a set of elements that must be solved simultaneously. More formally, a patch  $\Pi$  is a set of one or more elements with the following properties:

1. for every  $A \in \Pi$  there exists  $B \in \Pi$  such that  $A$  and  $B$  are coupled (dependency condition);
2. for every  $A \in \Pi$ , if there exists  $B \in \Omega$  such that  $A$  and  $B$  are coupled then  $B \in \Pi$  (maximality condition).

The *size* of a patch is the number of elements in it.

We have seen that causality defines a partial order over points in spacetime. We say that a subset  $\Omega'$  of spacetime is *causal* if and only if  $\Omega'$  is an anti-chain in the partial order, i.e., if and only if no two points of  $\Omega'$  influence each other. The boundary of a patch  $\Pi$  is necessarily causal because otherwise elements outside the patch would be coupled with elements in the patch, violating the maximality of  $\Pi$ . Patches are therefore partially ordered by causal dependence.

A spacetime mesh  $\Omega$  can be solved patch-by-patch in an order that respects the partial order of patches. The total computation time of such a patch-wise solution strategy is the sum over every patch  $\Pi$  in the mesh  $\Omega$  of the time to solve  $\Pi$ . We say that a patch-wise solution strategy is *efficient* if the total computation time is proportional to the number of elements in the mesh. Our meshing algorithms support an efficient solution strategy because both (i) the maximum size of a patch and (ii) the number of patches in a given spacetime volume are bounded. In a mesh constructed by other algorithms, either the maximum size of a patch or the number of patches or both are unbounded; furthermore, the solver must explicitly compute the partial order of patches or solve all patches together as a large coupled system. Therefore, a generic purpose meshing algorithm is inefficient in general; specialized algorithms are necessary for efficiently meshing in spacetime.

## 1.2.1 Terminology and notation

Before we proceed to the technical details of our spacetime meshing problem and a summary of the results in this thesis, we define some basic concepts and introduce the reader to the notation used in the rest of this thesis.

First, we review some basic concepts. See the references (Zie95) for further details.

A *simplex* of dimension  $k$ , also called a  $k$ -simplex, is the convex hull of  $k + 1$  affinely independent points. A simplex is a closed set of points. We identify a simplex with its vertices. Let  $p_0 p_1 p_2 \dots p_k$  be a  $k$ -simplex. Every subset of  $\{p_0, p_1, p_2, \dots, p_k\}$  defines a *face* of the simplex. Simplices of dimension 0, 1, 2, and 3 are called vertices, segments, triangles, and tetrahedra respectively. For a  $k$ -simplex  $S$ , let  $\text{aff } S$  denote the affine hull of  $S$ , i.e., the set of all linear combinations of vertices of  $S$ ; the affine hull  $\text{aff } S$  is a  $(k - 1)$ -flat (dBSvKO00). For example, the affine hull  $\text{aff } pq$  of two points  $p$  and  $q$  is the line  $pq$ .

A *simplicial complex* is a collection  $\mathcal{C}$  of simplices with the following properties: (i) if a simplex  $S \in \mathcal{C}$  then every face of  $S$  is in  $\mathcal{C}$ , and (ii) two simplices in  $\mathcal{C}$  either do not intersect, or their intersection is a simplex of smaller dimension which is their common face of maximal dimension. The empty simplex, whose dimension is  $-1$ , is a face of every simplex. The dimension of the simplicial complex  $\mathcal{C}$  is the highest dimension of any simplex in the collection  $\mathcal{C}$ . For a  $d$ -dimensional simplicial complex, the  $(d - 1)$ -dimensional faces are called the *facets*. A simplicial complex is a special type of *cell complex* (Zie95).

Two faces of a complex are *incident* if one is included in the other. Given a simplicial complex  $\mathcal{C}$ , the *star* of a face  $F$ , denoted by  $\text{star}(F)$ , is the sub-complex consisting of all simplices incident on  $F$ , and all their faces. The star of  $F$  is a closed set. The *link* of a face  $F$ , denoted by  $\text{link}(F)$ , is the sub-complex consisting of all faces  $G$  of simplices in  $\text{star}(F)$  such that  $G \cap F = \emptyset$ .

A particular type of simplicial complex is a triangulation. A  *$d$ -dimensional triangulation* is a  $d$ -dimensional simplicial complex such that all maximal faces are  $d$ -simplices. Note that a triangulation need not form a manifold. In a  $d$ -triangulation, every  $(d - 1)$ -face  $F$  belongs to one or more  $d$ -simplices; in the former case,  $F$  is a *boundary facet*, and in the latter case,  $F$  is an *interior facet*. All faces of a boundary facet are *boundary faces*; all other faces are *interior faces*. For example, if  $v$  is a vertex of a 2-dimensional triangulation, then  $\text{star}(v)$  consists of the vertex  $v$ , all edges incident on  $v$ , and all triangles incident on  $v$  together with their edges and vertices;  $\text{link}(v)$  is a set of edges

which form a closed loop if  $\text{star}(v)$  is homeomorphic to a disk.

Next, we define the terms and notation used to describe our spacetime meshing problem.

A  $d$ -dimensional *space mesh* is a  $d$ -dimensional triangulation. We visualize the  $(d+1)$ -dimensional spacetime domain with the time axis drawn vertically so that time increases upwards. We use uppercase letters like  $P, Q, R$  to denote points in spacetime and corresponding lowercase letters like  $p, q, r$  to denote their spatial projections.

A *front* is a maximal subset of spacetime that forms an anti-chain in the partial order of dependence; i.e., a front  $\tau$  is a maximal set of points such that no two points of  $\tau$  influence each other. An example of a front is the set of all points with a given time coordinate  $T$ , whose graph is the horizontal constant-time plane  $t = T$ .

The *front*  $\tau$  defines a piecewise linear function  $\tau : \mathbb{E}^d \rightarrow \mathbb{R}$ . Equivalently, the front  $\tau$  is a  $d$ -dimensional piecewise linear terrain (dBSvK000), a subset of  $\mathbb{E}^d \times \mathbb{R}$ . We will not distinguish between these two equivalent descriptions of the front—one as a function and the other as a set of points. Each point  $P$  on the front  $\tau$  can be written as  $P = (p, \tau(p))$  where  $p$  is the spatial projection of  $P$ . For a real  $T$  and front  $\tau$ , we use  $\tau \geq T$  to mean that every point  $P = (p, \tau(p))$  of  $\tau$  satisfies  $\tau(p) \geq T$ , i.e., the entire front  $\tau$  has achieved or exceeded time  $T$ . Arbitrary fronts  $\tau$  and  $\tau'$  satisfy  $\tau' \geq \tau$  if and only if  $\tau'(p) \geq \tau(p)$  for every point  $p$  such that  $P = (p, \tau(p)) \in \tau$  and  $P' = (p, \tau'(p)) \in \tau'$ .

We will frequently assume that the front  $\tau$  consists of a single  $k$ -simplex. In this case, we will not distinguish between the simplex and the corresponding time function  $\tau : \mathbb{E}^k \rightarrow \mathbb{R}$  whose graph is the  $k$ -flat in spacetime spanned by the simplex. In such a scenario, since  $\tau$  is a linear function, its gradient, denoted by  $\nabla \tau$ , is the same everywhere— $\nabla \tau$  is a vector in  $\mathbb{R}^k$  in the direction of steepest ascent and its  $L_2$ -norm is denoted by  $\|\nabla \tau\|$ .

The front at the beginning of each iteration of our algorithm represents the frontier of both the incremental mesh construction as well as the solution. Thus, if  $P = (p, \tau(p))$  is a point of the front  $\tau$  then  $p$  belongs to the space domain at time  $\tau(p)$ , i.e.,  $p \in M_{\tau(p)}$ ; the solution at  $P$  has been computed; and the set of points  $P^+ = (p, t^+)$  such that  $t^+ > \tau(p)$  remain to be meshed and the solution there is unknown.

A front is causal if and only if for every facet  $F$  of the front all characteristics cross  $F$  from one side to the other. For an element with a facet on the front  $\tau$ , this facet is an *outflow* facet of the element because influence travels from the interior of the element to the exterior across this facet. Equivalently, a front  $\tau$  is causal if and only if every point  $P = (p, \tau(p))$  depends only on points below the front, i.e., if  $P \succ Q$  then  $Q$  can be written as  $Q = (q, t_q)$  where  $t_q < \tau(p)$ . Symmetrically, every point of the front  $\tau$  influences only points above the front. By our earlier definition, every front is automatically causal.

For a simplex (of any dimension)  $S$  of the mesh  $M$ , let  $\tau|_S$  denote the time function  $\tau$  restricted to  $S$  and extended to the affine hull of  $S$ ; in other words,  $\tau|_S$  is a linear function that coincides with  $\tau$  for every point of  $S$ .

Let  $\tau_i : M \rightarrow \mathbb{R}$  denote the front after the  $i$ th step of the algorithm;  $\tau_0$  is the initial front. At every step  $\tau_i \rightarrow \tau_{i+1}$ , our algorithm will explicitly triangulate the new front  $\tau_{i+1}$ . Thus, every front constructed by our algorithm will be a triangulated terrain. For every  $i$ , the front  $\tau_i$  is a terrain whose facets are  $d$ -simplices.

A local minimum of the front  $\tau$  is a vertex  $p$  such that  $\tau(p) \leq \tau(q)$  for every vertex  $q$  that is a neighbor of  $p$ . Every front has a local minimum because it has at least one global minimum which is also a local minimum. When the current front  $\tau$  is clear from the context, for every point  $p \in M$  we use  $P$  to denote the corresponding point on the front, i.e.,  $P = (p, \tau(p))$ .

For an arbitrary simplex  $P_0P_1P_2 \dots P_d$  of the front  $\tau$ , we say that a vertex, say  $P_0$ , is a *lowest vertex* of the simplex if  $\tau(p_0) \leq \min_{0 \leq i < d} \tau(p_i)$ . Note that a simplex may have one or more lowest vertices. We say that a facet, say  $P_1P_2 \dots P_d$  is a *highest facet* if the opposite vertex  $P_0$  is a lowest vertex. Note that a simplex may have more than one highest facets.

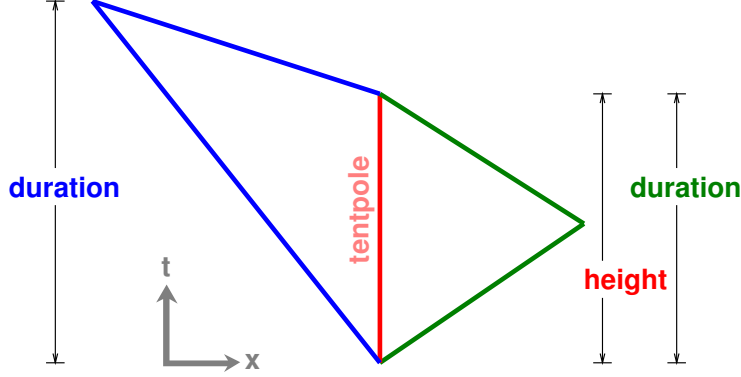


Figure 1.3: The temporal aspect ratio of a spacetime element is the ratio of its height to its duration. The height of both spacetime triangles in the figure is equal to the height of the tentpole they share. The spacetime triangle on the right has a better (larger) temporal aspect ratio than the triangle on the left.

We say that a front  $\tau'$  is obtained by advancing a vertex  $P = (p, \tau(p))$  of  $\tau$  by  $\Delta t \geq 0$  if  $\tau'(p) = \tau(p) + \Delta t$  and for every other vertex  $q \neq p$  we have  $\tau'(q) = \tau(q)$ . For every front  $\tau$ , vertex  $p$ , and real  $\Delta t \geq 0$ , let  $\tau' = \text{advance}(\tau, p, \Delta t)$  denote the front obtained from  $\tau$  by advancing  $p$  by  $\Delta t$ ; the functions  $\tau$  and  $\tau'$  coincide everywhere outside  $\text{star}(p)$ .

For a simplex  $\Delta$ , we use  $\sigma(\Delta)$  to denote the minimum slope  $\sigma(P)$  over all points  $P$  of  $\Delta$ ; we let  $\omega(\Delta)$  denote  $1/\sigma(\Delta)$ . Let  $\sigma_{\min}$  denote  $\min_{P \in \Omega} \{\sigma(P)\}$  and  $\sigma_{\max}$  denote  $\max_{P \in \Omega} \{\sigma(P)\}$ . We assume that  $0 < \sigma_{\min} \leq \sigma_{\max} < \infty$ . Thus, the slope  $\sigma(P)$  at an arbitrary point  $P$  is bounded:  $0 < \sigma_{\min} \leq \sigma(P) \leq \sigma_{\max} < \infty$ .

For a vertex  $P$  of the front  $\tau$ , define the quantity  $w_p$  in the spatial projection as

$$w_p := \min_{\Delta \in \text{link}(p)} \text{dist}(p, \text{aff } \Delta).$$

For an arbitrary subset  $K$  of  $\mathbb{E}^d \times \mathbb{R}$ , the *height* of  $K$  is the length of the longest time interval contained in the closure of  $K$ , and the *duration* of  $K$  is the length of the shortest time interval containing the interior of  $K$ . The *temporal aspect ratio* of a spacetime element is the ratio of the height of the element to its duration. See Figure 1.3. Note that the temporal aspect ratio is always in the range  $(0, 1]$  with a larger value corresponding to a “better” element. The temporal aspect ratio of an arbitrary subset of spacetime is unchanged if all time coordinates are uniformly translated and scaled by a non-zero constant.

## 1.2.2 Meshing objectives

We want a mesh of the spacetime domain  $\Omega$  consisting of spacetime simplices or *elements* such that every spacetime element has at least one causal outflow facet, a necessary condition for the numerical problem to be well-posed (JJ04). The sizes of the spacetime elements are controlled by a spacetime error indicator. The spacetime elements must form a *weak simplicial complex*; this property allows a simple strategy to compute integrals over the common intersection of any two spacetime elements—the intersection is an entire face of at least one of the two elements and has a natural parameterization that facilitates integration. Spacetime DG solvers are particularly suited to solve such weakly conforming meshes because of their discontinuous formulation.

**Definition 1.4** (Weak simplicial complex). A weak simplicial complex is a collection  $\mathcal{C}$  of simplices with the following properties:

1. if a simplex  $S \in \mathcal{C}$ , then every face of  $S$  is in  $\mathcal{C}$ ; and
2. the intersection of every two simplices of  $\mathcal{C}$  is a face of at least one of them.

We have seen that an efficient solution strategy is to solve the mesh  $\Omega$  patch-by-patch in an order that respects the partial order of patches. Every spacetime mesh can be partitioned into patches—giving a *causal partition*—and can be solved by this strategy. The total computation cost is the sum of the cost of solving each individual patch. A generic mesh of spacetime cannot be efficiently solved because either the size of a patch or the number of patches or both are not bounded. Our objective is to minimize the total computation cost. We give a meshing algorithm that incrementally constructs the spacetime mesh patch-by-patch explicitly in the order of causal dependence. We prove that both the size of each patch and the total number of patches in the mesh of a given spacetime volume are bounded; hence, the total computation cost is bounded.

We give an advancing front algorithm such that for every  $T \in \mathbb{R}^{\geq 0}$  there exists a finite integer  $k \geq 0$  such that the front  $\tau_k$  after the  $k$ th iteration of the algorithm satisfies  $\tau_k \geq T$ . The input to our problem is the initial front  $\tau_0$  and the initial conditions of the PDE. We obtain the spacetime mesh by triangulating the spacetime volume, called a *tent*, between each pair of successive fronts  $\tau_i$  and  $\tau_{i+1}$  such that each spacetime element has at least one facet on the front  $\tau_{i+1}$ , which by definition is causal. The elements in a tent are causally dependent and must be solved as a coupled system. We produce an efficient mesh such that the number of elements in a coupled system is small, depending on the maximum degree of the initial space mesh.

Our mesh is also efficient in the sense that elements are non-degenerate in the sense that each element has temporal aspect ratio bounded from below. We expect that the non-degeneracy guarantee means that in practice the numerical solution within each element can be computed with acceptable accuracy.

Our goal is to support an accurate solution of the underlying PDE as well as to reduce total computation time. It is challenging enough to devise meshing algorithms that provide a theoretical guarantee that the meshing algorithm would terminate after creating a finite number of non-degenerate elements. In addition, our goal is to provide an algorithm that is easy to implement and that performs significantly better in practice than the theoretical guarantee, for instance by a good choice of parameters to the algorithm and possibly using different heuristics. At the same time, we will never compromise on the ability to prove correctness of all algorithms described in this thesis. Some aspects of the meshing algorithm go beyond this basic goal and improve its performance in practice.

### Advancing front spacetime meshing

Given a simplicial mesh of some bounded domain  $M \subset \mathbb{E}^d$ , we give a meshing algorithm to incrementally construct a simplicial mesh of the spacetime domain using an advancing front method. The algorithm advances the front by moving a vertex forward in time, thus also advancing the local neighborhood  $\text{star}(v)$ , and adding simplices in the volume between the old and the new fronts. The inflow and outflow boundaries of each patch (Figure 1.5) are causal by construction, i.e., each boundary facet  $F$  separates the cone of influence from the cone of dependence for every point on  $F$  (Figure 1.4). Equivalently, for every point  $P$  on  $F$  we have  $\|\nabla F\| \leq \sigma(P)$ . If the outflow boundaries of a patch are causal, every point in the patch depends only on other points in the patch or points of inflow elements adjacent to the inflow boundaries of the patch. Therefore, the solution within the patch can be computed as soon as the patch is



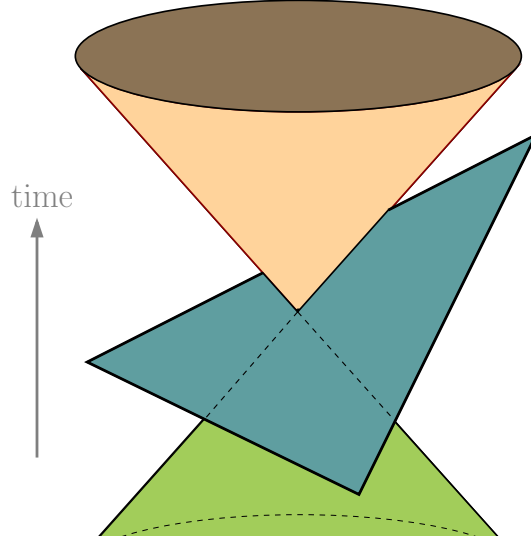


Figure 1.4: A causal triangle separates the cones of influence and dependence at every point on the face.

created, given only the inflow data from adjacent inflow elements and initial or boundary data where appropriate. The elements within a patch are causally dependent on each other and must be solved as a coupled system. Patches with no causal relationship can be solved independently. To minimize undesirable numerical dissipation and the number of patches, we would like the boundary facets of each patch to be as close as possible to the causality constraint without violating it.

We require that for every target time value  $T$  the algorithm will compute in a finite number of steps a mesh of the spacetime volume  $M \times [0, T]$  and the solution everywhere in this volume. The target time  $T$  may not be known *a priori* because it depends on the evolving physics.

Our algorithm ensures that every spacetime element in a patch has one facet on the new front, which is a causal outflow facet.

**TRIANGULATING A TENT** Our advancing front algorithm repeatedly advances a local neighborhood  $N$  of the current front  $\tau$  to a corresponding neighborhood  $N'$  of a new front  $\tau'$ , where  $\partial N = \partial N'$  and  $\tau = \tau'$  everywhere in  $\tau \setminus N$ . For instance, our algorithm pitches a local minimum of the current front creating a new front which is the input to the next iteration of the algorithm. *Pitching* a vertex  $P$  of the front  $\tau$  means advancing  $P = (p, \tau(p))$  to  $P' = (p, \tau'(p))$  where  $\tau$  and  $\tau'$  are the old and the new fronts respectively. Pitching  $P$  means advancing the neighborhood  $N = \text{star}(P)$  to  $N' = \text{star}(P')$  where  $\partial N = \partial N' = \text{link}(P)$ . The *progress* is defined to be the time difference  $\tau'(p) - \tau(p)$ .

The volume between the new front and the old front is called a *tent* and the edge  $PP'$  is called the *tentpole*. The tent is partitioned into spacetime elements (simplices); the set of elements in a tent forms a patch. Let  $F'$  denote an arbitrary facet on the new front  $\tau'$ . The tent is triangulated so that for each such facet  $F'$  the patch contains the element corresponding to the convex hull of  $F'$  and the vertex  $P$ , the bottom of the tentpole.

For each point  $U$  in the tent, the ray  $PU$  intersects a simplex  $F'$  on the new front  $\tau'$ . Therefore,  $U$  is contained in the convex hull of  $F' \cup \{P\}$ . Hence, the set of elements in a patch partition the tent.

By construction, each element  $E$  in the patch is the convex hull of  $F' \cup \{P\}$  for some facet  $F'$  on the new front  $\tau'$ . By construction,  $F'$  is a causal facet of  $E$ . For every point  $Q$  on  $F'$  the cone of influence of  $Q$  is entirely in the future

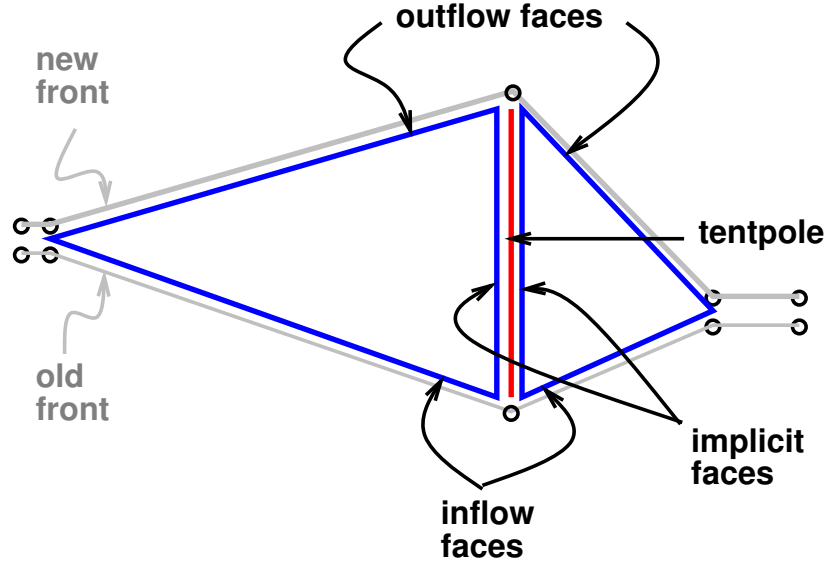


Figure 1.5: Cross-section of a patch of tetrahedra; the inflow and outflow faces are causal. Time increases up the page.

and does not intersect the element  $E$ ; therefore,  $F'$  is an outflow facet of  $E$ . Hence, every element in a patch has a causal outflow face.

Also, the intersection of every two elements is either (i) empty, (ii) a common vertex, (iii) the tentpole of a patch containing both elements, or (iii) the entire facet of at least one of the two elements. If the two elements belong to the same patch with tentpole  $PP'$ , then they share the vertex  $P$ ; they also share either the tentpole  $PP'$  or a common facet, or they share a common implicit facet containing the tentpole. On the other hand, if one element is an inflow into the other tetrahedron then their common intersection is either the entire outflow face of the first element or the entire inflow face of the second element.

When we generalize to other operations that advance the front we will ensure that these properties are always satisfied. For instance, an edge flip in  $2D \times \text{Time}$  creates a patch with a single tetrahedron, which has two causal inflow facets and two causal outflow facets.

### 1.2.3 Meshing challenges

We say that a front  $\tau$  is *valid* if there exists a positive real  $\delta$  bounded away from zero such that for every  $T \in \mathbb{R}^{\geq 0}$  there exists a sequence of fronts  $\tau, \tau_1, \tau_2, \dots, \tau_k$  where  $\tau_k \geq T$ , each front in the sequence obtained from the previous front by advancing some vertex by  $\delta$ . The minimum value of  $\delta$  for which we can guarantee that our algorithms construct only valid fronts is the *progress guarantee* of our algorithm. The progress guarantee is the same as the worst-case tentpole height. All our theoretical results, such as finite termination, worst-case temporal aspect ratios of spacetime elements, and near-size-optimality follow from the progress guarantee. What makes the definition of a valid front nontrivial is the requirement that all fronts be causal. The main difficulty in characterizing valid fronts arises when the wavespeed at a given point in the space domain increases discontinuously and unpredictably over time. In spatial dimensions  $d \geq 2$ , an additional complication is the changing front geometry due to adaptive refinement and coarsening, and mesh smoothing.

## 1.2.4 Summary of results

The main contribution of our work is an efficient incremental spacetime meshing algorithm that adapts quickly to changing geometric constraints, that supports an efficient parallelizable solution strategy, and that has provable worst-case guarantees on the temporal aspect ratio of spacetime elements.

**Theorem 1.5.** *Suppose we are given a simplicial mesh  $M \in \mathbb{E}^d$  as well as initial and boundary conditions of the underlying spacetime hyperbolic PDE. Our algorithm builds a simplicial mesh  $\Omega$  of the spacetime domain  $M \times [0, \infty)$  that satisfies all the following criteria:*

1. *the elements of  $\Omega$  form a weak simplicial complex that conforms to the initial mesh  $M$ ;*
2. *each spacetime element has at least one causal outflow facet;*
3. *for every  $T \geq 0$  the spacetime volume  $M \times [0, T]$  is contained in the union of a finite number of simplices of  $\Omega$ ;*
4. *the minimum temporal aspect ratio of every spacetime element is bounded from below.*

*Additionally, in 2D×Time, our algorithm adapts the size and duration of spacetime elements to a spacetime error indicator. We guarantee that the diameter of each tetrahedron is no larger than that allowed by the spacetime error indicator. Provided the error indicator does not reject any tetrahedra smaller than a bounded minimum size, our algorithm terminates with a finite mesh of  $M \times [0, T]$  for every target time  $T \geq 0$ .*

Given a triangulation  $M$  of the space domain and a target time  $T$ , we say that a simplicial spacetime mesh of  $M \times [0, T]$  is *solvable* if (i) each spacetime element has both a causal inflow facet and a causal outflow facet; and (ii) for every point  $x$  in the spatial projection  $\Delta$  of each spacetime element, the diameter of  $\Delta$  does not exceed the diameter of the simplex of  $M$  containing  $x$ .

**Theorem 1.6.** *Let  $\tilde{\epsilon}$  be an arbitrary constant, a parameter to our algorithm, in the range  $0 < \tilde{\epsilon} \leq \frac{1}{2}$ . The size of the mesh constructed by our algorithm is  $\tilde{O}\left(\frac{1}{\tilde{\epsilon}^2}\right)$  times the minimum size of any solvable mesh of the spacetime volume  $M \times [0, T]$ , where the hidden term in the  $\tilde{O}$ -notation depends on the dimension  $d$  and the worst-case spatial geometry of each front.*

An example of a tetrahedral mesh of 2D×Time constructed by our algorithm is given in Figure 1.6. Additional examples of meshes constructed using our algorithm appear in the references (ACE<sup>+</sup>04; ACF<sup>+</sup>04; AHTE05; Thi04).

## 1.2.5 Previous work

This thesis is part of an ongoing long-term project at the Center for Process Simulation and Design (CPSD), a multi-disciplinary research group at the University of Illinois (UIUC). See <http://www.cpsd.uiuc.edu/> for more about CPSD.

Building on ideas from earlier specialized algorithms, Üngör and Sheffer (ÜS02) and Erickson *et al.* (EGSÜ02) developed the first algorithm to build graded spacetime meshes over arbitrary simplicially meshed spatial domains, called Tent Pitcher. Unlike most traditional approaches, the Tent Pitcher algorithm does not impose a fixed global time step on the mesh, or even a local time step on small regions of the mesh. Rather, it produces a fully unstructured simplicial spacetime mesh, where the duration of each spacetime element depends on the local feature size and quality of the underlying space mesh. See Erickson *et al.* (EGSÜ02) for sample meshes constructed by Tent Pitcher. Figure 1.7 from the paper by Erickson *et al.* (EGSÜ02) illustrates the first few tent pitching steps of the algorithm.

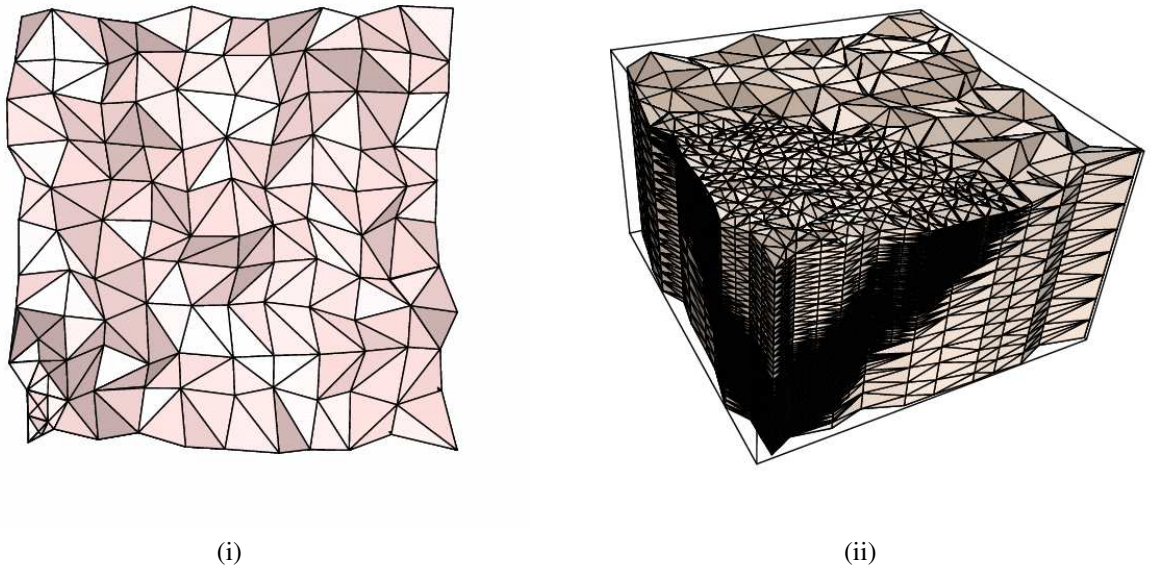


Figure 1.6: Given (i) a triangulated 2D space mesh, our algorithm constructs (ii) an unstructured tetrahedral spacetime mesh. Time increases upwards in (ii). In this example, the wavespeed at any point in spacetime is one of two distinct values: the maximum wavespeed occurs inside a circular cone where the tentpoles are shortest, the minimum wavespeed occurs everywhere else. The size of spacetime elements adapts to both changing wavespeed to maintain causality as well as to a simulated error metric which depends on the temporal aspect ratio.

The original Tent Pitcher algorithm proposed by Üngör and Sheffer (ÜS00) applied to one- and two-dimensional space domains. The algorithm could guarantee progress only if the input triangulation contained only angles less than 90 degrees and if the wavespeed did not increase or only increased smoothly. Üngör and Sheffer referred to the causality constraint as an angle constraint and assumed that this angle constraint was Lipschitz-continuous. They implemented Tent Pitcher and investigated several different heuristics to improve its performance.

Erickson *et al.* (EGSÜ02) extended Tent Pitcher to arbitrary spatial domains, even those with obtuse angles, in arbitrary dimensions by imposing additional constraints, called *progress constraints*. The progress constraint limits the amount of progress in time when some vertex of the simplex is pitched, in addition to the limit imposed by causality. The progress constraint is a function of the shape of the simplex and is necessary to guarantee progress only when the initial space mesh contains a non-acute angle.

The Tent Pitcher algorithm due to Üngör and Sheffer (ÜS00; Ü02) and extended by Erickson *et al.* (EGSÜ02) applied to the case where the wavespeed at a given point is either constant, decreasing, or increasing smoothly as a Lipschitz function. When the wavespeed changes, the previous algorithms take the global upper bound on the wavespeed and use that as a conservative upper bound on the wavespeed at every point. Limiting the progress at each step by a function of the global maximum wavespeed is unnecessarily restrictive. One would like an algorithm that adapts to increasing wavespeeds so that fewer spacetime elements, and therefore less computation time, are required to mesh a given volume. We develop such an algorithm, an extension to Tent Pitcher, in Chapter 3.

The size of spacetime elements affects the numerical accuracy of the approximate solution. Where the exact solution is constant or changing very little, large elements suffice to capture this small variation. Parts of the domain where the solution changes a lot need to be meshed with smaller elements. In Chapter 4 we extend Tent Pitcher to

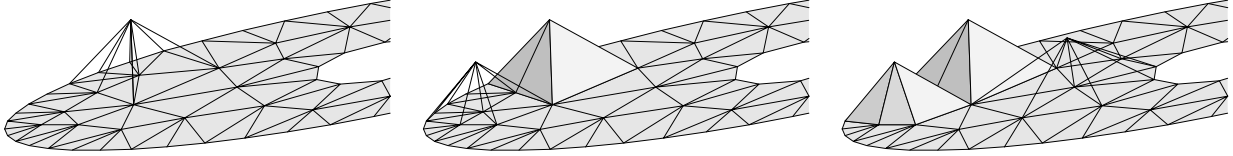


Figure 1.7: The first few tents pitched by Tent Pitcher (EGSÜ02).

make the size of spacetime elements adaptive to *a posteriori* error estimates.

Tent Pitcher is a good alternative to standard time-stepping methods. Global time-marching schemes advance the solution from one time value to another everywhere in the domain at once. Computing the solution for the new time value in this way has at least one of two disadvantages—either the maximum possible time step is constrained by the worst-quality element in the space mesh, or an arbitrarily large coupled system has to be solved simultaneously. The former would correspond to the constraint that the height of each tentpole erected by Tent Pitcher must be the same, and the latter would occur if the causality constraint were not satisfied by Tent Pitcher. Thus, the advancing front approach avoids both limitations associated with time-marching schemes. (Some recent advances have been made on adaptive explicit time-stepping methods for ODEs (EJL03).)

## Chapter summary

In this chapter, we gave a concise introduction to the properties of hyperbolic partial differential equations (PDEs) as they concern this thesis. We briefly discussed the challenging problem of generating good quality meshes to support fast and accurate numerical solutions to PDEs. We pointed out the advantages of spacetime discontinuous Galerkin (SDG) methods over conventional finite element methods. For more about DG methods, the reader is referred to the survey (CKS00) of discontinuous Galerkin methods and their applications.

We outlined the specific problem of meshing in spacetime to support SDG methods for solving hyperbolic PDEs, such as those modeling wave propagation. Meshing directly in spacetime presents unique challenges not encountered in classical meshing problems. It is hard to formulate geometric criteria for a good quality spacetime element and a good quality spacetime mesh, a problem that is already complicated and application-dependent in Euclidean domains. SDG methods, due to their discontinuous formulation, permit nonconforming meshes and more general mesh adaptivity operations. We will exploit this increased flexibility in developing meshing algorithms, extensions to the Tent Pitcher algorithm, in the remaining chapters.

An advancing front algorithm for generating a spacetime mesh, as exemplified by Tent Pitcher (Ü02; EGSÜ05), has several benefits. Elements are added to the mesh in small subsets called patches. Each element in a patch has at least one outflow facet. Since the front at every step is causal, the front represents all the information that is required for future iterations of the algorithm. The elements in a patch are coupled but two different patches erected over the same front are independent. Thus, the solution procedure is highly parallelizable. Solving each patch is equivalent to performing a small finite element computation limited to the patch. Memory requirements are low because patches are created in the order of causal dependence and hence can be discarded when they are no longer adjacent to the current front. The computation time required for the simulation is reduced due to the limited dependency only between elements in the same small patch and because the number of patches is bounded.

## Chapter 2

# Basic advancing front meshing algorithm

Tent Pitcher was the first provably correct spacetime meshing algorithm to support an efficient patch-wise solution strategy. Tent Pitcher was proposed by Üngör and Sheffer (ÜS00) and later extended by Erickson *et al.* (EGSÜ02; EGSÜ05). Our advancing front meshing algorithms are extensions to and augmentations of Tent Pitcher. In this chapter, we give an alternate derivation and proof of correctness of the Tent Pitcher algorithm. The style of the derivation in this chapter anticipates extensions to nonlinear problems and mesh adaptivity, problems that are considered in later chapters. Also, the alternate derivation in this chapter fixes an error in the paper by Erickson *et al.* (EGSÜ02) for the case of obtuse front triangles, an oversight that was corrected in a subsequent journal paper (EGSÜ05).

Our objective in this chapter is to set up a general framework for advancing front spacetime meshing algorithms and highlight Tent Pitcher as one specific member of this class of algorithms. The more sophisticated meshing algorithms described in later chapters fit in this general framework.

The Tent Pitcher algorithm is the first instance of an advancing front algorithm to mesh directly in spacetime. The algorithm proceeds by advancing a local neighborhood of the front in every step. The algorithm is simple because the geometric constraints that limit the amount of progress at each step are linear or quadratic functions of the coordinates. For linear problems, the wavespeed  $\omega$  is a fixed constant, determined by material properties, or can be conservatively bounded by the global maximum wavespeed. When the wavespeed is constant, the amount of progress made by the front in each local advancing step is limited only by local constraints.

### 2.1 Problem statement

The input is the initial front  $\tau_0$ , which is a triangulation of the space domain at time  $t = 0$ , and the causal slope  $\sigma$  (equivalently, the wavespeed  $\omega = 1/\sigma$ ), which is determined by the initial conditions of the PDE. In this chapter, we assume that the wavespeed  $\omega$  is a constant, either because the underlying hyperbolic PDE is linear or because  $\omega$  is the global maximum wavespeed. We give an advancing front algorithm such that for every  $T \in \mathbb{R}^{\geq 0}$  there exists a finite integer  $k \geq 0$  such that the front  $\tau_k$  after the  $k$ th iteration of the algorithm satisfies  $\tau_k \geq T$ , which means that the entire front has achieved or passed time  $T$ . The volume between each consecutive pair of fronts  $\tau_i$  and  $\tau_{i+1}$  is triangulated to give a patch.

We will generate meshes with geometrically non-degenerate elements. Specifically, we prove that each element has temporal aspect ratio bounded from below. Recall from Chapter 1 that the temporal aspect ratio of an element is the ratio of its height to its duration.

We say that a front  $\tau$  is *valid* if for every  $T \in \mathbb{R}^{\geq 0}$  there exists a finite sequence of fronts  $\tau, \tau_1, \tau_2, \dots, \tau_k$  where  $\tau_k \geq T$ , each front in the sequence obtained from the previous front by advancing some local neighborhood. Therefore, our problem can be defined as that of constructing a succession of valid fronts such that the volume between successive

fronts is triangulated with a small number of spacetime elements (simplices) each with bounded temporal aspect ratio.

**Definition 2.1** (Valid front). *A front  $\tau$  is valid if there exists a positive real  $\Delta t$  bounded away from zero such that for every  $T \in \mathfrak{R}^{\geq 0}$  there exists a finite sequence of fronts  $\tau, \tau_1, \tau_2, \dots, \tau_k$  where  $\tau_k \geq T$ , each front in the sequence obtained from the previous front by advancing some local neighborhood by  $\Delta t$ .*

The Tent Pitcher algorithm due to Üngör and Sheffer, and Erickson *et al.*, is obtained by making the following assumptions:

1. The front  $\tau \equiv 0$ , or more generally any constant time function  $\tau \equiv T$ , is valid.
2. The new front  $\tau' \in \text{advance}(\tau)$  is obtained by advancing a single vertex of  $\tau$  by a nonnegative amount, i.e.,  $N = \text{star}(P)$  for some vertex  $P$  of  $\tau$ .

We say that a front  $\tau'$  is obtained by advancing a vertex  $P$  of  $\tau$  by  $\Delta t \geq 0$  to the vertex  $P'$  of the front  $\tau'$  if  $\tau'(p) = \tau(p) + \Delta t$ , for every other vertex  $q \neq p$  we have  $\tau'(q) = \tau(q)$ , and every simplex incident on  $P'$  is in one-to-one correspondence with a simplex of  $\tau$  incident on  $P$ . For any front  $\tau$ , vertex  $p$ , and real  $\Delta t \geq 0$ , let  $\tau' = \text{advance}(\tau, p, \Delta t)$  denote the front obtained from  $\tau$  by advancing  $p$  by  $\Delta t$ .

We say that a front  $\tau'$  is obtained by advancing a neighborhood  $N$  of  $\tau$  by  $\Delta t \geq 0$  to the neighborhood  $N'$  of the front  $\tau'$  if  $\Delta t = \max_{P=(p, \tau(p)) \in N} \{\tau'(p) - \tau(p)\}$  and if  $\tau \setminus N$  and  $\tau' \setminus N'$  coincide.

**OUR SOLUTION** For one-dimensional space domains, we prove that every causal front is valid. In higher dimensions, we define *progressive* fronts, and we prove that if a front is progressive, then it is valid. We give an algorithm, a modification of Tent Pitcher, that given any progressive front  $\tau_i$  constructs a next front  $\tau_{i+1}$  such that  $\tau_{i+1}$  is progressive. The volume between  $\tau_i$  and  $\tau_{i+1}$  is partitioned into simplices. The new front  $\tau_{i+1}$  is obtained by advancing a local neighborhood of  $\tau_i$  by a positive amount bounded away from zero. The algorithm can be parallelized in a straightforward manner to solve several patches simultaneously by lifting any independent set of neighborhoods in parallel. Whenever the algorithm chooses to lift a local minimum vertex, it is guaranteed to be able to lift it by at least  $T_{\min} > 0$  where  $T_{\min}$  is a function of the input and bounded away from zero.

In this chapter, we will restrict front advancing operations to tent pitching, i.e., advancing  $N = \text{star}(p)$ , for some vertex  $p$ , to  $N'$  such that  $\partial N = \partial N' = \text{link}(p)$ . Since pitching a vertex does not change the spatial projection, the triangulation of every front is isomorphic to the initial space mesh. In this sense, we say that the meshing algorithm in this chapter is nonadaptive because the spatial projection of every front is the initial triangulation of the space domain. In this chapter, we will assume that the underlying PDE is linear and that  $\sigma$  denotes the causal slope, the reciprocal of the global wavespeed, a constant throughout spacetime. Alternatively, if the wavespeed is not constant, let  $\sigma$  denote  $\sigma_{\min}$ , a lower bound on the slope of any cone of influence in any spatial direction.

## 2.2 Meshing in 1D $\times$ Time

We begin by describing the linear nonadaptive Tent Pitcher algorithm to construct spacetime meshes over one-dimensional space domains. The input space mesh, denoted by  $M$ , is a one-dimensional simplicial complex, i.e., a set of vertices with pairs of vertices, say  $p$  and  $q$ , connected by a segment  $pq$ . Let  $|pq|$  denote the length of the segment  $pq$ , i.e., the Euclidean distance between  $p$  and  $q$ .

**Input:** A one-dimensional space mesh  $M \subset \mathbb{E}^1$

**Output:** A triangular mesh  $\Omega$  of  $M \times [0, \infty)$

The initial front  $\tau_0$  is  $M \times \{0\}$ , corresponding to time  $t = 0$  everywhere in space.

Repeat for  $i = 0, 1, 2, \dots$ :

1. Advance in time an arbitrary local minimum vertex  $P = (p, \tau_i(p))$  of the current front  $\tau_i$  to  $P' = (p, \tau_{i+1}(p))$  such that  $\tau_{i+1}$  is causal and  $\tau_{i+1}(p)$  is maximized.
2. Partition the spacetime volume between  $\tau_i$  and  $\tau_{i+1}$  into a patch of triangles, each sharing the tentpole edge  $PP'$ .
3. Call the numerical solver to compute the solution everywhere in the spacetime volume between  $\tau_i$  and  $\tau_{i+1}$  as well as the *a posteriori* error estimate. The solution on  $\tau_i$  is the inflow information to the solver.

---

Figure 2.1: Advancing front algorithm in 1D×Time.

At each step  $i$ , our algorithm chooses to advance an arbitrary local minimum  $p$  of the causal front  $\tau_i$  to construct the new causal front  $\tau_{i+1}$  such that  $\tau_{i+1}(p)$  is maximized. Since every front has at least one local minimum vertex, e.g., the global minimum, the algorithm has a nonempty subset of candidate vertices to pitch at each step.

Let  $AB$  be an arbitrary segment of the front  $\tau_{i+1}$ . Then,  $AB$  is causal if and only if the gradient of the time function  $\tau_{i+1}$  restricted to  $\text{aff } ab$  is less than the slope  $\sigma(AB)$ , i.e., if and only if

$$\|\nabla \tau_{i+1}|_{ab}\| := \frac{|\tau_{i+1}(b) - \tau_{i+1}(a)|}{|ab|} < \sigma(AB). \quad (2.1)$$

The new time coordinate  $\tau'(p)$  of  $p$  is constrained because every segment  $P'Q$  of the new front is constrained as in Equation 2.1 such that  $\tau'(p) < \tau(q) + |pq|\sigma$  for every segment  $pq \in \text{star}(p)$ .

Note that the inequality in Equation 2.1 is a strict inequality, so the set of all  $\tau_{i+1}(p)$ , such that the front  $\tau_{i+1}$  is causal, is an open, convex set, whose supremum value is not feasible. Therefore, to maximize  $\tau_{i+1}(p)$ , we compute the supremum time value  $T_{\text{sup}}$  that satisfies the causality constraint of Equation 2.1 and then take any time value less than  $T_{\text{sup}}$  but close enough to  $T_{\text{sup}}$  not to cause numerical errors due to loss of precision.

Figure 2.1 describes our linear nonadaptive advancing front meshing algorithm in 1D×Time. The solution everywhere in spacetime is computed patch-by-patch in an order consistent with the partial order of dependence until a particular target time  $T \geq 0$  has been met.

In the parallel setting, we repeatedly choose an independent set of local minima of the front  $\tau_i$ , equal to the number of processors, to be advanced in time simultaneously. The resulting patches can be solved independently. If a patch is accepted, the local neighborhood of the front is advanced without any conflicts with other patches.

It is easy to see that each spacetime triangle has one causal inflow facet (a segment) on the old front  $\tau_i$  and one causal outflow facet on the new front  $\tau_{i+1}$ .

### 2.2.1 Progress guarantee

It remains to show that the algorithm creates only a finite number of triangles to mesh the volume  $M \times [0, T]$  for any target time  $T \geq 0$  and that the minimum temporal aspect ratio of each triangle is bounded. Both requirements follow



from the following lower bound on the height of each tentpole. Recall from Section 1.2.1 that, for a vertex  $P$  of the one-dimensional front  $\tau$ , the distance  $w_p$  is the minimum distance of  $p$  from its nearest neighbor in the spatial projection of  $\tau$ .

**Theorem 2.2.** *Let  $\tau$  be a causal front and let  $p$  be an arbitrary local minimum of  $\tau$ . Then, for every  $\Delta t$  such that  $0 \leq \Delta t < w_p \sigma$ , the front  $\tau' = \text{advance}(\tau, p, \Delta t)$  is causal.*

*Proof of Theorem 2.2.* Only the segments of the front incident on  $P = (p, \tau(p))$  advance along with  $p$ . Consider an arbitrary segment  $pq$  incident on  $p$ . Since  $p$  is a local minimum, we have  $\tau(q) \geq \tau(p)$ . We have

$$\begin{aligned} \tau'(p) &\leq \tau(p) + \Delta t \\ &< \tau(p) + w_p \sigma \\ &\leq \tau(q) + |pq| \sigma(P'Q) \end{aligned}$$

Therefore, the slope of the segment  $P'Q$  is less than  $\sigma(P'Q)$  and hence  $P'Q$  is causal.  $\square$

Since each front  $\tau$  is causal, the difference between the maximum and the minimum time coordinate of points of  $\tau$  must be smaller than the diameter of the space domain  $M$  times the slope  $\sigma$  due to causality. Therefore, the algorithm must eventually advance the global minimum vertex of  $\tau$ . Thus, we have the following theorem.

**Theorem 2.3.** *For every  $i \geq 0$ , if the front  $\tau_i$  is causal then  $\tau_i$  is valid.*

*Proof of Theorem 2.3.* Let  $w_{\min}$  denote the smallest length of the spatial projection of a segment on any front. Since causality limits the gradient of the front, every vertex is pitched eventually when it becomes a local minimum; specifically, a vertex becomes a global minimum after only a finite number of iterations of the advancing front algorithm. By Theorem 2.2, each iteration advances the front in time by a bounded finite amount. Therefore, for any target time  $T \geq 0$ , after a finite number of iterations, the entire front has advanced past  $T$ . Specifically, we show next that after at most

$$\left\lceil \frac{n(T + \text{diam}(M)\sigma_{\max})}{w_{\min}\sigma} \right\rceil$$

iterations, the entire front has advanced up to or beyond the target time  $T$ . Here,  $n$  denotes the maximum number of vertices and  $w_{\min}$  denotes the minimum spatial length of any segment on any front constructed by our algorithm. Let  $T_{\min} = w_{\min}\sigma$ .

Consider step  $i + 1$  of the algorithm. By Theorem 2.2 the front  $\tau_{i+1}$  such that  $\tau_i(p) \leq \tau_{i+1}(p) < \tau_i(p) + T_{\min}$  is causal. Therefore, we have shown that if  $\tau_i$  is causal then there is a front  $\tau_{i+1} = \text{advance}(\tau_i, p, \Delta t)$  such that  $\tau_{i+1}$  is causal for every  $\Delta t \in [0, T_{\min})$ . Note that  $\sum_{p \in V(M)} \tau_{i+1}(p) = T_{\min} + \sum_{p \in V(M)} \tau_i(p)$ . By induction on  $i$ , and because  $\sigma$  is finite and  $M$  is bounded, there exists a finite  $k \geq i$  such that the front  $\tau_k$  satisfies

$$\sum_{p \in V(M)} \tau_k(p) \geq n(T + \text{diam}(M)\sigma)$$

for any real  $T$ . Hence,

$$\max_{p \in V(M)} \tau_k(p) \geq \frac{1}{n} \left( \sum_{p \in V(M)} \tau_k(p) \right) \geq T + \text{diam}(M)\sigma$$

Since  $\tau_k$  is causal

$$\left( \max_{p \in V(M)} \tau_k(p) \right) - \left( \min_{p \in V(M)} \tau_k(p) \right) \leq \text{diam}(M)\sigma.$$

Since  $\max_{p \in V(M)} \tau_k(p) \geq T + \text{diam}(M)\sigma$ , it follows that  $\min_{p \in V(M)} \tau_k(p) \geq T$  and so  $\tau_i$  is valid.  $\square$

In general, the Tent Pitcher algorithm is free to pitch any vertex, not just local minima; however, the progress guarantee of Theorem 2.2 applies only to local minima. Any causal front can be input as the initial front  $\tau_0$ ; thus, the solution can be saved after each step and the algorithm can be restarted from the last front.

## 2.3 Meshing in $2D \times \text{Time}$

In this section, we consider our advancing front algorithm in  $2D \times \text{Time}$ .

### 2.3.1 Need for progress constraints

It has been observed by Üngör and Sheffer and also by Erickson *et al.* that in spatial dimension  $d \geq 2$  the causality constraint is not enough to guarantee that spacetime elements created by Tent Pitcher are non-degenerate. With causality constraints alone, it was shown by Üngör and Sheffer (ÜS00), and by Erickson *et al.* (EGSÜ02) that if the space mesh contains an obtuse or a right triangle then Tent Pitcher will eventually construct a front such that no further progress is possible while maintaining causality. This is the case even for linear PDEs where the wavespeed everywhere in spacetime is a fixed constant.

Our algorithms advance a neighborhood  $N$  of the front  $\tau$  to the neighborhood  $N'$  of a new front  $\tau'$  where  $\partial N = \partial N'$ . It is necessary that the lower-dimensional simplices of  $\partial N$  satisfy gradient constraints stricter than the causal cone constraint.

Erickson *et al.* introduced so-called *progress constraints* on the front at each stage. Causality limits the magnitude of the gradient of every simplex on each front. The progress constraint is a gradient constraint on certain lower dimensional faces.

The progress constraint imposed on  $\tau$  is a gradient constraint on certain edges of the front  $\tau$ . For every local minimum vertex  $p$  of the front  $\tau$ , the progress constraint limits the gradient of the edges of  $\text{link}(p)$ . Figure 2.2 is the *vector diagram* that indicates the progress constraint imposed on a single triangle of the front  $\tau$ .

**INTERPRETING THE VECTOR DIAGRAM** Consider a single triangle  $PQR$  of the front  $\tau$ . Let  $pqr$  be the spatial projection of  $\triangle PQR$ . Triangle  $PQR$  defines a plane in spacetime which is the graph of the linear function  $\tau|_{pqr} : \mathbb{E}^2 \rightarrow \mathbb{R}$ . The gradient of  $\tau|_{pqr}$ , denoted by  $\nabla \tau|_{pqr}$  is a vector in  $\mathbb{R}^2$ . The direction of  $\nabla \tau|_{pqr}$  is the direction of steepest ascent along the plane of  $\triangle PQR$  and its magnitude is the slope of this plane.

Figure 2.2 shows the spatial projection  $\triangle pqr$  on the left and the vector space  $\mathbb{R}^2$  on the right. A vector in  $\mathbb{R}^2$  can be indicated by an arrow with its tail at the origin. In Figure 2.2, we simplify the depiction of vectors and indicate a vector by a point representing where the head of the arrow would be.

Triangle  $PQR$  is causal if and only if the point representing  $\nabla \tau|_{pqr}$  lies strictly inside the disk centered at the origin with radius equal to  $\sigma(PQR)$ . In Figure 2.2, we indicate the global slope  $\sigma$  by a disk centered at the origin with radius  $\sigma$ .

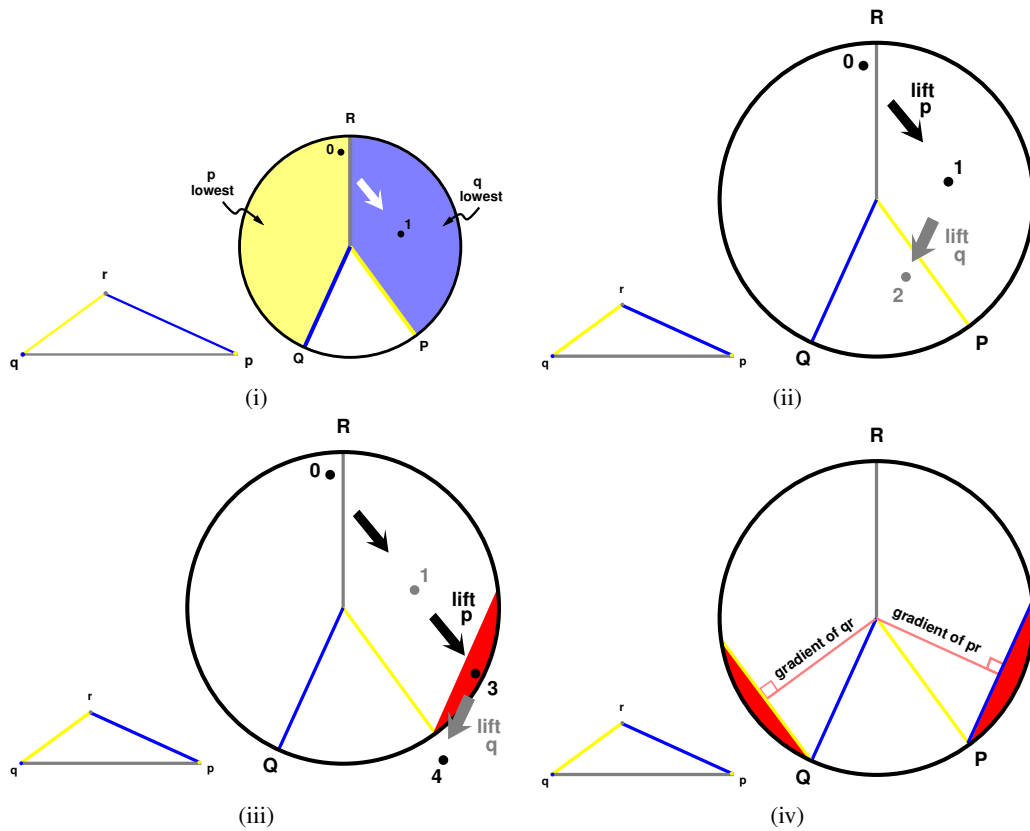


Figure 2.2: Vector diagram: Triangle  $PQR$  is causal if its gradient vector is inside the circular disc of radius  $\sigma$ . To ensure progress in the *next* step, the gradient vector must also lie outside the shaded red region. [Damrong Guoy, personal communication]

Suppose we advance  $P$  to  $P'$  giving the triangle  $P'QR$  of a new front  $\tau'$ . Lifting  $P$  keeps the gradient along  $\text{aff } qr$  unchanged, i.e.,  $\tau'|_{\text{aff } qr} = \tau|_{\text{aff } qr}$ , while increasing the magnitude of the component orthogonal to  $qr$  in the direction of  $p$ .

Vectors  $\mathbf{OP}$ ,  $\mathbf{OQ}$ , and  $\mathbf{OR}$  in Figure 2.2 are orthogonal to  $qr$ ,  $pr$ , and  $pq$  respectively and oriented in the direction of the third vertex in each case. These three normal vectors subdivide  $\mathbb{R}^2$  into three zones. Each zone is identified with a vertex of  $\triangle pqr$  because whenever  $\nabla \tau|_{pqr}$  lies in that zone the corresponding vertex is a local minimum vertex of  $\triangle PQR$ . For instance, if the gradient vector  $\nabla \tau|_{pqr}$  lies in zone  $p$ , bounded by the vectors  $\mathbf{OQ}$  and  $\mathbf{OR}$ , then  $\tau(p) \leq \tau(q)$  and  $\tau(p) \leq \tau(r)$ .

Consider the situation depicted in Figure 2.2(i). Points 0 and 1 indicate respectively the gradient vector of  $\triangle PQR$  where  $p$  is a local minimum vertex and the gradient vector of  $\triangle P'QR$  after pitching  $P$  to  $P'$  so that  $q$  is the new local minimum vertex. When  $P$  is pitched to  $P'$ , the gradient vector advances from 0 to 1 in the direction  $\mathbf{OP}$ . Advancing from point 0 to point 1 represents positive progress because both points are inside the disk (the corresponding triangles are causal) and  $p$  is no longer a local minimum.

Figure 2.2(ii) indicates the possible situation in the next iteration of the algorithm when the new local minimum  $Q$  is advanced—the gradient vector makes positive progress along direction  $\mathbf{OQ}$  from point 1 to point 2. If the algorithm is too greedy and advances from point 0 to point 3 in the current step, as shown in Figure 2.2(iii), then sufficient progress cannot be guaranteed in the next step because the gradient vector may leave the disk (point 4) and violate causality. Therefore, it is necessary to ensure the gradient vector of  $\triangle P'QR$  does not enter the shaded forbidden zone shown in Figure 2.2(iii). The forbidden zone in Figure 2.2(iii) limits the magnitude of the gradient of the edge  $pr$  on the new front  $\tau'$ , i.e., it imposes an upper bound on  $\tau'(p) - \tau(r)$ .

Symmetrically, when the local minimum  $q$  is pitched from  $Q$  to  $Q'$ , there is a corresponding forbidden zone that limits the slope of the edge  $Q'R$ . See Figure 2.2(iv).

Note that the forbidden zones (and therefore the progress constraint) depends solely on the shape and orientation of  $\triangle pqr$  and is invariant with respect to uniform scaling.

### 2.3.2 Progressive fronts in $2D \times \text{Time}$

Advancing a vertex  $p$  in time increases the gradient of simplices in  $\text{star}(p)$  but leaves unchanged the gradient of the lower-dimensional simplices in  $\text{link}(p)$ . For each face  $f \in \text{link}(p)$ , the gradient of the front in a direction orthogonal to  $f$  increases. Our algorithm advances an arbitrary local minimum vertex  $p$  of each front  $\tau$  to get a new front  $\tau'$ . The new front  $\tau'$  after advancing  $p$  is causal if and only if the gradient of  $f$  is strictly less than the slope of the causal cone constraint that limits the gradient of the simplex  $F \supset f$  such that  $F \in \text{star}(p)$ .

**Lemma 2.4.** *Let  $\triangle PQR$  be a triangle of the causal front  $\tau$  with  $P$  as its lowest vertex. Without loss of generality, assume  $\tau(p) \leq \tau(q) \leq \tau(r)$ . Let  $\sigma > 0$  be a slope such that  $\sigma \leq 1/\omega(PQR)$  and let  $d_p$  denote  $\text{dist}(p, \text{aff } qr)$ . Let  $\varepsilon$  be any real number in the range  $0 < \varepsilon < 1$ . Consider two cases:*

1. **Case  $\angle pqr \leq \pi/2$ :** *If  $\|\nabla \tau|_{qr}\| \leq (1 - \varepsilon)\sigma$ , then the front  $\tau' = \text{advance}(\tau, p, \Delta t)$  satisfies  $\|\nabla \tau'\| < \sigma$  for every  $\Delta t \in [0, \varepsilon d_p \sigma]$ .*
2. **Case  $\pi/2 < \angle pqr < \pi$ :** *If  $\|\nabla \tau|_{qr}\| \leq (1 - \varepsilon)\sigma \sin \angle pqr$ , then the front  $\tau' = \text{advance}(\tau, p, \Delta t)$  satisfies  $\|\nabla \tau'\| < \sigma$  for every  $\Delta t \in [0, \varepsilon d_p \sigma]$ .*

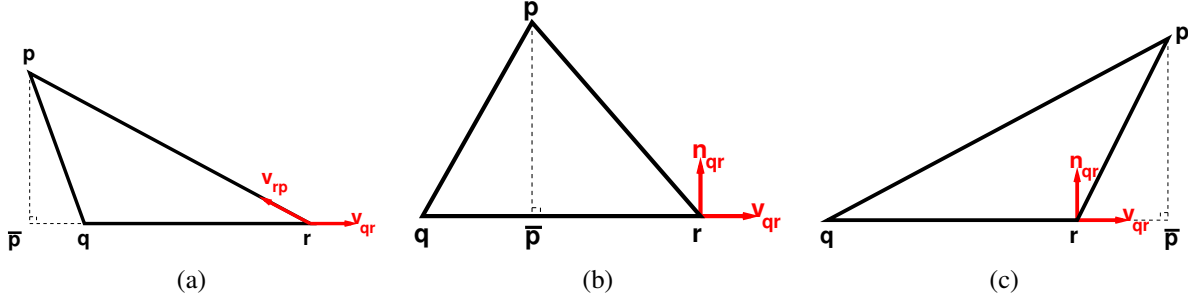


Figure 2.3: Triangle  $pqr$  of the front  $\tau$  where  $\tau(p) \leq \tau(q) \leq \tau(r)$

*Proof of Lemma 2.4.* Let  $\bar{p}$  be the orthogonal projection of  $p$  onto the line  $\text{aff } qr$ .

As long as  $\tau'(p) \leq \tau(q)$ , we have  $\|\nabla \tau'\| \leq \|\nabla \tau\|$  and the statement of the lemma follows. Hence, for the rest of this proof, assume  $\tau'(p) > \tau(q)$ .

Let  $\mathbf{n}_{qr}$  denote the unit vector normal to  $qr$  such that  $\mathbf{n}_{qr} \cdot (\mathbf{p} - \mathbf{q}) > 0$ . Let  $\mathbf{v}_{qr}$  be the unit vector parallel to  $qr$  such that  $\mathbf{v}_{qr} \cdot (\mathbf{r} - \mathbf{q}) > 0$ . Then,  $\{\mathbf{n}_{qr}, \mathbf{v}_{qr}\}$  form a basis for the vector space  $\mathbb{R}^2$ .

Lifting  $p$  does not change the gradient of the time function restricted to the opposite edge, so  $\nabla \tau' \cdot \mathbf{v}_{qr} = \nabla \tau \cdot \mathbf{v}_{qr}$ , i.e.,  $\nabla \tau'|_{qr} = \nabla \tau|_{qr}$ . The scalar product  $\nabla \tau' \cdot \mathbf{n}_{qr}$  can be written as

$$\nabla \tau' \cdot \mathbf{n}_{qr} = \frac{\tau'(p) - \tau(\bar{p})}{|p\bar{p}|}$$

Since  $q$  is the lowest vertex of  $qr$ , we have  $\nabla \tau' \cdot \mathbf{v}_{qr} \geq 0$ . Also, we are given that  $\nabla \tau \cdot \mathbf{v}_{qr} \leq (1 - \varepsilon)\sigma < \sigma$ . Note that  $\|\nabla \tau\| \leq \nabla \tau \cdot \mathbf{v}_{qr}$ . Therefore,  $\|\nabla \tau'\| < \sigma$  if and only if

$$\boxed{\frac{\tau'(p) - \tau(\bar{p})}{|p\bar{p}|} < \sqrt{\sigma^2 - \|\nabla \tau|_{qr}\|^2}} \quad (2.2)$$

**Case 1:  $\angle pqr$  is non-obtuse.** See Figure 2.3(b)–(c). In this case, we have  $\tau(\bar{p}) \geq \tau(q) \geq \tau(p)$ . We have

$$\tau'(p) = \tau(p) + \Delta t \leq \tau(\bar{p}) + \Delta t \leq \tau(\bar{p}) + \varepsilon\sigma|p\bar{p}|$$

Since  $0 < \varepsilon < 1$  we have  $\varepsilon < \sqrt{1 - (1 - \varepsilon)^2}$ . Therefore,

$$\tau'(p) < \tau(\bar{p}) + \sqrt{1 - (1 - \varepsilon)^2} \sigma|p\bar{p}| = \tau(\bar{p}) + \sqrt{\sigma^2 - (1 - \varepsilon)^2 \sigma^2} |p\bar{p}|$$

Since  $\|\nabla \tau|_{qr}\| \leq (1 - \varepsilon)\sigma$ , we have

$$\tau'(p) < \tau(\bar{p}) + |p\bar{p}| \sqrt{\sigma^2 - \|\nabla \tau|_{qr}\|^2}$$

which is precisely the causality constraint of Equation 2.2.

**Case 2:  $\angle pqr$  is obtuse.** See Figure 2.3(a). In this case, we have  $\tau(\bar{p}) < \tau(q)$ .

Let  $\beta = |\bar{p}q|/|p\bar{p}|$ . Since  $|\bar{p}q| \neq 0$ , we have

$$\frac{\tau'(p) - \tau(\bar{p})}{|p\bar{p}|} = \frac{\tau'(p) - \tau(q)}{|p\bar{p}|} + \frac{\tau(q) - \tau(\bar{p})}{|\bar{p}q|} \frac{|\bar{p}q|}{|p\bar{p}|} = \frac{\tau'(p) - \tau(q)}{|p\bar{p}|} + \beta \|\nabla \tau|_{qr}\| \quad (2.3)$$

Using Equation 2.3, the causality constraint (Equation 2.2) can be rewritten as

$$\frac{\tau'(p) - \tau(q)}{|p\bar{p}|} < \sqrt{\sigma^2 - \|\nabla \tau|_{qr}\|^2} - \beta \|\nabla \tau|_{qr}\| \quad (2.4)$$

We are given that  $\|\nabla \tau|_{qr}\| \leq (1 - \varepsilon)\sigma \sin \angle pqr$ . Substituting this upper bound on  $\|\nabla \tau|_{qr}\|$  into Equation 2.4, we obtain the following constraint:

$$\frac{\tau'(p) - \tau(q)}{|p\bar{p}|} < \sigma \left( \sqrt{1 - (1 - \varepsilon)^2 \sin^2 \angle pqr} \right) - \sigma(1 - \varepsilon)\beta \sin \angle pqr \quad (2.5)$$

which implies the causality constraint of Equation 2.4. Since  $\tau(p) \leq \tau(q)$  and  $\tau'(p) \leq \tau(p) + \varepsilon\sigma|p\bar{p}|$ , we have

$$\frac{\tau'(p) - \tau(q)}{|p\bar{p}|} \leq \frac{\tau'(p) - \tau(p)}{|p\bar{p}|} \leq \frac{\varepsilon\sigma|p\bar{p}|}{|p\bar{p}|} = \varepsilon\sigma.$$

Equation 2.5 is satisfied if

$$\varepsilon < \sqrt{1 - (1 - \varepsilon)^2 \sin^2 \angle pqr} - (1 - \varepsilon)\beta \sin \angle pqr$$

or equivalently

$$(\varepsilon + (1 - \varepsilon)\beta \sin \angle pqr)^2 + (1 - \varepsilon)^2 \sin^2 \angle pqr < 1$$

Let  $\lambda$  denote the left-hand side of the last inequality above.

We have

$$\begin{aligned} \lambda &= (\varepsilon + (1 - \varepsilon)\beta \sin \angle pqr)^2 + (1 - \varepsilon)^2 \sin^2 \angle pqr \\ &= \varepsilon^2 + (1 - \varepsilon)^2 \beta^2 \sin^2 \angle pqr + 2\varepsilon(1 - \varepsilon)\beta \sin \angle pqr + (1 - \varepsilon)^2 \sin^2 \angle pqr \\ &= \varepsilon^2 + (1 - \varepsilon)^2 (\beta^2 + 1) \sin^2 \angle pqr + 2\varepsilon(1 - \varepsilon)\beta \sin \angle pqr \end{aligned}$$

Note that

$$\beta^2 + 1 = \frac{|\bar{p}q|^2 + |p\bar{p}|^2}{|p\bar{p}|^2} = \frac{|pq|^2}{|p\bar{p}|^2}$$

by Pythagoras' theorem applied to  $\triangle puq$ . Also,  $\sin \angle pqr = |p\bar{p}|/|pq|$ . Hence,

$$(\beta^2 + 1) \sin^2 \angle pqr = 1.$$

Additionally,

$$\beta \sin \angle pqr = \frac{|\bar{p}q|}{|p\bar{p}|} \frac{|p\bar{p}|}{|pq|} = -\cos \angle pqr$$

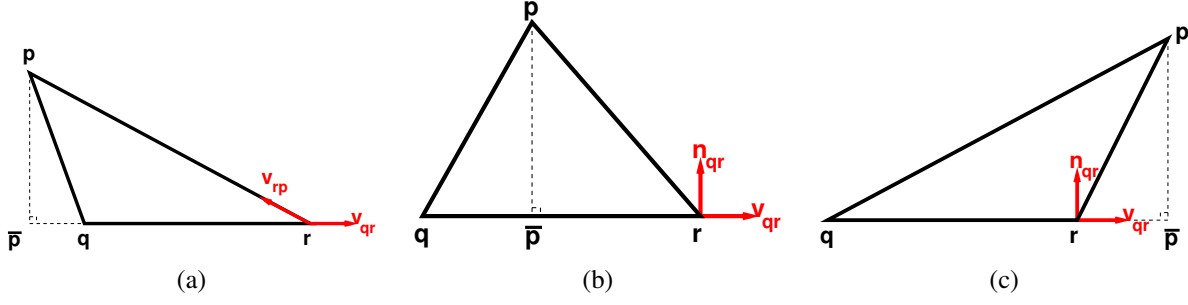


Figure 2.4: Triangle  $pqr$  with (a)  $\angle pqr$  obtuse, so  $\phi_{qr} = \sin \angle pqr < 1$ ,  $\phi(pqr) = \phi_{qr}$ ; (b)  $\angle pqr$  and  $\angle prq$  acute, so  $\phi_{qr} = 1$ ,  $\phi(pqr) = \sin \angle rqp < 1$ ; and (c)  $\angle prq$  obtuse, so  $\phi_{qr} = \sin \angle qrp < 1$ ,  $\phi(pqr) = \phi_{qr}$

Therefore,

$$\begin{aligned}
\lambda &= \varepsilon^2 + (1 - \varepsilon)^2 - 2\varepsilon(1 - \varepsilon) \cos \angle pqr \\
&= \varepsilon^2 + 1 + \varepsilon^2 - 2\varepsilon - 2\varepsilon(1 - \varepsilon) \cos \angle pqr \\
&= 1 + 2\varepsilon^2 - 2\varepsilon - 2\varepsilon(1 - \varepsilon) \cos \angle pqr \\
&= 1 - 2\varepsilon(-\varepsilon + 1 + (1 - \varepsilon) \cos \angle pqr) \\
&= 1 - 2\varepsilon(1 - \varepsilon)(1 + \cos \angle pqr) \\
&< 1
\end{aligned}$$

The last inequality follows because  $\triangle pqr$  is non-degenerate, so  $\cos \angle pqr \neq -1$ ; also, both  $\varepsilon$  and  $(1 - \varepsilon)$  are positive. Therefore, the causality constraint is satisfied.  $\square$

The progress constraint in  $2D \times \text{Time}$  is motivated by the Lemma 2.4 which states that if  $\triangle PQR$  is causal and satisfies progress constraint  $\sigma = 1/\omega(PQR)$  then  $\triangle P'QR$  obtained by advancing a lowest vertex  $P$  in time by  $\varepsilon \text{dist}(p, \text{aff } qr)$  is also causal.

For each simplex (an edge or a triangle)  $f$  in  $\text{star}(p) \cup \text{link}(p)$ , causality and the progress constraint limit the gradient of  $f$ , separately for each simplex  $f$ . Therefore, without loss of generality, we consider each such simplex  $f$  separately while defining and computing gradient constraints on  $f$ .

The progress constraint is parameterized by  $\varepsilon$  and a wavespeed  $\sigma$ . We are free to choose any value for  $\varepsilon$  in the allowed range. The bound on the gradient of  $\tau$  due to the progress constraint is proportional to the local geometry of the spatial projection of  $\tau$ .

**Definition 2.5.** For a triangle  $pqr$ , for any arbitrary edge of the triangle, say the edge  $qr$ , define  $\phi_{qr} := 1$  if both  $\angle pqr$  and  $\angle qrp$  are non-obtuse; otherwise let  $\phi_{qr}$  denote the sine of the obtuse angle of  $\triangle pqr$ , i.e.,  $\phi_{qr} := \max\{\sin \angle pqr, \sin \angle qrp\}$ . Define  $\phi(pqr)$  to be the minimum  $\phi_e$  over every edge  $e$  of the triangle. Note that  $0 < \phi(pqr) \leq 1$  and  $\phi(pqr) < 1$  if and only if  $\triangle pqr$  is obtuse (Figure 2.4).

**Definition 2.6** (Progress constraint  $\sigma$ ). Fix  $\varepsilon$  in the range  $0 < \varepsilon < 1$ . Let  $PQR$  be an arbitrary triangle of a front  $\tau$ . We say that the triangle  $PQR$  satisfies progress constraint  $\sigma$  if and only if for every lowest vertex  $P$ , equivalently for every highest edge  $QR$ , we have

$$\|\nabla \tau|_{qr}\| := \frac{\tau(r) - \tau(q)}{|qr|} \leq (1 - \varepsilon)\sigma\phi_{qr}.$$

**Input:** A bounded interval  $M \subset \mathbb{R}$   
 Fix  $\varepsilon \in (0, 1)$ , a parameter to the algorithm

**Output:** A triangular mesh  $\Omega$  of  $M \times [0, \infty)$

The initial front  $\tau_0$  is  $M \times \{0\}$ , corresponding to time  $t = 0$  everywhere in space.

Repeat the following sequence of steps for  $i = 0, 1, 2, \dots$ :

1. Advance in time an arbitrary local minimum vertex  $P = (p, \tau_i(p))$  of the current front  $\tau_i$  to  $P' = (p, \tau_{i+1}(p))$  such that  $\tau_{i+1}$  is *progressive* and  $\tau_{i+1}(p)$  is maximized.
2. Partition the spacetime volume between  $\tau$  and  $\tau_{i+1}$  into a patch of triangles, each sharing the tentpole edge  $PP'$ .
3. Call the numerical solver to compute the solution everywhere in the spacetime volume between  $\tau_i$  and  $\tau_{i+1}$  as well as the *a posteriori* error estimate. The solution on  $\tau_i$  is the inflow information to the solver and the solution on  $\tau_{i+1}$  is the outflow information.

---

Figure 2.5: Advancing front algorithm in  $2D \times \text{Time}$ .

We say that a triangle  $PQR$  is *progressive* if it satisfies progress constraint  $\sigma$ . We say that a front  $\tau$  is *progressive* if every triangle of  $\tau$  is progressive. Note that every progressive triangle or front is also causal.

Suppose a lowest vertex  $P$  is being advanced. As long as  $P$  is the lowest vertex of  $\triangle PQR$ , the progress constraint limits  $\|\nabla \tau'|_{qr}\|$  but  $\|\nabla \tau'|_{qr}\| = \|\nabla \tau|_{qr}\|$ . Assume without loss of generality that  $\tau(p) \leq \tau(q) \leq \tau(r)$ . When  $\tau'(p) > \tau(q)$ , the new lowest vertex is  $q$ , so the progress constraint limits  $\|\nabla \tau'|_{rp}\|$ . (We can interpret the progress constraint inductively as a causality constraint on the 1-dimensional facet  $pr$  opposite  $q$  where the relevant slope is  $(1 - \varepsilon)\sigma\phi_{rp}$ .)

In the parallel setting, we repeatedly choose an independent set of local minima of the front  $\tau_i$ , equal to the number of processors, to be advanced in time simultaneously. The resulting patches can be solved independently. If a patch is accepted, the local neighborhood of the front is advanced without any conflicts with other patches.

In subsequent sections, we will successively strengthen the progress constraint and correspondingly strengthen our notion of progressive fronts. When we refer to a front  $\tau$  simply as a progressive front, we will implicitly understand this to mean that  $\tau$  is causal and  $\tau$  satisfies the progress constraint as defined in the most recent definition.

The value of  $\tau_{i+1}(p)$  is constrained from above by causality and progress constraints separately for each of the simplices incident on  $p$ . The final value chosen by the algorithm must satisfy the constraints for each such triangle. Therefore, it is sufficient to consider each triangle  $pqr$  incident on  $p$  separately while deriving the causality and progress constraints that apply while pitching  $p$ .

The progress of the front at the  $(i+1)$ th step is defined to be  $\tau_{i+1}(p) - \tau_i(p)$ . We have already shown in Lemma 2.4 a lower bound on the amount of progress when subject to causality constraints alone. Next, we prove a lower bound on the amount of progress when subject to progress constraints alone. Thus, we obtain a lower bound on the worst-case amount of progress when subject to all causality and progress constraints simultaneously.

The next lemma states that if  $\triangle PQR$  is causal and satisfies progress constraint  $\sigma = 1/\omega(PQR)$  then  $\triangle P'QR$  obtained by advancing a lowest vertex  $P$  in time by  $(1 - \varepsilon)\phi(pqr) \text{dist}(p, \text{aff } qr)$  also satisfies progress constraint  $\sigma$ .



**Lemma 2.7.** Let  $PQR$  be a triangle of the causal front  $\tau$  with  $P$  as its lowest vertex. Let  $\sigma > 0$  denote a slope and let  $d_p$  denote  $\text{dist}(p, \text{aff}qr)$ . Let  $\varepsilon$  be any real number in the range  $0 < \varepsilon < 1$ .

If  $\triangle PQR$  satisfies progress constraint  $\sigma$ , then for every  $\Delta t \in [0, (1 - \varepsilon)\sigma d_p]$  the front  $\tau' = \text{advance}(\tau, p_0, \Delta t)$  satisfies progress constraint  $\sigma$ .

*Proof of Lemma 2.7.* By Definition 2.6, the front  $\tau'$  satisfies progress constraint  $\sigma$  if and only if

$$\begin{aligned}\|\nabla \tau'|_{pq}\| &\leq (1 - \varepsilon)\phi_{pq}\sigma \\ \|\nabla \tau'|_{qr}\| &\leq (1 - \varepsilon)\phi_{qr}\sigma \\ \|\nabla \tau'|_{rp}\| &\leq (1 - \varepsilon)\phi_{rp}\sigma\end{aligned}$$

Since  $\triangle PQR$  satisfies progress constraint  $\sigma$ , we have

$$\begin{aligned}\|\nabla \tau\|_{pq}\| &\leq (1 - \varepsilon)\phi_{pq}\sigma \\ \|\nabla \tau\|_{qr}\| &\leq (1 - \varepsilon)\phi_{qr}\sigma \\ \|\nabla \tau\|_{rp}\| &\leq (1 - \varepsilon)\phi_{rp}\sigma\end{aligned}$$

Also,  $p$  is a lowest vertex of  $\tau$ ; so  $\tau(p) \leq \min\{\tau(q), \tau(r)\}$ .

Since advancing  $p$  in time does not change the time function along  $qr$ , we have  $\|\nabla \tau'\|_{qr} = \|\nabla \tau\|_{qr} \leq (1 - \varepsilon)\phi_{qr}\sigma$ .

Consider the constraint  $\|\nabla \tau'\|_{pq} \leq (1 - \varepsilon)\phi_{pq}\sigma$ . As long as  $\tau'(p) \leq \tau(q)$ , we have  $\|\nabla \tau'\|_{pq} \leq \|\nabla \tau\|_{pq} \leq (1 - \varepsilon)\phi_{pq}\sigma$ . Similarly, as long as  $\tau'(p) \leq \tau(r)$ , the constraint  $\|\nabla \tau'\|_{rp} \leq (1 - \varepsilon)\phi_{rp}\sigma$  is automatically satisfied because  $\|\nabla \tau'\|_{rp} \leq \|\nabla \tau\|_{rp} \leq (1 - \varepsilon)\phi_{rp}\sigma$ .

When  $\tau'(p) > \tau(q)$ , the constraint  $\|\nabla \tau'\|_{pq} \leq (1 - \varepsilon)\phi_{pq}\sigma$  is equivalent to  $\tau'(p) \leq \tau(q) + |pq|(1 - \varepsilon)\phi_{pq}\sigma$ . We have

$$\begin{aligned}\tau'(p) &\leq \tau(p) + (1 - \varepsilon)\sigma d_p \\ &\leq \tau(q) + (1 - \varepsilon)\sigma \min\{|pq|, |pr|\}\phi_{qr} \\ &\leq \tau(q) + (1 - \varepsilon)\phi_{pq}\sigma |pq| \\ &\leq \tau(q) + (1 - \varepsilon)\phi(pqr)\sigma |pq|\end{aligned}$$

The last inequality follows because  $\phi(pqr) \leq \phi_{pq}$ .

Similarly, when  $\tau'(p) > \tau(r)$ , the constraint  $\|\nabla \tau'\|_{rp} \leq (1 - \varepsilon)\phi_{rp}\sigma$  is equivalent to  $\tau'(p) \leq \tau(r) + (1 - \varepsilon)\phi_{rp}\sigma |pr|$ . We have

$$\begin{aligned}\tau'(p) &\leq \tau(p) + (1 - \varepsilon)\sigma d_p \\ &\leq \tau(r) + (1 - \varepsilon)\sigma \min\{|pq|, |pr|\}\phi_{rp} \\ &\leq \tau(r) + (1 - \varepsilon)\phi_{rp}\sigma |rp| \\ &\leq \tau(r) + (1 - \varepsilon)\phi(pqr)\sigma |rp|\end{aligned}$$

□

Note that we have in fact proved the following two statements that imply Lemmas 2.4 and 2.7.

Let  $\triangle PQR$  be a triangle of the front  $\tau$  with  $P$  as one of its lowest vertices. Without loss of generality, assume  $\tau(p) \leq \tau(q) \leq \tau(r)$ . Let  $\varepsilon$  be any real number in the range  $0 < \varepsilon < 1$ . Let  $\sigma > 0$  be any slope.

1. If  $\|\nabla \tau|_{qr}\| \leq (1 - \varepsilon)\sigma\phi_{qr}$ , then  $\triangle P'QR$  satisfies  $\|\nabla \tau'\| < \sigma$  for every  $\tau'(p)$  in the range  $\tau(q) \leq \tau'(p) \leq \tau(q) + \varepsilon\sigma\text{dist}(p, \text{aff } qr)$ .
2.  $\triangle P'QR$  satisfies

$$\|\nabla \tau'|_{pq}\| \leq (1 - \varepsilon)\sigma\phi_{pq} \quad \text{and} \quad \|\nabla \tau'|_{pr}\| \leq (1 - \varepsilon)\sigma\phi_{pr}$$

for every  $\tau'(p)$  in the range  $\tau(q) \leq \tau'(p) \leq \tau(q) + (1 - \varepsilon)\sigma \min\{|pq|, |pr|\}$ .

The above claims are stronger than Lemmas 2.4 and 2.7 because we do not assume that  $\triangle PQR$  and the front  $\tau$  is progressive.

As a corollary to Lemmas 2.4 and 2.7, we conclude a positive lower bound on the minimum tentpole height, similar to that obtained by Erickson *et al.* (EGSÜ02) in the nonadaptive case when the wavespeed everywhere is a fixed constant  $\omega$ . Let  $\sigma$  denote the causal slope.

**Corollary 2.8.** *Let  $\tau$  be a causal front. Let  $\varepsilon$  be any real number in the range  $0 < \varepsilon < 1$ . If every triangle  $\triangle PQR$  of  $\tau$  satisfies progress constraint  $\sigma$ , then, for any local minimum  $p$  of  $\tau$ , the front  $\tau' = \text{advance}(\tau, p, \Delta t)$  is causal and satisfies the progress constraint  $\sigma$  for every  $\Delta t \in [0, \min\{\varepsilon, (1 - \varepsilon)\}w_p\sigma]$ .*

*Proof of Corollary 2.8.* Causality and progress constraints apply to each triangle  $PQR$  of the front incident on  $P$ . We show that each constraint individually guarantees a positive lower bound of  $\min\{\varepsilon, (1 - \varepsilon)\}w_p\sigma$  on the height  $\tau'(p) - \tau(p)$  of the height of the tentpole at  $p$ . Therefore, all the constraints together ensure a tentpole height of at least as much.

Applying Lemma 2.4 to each triangle  $PQR$ , we conclude that the front  $\tau'$  is causal for every  $\Delta t \in [0, \varepsilon w_p\sigma]$ .

Consider an arbitrary triangle  $PQR$  incident on  $P$ . Advancing  $p$  in time does not change the gradient of the front along  $qr$ . Therefore, the gradient of the new front is limited only along  $pq$  and  $pr$  by the progress constraint. By Lemma 2.4, we conclude that each of the gradient constraints along  $pq$  and  $pr$  guarantee a tentpole height of at least  $(1 - \varepsilon)\text{dist}(p, \text{aff } qr)\sigma$ . Applying Lemma 2.4 to each triangle  $PQR$ , we conclude that the front  $\tau'$  satisfies the progress constraint  $\sigma$  for every  $\Delta t \in [0, (1 - \varepsilon)w_p\sigma]$ .  $\square$

**Theorem 2.9.** *For any  $i \geq 0$ , if the front  $\tau_i$  is progressive then  $\tau_i$  is valid.*

*Proof of Theorem 2.9.* The proof is identical to that of Theorem 2.3 and follows because we choose  $\varepsilon > 0$  so that  $T_{\min} > 0$  is bounded away from zero.  $\square$

We thus have the following theorem.

**Theorem 2.10.** *Given a triangulation  $M$  of a bounded planar space domain where  $w_{\min}$  is the minimum width of a simplex of  $M$  and  $\sigma$  is the minimum slope anywhere in  $M \times [0, \infty)$ , for every  $\varepsilon$  such that  $0 < \varepsilon < 1$  our algorithm constructs a simplicial mesh of  $M \times [0, T]$  consisting of at most  $\left\lceil \frac{n(T + \text{diam}(M)\sigma)}{\min\{\varepsilon, 1 - \varepsilon\}\sigma w_{\min}} \Delta \right\rceil$  spacetime elements for every real  $T \geq 0$  in constant computation time per element, where  $\Delta$  is the maximum vertex degree.*

*Proof of Theorem 2.10.* By Lemmas 2.4 and 2.7, it follows that the height of each tentpole constructed by the algorithm is at least  $T_{\min} = \min\{\varepsilon, 1 - \varepsilon\}\sigma w_{\min}$ . By Theorem 2.9, after constructing at most  $k \leq \left\lceil \frac{n(T + \text{diam}(M)\sigma)}{T_{\min}} \right\rceil$  patches, the entire front  $\tau_k$  is past the target time  $T$ . Since each patch consists of at most  $\Delta$  elements, where  $\Delta$  is the maximum number of simplices in the star of any vertex of  $M$ , the theorem follows.  $\square$

## 2.4 Meshing in arbitrary dimensions $d\mathbf{D} \times \mathbf{Time}$

For spatial dimension  $d \geq 3$ , we prove results analogous to those in Section 2.3. For each front  $\tau_i$ , causality limits the gradient of 1-dimensional simplices, and causality and progress constraints together limit the gradient of  $k$ -dimensional simplices for each  $2 \leq k \leq d$ .

Pitching vertex  $p_0$ , a local minimum of the front  $\tau$ , alters the gradient of all faces of  $\text{star}(p_0)$  of all dimensions and each of these faces limits the progress of  $p_0$  in time because of causality and progress constraints on their gradient in time. Our objective is to impose gradient constraints on each  $k$ -dimensional simplex such that each constraint individually guarantees a minimum positive progress in time for  $p_0$ . Hence, all these gradient constraints taken together also imply positive progress which in turn implies a lower bound on the height and therefore the temporal aspect ratio of each spacetime element.

Fix  $\varepsilon \in (0, 1)$ . The progress constraint is parameterized by  $\varepsilon$  and the wavespeed  $\sigma$ . We are free to choose any value for  $\varepsilon$  in the allowed range.

Consider an arbitrary  $k$ -dimensional face  $P_0P_1P_2 \dots P_k$  incident on a vertex  $P_0$  of a front  $\tau$  where  $2 \leq k \leq d$ . Let  $p_0p_1p_2 \dots p_k$  denote the spatial projection of this simplex. The extent to which progress constraint  $\sigma$  limits the gradient of  $P_0P_1P_2 \dots P_k$ , i.e., the gradient of the time function  $\tau$  restricted to  $P_0P_1P_2 \dots P_k$ , depends on the geometry of the simplex  $p_0p_1p_2 \dots p_k$  in space.

For each integer  $i$  such that  $0 \leq i \leq k$ , let  $\Delta_i$  denote the facet  $p_0p_1p_2 \dots p_{i-1}p_{i+1} \dots p_k$  opposite  $p_i$ , let  $\bar{p}_i$  denote the orthogonal projection of  $p_i$  onto  $\text{aff}\Delta_i$ , let  $u_i$  denote the point of  $\Delta_i$  closest to  $\bar{p}_i$ , and let  $\theta_i$  denote  $\angle p_i u_i \bar{p}_i$ . We say that the simplex  $p_0p_1p_2 \dots p_k$  is *obtuse* if  $\bar{p}_i \notin \Delta_i$  for some  $i$ .

**Definition 2.11.** For the  $k$ -dimensional simplex  $p_0p_1p_2 \dots p_k$  define

$$\phi(p_0p_1p_2 \dots p_k) := \min_{0 \leq i \leq k} \{ \sin \theta_i \}$$

As in  $2\mathbf{D} \times \mathbf{Time}$ , there are two key lemmas in higher dimensions that imply a lower bound on the worst-case height of any tentpole. Lemma 2.12 was proved implicitly in the paper by Erickson *et al.* (EGSÜ02) but was applied only to the case of constant wavespeed.

The first lemma states that if  $P_0P_1P_2 \dots P_k$  is causal and satisfies progress constraint  $\sigma$  then  $P'_0P_1P_2 \dots P_k$  obtained by advancing a lowest vertex  $P'_0$  in time by  $\varepsilon\sigma \text{dist}(p_0, \text{aff } p_1p_2 \dots p_k)$  is also causal.

**Lemma 2.12.** Let  $P_0P_1P_2 \dots P_k$  be any  $k$ -dimensional simplex of the causal front  $\tau$  for arbitrary  $1 \leq k \leq d$  with  $P_0$  as its lowest vertex. Let  $\bar{p}_0$  denote the orthogonal projection of  $p_0$  onto  $\text{aff } p_1p_2 \dots p_k$ . Let  $\sigma > 0$  be a slope such that  $\sigma \leq 1/\omega(P_0P_1P_2 \dots P_k)$  and let  $d_{p_0}$  denote  $\text{dist}(p_0, \text{aff } p_1p_2 \dots p_k) = |p_0\bar{p}_0|$ . Let  $\varepsilon$  be any real number in the range  $0 < \varepsilon < 1$ . Consider two cases:

1. Case  $\bar{p}_0 \in \mathbf{p}_1\mathbf{p}_2 \dots \mathbf{p}_k$  : If  $\|\nabla \tau|_{p_1p_2 \dots p_k}\| \leq (1 - \varepsilon)\sigma$ , then, for every  $\Delta t \in [0, \varepsilon d_{p_0} \sigma]$ , the front  $\tau' = \text{advance}(\tau, p_0, \Delta t)$  satisfies  $\|\nabla \tau'|_{p_0p_1p_2 \dots p_k}\| < \sigma$ .
2. Case  $\bar{p}_0 \notin \mathbf{p}_1\mathbf{p}_2 \dots \mathbf{p}_k$  : Let  $u$  denote the point of the facet  $p_1p_2 \dots p_k$  closest to  $\bar{p}_0$ . If  $\|\nabla \tau|_{p_1p_2 \dots p_k}\| \leq (1 - \varepsilon)\sigma \sin \angle p_0 u \bar{p}_0$ , then, for every  $\Delta t \in [0, \varepsilon d_{p_0} \sigma]$ , the front  $\tau' = \text{advance}(\tau, p_0, \Delta t)$  satisfies  $\|\nabla \tau'|_{p_0p_1p_2 \dots p_k}\| < \sigma$ .

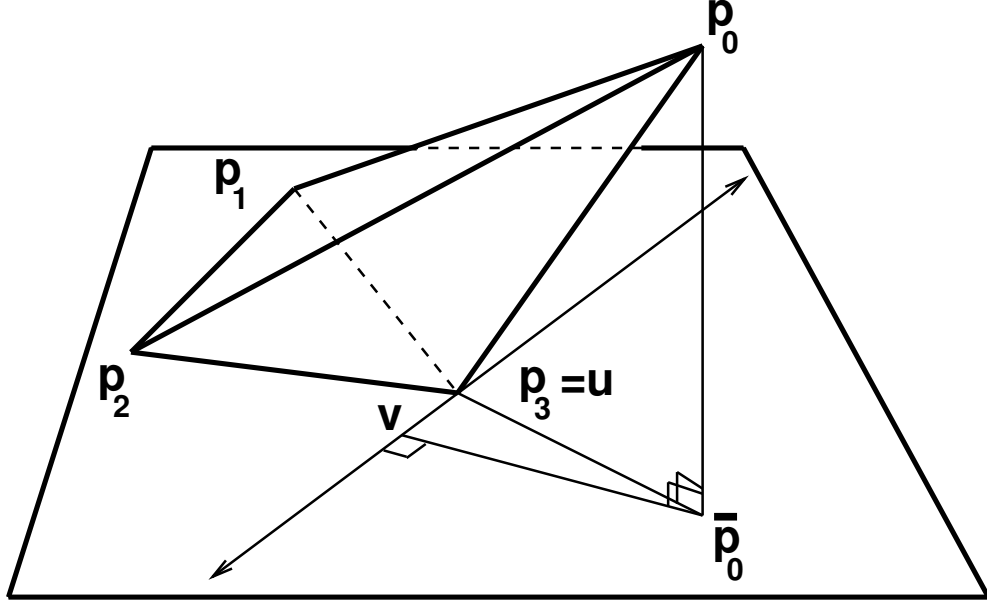


Figure 2.6: An obtuse tetrahedron with  $\bar{p}_0 \notin p_1p_2 \dots p_k$ .

*Proof of Lemma 2.12.* The constraint on  $P'_0P_1P_2 \dots P_k$  is equivalent to the following:

$$\frac{\tau'(p_0) - \tau(\bar{p}_0)}{|p_0\bar{p}_0|} < \sqrt{\sigma^2 - \|\nabla \tau|_{p_1p_2 \dots p_k}\|^2}$$

Without loss of generality, assume  $\tau(p_0) \leq \tau(p_1) \leq \tau(p_2) \leq \dots \leq \tau(p_k)$ .

**Case 1:**  $\bar{p}_0 \in p_1p_2 \dots p_k$ . In this case, we have  $\tau(\bar{p}_0) \geq \tau(p_1) \geq \tau(p_0)$ . Hence,

$$\frac{\tau'(p_0) - \tau(\bar{p}_0)}{|p_0\bar{p}_0|} \leq \frac{\tau'(p_0) - \tau(p_0)}{|p_0\bar{p}_0|}$$

Since  $\tau'(p_0) - \tau(p_0) \leq \varepsilon\sigma|p_0\bar{p}_0|$ , it suffices to show that

$$\varepsilon\sigma < \sqrt{\sigma^2 - \|\nabla \tau|_{p_1p_2 \dots p_k}\|^2}$$

Since  $\|\nabla \tau|_{p_1p_2 \dots p_k}\| \leq (1 - \varepsilon)\sigma$ , it suffices to show that

$$\varepsilon^2 < 1 - (1 - \varepsilon)^2$$

i.e.,

$$2\varepsilon^2 < 2\varepsilon$$

which is true whenever  $0 < \varepsilon < 1$ .

**Case 2:**  $\bar{p}_0 \notin p_1p_2 \dots p_k$ .

Note that  $u \neq \bar{p}_0$ , hence,  $|p_0\bar{p}_0|/|p_0u| = \sin \angle p_0u\bar{p}_0 < 1$ . We consider two sub-cases separately: (a)  $\tau(\bar{p}_0) \geq \tau(p_0)$  and (b)  $\tau(\bar{p}_0) < \tau(p_0)$ . See Figure 2.6.

Note that we could have merged case 2(a) with case 1; however, then the antecedent of the theorem would have depended on the current front  $\tau$ . This would have, in turn, complicated the implementation of the algorithm and the proof of the subsequent theorems.

**Case 2(a):**  $\tau(\bar{\mathbf{p}}_0) \geq \tau(\mathbf{p}_0)$ . In this case, since  $\tau(\bar{p}_0) \geq \tau(p_0)$ , we have

$$\frac{\tau'(p_0) - \tau(\bar{p}_0)}{|p_0\bar{p}_0|} \leq \frac{\tau'(p_0) - \tau(p_0)}{|p_0\bar{p}_0|}$$

Since  $\tau'(p_0) - \tau(p_0) \leq \varepsilon\sigma|p_0\bar{p}_0|$ , it suffices to show that

$$\varepsilon\sigma < \sqrt{\sigma^2 - \|\nabla \tau|_{p_1p_2\dots p_k}\|^2}$$

Since  $\|\nabla \tau|_{p_1p_2\dots p_k}\| \leq (1 - \varepsilon)\sigma \sin \angle p_0u\bar{p}_0 < (1 - \varepsilon)\sigma$ , it suffices to show that

$$\varepsilon^2 < 1 - (1 - \varepsilon)^2$$

i.e.,

$$2\varepsilon^2 < 2\varepsilon$$

which is true whenever  $0 < \varepsilon < 1$ .

**Case 2(b):**  $\tau(\bar{\mathbf{p}}_0) < \tau(\mathbf{p}_0)$ . In fact, we will handle this case with a potentially weaker antecedent than the one in the statement of the theorem. Let  $v$  denote the point of aff  $p_1p_2\dots p_k$  closest to  $\bar{p}_0$  among all points such that  $\tau(v) \geq \tau(p_0)$ . Since  $u \in p_1p_2\dots p_k$  we have  $\tau(\bar{p}) \geq \tau(p_0)$ ; hence,  $|\bar{p}_0v| \leq |\bar{p}_0u|$  and  $|p_0v| \leq |p_0u|$ . Hence,

$$\sin \angle p_0v\bar{p}_0 = \frac{|p_0\bar{p}_0|}{|p_0v|} \geq \frac{|p_0\bar{p}_0|}{|p_0u|} = \sin \angle p_0u\bar{p}_0 \quad (2.6)$$

We will prove the following statement which, by the inequality of Equation 2.6, implies the theorem:

If  $\|\nabla \tau|_{p_1p_2\dots p_k}\| \leq (1 - \varepsilon)\sigma \sin \angle p_0v\bar{p}_0$ , then, for every  $\Delta t \in [0, \varepsilon|p_0\bar{p}_0|\sigma]$ , the front  $\tau' = \text{advance}(\tau, p_0, \Delta t)$  satisfies  $\|\nabla \tau'|_{p_0p_1p_2\dots p_k}\| < \sigma$ .

Let  $\beta = |\bar{p}_0v|/|p_0\bar{p}_0|$ . By our choice of  $v$ ,  $\nabla \tau|_{p_1p_2\dots p_k}$  is a vector pointing in the direction from  $\bar{p}_0$  to  $v$ . Hence,

$$\frac{\tau'(p_0) - \tau(\bar{p}_0)}{|p_0\bar{p}_0|} = \frac{\tau'(p_0) - \tau(v)}{|p_0\bar{p}_0|} + \beta \|\nabla \tau|_{p_1p_2\dots p_k}\| \quad (2.7)$$

Using Equation 2.7, the constraint on  $P'_0P_1P_2\dots P_k$  can be rewritten as

$$\frac{\tau'(p_0) - \tau(v)}{|p_0\bar{p}_0|} < \sqrt{\sigma^2 - \|\nabla \tau|_{p_1p_2\dots p_k}\|^2} - \beta \|\nabla \tau|_{p_1p_2\dots p_k}\|$$

Now,

$$\frac{\tau'(p_0) - \tau(v)}{|p_0\bar{p}_0|} \leq \frac{\tau'(p_0) - \tau(p_0)}{|p_0\bar{p}_0|}$$

Since  $\tau'(p_0) - \tau(p_0) \leq \varepsilon\sigma|p_0\bar{p}_0|$ , it suffices to show that

$$\varepsilon\sigma < \sqrt{\sigma^2 - \|\nabla \tau|_{p_1p_2\dots p_k}\|^2} - \beta \|\nabla \tau|_{p_1p_2\dots p_k}\|$$

By the antecedent, we have  $\|\nabla \tau|_{p_1 p_2 \dots p_k}\| \leq (1 - \varepsilon)\sigma \sin \angle p_0 v \bar{p}_0$ . Hence, it suffices to show that

$$\varepsilon < \sqrt{1 - (1 - \varepsilon)^2 \sin^2 \angle p_0 v \bar{p}_0} - \beta (1 - \varepsilon) \sin \angle p_0 v \bar{p}_0$$

i.e.,

$$(\varepsilon + \beta (1 - \varepsilon) \sin \angle p_0 v \bar{p}_0)^2 < 1 - (1 - \varepsilon)^2 \sin^2 \angle p_0 v \bar{p}_0$$

i.e.,

$$\varepsilon^2 + (\beta (1 - \varepsilon) \sin \angle p_0 v \bar{p}_0)^2 + 2\beta \varepsilon (1 - \varepsilon) \sin \angle p_0 v \bar{p}_0 + (1 - \varepsilon)^2 \sin^2 \angle p_0 v \bar{p}_0 < 1$$

i.e.,

$$\varepsilon^2 + 2\varepsilon (1 - \varepsilon)\beta \sin \angle p_0 v \bar{p}_0 + (1 - \varepsilon)^2(\beta^2 + 1) \sin^2 \angle p_0 v \bar{p}_0 < 1$$

Note that

$$\begin{aligned} \beta^2 + 1 &= \frac{|\bar{p}_0 v|^2 + |p_0 \bar{p}_0|^2}{|p_0 \bar{p}_0|^2} \\ &= \frac{|p_0 v|^2}{|p_0 \bar{p}_0|^2} \end{aligned}$$

where the last equality follows by Pythagoras' theorem applied to  $\triangle p_0 \bar{p}_0 v$ . (See Figure 2.6.) Also,  $\sin \angle p_0 v \bar{p}_0 = |p_0 \bar{p}_0|/|p_0 v|$ . Hence,  $(\beta^2 + 1) \sin^2 \angle p_0 v \bar{p}_0 = 1$ .

Additionally,

$$\begin{aligned} \beta \sin \angle p_0 v \bar{p}_0 &= \frac{|\bar{p}_0 v|}{|p_0 \bar{p}_0|} \frac{|p_0 \bar{p}_0|}{|p_0 v|} \\ &= \cos \angle p_0 v \bar{p}_0 \end{aligned}$$

Therefore, it suffices to show that

$$\varepsilon^2 + 2\varepsilon (1 - \varepsilon) \cos \angle p_0 v \bar{p}_0 + (1 - \varepsilon)^2 < 1$$

Observe that  $\varepsilon^2 + 2\varepsilon (1 - \varepsilon) + (1 - \varepsilon)^2 = (\varepsilon + (1 - \varepsilon))^2 = 1$ . Therefore,

$$\varepsilon^2 + 2\varepsilon (1 - \varepsilon) \cos \angle p_0 v \bar{p}_0 + (1 - \varepsilon)^2 = 1 - 2\varepsilon (1 - \varepsilon) (1 - \cos \angle p_0 v \bar{p}_0)$$

Hence, it suffices to show that

$$1 - 2\varepsilon (1 - \varepsilon) (1 - \cos \angle p_0 v \bar{p}_0) < 1$$

Recall that  $\angle p_0 v \bar{p}_0$  is acute, so  $0 < \cos \angle p_0 v \bar{p}_0 < 1$ , i.e.,  $1 - \cos \angle p_0 v \bar{p}_0 > 0$ . Hence, the claim follows whenever  $0 < \varepsilon < 1$ .  $\square$

#### 2.4.1 Progress constraint for a $k$ -dimensional simplex

Motivated by Lemma 2.12, we derive progress constraints that are sufficient to ensure that the antecedent of Lemma 2.12 is satisfied in the *next* step by the front  $\tau'$ .

Consider an arbitrary  $k$ -dimensional face  $p_0 p_1 p_2 \dots p_k$  incident on  $p_0$  for any  $k$  in the range  $2 \leq k \leq d$ .

**Definition 2.13** (Progress constraint). *We say that a simplex  $P_0P_1P_2\dots P_k$  of the front  $\tau$  satisfies the progress constraint  $\sigma$  if and only if for every highest facet  $\Delta_i$  where  $0 \leq i \leq k$  we have  $\|\nabla \tau|_{\Delta_i}\| \leq (1 - \varepsilon)\phi(p_0p_1p_2\dots p_k)\sigma$ .*

Note that if  $P_0P_1P_2\dots P_k$  with  $P_0$  as its lowest vertex satisfies the progress constraint  $\sigma$  (Definition 2.13) then  $\|\nabla \tau|_{p_1p_2\dots p_k}\| \leq (1 - \varepsilon)\phi(p_0p_1p_2\dots p_k)\sigma$ .

**Lemma 2.14.** *Let  $P_0P_1P_2\dots P_k$  be any  $k$ -dimensional simplex of the causal front  $\tau$  for arbitrary  $2 \leq k \leq d$  with  $P_0$  as its lowest vertex. Let  $\phi$  denote  $\phi(p_0p_1p_2\dots p_k)$ . For each  $i$  with  $0 \leq i \leq k$ , let  $v_i$  denote the point of  $\text{aff}(\Delta_i \cap \Delta_0)$  closest to  $p_0$ .*

*If  $P_0P_1P_2\dots P_k$  satisfies progress constraint  $\sigma$ , then for every  $\Delta t \in [0, (1 - \varepsilon)\phi\sigma|v_i p_0|]$  the front  $\tau' = \text{advance}(\tau, p_0, \Delta t)$  satisfies  $\|\nabla \tau'|_{\Delta_i}\| \leq (1 - \varepsilon)\phi\sigma$  for every  $i$  such that  $0 \leq i \leq k$ .*

*Proof of Lemma 2.14.* Note that  $\tau'|_{\Delta_0} = \tau|_{\Delta_0}$ ; hence, the statement is trivial for  $i = 0$ .

Since  $P_0P_1P_2\dots P_k$  satisfies progress constraint  $\sigma$ , by Definition 2.13, we have  $\|\nabla \tau|_{\Delta_i}\| \leq (1 - \varepsilon)\phi\sigma$  for every  $i$  such that  $0 \leq i \leq k$ .

Consider an arbitrary  $i$  in the range  $1 \leq i \leq k$  such that  $\Delta_i$  is a highest facet.

Note that for every simplex  $f \in \text{link}(p_0)$ , the time function  $\tau$  restricted to  $\text{aff} f$  is unchanged by pitching  $p_0$ . Therefore, pitching  $p_0$  increases  $\nabla \tau|_{\Delta_i}$  in a direction orthogonal to  $\text{aff} \Delta_i \cap \Delta_0$  while keeping the component of  $\tau$  along  $\Delta_i \cap \Delta_0$  unchanged. Hence,

$$\|\nabla \tau'|_{\Delta_i}\| - \|\nabla \tau|_{\Delta_i}\| = \frac{\tau'(p_0) - \tau(p_0)}{|v_i p_0|}$$

Since  $\|\nabla \tau|_{\Delta_i}\| \geq 0$  and  $\tau'(p_0) \leq \tau(p_0) + (1 - \varepsilon)\phi\sigma|v_i p_0|$ , we have

$$\|\nabla \tau'|_{\Delta_i}\| \leq \frac{\tau'(p_0) - \tau(p_0)}{|v_i p_0|} \leq \frac{(1 - \varepsilon)\phi\sigma|v_i p_0|}{|v_i p_0|} = (1 - \varepsilon)\phi\sigma.$$

Therefore,  $P'_0P_1P_2\dots P_k$  satisfies the constraint in the statement of the lemma.  $\square$

Note that we have in fact proved the following two statements that imply Lemmas 2.12 and 2.14.

Let  $P_0P_1P_2\dots P_k$  be any  $k$ -dimensional simplex with  $P_0$  as its lowest vertex. Without loss of generality, assume  $\tau(p_0) \leq \tau(p_1) \leq \tau(p_2) \leq \dots \leq \tau(p_k)$ . For each  $i$  with  $0 \leq i \leq k$ , let  $v_i$  denote the point of  $\text{aff}(\Delta_i \cap \Delta_0)$  closest to  $p_0$ . Let  $\varepsilon$  be any real number in the range  $0 < \varepsilon < 1$ . Let  $\sigma > 0$  be any slope.

1. If  $\|\nabla \tau|_{p_1p_2\dots p_k}\| \leq (1 - \varepsilon)\sigma\phi(p_1p_2\dots p_k)$ , then  $P'_0P_1P_2\dots P_k$  satisfies  $\|\nabla \tau'|_{p_0p_1p_2\dots p_k}\| < \sigma$  for every  $\tau'(p_0)$  in the range  $\tau(p_1) \leq \tau'(p_0) \leq \tau(p_1) + \varepsilon\sigma\text{dist}(p_0, \text{aff} p_1p_2\dots p_k)$ .

2.  $P'_0P_1P_2\dots P_k$  satisfies

$$\forall i, 0 \leq i \leq k \quad \|\nabla \tau'|_{\Delta_i}\| \leq (1 - \varepsilon)\sigma\phi(\Delta_i)$$

for every  $\tau'(p_0)$  in the range  $\tau(p_1) \leq \tau'(p_0) \leq \tau(p_1) + (1 - \varepsilon)\sigma \min_{0 \leq i \leq k} \{|v_i p_0|\}$ .

The above claims are stronger than Lemmas 2.12 and 2.14 because we do not assume that  $P_0P_1P_2\dots P_k$  and the front  $\tau$  are progressive.

## 2.4.2 Combining constraints for all dimensions

Pitching vertex  $p$  alters the gradients of all faces of  $\text{star}(p)$  of all dimensions and each of these faces limits the progress of  $p$  in time. We interpret the progress constraints mentioned in the previous lemmas as gradient constraints on lower dimensional faces of the front. These gradient constraints are imposed simultaneously on all facets of dimension from 2 through  $d$  of the front  $\tau_i$  at each step. The previous lemmas guarantee that for each  $k$ , where  $1 \leq k \leq d$ , the causality and progress constraint for each  $k$ -dimensional face  $f$  ensures positive progress of  $p$  so that the corresponding face  $f'$  on the new front also satisfies the relevant causality and progress constraints.

Thus, every  $k$ -dimensional highest face  $\Delta$  has a gradient constraint imposed on it for every  $(k + 1)$ -dimensional highest face  $\Gamma$  such that  $\Delta \subset \Gamma$ .

**Theorem 2.15.** *For any  $i \geq 0$ , if the front  $\tau_i$  is progressive then  $\tau_i$  is valid.*

*Proof of Theorem 2.15.* The proof is identical to that of Theorem 2.3. □

We thus have the following theorem.

**Theorem 2.16.** *Given a triangulation  $M$  of a bounded planar space domain where  $w_{\min}$  is the minimum width of a simplex of  $M$  and  $\sigma$  is the minimum slope anywhere in  $M \times [0, \infty)$ , for every  $\varepsilon$  such that  $0 < \varepsilon < 1$  our algorithm constructs a simplicial mesh of  $M \times [0, T]$  consisting of at most  $\left\lceil \frac{n(T + \text{diam}(M)\sigma)}{\min T} \right\rceil$  spacetime elements for every real  $T \geq 0$  in constant computation time per element.*

*Proof of Theorem 2.16.* By Lemmas 2.12 and 2.14, it follows that the height of each tentpole constructed by the algorithm is at least  $T_{\min} = \varepsilon\sigma w_{\min}$ . By Theorem 2.15, after constructing at most  $k \leq \left\lceil \frac{\text{diam}(M)\sigma}{T_{\min}} T \right\rceil$  patches, the entire front  $\tau_k$  is past the target time  $T$ . Since each patch consists of at most  $\Delta(M)$  elements, the theorem follows. □

## 2.5 Element quality

Various definitions of quality exist for linear elements in Euclidean space, such as ratio of circumradius to inradius, circumradius to shortest edge length, radius of minimum enclosing ball to maximum enclosed ball, etc.. Each definition is useful to quantify the suitability of the element for the particular numerical technique being used. In  $\mathbb{E}^2$ , all measures of quality are within constant factors of each other, which is not true in higher dimensions. We recommend the excellent survey due to Shewchuk (She02) on various aspects of element quality.

The spacetime domain  $\mathbb{E}^d \times \mathbb{R}$  is not Euclidean because the time axis can be scaled independently of space. It is therefore nontrivial to define the quality of a spacetime element. We consider the temporal aspect ratio of an element as a measure of its quality. The temporal aspect ratio of an element was defined in Chapter 2 as the ratio of its height to its duration. We prove that our worst-case guarantees on the height of each tentpole lead to a lower bound on the worst-case temporal aspect ratio of any spacetime element constructed by our algorithm.

In this chapter, we have proved a lower bound on the worst-case height of each tentpole, a progress guarantee similar to that of Erickson *et al.* (EGSÜ02) and Abedi *et al.* (ACE<sup>+</sup>04). For the linear nonadaptive version of our algorithm, where the slope is  $\sigma$  everywhere, this progress guarantee can be rephrased as follows: the height of each spacetime tetrahedra in the tent pitched at  $P$  is at least  $\tilde{\varepsilon}\sigma w_p$  where  $\tilde{\varepsilon} \in (0, \frac{1}{2}]$  is a fixed parameter and  $w_p$  denotes the distance of  $p$  from the boundary of the kernel of  $\text{link}(p)$  in the spatial projection. Thus, the height of the tentpole at  $P$  is bounded from below by a positive function of  $\varepsilon$ , the slope  $\sigma$ , and the shape of the triangles in  $\text{star}(p)$ .



Note that the temporal aspect ratio is always in the range  $(0, 1]$  with a larger value corresponding to a “better” element. The duration of the tetrahedron  $P'PQR$  can be at most  $2\sigma w_p$  because both facets  $PQR$  and  $P'QR$  are causal. Together with the lower bound on the height of the tetrahedron, this implies the following theorem.

**Theorem 2.17.** *The temporal aspect ratio of any tetrahedron in  $\Omega$  is at least  $\tilde{\epsilon}/2$ .*

When the wavespeed is not constant, the worst-case temporal aspect ratio that we can prove is smaller by a factor  $\sigma_{\min}/\sigma_{\max}$ , i.e., proportional to the ratio of maximum to minimum wavespeeds or the *Mach factor*.

Bisecting a triangle on the front can improve the temporal aspect ratio of future tetrahedra because the smaller triangles may be limited by a smaller wavespeed than their larger ancestors. However, newest vertex bisection does not improve the quality of the spatial projection of front triangles, beyond a very limited amount. Repeatedly bisecting a single triangle produces smaller triangles from at most four different similarity classes. To improve the temporal aspect ratio, mesh smoothing and other generalized mesh adaptivity operations are more useful because they improve the quality of the spatial projection of the front.

## 2.6 Size optimality

The computation time of any solution strategy increases with the number of patches—computing the solution within each patch is expensive and, in our scenario, much more computationally expensive than the mesh generation, especially for high polynomial orders. Therefore, it is important to generate a mesh with close to the fewest number of patches necessary for a given accuracy.

Our algorithm constructs groups of coupled spacetime elements inside each tent such that the boundary of the tent is causal. The number of elements in the resulting patch is at most the maximum vertex degree of the underlying space mesh. Each element constructed by our algorithm has both a causal inflow facet and a causal outflow facet; additionally, the spatial projection of each element  $P'_0P_0P_1P_2\dots P_d$  is the simplex  $p_0p_1p_2\dots p_d$  in the original space mesh. Given a triangulation  $M$  of the space domain and a target time  $T$ , we say that a simplicial spacetime mesh of  $M \times [0, T]$  is *solvable* if (i) each element has both a causal inflow facet and a causal outflow facet; and (ii) for every point  $x$  in the spatial projection  $\Delta$  of each element, the diameter of  $\Delta$  does not exceed the diameter of the simplex of  $M$  containing  $x$ .

Fix an arbitrary point  $x$  in space. The *size* of a spacetime mesh of  $M \times [0, T]$  is the maximum over  $x \in M$  of the number of spacetime elements that intersect the temporal segment  $x \times [0, T]$ .

Consider the linear nonadaptive instance of our algorithm. The wavespeed everywhere in spacetime is constant, equal to  $\sigma$ .

**Theorem 2.18.** *The size of the mesh constructed by our algorithm is  $\tilde{O}(1/\epsilon^2)$  times the minimum size of any valid mesh of the spacetime volume  $M \times [0, T]$ .*

*Proof.* Let  $D$  and  $\rho$  denote the diameter and inradius respectively of the simplex  $p_0p_1p_2\dots p_d$  of  $M$  containing  $x$ . Causality limits the gradient of any edge of the  $d$ -simplex to less than  $\sigma$ . Therefore, any temporal segment of duration  $(d-1)\sigma D$  must intersect at least two distinct elements in a solvable mesh; therefore, the number of spacetime elements in a solvable mesh that intersect  $x \times [0, T]$  is at least  $\lfloor T/((d-1)\sigma D) \rfloor$ .

Consider a minimal sequence of tent pitching steps, called a *superstep*, in which each vertex of  $p_0p_1p_2\dots p_d$  is

lifted at least once. When  $p_0$  is pitched, the amount of progress made by  $x$  is proportional to  $\text{dist}(x, \text{aff}\Delta_0)$ . Since

$$\sum_{0 \leq i \leq k} \text{dist}(x, \text{aff}\Delta_i) \geq \rho$$

the amount of progress made by  $x$  during a superstep is at least  $\varepsilon\sigma\gamma\rho$ , where  $\gamma \in (0, 1]$  denotes the minimum over all  $i$  such that  $0 \leq i \leq k$  of  $w_{p_i}/\text{dist}(p_i, \text{aff}\Delta_i)$ . Hence, after at most  $\lceil T/(\varepsilon\sigma\gamma\rho) \rceil$  supersteps, the point  $x$  achieves or exceeds the target time  $T$ .

Causality limits the gradient of any edge of the simplex  $p_0p_1p_2 \dots p_d$  to less than  $\sigma$ . Therefore, any  $d-1$  vertices of  $p_0p_1p_2 \dots p_d$  can advance less than  $2(d-1)\sigma D$  units of time total without also advancing the  $d$ th vertex. Therefore, the number of steps in each superstep is at most  $\lfloor (2(d-1)\sigma D)/(\varepsilon\sigma w) \rfloor$  where  $w = \min_{0 \leq i \leq k} w_{p_i}$ . It follows that the number of tetrahedra in the spacetime mesh constructed by our algorithm intersected by  $x \times [0, T]$  is at most  $\lceil T/(\varepsilon\sigma\gamma\rho) \rceil \cdot \lfloor (2(d-1)\sigma D)/(\varepsilon\sigma w) \rfloor$ .

The ratio of the upper bound to the lower bound on the size is

$$O\left(d \frac{1}{\varepsilon^2} \frac{D^2}{\gamma\rho w}\right).$$

□

Note that for every fixed input space mesh  $M$ , the size of the spacetime mesh of  $M \times [0, T]$  constructed by our algorithm is at most  $O(1/\varepsilon^2)$  times that of a solvable mesh of the same spacetime volume, where the constant in the big-Oh notation depends on  $M$ .

When the wavespeed is not constant, the size-optimality factor that we can prove is larger by a factor  $\sigma_{\max}/\sigma_{\min}$ , i.e., inversely proportional to the *Mach factor*.

When the spacetime error indicator demands different mesh resolution in different portions of the spacetime domain, we can prove that the mesh constructed by our algorithm is still near-optimal where the approximation ratio is worse by a factor proportional to the ratio of maximum to minimum element sizes allowed by the error tolerance.

Our advancing front meshing algorithms are parameterized by real numbers like  $\varepsilon$  that control the extent to which they greedily maximize the height (and hence the temporal aspect ratio) of new elements. Being greedy at each step is not always a good choice for maximizing the worst-case temporal aspect ratio and for minimizing the total number of spacetime elements. We have especially clear evidence that while attempting to satisfy coplanarity constraints in order to coarsen parts of the front it may be necessary to reduce the heights of tentpoles. As a result of being less greedy at each step, do we actually increase the number of spacetime elements to an unbounded extent? Theorem 2.18 says that by being less greedy, our advancing front algorithm is near-optimal in the number of elements compared to a solvable mesh.

## 2.7 Geometric primitives

Maximizing the height of each tentpole subject to causality and progress constraints is equivalent to shooting a ray in an arrangement of (a small number of) planes and infinite cones. Consider the case where the wavespeed everywhere in spacetime is the same, i.e., the slope of every cone of influence is equal to  $\sigma$ .

When a vertex  $p$  of the causal front  $\tau$  is advanced in time to get the front  $\tau'$  by pitching a tentpole from  $P = (p, \tau(p))$  to  $P' = (p, \tau'(p))$ , the new front  $\tau'$  is causal if and only if for every triangle  $pqr$  incident on  $p$  the slope of triangle

$P'QR$  is less than  $\sigma$ . Let  $\pi_{qr}$  denote the plane through  $QR$  making a slope of  $\sigma$  with the space domain. The slope of  $\triangle P''QR$  is equal to  $\sigma$  if and only if  $P'' = (p, \tau''(p))$  is on the plane  $\pi_{qr}$  and the slope of  $\triangle P'QR$  is less than  $\sigma$  if and only if  $\tau(p) \leq \tau'(p) < \tau''(p)$ . Thus,  $\tau''(p)$  can be computed by shooting a ray in spacetime with origin at  $P$  oriented in the positive time direction and finding the point of intersection of this ray with the plane  $\pi_{qr}$ . The triangle  $P'QR$  is causal only if  $|PP'| < |PP''|$ . Finding the supremum height of the tentpole at  $P$  subject to causality constraint alone is equivalent to finding the distance along the tentpole direction before the ray originating at  $P$  in the tentpole direction first intersects any plane  $\pi_{qr}$  among all such planes for every edge  $qr \in \text{link}(p)$ .

The progress constraint  $\|\nabla \tau'_{pq}\| \leq (1 - \varepsilon)\phi_{pq}\sigma$  is satisfied if and only if the edge  $P'Q$  is below or on the infinite right circular cone  $C_q$  with apex at  $Q = (q, \tau(q))$  and axis in the positive time direction. Thus, maximizing the height of the tentpole  $PP'$  is equivalent to shooting a ray with origin at  $P$  in the tentpole direction and determining its first intersection with  $C_q$ .

Thus, finding the supremum height of the tentpole at  $P$  subject to causality and progress constraints is equivalent to answering ray shooting queries among an arrangement of planes, one for each edge  $qr \in \text{link}(p)$ , and infinite circular cones, one for each vertex  $q$  neighboring  $p$ .

**RUNNING TIME** The running time is  $O(\text{deg}(p))$  for constructing the patch at  $p$ , where  $\text{deg}(p)$  is the number of simplices in  $\text{star}(p)$  of any dimension, hence  $O(1)$  amortized per spacetime element. Additional complexity at each step comes from the need to choose the local minimum vertex to pitch; the choice of local minimum can be arbitrarily complicated. Advancing  $p$  destroys at most one local minimum ( $p$  itself) and creates at most  $\text{deg}(p)$  new local minima (the neighbors of  $p$ ). Thus, the set of local minima of each front can be maintained efficiently.

If the tentpole is inclined, for instance to track a moving boundary or shock interface, then the problem of maximizing tentpole height is still equivalent to answering ray shooting queries. The problem is a little more complicated if the choice of tentpole direction is not specified and must be chosen to optimize some geometric or numerical quality criteria.

Note that if the wavespeed is not uniform everywhere, the problem is more complicated by the fact that nonlocal cones can limit the height of a tentpole and that progress constraints must anticipate future wavespeeds. In problems with nonuniform wavespeeds, maximizing the height of a tentpole is not always equivalent to answering a ray shooting query—a triangle of the new front can be tangent to a remote cone of influence even if the corresponding tentpole is still below the cone.

We will postpone discussions of geometric primitives for greedily maximizing the height of each tentpole for such more general problems to later chapters.

## Chapter summary

The Tent Pitcher algorithm is the first instance of an advancing front algorithm to mesh directly in spacetime. The algorithm is simple because the geometric constraints that limit the height of each tentpole are linear functions of the coordinates. The height of each tentpole depends on the size of the space elements incident on the tentpole only and not on any global property of the space mesh. Consequently, we were able to prove a lower bound on the temporal aspect ratios of spacetime tetrahedra constructed by our algorithm. Progress constraints are artifacts of our algorithm, necessitated by its local advancement strategy, and not required explicitly to satisfy causality. Even though progress constraints limit the progress in time at each step, we were able to prove that the number of elements produced by our

algorithm for meshing a given spacetime volume is not much more than that in a size optimal causal mesh of the same volume.

In this chapter, we described the constant wavespeed case where the height of each tentpole is limited only by local constraints, as in the case of linear PDEs. We were able to generalize Tent Pitcher to pitch inclined tentpoles corresponding to advancing the front in time as well as changing the spatial projection of the front vertices. We were also able to incorporate additional operations such as edge flips. These new operations allow the algorithm to recover from a bad quality initial front (the space mesh  $M$ ). In Chapter 7, we will also use these operations to track spacetime features such as moving boundaries by aligning the tentpole direction and/or causal facets of the front with these features.

## Chapter 3

# Meshing with nonlocal cone constraints

The basic advancing front algorithm of Chapter 2 relied on a fixed lower bound  $\sigma = \sigma_{\min}$  on the globally minimum slope. The progress constraint was a function of this minimum slope  $\sigma_{\min}$  and this constraint restricted the progress at every step of the algorithm. Due to nonlinearity, the speed at which a wave propagates may be different in different parts of the domain. Even at the same point in space, the wavespeed may change with time. In general, the wavespeed may be a function of the solution. In this chapter, we consider the problem of meshing the spacetime domain when causality limits the gradient of mesh facets differently in different parts of the domain because the causal slope is not a constant everywhere.

In this chapter, we make our algorithm respond to changes in the causal slope (the reciprocal of the wavespeed), even if such changes are discontinuous and unpredictable, subject to the no-focusing assumption. When the wavespeed is not constant, a fast distant wave corresponding to a shallow cone of influence can limit the amount of local progress made by our advancing front algorithm. Thus, when the wavespeed is not constant, the most limiting cone constraint can be nonlocal. Nonlinear PDEs or even linear PDEs with discontinuous initial conditions can exhibit such behavior. The no-focusing assumption, Axiom 1.1 and its anisotropic version Axiom 1.3, allows us to conservatively estimate the slope at a point  $P$  in spacetime where the solution has not been computed yet, given the cone of influence of every point on the current front. The slope  $\sigma(P)$  is bounded by the minimum and maximum slopes of all cones of influence that contain  $P$ . We extend the algorithm of Chapter 2 to construct only causal fronts, making use of the no-focusing assumption to estimate the causality constraint in the unmeshed and unsolved portion of the spacetime domain ahead of the current front.

### 3.1 Problem statement

Just like in Chapter 2, the input to our problem is the initial front  $\tau_0$  and the initial conditions of the underlying hyperbolic PDE in the form of the causal slope  $\sigma(P)$  for every point  $P$  of  $\tau_0$ . We want an advancing front algorithm such that for every nonnegative real  $T$  there exists a finite integer  $k \geq 0$  such that the front  $\tau_k$  after the  $k$ th iteration of the algorithm satisfies  $\tau_k \geq T$ . As before, we would like to characterize *valid* fronts as those that are guaranteed to make finite progress at each step.

The main difficulty in characterizing valid fronts arises when the causal slope at a given point in the space domain decreases over time, i.e., the wavespeed increases. For instance, suppose  $\triangle PQR$  is causal. However, as soon as the local minimum vertex, say  $P$ , is advanced in time by an arbitrarily small positive amount to  $P'$ , the triangle  $P'QR$  may intersect a cone of influence with a much smaller slope, i.e.,  $\sigma(P'QR) \ll \sigma(PQR)$ . Consequently,  $\triangle P'QR$  is not causal. The decrease in causal slope from  $\sigma(PQR)$  to  $\sigma(P'QR)$  prevents the front from making nontrivial progress by advancing the local minimum vertex  $P$ .

**OUR SOLUTION** For one-dimensional space domains, we prove that every causal front is valid. We give an algorithm that given an arbitrary causal front  $\tau_i$  constructs a next front  $\tau_{i+1} = \text{advance}(\tau_i, p, \Delta t)$  such that  $\tau_{i+1}$  is causal and  $\tau_{i+1}(p)$  is maximized.

In higher dimensions, i.e.,  $d \geq 2$ , we define *progressive* fronts and prove that if a front is progressive then it is valid. We give an algorithm that given any progressive front  $\tau_i$  constructs a next front  $\tau_{i+1} = \text{advance}(\tau_i, p, \Delta t)$  such that  $\tau_{i+1}$  is progressive and  $\tau_{i+1}(p)$  is maximized. Whenever  $p$  is a local minimum of  $\tau_i$ , the progress  $\tau_{i+1}(p) - \tau_i(p)$  is positive and bounded away from zero.

Our algorithm resolves the following conundrum. The progress of the front at each step  $i$  is limited by the progress constraint that must be satisfied by the next front at step  $i+1$ . However, we do not know what the next front is unless we know how much progress is possible at step  $i$ . Intuitively, the geometric constraints that apply at any given iteration of the algorithm are predicted by simulating the  $h$  next tent pitching steps for some parameter  $h \geq 0$ . We initially make conservative assumptions about the future wavespeed and successively refine the estimate of the wavespeed encountered in the next  $h$  iterations.

Our algorithm is the first algorithm to build spacetime meshes over arbitrary-dimensional triangulated spatial domains suitable for solving nonlinear hyperbolic PDEs, where the wavespeed at any point in spacetime depends on the solution and cannot be computed in advance. Moreover, the solution can change discontinuously, for instance when a *shock* propagates through the domain. As long as the no-focusing condition (Axiom 1.1) holds, the resulting mesh is efficiently solvable patch-by-patch by SDG methods.

## 3.2 Nonlocal cone constraints in $1D \times \text{Time}$

To complete the description of the algorithm in  $1D \times \text{Time}$ , it remains only to describe how to maximize the height  $\tau_{i+1}(p) - \tau_i(p)$  of the tentpole subject to the causality constraint. Even in  $1D \times \text{Time}$ , this optimization problem is not trivial in the presence of nonlinearity because of nonlocal cone constraints. Nonlocal cone constraints are handled in the same way in higher dimensions but the algorithm is more complicated because of progress constraints.

Recall that the *cone of influence* of a point  $P$  has its apex at  $P$  and its slope in any spatial direction is the maximum slope of any characteristic through  $P$  in that direction; fast waves correspond to cones with smaller slope.

When the PDE is nonlinear, a distant but fast wave, i.e., a *nonlocal* cone, can overtake a slower wave and hence limit the duration of new elements. See Figure 3.1. *We assume as a conservative estimate that the wave travels through the space domain  $M$  along the shortest path in the ambient Euclidean space.* When the medium is *anisotropic*, waves travel faster in one direction than the other, so the cones are non-circular, for instance, with elliptical cross-sections. We will discuss the situation for anisotropic problems in Chapter 7; it should be noted that the discussion in the current chapter is not restricted to circular cones.

Our algorithms advance a local neighborhood  $N$  of the front  $\tau$  at each step to the neighborhood  $N'$  of a new causal front  $\tau'$ . Hence,  $\tau'$  is causal if and only if (i) the gradient of  $\tau'$  at every point of  $N'$  is less than the minimum slope anywhere in  $N$ , and (ii) the neighborhood  $N'$  lies below (i.e., does not intersect) the cone of influence  $C_q$  for every point  $Q \in \tau \setminus N$ . Each such cone of influence corresponds to a *causal cone constraint*. In  $1D \times \text{Time}$ , a cone of influence is defined by two rays with common apex.

Thus, maximizing the progress of  $P$ , and hence the duration of new spacetime elements, requires querying the lower hull of cones of influence of points in  $\tau \setminus N$ . After the solution is computed on the new front  $\tau'$ , including the causal slope at every point of  $\tau'$ , we obtain a new set of cone constraints.

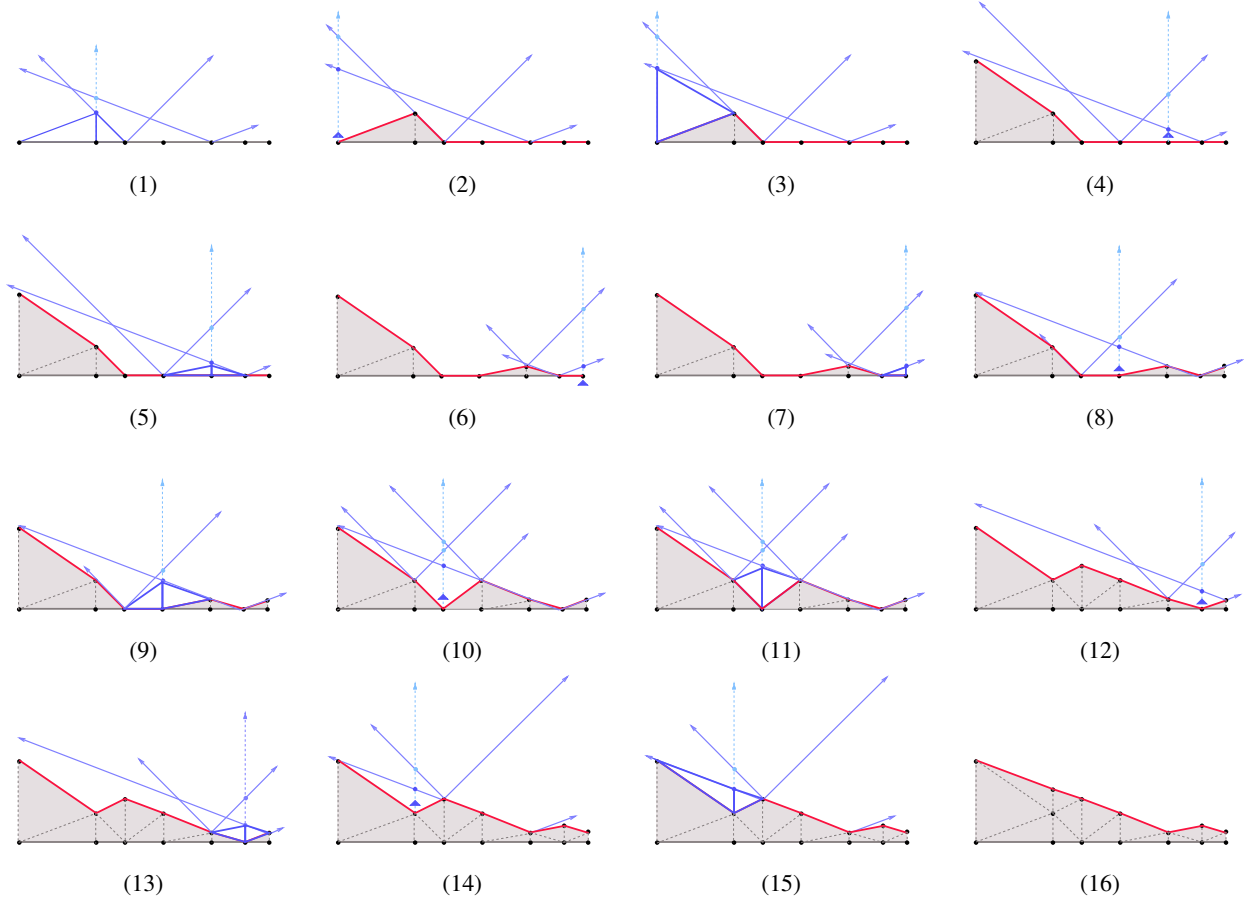


Figure 3.1: A sequence of tent pitching steps in  $1D \times \text{Time}$ . Maximizing the height of each tentpole while staying below every cone of influence may require examining remote cones arbitrarily far away.

For a fixed segment  $pq$  incident on  $p$  let  $T_{\text{sup}}(p, Q)$  denote the supremum upper bound on  $\tau_{i+1}(p)$  such that  $P'Q$  on the front  $\tau_{i+1}$  is causal, i.e.,

$$T_{\text{sup}}(p, Q) := \sup \{t : P'Q \text{ is causal where } P' = (p, t)\}.$$

Let  $T_{\text{sup}}(p)$  denote the maximum  $T_{\text{sup}}(p, Q)$  for every neighbor  $Q$  of  $P$ . To maximize the progress at step  $i + 1$ , we would like to compute  $T_{\text{sup}}(p)$ . The segment  $P'Q$  is causal if and only if the slope of  $P'Q$  is less than the slope of the cone of influence from every point on the front that intersects  $P'Q$ . In  $1D \times \text{Time}$ , a cone of influence intersects  $P'Q$  if and only if the cone intersects the tentpole  $PP'$ .

In general, a cone of influence from arbitrarily far away can intersect the tentpole at  $p$ . See Figure 3.1. (Nonlocal cone constraints do not dominate local cone constraints when the wavespeed everywhere is the same.) Therefore, in general,  $T_{\text{sup}}(p)$  could be determined by a cone of influence of a point arbitrarily distant from  $p$ . In this section, we give two algorithms—one to compute  $T_{\text{sup}}(p, Q)$  exactly using ray shooting in an arrangement of rays (lines) and the other to approximate  $T_{\text{sup}}(p)$  numerically using a binary search.

**LOCAL AND NONLOCAL CONE CONSTRAINTS** Partition the front into two subsets of points: (i) points in the star of  $P$  (“local” points), and (ii) points everywhere else on the front (“remote” points). Corresponding to each subset we have two disjoint subsets of cones of influence— $\mathcal{C}_{\text{local}}$  and  $\mathcal{C}_{\text{remote}}$  respectively. Each subset of cones limits the new time value of  $p$  and so the final time value is the smaller of the two values for each of  $\mathcal{C}_{\text{local}}$  and  $\mathcal{C}_{\text{remote}}$  taken separately.

Consider the subset  $\mathcal{C}_{\text{local}}$ . Let  $\sigma_{\text{local}}$  denote the smallest slope among all cones of influence in  $\mathcal{C}_{\text{local}}$ . The segment  $P'Q$  is causal only if its slope is less than  $\sigma_{\text{local}}$ . Let  $t_{\text{local}}$  be the supremum time value of  $P'$  for which the slope of  $P'Q$  is less than  $\sigma_{\text{local}}$ . To compute  $t_{\text{local}}$  we substitute  $\sigma_{\text{local}}$  in the condition for causality of  $P'Q$  (Equation 2.1).

Next consider the subset  $\mathcal{C}_{\text{remote}}$ . The front  $\tau_i$  is strictly below every cone in  $\mathcal{C}_{\text{remote}}$  because  $\tau_i$  is causal. The segment  $P'Q$  is causal only if it is also strictly below every cone in  $\mathcal{C}_{\text{remote}}$ . Given a cone  $C \in \mathcal{C}_{\text{remote}}$ ,  $C$  intersects  $P'Q$  if and only if  $C$  intersects the tentpole  $PP'$ . Let  $t_{\text{remote}}$  denote the smallest time value  $T$  for which the tentpole  $PP'$  where  $P' = (p, T)$  intersects exactly one cone in  $\mathcal{C}_{\text{remote}}$ . The segment  $P'Q$  is causal only if  $T < t_{\text{remote}}$ .

Therefore, the progress  $\tau_{i+1}(p) - \tau_i(p)$  at step  $i + 1$  is limited because

$$T_{\text{sup}}(p) = \min\{t_{\text{local}}, t_{\text{remote}}\}.$$

To maximize the progress at the current step, we choose  $\tau_{i+1}(p)$  less than  $T_{\text{sup}}(p)$ , e.g., equal to  $T_{\text{sup}}(p)$  minus the machine precision.

We have the following theorem.

**Theorem 3.1.** *Let  $\tau$  be a causal front and let  $p$  be an arbitrary local minimum of  $\tau$ . Let  $w_p$  denote the spatial distance from  $p$  to its nearest neighbor. Then, for every  $\Delta t$  such that  $0 \leq \Delta t < w_p \sigma_{\text{min}}$  the front  $\tau' = \text{advance}(\tau, p, \Delta t)$  is causal.*

*Proof of Theorem 2.2.* Only the segments of the front incident on  $P = (p, \tau(p))$  advance along with  $p$ . Consider an arbitrary segment  $pq$  incident on  $p$ . Since  $p$  is a local minimum, we have  $\tau(q) \geq \tau(p)$ . We have

$$\begin{aligned} \tau'(p) &\leq \tau(p) + \Delta t \\ &< \tau(p) + w_p \sigma_{\text{min}} \\ &\leq \tau(q) + |pq| \sigma_{\text{min}} \\ &\leq \tau(q) + |pq| \sigma(P'Q) \end{aligned}$$

Therefore, the slope of the segment  $P'Q$  is less than  $\sigma(P'Q)$  and hence  $P'Q$  is causal.  $\square$

**COMPUTING  $t_{\text{REMOTE}}$  EXACTLY** Computing  $t_{\text{remote}}$  is equivalent to answering a ray shooting query in the arrangement of the cones in  $\mathcal{C}_{\text{remote}}$ . We use a bounding cone hierarchy  $\mathcal{H}$ , i.e., a binary tree, obtained from a hierarchical decomposition of the space domain to efficiently answer the ray shooting query. The hierarchical decomposition of the space domain induces a corresponding hierarchical decomposition of every front. For each element of this hierarchy, we store a cone that bounds the cone of influence of every point of the corresponding subset of the front. To answer the ray shooting query, we traverse the cone hierarchy from top to bottom starting at the root. At every stage, we store a subset  $\mathcal{C}$  of bounding cones such that every cone in  $\mathcal{C}_{\text{remote}}$  is contained in some cone in the subset  $\mathcal{C}$ . The cones in  $\mathcal{C}$  are stored in a priority queue in non-decreasing order of the time value at which the vertical ray at  $P$  intersects each cone. Initially,  $\mathcal{C}$  consists solely of the cone at the root of the hierarchy. At every stage, if the cone in  $\mathcal{C}$  that



has the earliest intersection in time does not come from a leaf in the hierarchy then we replace it in the priority queue with its children. Continuing in this fashion, we eventually determine the single facet of the front such that the cone of influence from some point on this facet is intersected first by the vertical ray at  $P$ . The time coordinate of the point of intersection is  $t_{\text{remote}}$ , the answer to the ray shooting query.

Because the hierarchy is balanced its depth is  $O(\log m)$ , where  $m$  is the number of simplices in the space mesh. The tighter the bounding cones, i.e., the better they approximate the actual cones of influence, the better is the efficiency of the algorithm. In  $1D \times \text{Time}$ , we observed empirically that on average only a few nodes in the cone hierarchy were examined by this algorithm to determine the most constraining cone of influence.

**APPROXIMATING  $t_{\text{REMOTE}}$**  Since we know a range of values  $[\tau_i(p) + T_{\min}, t_{\text{local}}]$  that contains  $t_{\text{remote}}$ , we can approximate  $t_{\text{remote}}$  up to any desired numerical accuracy by performing a binary search in this interval. At every iteration, we speculatively lift  $P$  to the midpoint of the current search interval. Let  $P''$  be the speculative top of the tentpole at  $P$ . We query the cones of influence in  $\mathcal{C}_{\text{remote}}$  to determine the minimum slope  $\sigma_{\text{remote}}$  among all cones that intersect  $PP''$ . If the maximum slope of the outflow faces incident on  $P''$  is less than  $\sigma_{\text{remote}}$  then we can continue searching in the top half of the current interval; otherwise, the binary search continues in the bottom half of the current interval. The search terminates when the search interval is smaller than our desired additive error. A bounding cone hierarchy helps in the same manner as before to determine the minimum slope among all cones in  $\mathcal{C}_{\text{remote}}$  that intersect  $PP''$ , i.e., all cones of influence that contain  $P''$ .

### 3.3 Nonlocal cone constraints in $2D \times \text{Time}$

In  $2D \times \text{Time}$ , the algorithm to maximize the progress at each step is complicated by the presence of progress constraints in addition to causality constraints. In this section, we give an algorithm for which the progress guarantee at each step is finite and bounded away from zero. The minimum progress guarantee is a function of the local geometry of the spatial projection of the front  $\tau_i$  and the global minimum causal slope, analogous to the progress guarantee proved in Chapter 2 for the constant-wavespeed case.

Our algorithm anticipates changing wavespeeds by simulating the next few iterations at each step. The purpose of this lookahead is to estimate the actual causal slope encountered in the next few iterations. As a result, we expect that, in practice, the actual progress is proportional to the (possibly nonlocal) slope that most constrains causality at the current step and in the next few iterations of the algorithm, which may be significantly larger than the global minimum slope. Hence, we expect our algorithm to create spacetime elements whose sizes are proportional to the local geometry and adapt rapidly to changing causal cone constraints.

#### 3.3.1 Looking ahead

From Theorem 2.4, we observe that the new front  $P'QR$  is causal if the old front  $PQR$  satisfies progress constraint  $\sigma(P'QR)$ . We need to estimate the slope  $\sigma(P'QR)$  in the next step in order to enforce a progress constraint in the current step. This dependency on the future wavespeed creates the following conundrum. The progress of the front at each step  $i$  is limited by the progress constraint that must be satisfied by the next front at step  $i + 1$ . However, we do not know what the next front is unless we know how much progress is possible at step  $i$ . Of course, we can always use the global maximum wavespeed as a conservative estimate of the slope  $\sigma(P'QR)$ ; however, this excessively conservative

estimate implies a very low progress guarantee for problems where the ratio of maximum to minimum wavespeeds is very large.

To solve this conundrum, we develop a lookahead algorithm that adaptively estimates future wavespeed. For a fixed positive integer  $h$ , called the *horizon*, the algorithm at the  $i$ th step computes an estimated slope  $\tilde{\sigma}_h(PQR)$  for every triangle  $PQR$  of the current front. The horizon  $h$  can be fixed or chosen adaptively at each step.

When  $h = 0$ , we use the minimum slope  $\sigma_{\min}$  as an estimate of the actual causal slope on the front in the next step, so our estimate of future slope is  $\tilde{\sigma}_0(PQR) = \sigma_{\min}$ . When  $h > 0$ , we can use the current estimate to compute the next front and the actual slope on this new front to refine our previous estimate.

**Definition 3.2** ( $h$ -progressive). *Let  $h$  be a nonnegative integer, called the horizon.*

*Let  $PQR$  be a given triangle. We inductively define  $\triangle PQR$  as  $h$ -progressive as follows.*

**Base case  $h = 0$ :** *Triangle  $PQR$  is 0-progressive if and only if it is causal and satisfies progress constraint  $\sigma_{\min}$  (Definition 2.6).*

**Case  $h > 0$ :** *Triangle  $PQR$  is  $h$ -progressive if and only if all the following conditions are satisfied:*

1.  $PQR$  is causal;
2. *Let  $P$  be an arbitrary local minimum vertex of  $\triangle PQR$ . Let  $d_p$  denote  $\text{dist}(p, \text{aff } qr)$  and let  $T_{\min} = \min\{\varepsilon, 1 - \varepsilon\} \sigma_{\min} d_p$ . Let  $P'QR = \text{advance}(PQR, p, T_{\min})$  be the triangle obtained by advancing  $P$  by  $T_{\min}$ . Then,  $PQR$  must satisfy progress constraint  $\sigma(P'QR)$  and  $P'QR$  must be  $\max\{h - 1, 0\}$ -progressive.*

Note that an  $h$ -progressive triangle is also causal.

**Lemma 3.3.** *For every  $h \geq 0$ , if  $\triangle PQR$  is  $h$ -progressive, then  $\triangle PQR$  is  $(h + 1)$ -progressive.*

*Proof of Lemma 3.3.* If a triangle  $PQR$  satisfies progress constraint  $\sigma$  (Definition 2.6), then  $\triangle PQR$  satisfies progress constraint  $\sigma'$  for every  $\sigma' \geq \sigma$ . By Lemmas 2.4 and 2.7, if  $\triangle PQR$  satisfies progress constraint  $\sigma_{\min}$ , then the triangle  $P'QR$  after pitching a local minimum  $P$  by  $T_{\min}$ , where  $T_{\min}$  is the quantity in Definition 3.2, is causal and satisfies progress constraint  $\sigma_{\min}$ ; since  $\sigma_{\min}$  is a lower bound on the causal slope anywhere in spacetime, we conclude that triangle  $P'QR$  is 0-progressive. Therefore, by Definition 3.2, if  $\triangle PQR$  is 0-progressive, then it is  $h$ -progressive for every  $h \geq 0$ . Hence, if  $\triangle PQR$  is  $h$ -progressive, then it is  $h'$ -progressive for every  $h' \geq h$ .  $\square$

We are now ready to describe our advancing front algorithm in  $2D \times \text{Time}$ . Recall the causality constraint (Equation 2.2) and the progress constraint (Definition 2.6) that applies at each step.

The causal slope on the new front is computed by the solver; cone constraints can change as a result. In the parallel setting, nonlocal cone constraints and updates to the cone hierarchy due to changes in the cone constraints must be communicated across processors.

We claim that being  $h$ -progressive guarantees finite positive progress at each step. If  $\triangle PQR$  is  $h$ -progressive then for every  $\Delta t$  in the range  $0 \leq \Delta t \leq \min\{\varepsilon, 1 - \varepsilon\} \sigma_{\min} \text{width}(pqr)$  the triangle  $P'QR$  obtained by pitching an arbitrary local minimum vertex  $P$  by  $\Delta t$ , is  $h$ -progressive. The amount of progress is a function of  $\triangle pqr$ , the distribution of wavespeeds, and the parameters  $\varepsilon$  and  $h$ .

**Lemma 3.4.** *Suppose  $PQR$  is a triangle of an  $h$ -progressive front  $\tau$  for some  $h \geq 0$ . Let  $P$  be an arbitrary local minimum vertex of  $\triangle PQR$ . Let  $d_p$  denote  $\text{dist}(p, \text{aff } qr)$  and let  $T_{\min} = \min\{\varepsilon, 1 - \varepsilon\} \sigma_{\min} d_p$ . Let  $P'QR$  denote the corresponding triangle where  $P' = (p, \tau(p) + \Delta t)$  for an arbitrary  $\Delta t \in [0, T_{\min}]$ .*

*Then,  $\triangle P'QR$  is  $h$ -progressive.*

**Input:** A triangulated space domain  $M \subset \mathbb{E}^2$

**Output:** A tetrahedral mesh  $\Omega$  of  $M \times [0, \infty)$

The initial front  $\tau_0$  is  $M \times \{0\}$ , corresponding to time  $t = 0$  everywhere in space.

Fix  $h \geq 0$ .

Repeat for  $i = 0, 1, 2, \dots$ :

1. Advance in time an arbitrary local minimum vertex  $P = (p, \tau_i(p))$  of the current front  $\tau_i$  to  $P' = (p, \tau_{i+1}(p))$  such that  $\tau_{i+1}$  is  $h$ -progressive, and  $\tau_{i+1}(p)$  is maximized.
2. Partition the spacetime volume between  $\tau$  and  $\tau_{i+1}$  into a patch of tetrahedra, each sharing the tentpole edge  $PP'$ .
3. Call the numerical solver to compute the solution in the spacetime volume between  $\tau_i$  and  $\tau_{i+1}$ .

---

Figure 3.2: Algorithm in 2D×Time with nonlocal cone constraints.

---

*Proof of Lemma 3.4.* By Definition 3.2, triangle  $P'QR$  is  $(h-1)$ -progressive. By Lemma 3.3, triangle  $P'QR$  is also  $h$ -progressive.  $\square$

By Lemma 3.4, if the amount of progress made by  $p$  in every step is no more than the minimum  $T_{\min} = \min\{\varepsilon, 1 - \varepsilon\} \sigma_{\min} \text{dist}(p, \text{aff } qr)$  for every triangle  $pqr$ , then every front is  $h$ -progressive. However, the actual progress at each step would be no more than the progress guarantee obtained by imposing the progress constraint  $\sigma_{\min}$  of Definition 2.6 at each step. It is important to minimize the number of spacetime elements by exploiting the fact that the actual wave-speed in the next step may be significantly smaller than the global maximum wavespeed; i.e., to take advantage of the possibility that  $\sigma(P'QR) \gg \sigma_{\min}$  in Definition 3.2. In the next section, we give an algorithm to greedily maximize the progress of local minimum vertex  $P$  at each step, possibly at the expense of the progress in subsequent steps, but still retain the minimum progress guarantee of  $T_{\min}$  when pitching  $P$ .

### 3.3.2 Greedily maximizing progress

We want to maximize the progress at each step in a greedy fashion, i.e., at the  $i$ th step given an arbitrary local minimum vertex  $p$  of the front  $\tau_i$  we want to maximize  $\tau_{i+1}(p)$  where  $\tau_{i+1} = \text{advance}(\tau_i, p, \Delta t)$  subject to the constraint that  $\tau_{i+1}$  is causal and  $h$ -progressive.

For a fixed triangle  $pqr$  incident on  $p$  let  $T_{\text{sup}}(p, QR)$  denote

$$T_{\text{sup}}(p, QR) := \sup\{t : P'QR \text{ is causal and } h\text{-progressive, where } P' = (p, t)\}$$

To maximize the progress at step  $i$ , we would like to compute  $T_{\text{sup}}(p, QR)$ .

Similar to the 1D×Time case, partition the set of cones of influence from points on the front  $\tau_i$  into local and remote subsets. Let  $\sigma_{\text{local}}$  denote the smallest slope among all local cones of influence. The simplex  $P'QR$  is causal only if its slope is less than  $\sigma_{\text{local}}$ . Let  $t_{\text{local}}$  be the supremum time value of  $P'$  for which the slope of  $P'QR$  is less than  $\sigma_{\text{local}}$ . To compute  $t_{\text{local}}$  we substitute  $\sigma_{\text{local}}$  in the condition for causality of  $P'QR$  (Equation 2.2).

Unlike the 1D×Time case,  $T_{\text{sup}}(p, QR)$  cannot be computed by ray shooting queries. In 2D×Time, we need an oracle to determine which among several cones is intersected for the smallest  $T$  by a triangle  $P'QR$  when the vertex  $P$

```

MAXIMIZEPROGRESS( Front  $\triangle PQR$ , Vertex  $P$ , Integer  $h > 0$  ):
1. Comment:  $\tilde{\sigma}_h(PQR)$  is the current estimate of the slope in the next step.
2.  $\tilde{\sigma}_h \leftarrow \sigma_{\min}$ ;
3. done  $\leftarrow$  false;
4. while not done:
    4.1. compute the maximum time value  $T^*$  such that
            $\triangle P'QR$  where  $P' = (p, T^*)$ 
           is causal and satisfies progress constraint  $\tilde{\sigma}_h$ ;
    4.2. lift  $p$  to time value  $T^*$  giving  $\triangle P^*QR$ ;
    4.3. Comment: recursively compute  $\tilde{\sigma}_{h-1}(P^*QR)$ .
    4.4.  $\sigma' \leftarrow \text{FUTURESLOPE}(P^*QR, h - 1)$ ;
    4.5. done  $\leftarrow$  true;
    4.6. let  $P''QR$  denote the triangle after advancing  $P$ 
           so that  $P''QR$  is causal, it satisfies progress constraint  $\sigma'$ ,
           and the height of  $PP''$  is maximized;
    4.7. if  $\sigma(P''QR) > \tilde{\sigma}_h$ :
        4.7.1. {Comment: Improve the current estimate  $\tilde{\sigma}_h$ .}
        4.7.2.  $\tilde{\sigma}_h \leftarrow \sigma(P''QR)$ ;
        4.7.3. done  $\leftarrow$  false;
5. return  $T^*$ ;

```

```

FUTURESLOPE( Front  $\triangle ABC$ , Integer  $h' \geq 0$  ):
1. if  $h' = 0$ :
    1.1. return  $\sigma_{\min}$ ;
2.  $\tilde{\sigma} \leftarrow \infty$ ;
3. for every local minimum, say  $A$ , of  $\triangle ABC$ :
    3.1.  $T' \leftarrow \text{MAXIMIZEPROGRESS}(\triangle ABC, A, h')$ ;
    3.2. let  $\triangle A'BC$  be the triangle after advancing  $A$  to  $A' = (a, T')$ ;
    3.3.  $\tilde{\sigma} \leftarrow \min\{\tilde{\sigma}, \sigma(A'BC)\}$ ;
4. return  $\tilde{\sigma}$ ;

```

Figure 3.3: Algorithm to maximize height of tentpole  $PP'$  subject to  $h$ -progressive constraints

of  $\triangle PQR$  is lifted to  $P' = (p, T)$  while also lifting  $Q$  by a positive amount.. In spatial dimension  $d \geq 2$ , the algorithm to compute  $T_{\text{sup}}(p, QR)$  requires queries involving shooting  $(d - 1)$ -dimensional faces of the current front.

Definition 3.2 immediately gives an algorithm to answer the following question: given a triangle  $PQR$  in spacetime and an integer  $h \geq 0$ , is  $\triangle PQR$   $h$ -progressive? Using the algorithm to answer this decision question, we can approximate  $T_{\text{sup}}(p, QR)$  up to any given numerical accuracy by performing a binary search in the interval  $(\tau_i(p), t_{\text{local}}]$  which we know contains  $T_{\text{sup}}(p, QR)$ . The eventual height of the tentpole  $PP'$  is at least  $T_{\text{min}}$ , i.e., positive and bounded away from zero.

Algorithm MAXIMIZEPROGRESS of Figure 3.3 computes  $T_{\text{sup}}(p, QR)$ . The correctness of the algorithm follows from the following observation that FUTURESLOPE estimates the causal slope of the triangle in the next step after advancing sufficiently in time. By Lemmas 2.4 and 2.7, FUTURESLOPE advances the local minimum  $A$  by at least  $T_{\text{min}} = \min\{\varepsilon, 1 - \varepsilon\} \sigma_{\min} \text{dist}(a, \text{aff } bc)$  to  $A'$ . Therefore, the estimated slope  $\tilde{\sigma}$  computed by FUTURESLOPE is a sufficiently accurate estimate of the future slope to ensure that the triangle  $P'QR$  obtained by advancing the local minimum  $P$  to the time value  $T^*$  computed by MAXIMIZEPROGRESS satisfies the definition of an  $h$ -progressive triangle (Definition 3.2).

Maximizing the progress at the current step going from  $\triangle PQR$  to  $\triangle P'QR$  is equivalent to computing the maximum slope  $\tilde{\sigma}_h(P'QR)$  such that  $\triangle P'QR$  is  $h$ -progressive. Algorithm MAXIMIZEPROGRESS relies on a procedure to compute the slope anywhere on a triangle  $\triangle'$  in the future. We need a procedure to compute the minimum slope among all cones of influence emanating from the current front that intersect  $\triangle'$ . The algorithm also uses geometric primitives such as ray shooting to maximize the height of a tentpole subject to given causality and progress constraints. We will postpone discussion of the implementation of these low-level subroutines to a later section.

We thus have the following theorems.

**Theorem 3.5.** *For every  $i \geq 0$ , if the front  $\tau_i$  is  $h$ -progressive, then  $\tau_i$  is valid.*

*Proof of Theorem 3.5.* We prove the statement by induction on  $i$ . The proof is almost identical to that of Theorem 2.3 except with the additional complication of progress constraints in  $2D \times \text{Time}$ . The initial front  $\tau_0$  is progressive by definition. By Lemma 2.4 and Lemma 3.4, at each step  $i$  the algorithm advances a local minimum vertex  $p$  of the the  $h$ -progressive front  $\tau_i$  to the front  $\tau_{i+1}$  such that  $\tau_{i+1}$  is  $h$ -progressive. Let  $w_p$  denote the minimum distance  $\text{dist}(p, \text{aff } qr)$  for every edge  $qr$  in  $\text{link}(p)$ . By Lemma 3.4, we know that  $\tau_{i+1} \geq \tau_i(p) + T_{\min}$  where  $T_{\min} = \min\{\varepsilon, 1 - \varepsilon\}w_p\sigma_{\min}$ . Therefore, for every target time  $T \geq 0$ , the entire front achieves or exceeds time  $T$  in a finite number of steps.  $\square$

Thus, we obtain a theorem analogous to Theorem 2.10.

**Theorem 3.6.** *Given a triangulation  $M$  of a bounded planar space domain where  $w_{\min}$  is the minimum width of a simplex of  $M$  and  $\sigma$  is the minimum slope anywhere in  $M \times [0, \infty)$ , for every  $\varepsilon$  such that  $0 < \varepsilon < 1$  our algorithm constructs a simplicial mesh of  $M \times [0, T]$  consisting of at most  $\left\lceil \frac{n(T + \text{diam}(M)\sigma_{\max})}{\min\{\varepsilon, 1 - \varepsilon\}w_{\min}\sigma_{\min}} \Delta \right\rceil$  spacetime elements for every real  $T \geq 0$ , where  $\Delta$  is the maximum vertex degree.*

*Proof of Theorem 3.6.* By Lemmas 2.4 and 2.7, it follows that the height of each tentpole constructed by the algorithm is at least  $T_{\min} = \min\{\varepsilon, 1 - \varepsilon\}w_{\min}\sigma_{\min}$ . By Theorem 2.9, after constructing at most  $k \leq \left\lceil \frac{n(T + \text{diam}(M)\sigma_{\max})}{T_{\min}} \right\rceil$  patches, the entire front  $\tau_k$  is past the target time  $T$ . Since each patch consists of at most  $\Delta$  elements, where  $\Delta$  is the maximum number of simplices in the star of any vertex of  $M$ , the theorem follows.  $\square$

### 3.4 Nonlocal cone constraints in arbitrary dimensions $dD \times \text{Time}$

The algorithm and analysis of Section 3.3 extends in a straightforward manner to higher dimensions  $d \geq 3$ . The only additional complications involve the bounding cone hierarchy and queries to this hierarchy. For instance, for  $d = 3$ , whenever a vertex  $p$  of tetrahedron  $pqrs$  is advanced in time, we need to query whether the spacetime triangle corresponding to  $\triangle pqr \in \text{star}(p)$  intersects any four-dimensional cone of influence.

We give in this section the definitions in arbitrary dimensions corresponding to those in Section 3.3 and state the equivalent theorems without repeating their proofs because they are analogous to the corresponding theorems in  $2D \times \text{Time}$ .

Consider an arbitrary  $k$ -dimensional face  $p_0p_1p_2 \dots p_k$  incident on  $p_0$ .

**Definition 3.7** ( $h$ -progressive). *Let  $h$  be a nonnegative integer, called the horizon.*

*Let  $P_0P_1P_2 \dots P_k$  be a given  $k$ -simplex. We inductively define  $P_0P_1P_2 \dots P_k$  as  $h$ -progressive as follows.*

**Base case**  $h = 0$ :  $P_0P_1P_2 \dots P_k$  is  $0$ -progressive if and only if it is causal and satisfies progress constraint  $\sigma_{\min}$  (Definition 2.13).

**Case**  $h > 0$ :  $P_0P_1P_2 \dots P_k$  is  $h$ -progressive if and only if all the following conditions are satisfied:

1.  $P_0P_1P_2\dots P_k$  is causal;
2. Let  $P_0$  be an arbitrary local minimum vertex of  $P_0P_1P_2\dots P_k$ . Let  $d_{p_0}$  denote  $\text{dist}(p_0, \text{aff } p_1p_2\dots p_k)$  and let  $T_{\min} = \min\{\varepsilon, 1 - \varepsilon\}\sigma_{\min}d_{p_0}$ . Let  $P'_0P_1P_2\dots P_k = \text{advance}(P_0P_1P_2\dots P_k, p_0, T_{\min})$  be the simplex obtained by advancing  $P_0$  by  $T_{\min}$ . Then,  $P_0P_1P_2\dots P_k$  must satisfy progress constraint  $\sigma(P'_0P_1P_2\dots P_k)$  and  $P'_0P_1P_2\dots P_k$  must be  $\max\{h - 1, 0\}$ -progressive.

Note that an  $h$ -progressive simplex is also causal.

**Lemma 3.8.** *Suppose  $P_0P_1P_2\dots P_k$  is a simplex of an  $h$ -progressive front  $\tau$  for some  $h \geq 0$ . Let  $P_0$  be an arbitrary local minimum vertex of  $P_0P_1P_2\dots P_k$ . Let  $d_{p_0}$  denote  $\text{dist}(p_0, \text{aff } p_1p_2\dots p_k)$  and let  $T_{\min} = \min\{\varepsilon, 1 - \varepsilon\}\sigma_{\min}d_{p_0}$ . Let  $P'_0P_1P_2\dots P_k$  denote the corresponding simplex where  $P'_0 = (p_0, \tau(p_0) + \Delta t)$  for an arbitrary  $\Delta t \in [0, T_{\min}]$ .*

*Then,  $P'_0P_1P_2\dots P_k$  is  $h$ -progressive.*

We have thus shown the finite termination of the algorithm.

**Theorem 3.9.** *Given a triangulation  $M$  of a bounded  $d$ -dimensional space domain where  $w_{\min}$  is the minimum width of a simplex of  $M$ , for every  $\varepsilon$  such that  $0 < \varepsilon < 1$  our algorithm constructs a simplicial mesh of  $M \times [0, T]$  consisting of at most  $\left\lceil \frac{n(T + \text{diam}(M)\sigma_{\max})}{\min\{\varepsilon, 1 - \varepsilon\}w_{\min}\sigma_{\min}} \Delta \right\rceil$  spacetime elements for every real  $T \geq 0$ , where  $\Delta$  is the maximum vertex degree.*

*Proof of Theorem 3.6.* By Lemmas 2.12 and 2.14, it follows that the height of each tentpole constructed by the algorithm is at least  $T_{\min} = \min\{\varepsilon, 1 - \varepsilon\}w_{\min}\sigma_{\min}$ . By Theorem 2.9, after constructing at most  $k \leq \left\lceil \frac{n(T + \text{diam}(M)\sigma_{\max})}{T_{\min}} \right\rceil$  patches, the entire front  $\tau_k$  is past the target time  $T$ . Since each patch consists of at most  $\Delta$  elements, where  $\Delta$  is the maximum number of simplices in the star of any vertex of  $M$ , the theorem follows.  $\square$

### 3.5 Estimating future slope

The algorithms of previous sections rely on efficient answers to the following questions:

1. Given a triangle  $PQR$  and a set of cones of influence, what is the slope of the fastest cone of influence that intersects  $\triangle PQR$ ?
2. Given a triangle  $PQR$  with  $P$  as a lowest vertex and a slope  $\sigma$ , what is the supremum height of the tentpole  $PP'$  such that  $\triangle P'QR$  has slope less than  $\sigma$ ?

Maintaining the entire arrangement of cones of influence is expensive and unnecessary for our purpose; it suffices to obtain a cone that bounds (tightly) the actual cone of influence at  $P$ . In the absence of focusing, the cone of influence of any point  $P$  is contained in the cone of influence of every point  $Q$  of the front such that  $P \in \text{cone}^+(Q)$ .

At each step, we maintain a hierarchical decomposition of the front. We build a bounding cone hierarchy corresponding to this hierarchical partition. See Figure 3.4. We query the cone hierarchy to efficiently maximize the progress in time at each tent pitching step. In  $1D \times \text{Time}$ , this query is equivalent to shooting a ray (the infinite extension of the tentpole into the future) and determining its earliest intersection with any cone of influence. After each step, we update the cones stored in the cone hierarchy to reflect the new wavespeeds computed on the new front.

Because of no-focusing (Axiom 1.1), we can determine (a lower bound on) the slope at a point  $P$  in the future by computing all cones of influence from points  $Q$  on the current front that contain  $P$ . The shallowest such cone determines a lower bound on  $\sigma(P)$ . It can be computationally very expensive to determine the shallowest cone of influence

that contains a given point  $P$ . In particular, the shallowest cone of influence containing  $P$  may correspond to a point  $Q$  arbitrarily far from  $P$ . To compute this nonlocal cone constraint efficiently, we use a standard hierarchical decomposition, called a *bounding cone hierarchy*, of the space domain. The elements in the hierarchy correspond to subsets of the space domain. For each element of the hierarchy, we compute the minimum slope within the corresponding subset of the space domain. The smallest element in the hierarchy is a single simplex. In order to determine the strictest cone constraint that applies locally, we traverse the hierarchy until we determine the simplex with minimum slope whose cone of influence contains  $P$ . In practice, we expect that our algorithm has to examine only a small subset of the hierarchy; we have observed the resulting speed-up in  $1D \times \text{Time}$ . In the worst case, the algorithm has to examine every simplex of the front, but in that case the algorithm will be at most a constant factor slower than one that does not use a bounding cone hierarchy. When a patch is solved, the bounding cones are updated with the new slopes by traversing a path from a leaf to the root of the hierarchy. This hierarchical approximation technique has been applied very successfully to numerous simulation problems, such as the Barnes-Hut divide-and-conquer method (BH86) for  $N$ -body simulations, as well as to collision detection in computer graphics and robot motion planning (LMCG96) and for indexing multi-dimensional data in geographic information systems (Gut84).

## Chapter summary

We have shown how to extend the Tent Pitcher algorithm for arbitrary dimensions to nonlinear problems where the wavespeed is not constant. Our expressions for the causality and progress constraints that apply at each step make explicit the dependence on the slope of the cone of influence most constraining the progress at that step. This dependence is not explicit in the formulæ of Erickson *et al.* because they assume without loss of generality that the slope is 1 everywhere in spacetime. For the constant wavespeed case, the algorithm in this paper is an alternative to the algorithm due to Erickson *et al.* with potentially weaker progress constraints. We can view the algorithm of Erickson *et al.* as looking one step ahead in the sense that the progress constraint at step  $i$  guarantees that the front constructed in step  $i + 1$  is causal. Our algorithm can be viewed as looking further—our progress constraint at step  $i$  guarantees that the front constructed in step  $i + h$  is causal. It needs to be investigated whether the extra complexity of the algorithm for  $h > 2$  or adaptively choosing  $h$  at each step is justified by a more efficient simulation overall.

The nonlocal nature of the cone constraints pose significant challenges while implementing the algorithm in this chapter in parallel. Maintaining a cone hierarchy and performing queries of the sort needed by our algorithm is also a significant challenge for spatial dimensions  $d \geq 3$ .

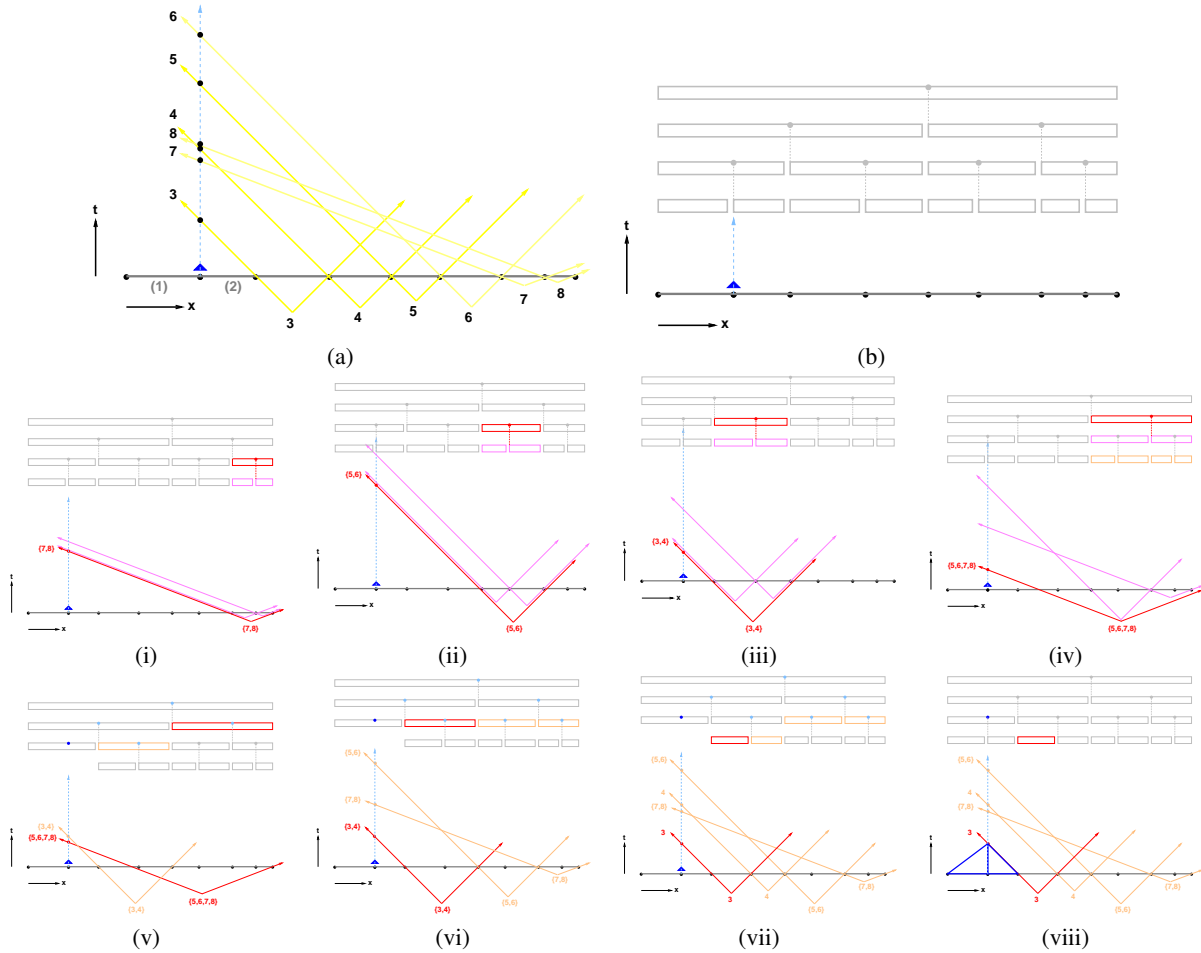


Figure 3.4: Constructing and traversing a bounding cone hierarchy. (i) All the nonlocal cone constraints limiting the height of a tentpole are grouped into (ii) a cone hierarchy (a binary tree) induced by a recursive subdivision of the front. (i)–(iv) The cone hierarchy is built bottom-up by merging pairs of bounding cones at each step. (v)–(viii) The hierarchy is expanded top-down until the strictest cone constraint is a leaf in the hierarchy. Only a fraction of all cone constraints in the hierarchy are examined while traversing the cone hierarchy.



## Chapter 4

# Adaptive refinement and coarsening

The duration of spacetime elements constructed by our algorithm is constrained by causality; however, all spacetime elements constructed by pitching a simplex of the front have the same spatial diameter as the corresponding simplex of the initial front, i.e., the space mesh  $M$ . In other words, every front constructed by our algorithm so far is only as refined as the initial mesh  $M$ . Parts of the spacetime domain, where the solution changes rapidly, need to be meshed with smaller elements to achieve the given error tolerance. In this chapter, we make our meshing algorithms adaptive to local *a posteriori* estimates of the numerical error in response to which we refine or coarsen the current front. Refinement of the current front means that spacetime elements constructed in future steps will have smaller size, and, after a finite number of refinement steps, reduced error. By adapting the size of the spacetime elements to the error estimate, we are able to compute a more efficient mesh for a given error bound. Without adaptivity, we would require the initial space mesh to be as refined as the finest resolution required at any time, which would necessitate many more elements for meshing the same spacetime volume.

In this chapter, we concentrate on the case of constant slope (i.e., constant wavespeed) where  $\sigma$  denotes the slope everywhere in spacetime or more generally  $\sigma = \sigma_{\min}$  is the reciprocal of the globally maximum wavespeed. In Chapter 5 we will discuss adaptive refinement and coarsening in the presence of changing wavespeeds.

Also, in this chapter, we rectify an oversight in the proof of correctness in our paper (ACE<sup>+</sup>04) by including a case in the proof of Theorem 4.3 that was missing from the corresponding theorem in the paper.

### 4.1 Problem statement

Mesh adaptivity in our advancing front framework is the problem of adapting the spatial size of front facets. We require an algorithm that responds to error tolerance requirements by reducing the spatial size of front facets where necessary so that future spacetime elements are smaller and therefore have reduced error. When the error estimate is sufficiently greater than the allowed error, we want the algorithm to increase the spatial size of front facets wherever permitted so that future spacetime elements are bigger. Reducing the error is a requirement for the solution strategy to advance; hence, it is necessary for the algorithm to respond immediately to refinement demands. However, coarsening is a request—an excessively refined mesh still gives a sufficiently accurate solution but it is not efficient. The algorithm should coarsen aggressively to be efficient but it can decide to postpone a coarsening request until a later step.

Our main challenge is to incorporate refinement and coarsening of the front at each step into our advancing front framework. Each iteration of the advancing front algorithm, i.e., each application of the advance function, is understood to be a tent pitching step followed by zero or more refinement and coarsening operations. The actual operations for refining and coarsening the current front are described in detail later in this chapter.

Mesh refinement and coarsening affects spacetime elements in the future when some vertex of the currently refined

front is pitched. Since our algorithm coarsens only a pair of triangles that have been previously obtained by refinement, it is advantageous to start with the coarsest acceptable space mesh, e.g., the coarsest mesh that is still a good enough piecewise linear approximation to the space domain, and let the meshing algorithm adapt the mesh locally as necessary in response to the demands for numerical accuracy. In Chapter 7 we discuss generalization of coarsening beyond a simple undoing of a previous refinement.

In dimension  $d \geq 2$ , we saw in Chapter 2 that nontrivial progress constraints are necessary to guarantee positive progress at each step. These progress constraints are functions of the shape of the triangles on the front. But the shape of front facets, or more accurately the shape of the spatial projection of the front facets, is changing as a result of refinement and coarsening! Therefore, the challenge is to modify the progress constraint to anticipate changes in shape due to an arbitrary amount of refinement.

**OUR SOLUTION** For one-dimensional space domains, we have proved in Chapter 2 that every (causal) front is valid. Therefore, modifying Tent Pitcher to make it adaptive in  $1D \times \text{Time}$  is very easy. The input space mesh is a one-dimensional simplicial complex. To refine the front, we bisect a front segment into two parts, say two equal halves; coarsening reverses this operation by merging two segments that are collinear in spacetime. Since refinement and coarsening does not alter the gradient of the time function restricted to the elements involved in these operations, refinement and coarsening preserve causality.

Note that when pitching a local minimum vertex  $P$ , an interior vertex, the smaller of the temporal aspect ratios of the resulting two triangles is maximized if the two edges incident on  $P$  have approximately equal lengths of their spatial projections. We use this fact to guide our choice of where to subdivide a front segment.

In higher dimensions, we define *progressive* fronts and prove that if a front is progressive then it is valid. For  $d = 2$ , we give an algorithm that, given any progressive front  $\tau_i$ , constructs a next front  $\tau_{i+1} = \text{advance}(\tau_i, p, \Delta t)$  such that  $\tau_{i+1}$  is progressive and  $\tau_{i+1}(p)$  is maximized. Whenever  $p$  is a local minimum of  $\tau_i$ , the progress  $\tau_{i+1}(p) - \tau_i(p)$  is guaranteed to be at least  $T_{\min}$ , which is a function of the input and bounded away from zero. It is necessary to predict the shape of the spatial projections of triangles on the new front  $\tau_{i+1}$  and ensure that  $\tau_i$  satisfies progress constraints that anticipate refinement and coarsening of the new front. We choose a refinement method, called *newest vertex bisection*, that allows us to predict all possible shapes of triangles on any front in the future after an arbitrary number of refinement and coarsening steps. We incorporate constraints associated with every such shape in the progress constraints that must be satisfied by the front at each step, and call such a front a *progressive* front. The details and formal definitions are in Section 4.2.4.

Our algorithm adapts to *a posteriori* estimates of numerical error as follows. A patch is solved as soon as it is created. If the estimated numerical error, i.e., estimated energy dissipation, for any element in the patch is greater than some threshold  $\xi_1$  then the element is marked for refinement and the patch is rejected. If no element is marked for refinement, then the patch is accepted. If the largest estimated numerical error for an element is less than some threshold  $\xi_2$ , where  $\xi_2 < \xi_1$ , then the element is marked as coarsenable. If a patch is rejected, then the front is not advanced and for every element marked for refinement, the corresponding facet of the current front is bisected. Since repeated bisection decreases the spatial diameter, the size of future spacetime elements decreases; we assume that a finite number of refinement steps eventually reduces the numerical error.

For now, we consider only the case  $d = 2$ , i.e., space domains  $M$  that are 2D simplicial complexes consisting of triangles, edges, and vertices embedded in some ambient Euclidean space. Adaptive refinement and coarsening in dimensions  $d > 2$  remains an open problem and we postpone a discussion of higher dimensions until Section 4.3.

**Input:** A one-dimensional space mesh  $M \subset \mathbb{E}^1$

**Output:** A triangular mesh  $\Omega$  of  $M \times [0, \infty)$

The initial front  $\tau_0$  is  $M \times \{0\}$ , corresponding to time  $t = 0$  everywhere in space.

Repeat for  $i = 0, 1, 2, \dots$ :

1. Advance in time an arbitrary local minimum vertex  $P = (p, \tau_i(p))$  of the current front  $\tau_i$  to  $P' = (p, \tau_{i+1}(p))$  such that  $\tau_{i+1}$  is causal and  $\tau_{i+1}(p)$  is maximized.  
If all segments of  $\tau_i$  incident on  $P$  are marked as coarsenable by the solution during the previous iteration, then choose  $P'$  so that the coarsenable segments become collinear in time, unless the height  $\tau_{i+1}(p) - \tau_i(p)$  of the resulting tentpole is too small.
2. Partition the spacetime volume between  $\tau_i$  and  $\tau_{i+1}$  into a patch of triangles, each sharing the tentpole edge  $PP'$ .
3. Compute the solution in the spacetime volume between  $\tau_i$  and  $\tau_{i+1}$  as well as the *a posteriori* error estimate.
4. If the spacetime error indicator tolerates the error in the patch, then advance the front to  $\tau_{i+1}$  and merge every adjacent pair of coarsenable collinear segments.
5. Otherwise, some segments of the front are marked for refinement; bisect each such segment to get the new front  $\tau_{i+1}$ .

---

Figure 4.1: Adaptive meshing algorithm in  $1D \times \text{Time}$

---

If a patch is rejected, then for every tetrahedron  $PP'Q'R'$  marked for refinement the triangle  $pqr$  in the spatial projection is bisected. A pair of triangles can be coarsened by merging them if the result is a single triangle. If the two triangles were previously obtained by bisecting a larger triangle, then they can always be merged whenever they are coplanar in spacetime.

Figure 4.1 describes our adaptive meshing algorithm in  $1D \times \text{Time}$ ; figure 4.15 describes the adaptive algorithm in  $2D \times \text{Time}$ . Both algorithms proceed by pitching local minima, and they refine and coarsen the front in response to error estimates. In the parallel setting, we repeatedly choose an independent set of local minima of the current front, equal to the number of processors, to be advanced in time simultaneously. The resulting patches can be solved independently. If a patch is accepted, the local neighborhood of the front is advanced without any conflicts with other patches. Thus, the solution everywhere in spacetime is computed patch-by-patch in an order consistent with the partial order of dependence of patches.

## 4.2 Meshing in $2D \times \text{Time}$

In this section, we give new adaptive progress constraints in  $2D \times \text{Time}$  that guarantee that each front, even after an arbitrary number of refinement and coarsening steps, is able to make positive progress by tent pitching.

First, we describe our mesh refinement procedure.

### 4.2.1 Hierarchical front refinement

Mesh refinement is needed to achieve the desired numerical accuracy. Intuitively, the larger is the variation in the solution within a subdomain, the smaller is the desired element size. Where the solution is changing slowly and smoothly, it is sufficient to use larger elements—since the number of elements is smaller, the solution procedure is more efficient for the given numerical accuracy. Therefore, the mesh should be only as refined as necessary.

For tracking evolving phenomena efficiently, it is also necessary to coarsen previously refined elements when the phenomenon recedes and the solution is no longer changing rapidly. Thus, coarsening is desirable for computational efficiency. However, over-refinement does not hurt the quality of the solution.

Since our DG method uses a discontinuous formulation, we do not require a smooth grading of element size. In fact, experimental results suggest that if the mesh successfully tracks a sharp shock, then it is perfectly acceptable to use very coarse elements aligned with the shock trajectory.

In the terminology of the different kinds of adaptivity that have been studied in the literature— $p$ -adaptivity (adapt the degree of the polynomial basis functions),  $h$ -adaptivity (adapt the size and number of elements in the mesh), and  $r$ -adaptivity (adapt the locations of nodes in the mesh, e.g., smoothing)—we perform  $h$ -adaptivity to adapt the size of spacetime elements.

**THE CHOICE OF BISECTION METHOD** There is a vast body of literature on mesh refinement for both structured and unstructured meshes. See the survey by Jones and Plassman (JP97) for an introduction. Specifically, we are interested in hierarchical mesh refinement by recursive bisection. Regular subdivisions of a simplex were studied by Bank *et al.* (BSW83) in 2D, and Edelsbrunner and Grayson (EG00) in higher dimensions. Mesh refinement in 2D requires bisecting specified triangles to decrease their diameter as well as propagating to neighboring triangles to maintain a triangulation. The longest edge refinement introduced by Rosenberg and Stenger (RS75) has been later popularized by Rivara (Riv97; Riv84; Riv96). Newest vertex bisection was originally developed by Sewell (Sew72) and later adapted by Mitchell (Mit88; Mit89; Mit91). Arnold *et al.* (AMP00), Bey (Bey95), Bänsch (Bän91), Liu and Joe (LJ94; LJ95), Maubach (Mau95), and Bey (Bey00) extended newest vertex bisection to higher dimensions. Most importantly, Arnold *et al.* (AMP00) proved that the number of shapes generated by their recursive bisection of a simplex is finite.

Our adaptive algorithm uses the *newest vertex bisection* refinement method, originally developed by Sewell (Sew72), later adapted by Mitchell (Mit88; Mit89; Mit91) in the context of multigrid methods, and still later studied and generalized to three dimensions by Bänsch (Bän91). This method is similar to, but not identical to, *longest-edge* refinement (RS75; Riv84; Riv96).

We call the newest vertex of a triangle its *apex* and the opposite edge its *base*. Initially, one vertex of each triangle in the mesh is chosen arbitrarily as its apex. Newest vertex bisection replaces a triangle with two smaller triangles, each with half the area of the original triangle, obtained by bisecting along the line segment through the apex and the midpoint of the base. The new vertex introduced at the midpoint is the newest vertex of both smaller triangles. See Figure 4.2.

The descendants of any marked triangle under newest vertex bisection fall into only eight homothetic classes (Figure 4.2). There are only four directions along which the triangle or any of its descendants can be further bisected. These four directions are parallel to the three edges of the triangle and the bisecting segment. Each of the four ways to choose three of the four directions gives two similar triangle shapes that are mirror images of each other, for a total of eight triangle shapes, equivalent up to translation and scaling. Any two triangles in the same equivalence class have

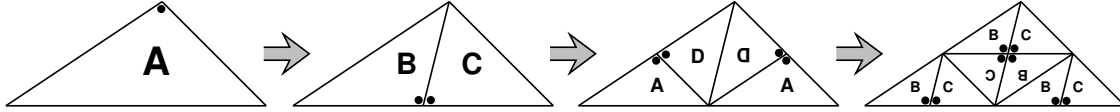


Figure 4.2: Newest vertex refinement (ACE<sup>+</sup>04). Newest vertices of each triangle are marked.

corresponding newest vertices. Refinement by three levels is guaranteed to decrease the diameter by at least a half.

A front triangle  $PQR$  and its grandparent  $\triangle ABC$  create homothetic tetrahedra when their corresponding vertices are pitched. This is because causality and progress constraints are gradient constraints that scale with the spatial geometry of front triangles. Therefore, our refinement algorithm using newest vertex bisection adapts the resolution of the spacetime mesh but is limited in its ability to adapt the shape and temporal aspect ratio of spacetime tetrahedra.

**PROPAGATION** When we refine one triangle in a mesh, we may be forced to refine other nearby triangles in order to maintain a conforming triangulation. Maintaining a triangulated front is necessary for our algorithm—nonconforming or dangling vertices create complications that we do not know how to solve yet.

We call an edge of the triangulation a *terminal edge* if it is the base of every triangle incident on it.

Suppose vertex  $a$  is the apex of a  $\triangle abc$  that is bisected (Figure 4.3). If  $bc$  is not a boundary edge then some neighboring triangle  $\triangle cbe$  shares the edge  $bc$ . To maintain a triangulation,  $\triangle cbe$  must be bisected also. If  $bc$  is not the base of  $\triangle cbe$ , then the child of  $\triangle cbe$  sharing edge  $bc$  must be bisected as well, and the bisection of  $\triangle cbe$  will propagate recursively; see Figure 4.3.

It is easy to prove that this propagation terminates, regardless of which vertex is chosen as the apex of each triangle. Suppose a refinement of  $\triangle abc$  with apex  $a$  propagates to a neighboring triangle sharing the edge  $bc$ . A single newest vertex bisection of  $\triangle abc$  makes the edges  $ab$  and  $ac$  the bases respectively of the two children of  $\triangle abc$ . If the propagation revisits  $\triangle abc$ , it must return by bisecting either the edge  $ab$  or the edge  $ac$ . But since these edges are now terminal edges, the propagation terminates at that step.

The propagation path touches every triangle in the worst case, but in practice, the propagation path usually has small constant length; see Suárez *et al.* (SPC03) for an analysis of a similar refinement algorithm. Because we bisect triangles first and then propagate, instead of the other way round, our algorithm terminates, regardless of which vertices are marked in each triangle: each triangle in the mesh is bisected at most twice. (Mitchell’s original head-recursive algorithm (Mit88; Mit89; Mit91) can enter an infinite loop if the initial selection of marks does not satisfy a certain matching condition.)

The propagation follows a directed path in the dual graph of the triangulation, leaving each triangle along the dual edge corresponding to the base of the triangle. The propagation terminates when the base of the last triangle bisected is a terminal edge. The propagation either encounters a boundary edge or the propagation revisits one of the children of a triangle that was bisected earlier along the propagation path; see Figure 4.4.

Newest vertex bisection never subdivides any angle of a triangle more than once. If the apex of each triangle in the initial mesh is the vertex with largest angle, then every vertex  $v$  is the apex of at most 5 triangles incident on  $v$ . (In the degenerate case where six equilateral triangles meet at a vertex, we can break ties using a straightforward symbolic perturbation scheme.) Thus, the degree of a vertex  $v$  in the initial space mesh increases by at most 5 as a result of refinement. If  $v$  is not a vertex of the initial space mesh then the degree of  $v$  is 4 when  $v$  is inserted and is at most 8 at any subsequent step. We conclude that if a triangulation has maximum degree  $\Delta$ , then any refinement of that triangulation has maximum degree at most  $\max\{\Delta + 5, 8\}$ .

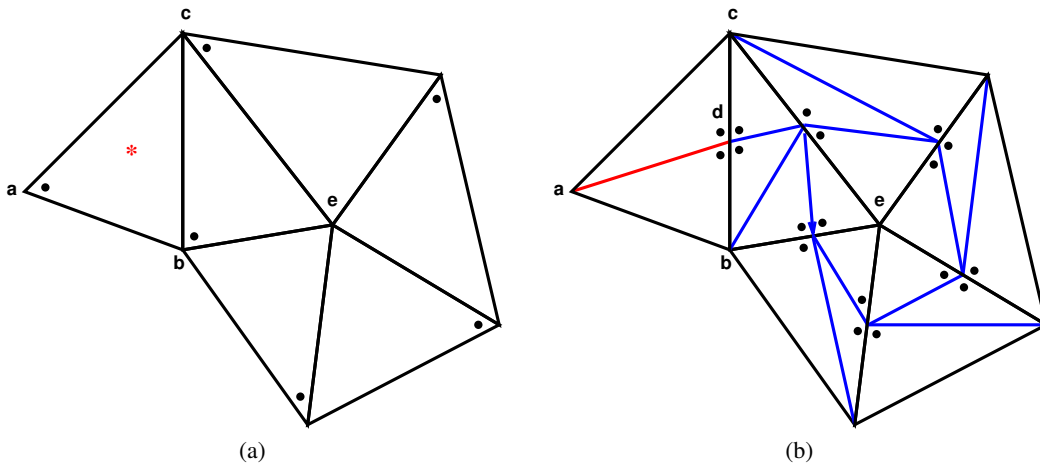


Figure 4.3: Refining  $\triangle abc$  propagates to neighboring triangles: (a) before and (b) after refinement.

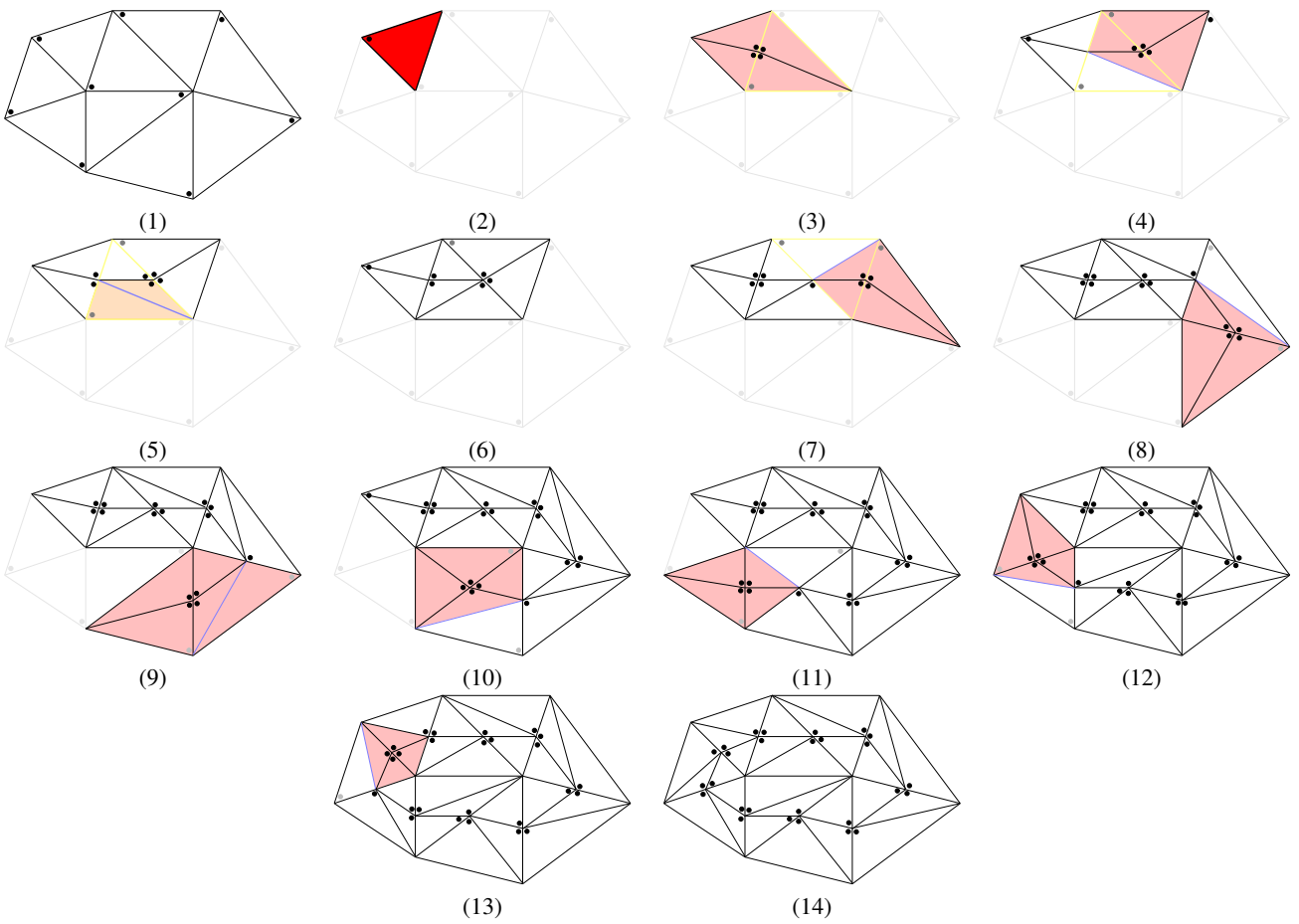


Figure 4.4: Refinement propagation path terminates when it revisits a triangle.

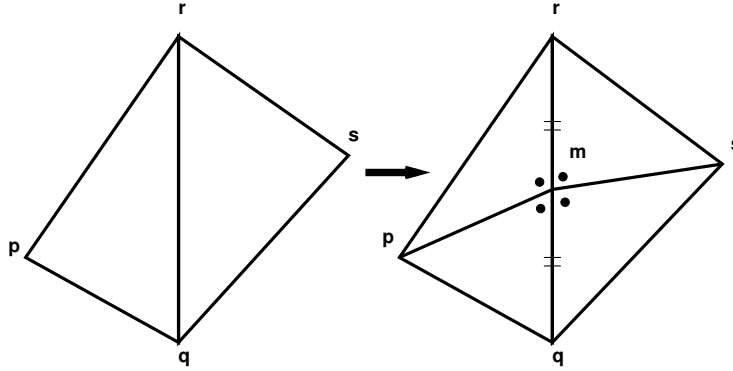


Figure 4.5: Bisecting an edge and the two triangles incident on it

BISECTTRIANGLE(Triangle  $\triangle pqr$ ):

1. Let  $qr$  be the base of  $\triangle pqr$ ;
2. Let  $\triangle qrs$  be the neighbor of  $\triangle pqr$  sharing the edge  $qr$ ;
3. Comment: If  $qr$  is a boundary edge, there is no such neighbor.
4. Bisect the edge  $qr$  by inserting a new vertex  $m$  at its midpoint;
5. Insert the edges  $pm$  and  $ms$ ;
6. Mark all four angles at  $m$ ;
7. If  $qr$  is not the base of  $\triangle qrs$ :
8.     Mark  $\triangle qrs$ ;

Figure 4.6: Bisecting a triangle and its neighbor.

**BASIC MESH OPERATIONS** The entire refinement propagation can be expressed as a sequence of edge bisection and edge flip operations. Bisecting a terminal edge achieves newest-vertex bisection of all triangles incident on it. However, if an edge  $e$  is not a terminal edge, then bisecting  $e$  leaves at least one of the triangles incident on  $e$  in a *dirty* state because an edge of this triangle other than its base has been bisected. To rectify this situation, we *clean* the dirty triangle by another edge bisection followed by an edge flip. In this fashion, every clean triangle is subdivided according to the rules of newest-vertex bisection. Dirty triangles are transient and are cleaned before the surrounding neighborhood of the front is advanced.

**Edge bisection** This operation bisects an edge shared by one or two triangles; see Figure 4.5. The new vertex is the apex of all four new triangles. Bisecting a triangle at *level*  $l$  produces two new *children* at level  $l + 1$ ; every triangle in the original space mesh is at level zero. The set of all triangles that ever appear on any front form a forest of rooted binary trees with each triangle in the initial space mesh as the root of some tree in the forest. The *height* of a node in the refinement tree is the number of edges on a longest path from the node to any of its descendants.

**Edge flip** An edge flip replaces one diagonal of a convex quadrilateral with the other diagonal. Note how in Figure 4.7, the apex of the adjacent triangle (shown dashed) is changed. On the left, we see  $\triangle pqr$  first split into  $\triangle pqu$  and  $\triangle uqr$ , then  $\triangle uqr$  is split into  $\triangle uqv$  and  $\triangle uvr$ . On the right, after the flip operation, we have  $\triangle pqr$  first split into  $\triangle pqv$  and  $\triangle pvr$ , and then  $\triangle pvr$  split into  $\triangle pvu$  and  $\triangle uvr$ . Vertex  $p$  is the apex of  $\triangle pqr$ . The refinement subtree rooted at  $\triangle pqr$  changes as a result of the edge flip.

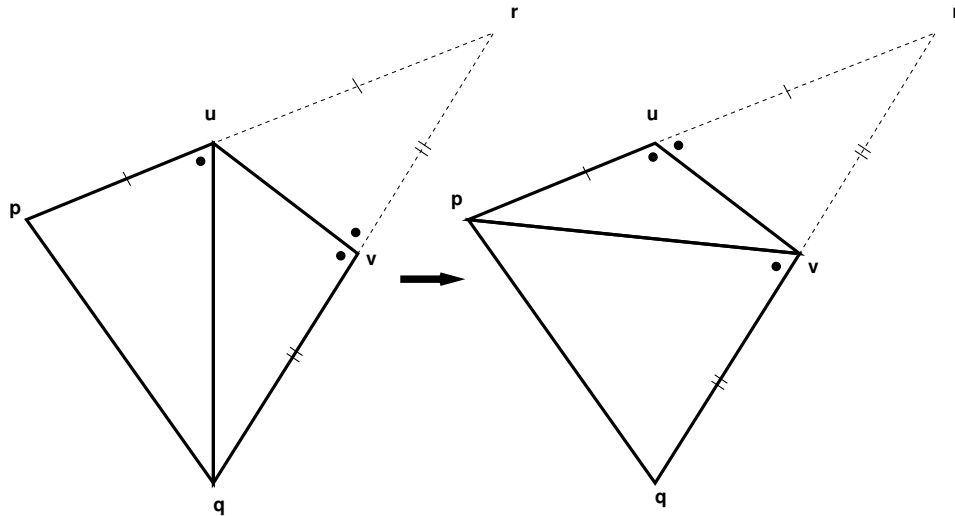


Figure 4.7: Edge flip

**LAZY PROPAGATION** Edge bisections caused by propagation unnecessarily create smaller triangles in parts of the front even where the error estimate is sufficiently below the acceptable threshold. If the propagation were delayed until a later step, the spacetime mesh would contain fewer tetrahedra. In a parallel setting, interprocessor communication is inefficient; so, it is useful to allow the algorithm to proceed on unrelated processors and not require all processors to wait until the entire propagation sequence has been executed.

Therefore, we propagate refinements *lazily*, by temporarily bisecting an edge of a neighboring triangle other than its base and marking this triangle as *dirty*. A dirty triangle can be cleaned up later by performing one edge bisection, which in turn can be propagated lazily, plus one edge flip. Lazy propagation is particularly useful for parallel implementation, where the mesh may be distributed over multiple processors, because it minimizes both communication costs and deadlocks. If a processor needs to refine a triangle in its subset of the mesh, it need not wait for the entire propagation sequence (which may be controlled by other processors) to be completed before proceeding with its next task. Even in the serial case, lazy refinement may reduce the number of changes to the mesh, since later coarsening may stop the propagation of refinement early.

**Earnest vs. lazy propagation** Algorithm REFINE is called to refine a triangle currently on the front. By definition, this triangle is a leaf in the refinement forest. The contrast between earnest propagation (Figure 4.8) and lazy propagation (Figure 4.9) is shown in Figure 4.12. Earnest propagation causes the adjacent triangle to be split which may propagate further. Lazy propagation (bottom path) splits the adjacent triangle but does not propagate further immediately—the gray arrows in Figure 4.12 are not traversed until later. Instead, the propagation is delayed until the adjacent triangle needs to be refined or pitched. In the interim, the triangulation may consist of transient dirty triangles. After cleaning up, the final result is the same.

### Refinement with lazy propagation

As long as all dirty triangles are cleaned up, refinement with lazy propagation is identical to refinement with earnest propagation; see Figure 4.12.



```

REFINE(Triangle  $\triangle pqr$ ):
1.  REFINEANDPROPAGATE( $\triangle pqr$ );

REFINEANDPROPAGATE(Triangle  $\triangle pqr$ ):
1.  Let  $e$  be the base of  $\triangle pqr$ ;
2.  Let  $\tau$  be the neighboring triangle that shares the edge  $e$ ;
3.  BISECTTRIANGLE( $\triangle pqr$ ); (Figure 4.6)
4.  If  $\tau$  is marked:
4.1.  CLEANUP( $\tau$ );

CLEANUP(Triangle  $\triangle pqr$ ):
1.  Let  $p$  be the apex of  $\triangle pqr$ ;
2.  Let  $\triangle pqs$  and  $\triangle sqr$  be the current children of  $\triangle pqr$ ;
3.  {Comment: The edge opposite  $q$  is currently bisected.}
4.  REFINEANDPROPAGATE( $\triangle sqr$ );
5.  Flip the edge  $qs$ ;

```

Figure 4.8: Refinement with earnest propagation.

## 4.2.2 Coarsening

Coarsening is the opposite of refinement and hence called *de-refinement*; we coarsen locally by undoing a single edge bisection. Unlike refinement, coarsening does not require propagation further into the mesh to maintain a conforming triangulation, although one coarsening step may make other coarsenings possible. In particular, if we refine a triangle and then immediately coarsen, we can (but need not) coarsen along the entire refinement path.

DEREFINE is called to coarsen a triangle currently on the front that is a strict descendant of some triangle in the original mesh. By definition, the triangle being coarsened is a leaf in the refinement forest and its parent exists. See Figure 4.13.

When the propagation path of a refinement loops back on itself, there will be no degree-4 vertex in the portion of the mesh corresponding to this loop (Figure 4.14), and algorithm DEREFINE will not apply. The solution is to perform an edge flip to create a degree-4 vertex and then call DEREFINE. The edge flip will create a dirty triangle, and this dirty triangle can be coarsened immediately by DEREFINE along with its neighbor.

## 4.2.3 Adaptive meshing in $2D \times \text{Time}$

We are now ready to describe an iteration of our advancing front algorithm. Advance a single vertex  $p$  by a positive amount, where  $p$  is any local minimum of the current front  $\tau_i$ , to get the new front  $\tau_{i+1}$  such that every triangle  $pqr$  on  $\tau_{i+1}$  is progressive. In the parallel setting, advance any independent set of local minima forward in time, each subject to the above constraint.

To incorporate adaptivity into our meshing algorithm, we make a small change to the main loop. At each iteration, just as before, we choose a local minimum vertex  $P$  of the front, move it forward in time to create a tent, and pass the tent and its inflow data to the spacetime DG solver. We assume that the solver also computes an *a posteriori* estimate of its own numerical error. If the error within any element of the tent is above some threshold, the solver *rejects* the patch, at which point the meshing algorithm throws away the tent and refines the facets of the front whose elements had high error. (Alternately, we could refine the facets until their diameter is smaller than a target length scale computed by the

```

LAZYREFINE(Triangle  $\triangle pqr$ ):
1. If parent( $\triangle pqr$ ) exists and is marked dirty:
1.1.   {Comment:  $\triangle pqr$  is transient and so we cannot refine  $\triangle pqr$ .}
1.2.   CLEANUP1(parent( $\triangle pqr$ ));
2. Else:
2.1.   LAZYREFINEANDPROPAGATE( $\triangle pqr$ );
LAZYREFINEANDPROPAGATE(Triangle  $\triangle pqr$ ):
1. Let  $e$  be the base of  $\triangle pqr$ ;
2. Let  $\tau$  be the neighboring triangle that shares the edge  $e$ ;
3. BISECTTRIANGLE( $\triangle pqr$ ); (Figure 4.6)
4. If parent( $\tau$ ) exists and is marked dirty:
4.1.   {Comment:  $\tau$  is transient.}
4.2.   CLEANUP2(parent( $\tau$ ));
CLEANUP1(Triangle  $\triangle pqr$ ): (Figure 4.10)
1. {Comment:  $\triangle pqr$  is marked and has height 1.}
2. Let  $p$  be the apex of  $\triangle pqr$ ;
3. Let  $\triangle pqs$  and  $\triangle sqr$  be the current children of  $\triangle pqr$ ;
4. {Comment: The edge opposite  $q$  is currently bisected.}
5. LAZYREFINEANDPROPAGATE( $\triangle sqr$ );
6. Flip the edge  $qs$ ;
CLEANUP2(Triangle  $\triangle pqr$ ): (Figure 4.11)
1. {Comment:  $\triangle pqr$  is marked and has height 2.}
2. Let  $p$  be the apex of  $\triangle pqr$ ;
3. Let  $\triangle pqs$  and  $\triangle sqr$  be the current children of  $\triangle pqr$ ;
4. {Comment: The edge opposite  $q$  is currently bisected.}
5. If  $\triangle pqs$  is a leaf:
5.1.   {Comment:  $\triangle sqr$  is subdivided.}
5.2.   Flip the edge  $qs$ ;
6. Else if  $\triangle sqr$  is a leaf:
6.1.   {Comment:  $\triangle pqs$  is subdivided.}
6.2.   Let  $\triangle pst$  and  $\triangle tsq$  be the children of  $\triangle pqs$ ;
6.3.   REFINEANDPROPAGATE( $\triangle sqr$ );
6.4.   Flip the edge  $qs$ ;
6.5.   Flip the edge  $st$ ;

```

Figure 4.9: Refinement with lazy propagation.

solver.) Note that this refinement may propagate far outside the neighborhood of  $P$ . We accept the numerical solution and update the front only if the error within every element of the patch is acceptable.

On the other hand, the error estimate within an element may fall below some second threshold, indicating that the mesh is finer than necessary to compute the desired result. In this case, the DG solver marks the outflow face of that element as *coarsenable*. We can coarsen four facets of the front into two only if they are the result of an earlier refinement, they are all marked as coarsenable, and each pair of triangles to be merged is coplanar. To make coarsening possible, our algorithm tries to make coarsenable siblings coplanar, by lowering the top of the tent. However, to avoid very thin elements, we accept the lower tent only if its height is above some threshold. If the lower tent is accepted and its outflow faces are still marked coarsenable, then we coarsen the front. This means, of course, that merging a pair of coarsenable triangles may be delayed due to the coplanarity constraint imposing a too-small tentpole height. We definitely observe this in practice, leading to a more inefficient mesh than absolutely necessary. In fact, coarsening

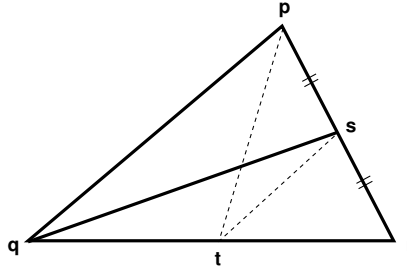


Figure 4.10: Before (solid) and after (dotted) one edge bisection and an edge flip performed by CLEANUP1

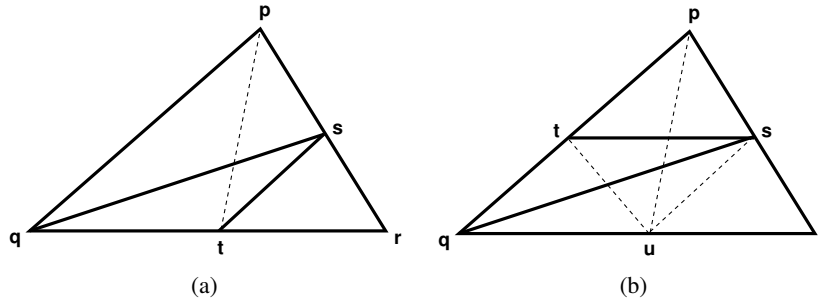


Figure 4.11: Before (solid) and after (dotted) CLEANUP2: (a) only an edge flip is required; (b) an edge bisection followed by two edge flips are required

may be delayed several steps. In Chapter 6, we give an algorithm to ensure that every coarsenable pair of triangles will eventually be made coplanar and merged, while still guaranteeing a bounded minimum tentpole height.

See Figure 4.15 for an outline of the adaptive Tent Pitcher algorithm. See Figure 4.16 for an illustration of the effect of refine and coarsen operations interspersed with tent pitching steps.

**CLEANING UP AFTER A LAZY PROPAGATION** If refinement is being propagated lazily, we must ensure that the triangles incident on  $p$  are clean.

CLEANUPBEFOREPITCHING(Vertex  $p$ ):

1. For every triangle  $\triangle pqr$  incident on  $p$ :
2.     If  $\text{parent}(\triangle pqr)$  exists and is marked dirty:
3.         CLEANUP1( $\text{parent}(\triangle pqr)$ );

**COPLANARITY CONSTRAINTS** While pitching  $p$ , we see whether coarsenable triangles adjacent to  $p$  can be made coplanar with their siblings after pitching. For each triangle  $\triangle pqs$  incident on  $p$ , consider the four triangles neighboring  $\triangle pqs$  referred to in DEREFINE. If all the four triangles are currently marked as coarsenable, we solve for  $\tau'(p)$  to compute the new value of  $\tau'(p)$  that would make  $p$  coplanar with  $q$ ,  $r$ , and  $u$ . This is the value of  $\tau'(p)$  that satisfies what we call the *coplanarity constraint*. Satisfying the coplanarity constraint may require a shorter tentpole at  $p$ ; if the shorter height is less than some constant (such as  $1/10$ ) times the height *without* the constraint, then we choose to ignore the coplanarity constraint to avoid creating degenerate elements. Otherwise, the final height of the tentpole at  $p$  is limited by the coplanarity constraint and coarsenable triangles can be merged immediately after pitching  $p$ .

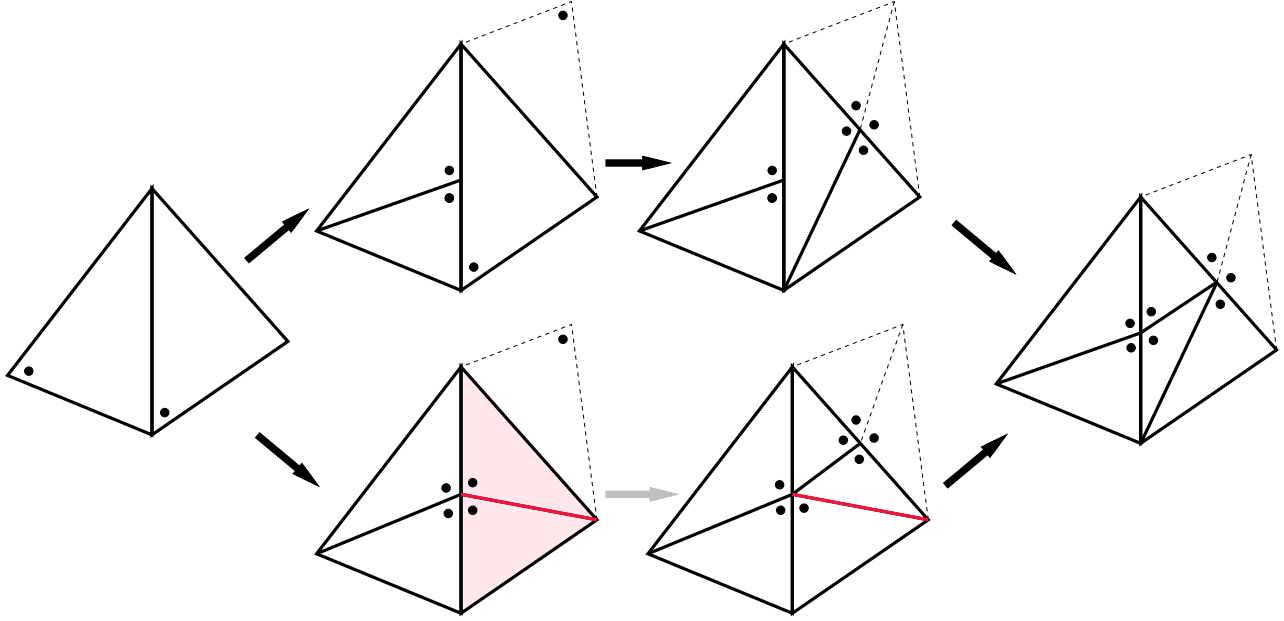


Figure 4.12: Earnest propagation (top path) vs. lazy propagation (bottom path)

#### 4.2.4 Causality and Progress Constraints

To complete the description of our adaptive version of Tent Pitcher, all that remains is to define *progressive* triangles and fronts, i.e., to define the progress constraints that limit the new time value for each vertex to be pitched. Each triangle in the space mesh imposes constraints on the time values at each of its vertices. When we pitch a tent over a local minimum vertex  $P$ , the new time value  $\tau_{i+1}(p)$  is simply the largest value that satisfies the constraints for every triangle  $pqr$  incident on  $p$  in the space mesh.

One constraint is of course the causality constraint of Equation 2.2, repeated below:

$$\frac{\tau_{i+1}(p) - \tau_i(\bar{p})}{|p\bar{p}|} < \sqrt{\sigma^2 - \|\nabla \tau_i|_{qr}\|^2}$$

The more subtle and important change in our algorithm is the introduction of new progress constraints. In the earlier non-adaptive algorithm (EGSÜ02), the progress constraint was a function of the shape of the underlying space elements. In our new algorithm, the shape of the underlying element is subject to change; each triangle in the current front may be the result of any number of refinements since the last time any ancestor or descendant of that triangle was pitched. Consequently, our progress constraints must take into account the shapes of *all possible* descendants of a triangle simultaneously. This requirement motivates our choice of newest vertex refinement; because the descendants of any triangle fall into only a finite number of homothety classes, we have only a finite number of simultaneous progress constraints.

We can visualize these constraints by referring back to our circle diagram; see Figure 4.18. A minimal set of progress constraints can be obtained by simply taking the union of the non-adaptive progress constraints of the eight shapes in the hierarchy. Recall that each of the eight shapes, corresponding to a descendant of  $\triangle pqr$ , defines a forbidden zone where the gradient vector of  $\triangle pqr$  must not lie. We call these the “primary” forbidden zones. The

DEREFINE(Triangle  $\triangle pqs$ ):

1. Let  $\triangle psr$  be the sibling of  $\triangle pqs$ , i.e., edge  $qr$  is currently bisected;
2. Verify that  $\triangle pqs$  and  $\triangle psr$  are leaves and are coplanar;
3. Verify that  $s$  has degree 4;
4. Let  $u$  be the fourth neighbor of  $s$  other than  $\{p, q, r\}$ ;
5. Verify that  $\triangle rsu$  and  $\triangle usq$  are leaves and are coplanar;
6. {Comment: Equivalently,  $r-s-q$  must be collinear.}
7. {Comment: All four triangles incident on  $s$  need NOT be coplanar.}
8. Replace  $\triangle pqs$  and  $\triangle psr$  with their parent  $\triangle pqr$ ;
9. Replace  $\triangle rsu$  and  $\triangle usq$  with their parent  $\triangle rqu$ ;
10. {Comment: The two new triangles  $\triangle pqr$  and  $\triangle rqu$  are not dirty.}
11. If parent( $\triangle pqr$ ) exists and is coarsenable:
12.     DEREFINE( $\triangle pqr$ );
13. If parent( $\triangle rqu$ ) exists and is coarsenable:
14.     DEREFINE( $\triangle rqu$ );

Figure 4.13: Algorithm to de-refine

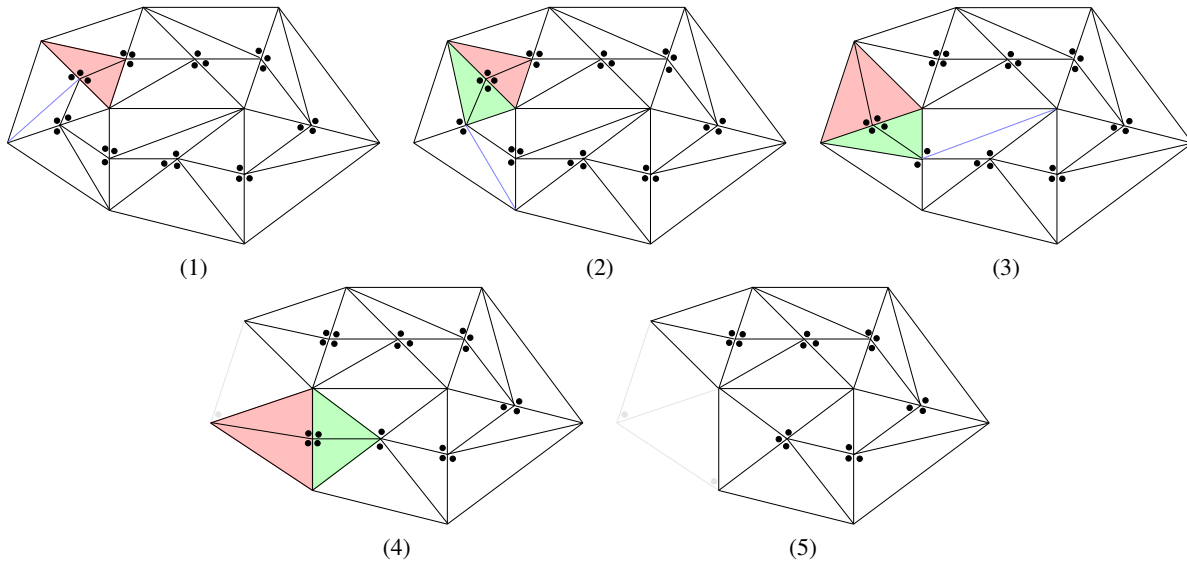


Figure 4.14: De-refining a loop in the refinement propagation path requires edge flips to create degree-4 vertices. To merge the first pair of triangles, an edge flip is necessary, (1)→(2), to create a degree-4 vertex that can now be deleted. Subsequent coarsening steps (2)→(3) and (3)→(4) each require an edge flip.

**Input:** A triangulation  $M \subset \mathbb{R}^2$

**Output:** A tetrahedral mesh of  $M \times [0, \infty)$

Initial front  $\tau_0$  is the space mesh at time  $t = 0$ , i.e.,  $\tau_0(p) = 0$  for every  $p \in V(M)$

Repeat for  $i = 0, 1, 2, \dots$ :

- Lift a local minimum vertex  $p$  of the current front  $\tau_i$  to obtain the new front  $\tau_{i+1}$  such that every triangle  $pqr$  on  $\tau_{i+1}$  is progressive.
- Solve the resulting patch.
- If the patch is rejected by solver, one or more elements in the patch are marked for refinement.
- For every element marked for refinement, bisect its inflow facet; otherwise, advance the front.
- If any pair of coarsenable siblings are coplanar, then coarsen this pair.

Figure 4.15: Adaptive Tent Pitcher algorithm with refinement and coarsening

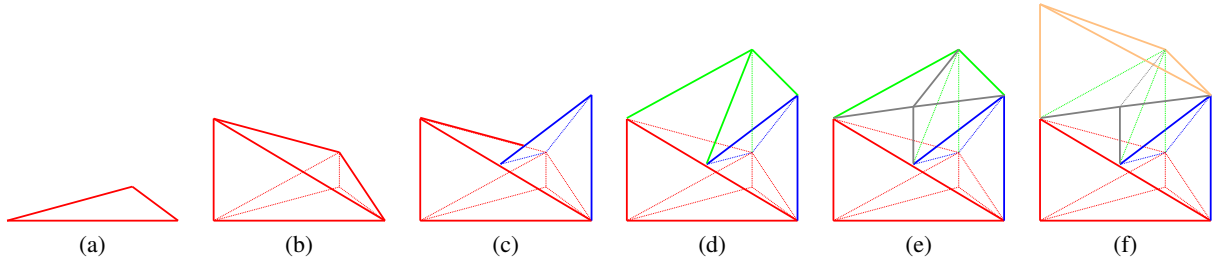


Figure 4.16: A sequence of 5 tents pitched by the adaptive algorithm: (a)→(b) pitch twice, (b)→(c) refine and pitch, (c)→(d) pitch, (d)→(e) pitch, (e)→(f) coarsen and pitch

progress constraint that the corresponding triangle  $PQR$  on the front must satisfy is the conjunction of the progress constraint for each of these eight shapes. In addition, we must also forbid “secondary zones” from which the only alternative, due to the nature of Tent Pitcher, is to enter a primary forbidden zone. Staying outside the primary and secondary forbidden zones is sufficient to guarantee that the progress at each step is bounded away from zero.

Fix two real numbers  $\varepsilon$  and  $\varphi$  such that  $0 < \varepsilon < \varphi < (1 + \varepsilon)/2 < 1$ . For any triangle  $\triangle abc$  with apex  $a$ , we define the *diminished width* of  $\triangle abc$  as follows.

**Definition 4.1** (Diminished width (ACE<sup>+</sup>04)). *Let  $abc$  be an arbitrary triangle, where  $a$  is the apex. (See Figure 4.17.) The diminished width of  $\triangle abc$  is defined as*

$$\tilde{w}(abc) := \min \left\{ \begin{array}{l} (1 - \varepsilon)\text{dist}(a, \text{aff } bc), \\ (1 - \varphi)\text{dist}(b, \text{aff } ac), \\ (1 - \varphi)\text{dist}(c, \text{aff } ab) \end{array} \right\}$$

The first distance is measured from the apex to the opposite edge and is scaled differently from the other two

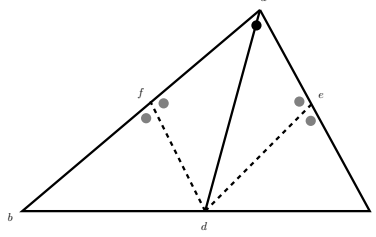


Figure 4.17:  $\triangle abc$  where  $a$  is the apex.

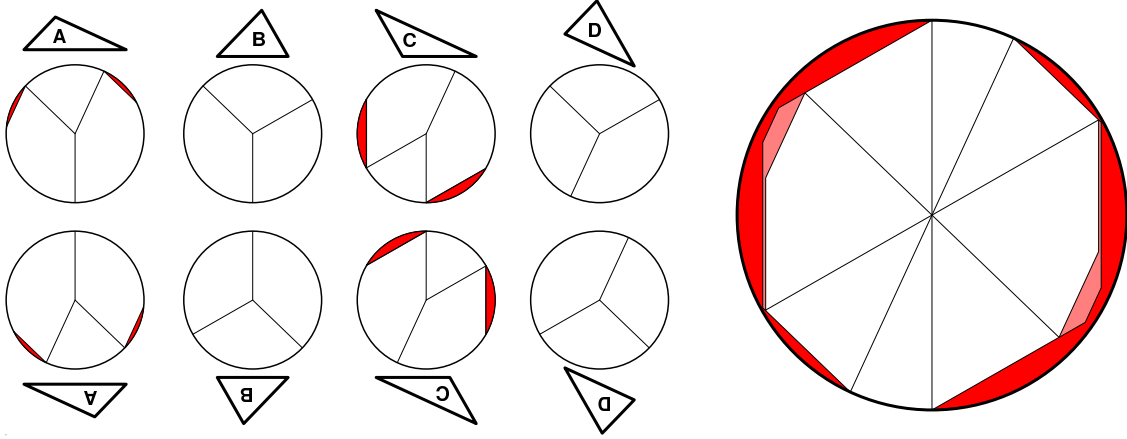


Figure 4.18: The adaptive progress constraint is obtained from the progress constraint for each of the eight different shapes of descendant triangles.

altitudes. This definition extends recursively to any descendants of  $\triangle abc$  obtained by newest vertex subdivision; in the interest of readability, we will always list the vertices of any triangle with the apex first. We express our new progress constraints algebraically by limiting the difference in time values along each edge in the subdivided triangle, as follows.

**Definition 4.2** (Adaptive progress constraint  $\sigma$ ). *Fix  $\varepsilon$  and  $\varphi$  such that  $0 < \varepsilon < \varphi < (1 + \varepsilon)/2 < 1$ . Let  $\triangle ABC$  be an arbitrary triangle of a front  $\tau$  with apex  $A$ . Let  $d$ ,  $e$ , and  $f$  be midpoints of sides  $bc$ ,  $ac$ , and  $ab$  respectively (Figure 4.17). We say that the triangle  $ABC$  satisfies adaptive progress constraint  $\sigma$  if and only if*

$$\begin{aligned}
 |\tau(a) - \tau(b)| &\leq 2\tilde{w}(dca)\sigma \\
 |\tau(a) - \tau(d)| &\leq \tilde{w}(abc)\sigma \\
 |\tau(a) - \tau(c)| &\leq 2\tilde{w}(dab)\sigma \\
 |\tau(b) - \tau(c)| &\leq 4\tilde{w}(ead)\sigma
 \end{aligned}$$

The constraints in the definition of the progress constraint apply recursively to all descendants of the triangle  $\triangle abc$ , but these recursive constraints are equivalent to one of the four constraints above.

Now suppose we are pitching a triangle  $\triangle pqr$  of the front  $\tau$ , where  $\tau(p) \leq \tau(q) \leq \tau(r)$ . Let  $w$  be the midpoint of  $qr$ ; let  $u$  be the midpoint of  $pr$ ; and let  $v$  be the midpoint of  $pq$ ; see Figures 4.19 and 4.20. Depending on which of

the three vertices is marked as the apex, the new time value  $\tau'(p)$  is bounded as a result of these progress constraints in the three different ways enumerated below. Notice that when  $p$  is not the apex, lifting  $p$  also lifts either  $u$  or  $v$ , so progress constraints along edges  $qu$  or  $rv$  also indirectly limit  $\tau'(p)$ .

If  $p$  is the apex:

$$\tau'(p) \leq \min \left\{ \begin{array}{l} \tau(q) + 2\tilde{w}(rpw)\sigma, \\ \tau(s) + \tilde{w}(pqr)\sigma, \\ \tau(r) + 2\tilde{w}(wpq)\sigma \end{array} \right\} \quad (4.1)$$

If  $r$  is the apex:

$$\tau'(p) \leq \min \left\{ \begin{array}{l} \tau(q) + 4\tilde{w}(uvr)\sigma, \\ \tau(r) + 2\tilde{w}(vqr)\sigma, \\ 2\tau(r) - \tau(q) + 2\tilde{w}(rpq)\sigma \end{array} \right\} \quad (4.2)$$

If  $q$  is the apex:

$$\tau'(p) \leq \min \left\{ \begin{array}{l} \tau(q) + 2\tilde{w}(uqr)\sigma, \\ \tau(r) + 4\tilde{w}(wuq)\sigma, \\ \tau(q) - \tau(r) + 2\tilde{w}(rpq)\sigma \end{array} \right\} \quad (4.3)$$

The adaptive progress constraint (Definition 4.2) is stronger than the non-adaptive progress constraint (Definition 2.6); in particular, the new progress constraint limits the gradient of all three edges of  $\triangle PQR$ , not just the highest edges, and anticipates future refinement and coarsening of triangles on the front by newest vertex bisection by also limiting the gradient along the bisector edge. Of course, our algorithm works even when no refinement or coarsening operations are actually performed.

The following theorems were proved by Abedi *et al.*. In this section, we rectify an oversight in the proof of correctness in the paper by Abedi *et al.* (ACE<sup>+</sup>04) by including a case in the proof of Theorem 4.3 that was missing.

**Theorem 4.3.** *If a front  $\tau_i$  is progressive, then for every local minimum vertex  $p$ , for every  $\Delta t \in [0, \varepsilon w_p \sigma_{min}]$ , the front  $\tau_{i+1} = \text{advance}(\tau_i, p, \Delta t)$  is causal.*

*Proof.* Since only the triangles of the front incident on  $P$  advance along with  $p$ , we can restrict our attention to an arbitrary triangle  $pqr$  incident on  $p$ . Let  $\tau$  and  $\tau'$  denote  $\tau_i|_{pqr}$  and  $\tau_{i+1}|_{pqr}$  respectively. Let  $\bar{p}$  be the orthogonal projection of  $p$  onto line  $qr$ .

We consider two cases separately.

**CASE 1:**  $\tau(\bar{p}) \geq \tau(\mathbf{q}) \geq \tau(\mathbf{p})$  See Figure 4.19. In this case, we have  $\angle pqr \leq \pi/2$ . We will show that

$$\|\nabla \tau|_{qr}\| \leq (1 - \varepsilon)\sigma$$



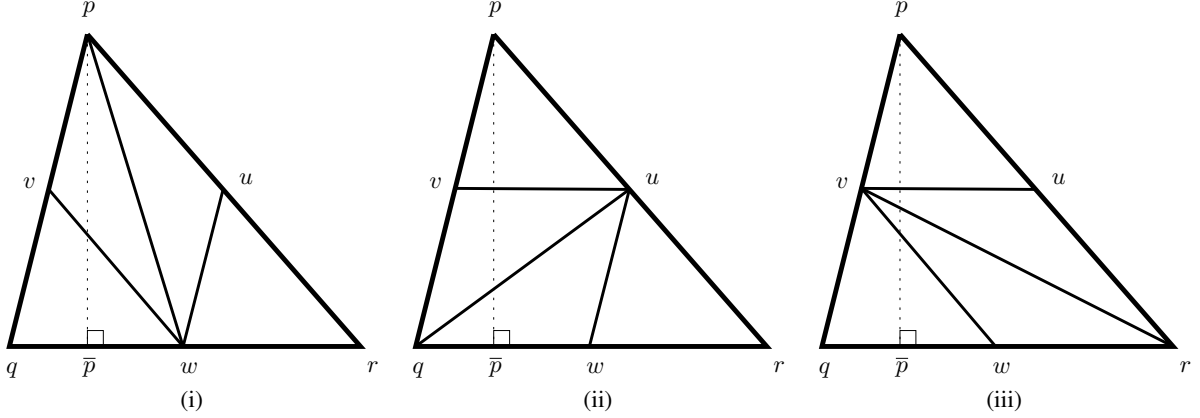


Figure 4.19: Triangle  $pqr$  with  $\angle pqr \leq \pi/2$  with apex at  $p$ ,  $q$ , and  $r$  respectively.

i.e., that

$$\tau(r) - \tau(q) \leq (1 - \varepsilon)|qr|\sigma.$$

The proof then follows from Lemma 2.4 because the antecedent of the lemma is satisfied.

We consider three cases depending on which vertex of  $\triangle pqr$  is the apex.

If  $p$  is the apex, then

$$\begin{aligned} \tau(r) - \tau(q) &\leq 4\tilde{w}(upw)\sigma && \text{(by the progress constraint)} \\ &\leq 4(1 - \varepsilon)\text{dist}(u, \text{aff } pw)\sigma && \text{(by definition of diminished width)} \\ &= 2(1 - \varepsilon)\text{dist}(r, \text{aff } pw)\sigma && (2\text{dist}(u, \text{aff } pw) = \text{dist}(r, \text{aff } pw)) \\ &\leq 2(1 - \varepsilon)|wr|\sigma && (\text{dist}(r, \text{aff } pw) \leq |wr|) \\ &= (1 - \varepsilon)|qr|\sigma && (2|wr| = |qr|) \end{aligned}$$

If  $r$  is the apex, then

$$\begin{aligned} \tau(r) - \tau(q) &\leq 2\tilde{w}(vrp)\sigma && \text{(by the progress constraint)} \\ &\leq 2(1 - \varepsilon)\text{dist}(v, \text{aff } pr)\sigma && \text{(by definition of diminished width)} \\ &= (1 - \varepsilon)\text{dist}(q, \text{aff } pr)\sigma && (2\text{dist}(v, \text{aff } pr) = \text{dist}(q, \text{aff } pr)) \\ &\leq (1 - \varepsilon)|qr|\sigma && (\text{dist}(q, \text{aff } pr) \leq |qr|) \end{aligned}$$

If  $q$  is the apex, then

$$\begin{aligned} \tau(r) - \tau(q) &\leq 2\tilde{w}(upq)\sigma && \text{(by the progress constraint)} \\ &\leq 2(1 - \varepsilon)\text{dist}(u, \text{aff } pq)\sigma && \text{(by definition of diminished width)} \\ &= (1 - \varepsilon)\text{dist}(r, \text{aff } pq)\sigma && (2\text{dist}(u, \text{aff } pq) = \text{dist}(r, \text{aff } pq)) \\ &\leq (1 - \varepsilon)|qr|\sigma && (\text{dist}(r, \text{aff } pq) \leq |qr|) \end{aligned}$$

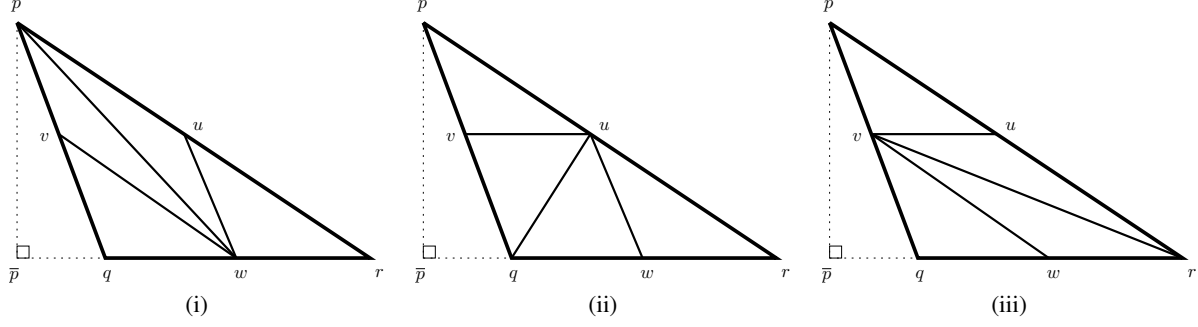


Figure 4.20: Triangle  $pqr$  with  $\angle pqr > \pi/2$  with apex at  $p$ ,  $q$ , and  $r$  respectively.

**CASE 2:**  $\tau(\bar{p}) < \tau(\mathbf{q})$  See Figure 4.20. In this case, we have  $\angle pqr > \pi/2$ . We will show that

$$\|\nabla \tau|_{qr}\| \leq (1 - \varepsilon)\sigma \sin \angle pqr$$

i.e., that

$$\tau(r) - \tau(q) \leq (1 - \varepsilon)|qr|\sigma \sin \angle pqr.$$

The proof then follows from Lemma 2.4 because the antecedent of the lemma is satisfied.

See Figure 4.20(a). Let  $\beta = |\bar{p}q|/|\bar{p}p|$ . Since  $|\bar{p}q| \neq 0$ , we have

$$\begin{aligned} \frac{\tau'(p) - \tau(\bar{p})}{|\bar{p}p|} &= \frac{\tau'(p) - \tau(q)}{|\bar{p}p|} + \frac{\tau(q) - \tau(\bar{p})}{|\bar{p}q|} \frac{|\bar{p}q|}{|\bar{p}p|} \\ &= \frac{\tau'(p) - \tau(q)}{|\bar{p}p|} + \beta \|\nabla \tau|_{qr}\| \end{aligned} \quad (4.4)$$

Using Equation 4.4, the causality constraint (Equation 2.2) can be rewritten as

$$\begin{aligned} \frac{\tau'(p) - \tau(q)}{|\bar{p}p|} &\leq \sqrt{\sigma^2 - \|\nabla \tau|_{qr}\|^2} \\ &\quad - \beta \|\nabla \tau|_{qr}\| \end{aligned} \quad (4.5)$$

We consider three cases depending on which vertex of  $\triangle pqr$  is the apex.

If  $p$  is the apex, then

$$\begin{aligned} \tau(r) - \tau(q) &\leq 4\tilde{w}(upw)\sigma && \text{(by the progress constraint)} \\ &\leq 4(1 - \varepsilon)\text{dist}(u, \text{aff } pw)\sigma && \text{(by definition of diminished width)} \\ &= 2(1 - \varepsilon)\text{dist}(r, \text{aff } pw)\sigma && (2\text{dist}(u, \text{aff } pw) = \text{dist}(r, \text{aff } pw)) \end{aligned}$$

Hence,

$$\begin{aligned}
\frac{\tau(r) - \tau(q)}{|qr|} &\leq (1 - \varepsilon) \frac{\text{dist}(r, \text{aff } pw)}{|qr|/2} \sigma \\
&= (1 - \varepsilon) \frac{\text{dist}(r, \text{aff } pw)}{|wr|} \sigma \\
&= (1 - \varepsilon) \sigma \sin \angle pwr \\
&= (1 - \varepsilon) \sigma \frac{|\bar{p}p|}{|pw|} \\
&< (1 - \varepsilon) \sigma \frac{|\bar{p}p|}{|pq|} && \text{because } |pw| > |pq| \\
&= (1 - \varepsilon) \sigma \sin \angle pqr
\end{aligned}$$

If  $r$  is the apex, then

$$\begin{aligned}
\tau(r) - \tau(q) &\leq 2\tilde{w}(vrp) \sigma && \text{(by the progress constraint)} \\
&\leq 2(1 - \varepsilon) \text{dist}(v, \text{aff } pr) \sigma && \text{(by definition of diminished width)} \\
&= (1 - \varepsilon) \text{dist}(q, \text{aff } pr) \sigma && (2\text{dist}(v, \text{aff } pr) = \text{dist}(q, \text{aff } pr))
\end{aligned}$$

Hence,

$$\begin{aligned}
\frac{\tau(r) - \tau(q)}{|qr|} &\leq (1 - \varepsilon) \sigma \frac{\text{dist}(q, \text{aff } pr)}{|qr|} \\
&= (1 - \varepsilon) \sigma \sin \angle qrp \\
&= (1 - \varepsilon) \sigma \frac{|\bar{p}p|}{|pr|} \\
&< (1 - \varepsilon) \sigma \frac{|\bar{p}p|}{|pq|} && \text{because } |pr| > |pq| \\
&= (1 - \varepsilon) \sigma \sin \angle pqr
\end{aligned}$$

If  $q$  is the apex, then

$$\begin{aligned}
\tau(r) - \tau(q) &\leq 2\tilde{w}(upq) \sigma && \text{(by the progress constraint)} \\
&\leq 2(1 - \varepsilon) \text{dist}(u, \text{aff } pq) \sigma && \text{(by definition of diminished width)} \\
&= (1 - \varepsilon) \text{dist}(r, \text{aff } pq) \sigma && (2\text{dist}(u, \text{aff } pq) = \text{dist}(r, \text{aff } pq))
\end{aligned}$$

Hence,

$$\begin{aligned}
\frac{\tau(r) - \tau(q)}{|qr|} &\leq (1 - \varepsilon) \frac{\text{dist}(r, \text{aff } pq)}{|qr|} \sigma \\
&= (1 - \varepsilon) \sigma \sin(\pi - \angle pqr) \\
&= (1 - \varepsilon) \sigma \sin \angle pqr
\end{aligned}$$

□

**Theorem 4.4.** *If a front  $\tau_i$  is progressive and if  $0 < \varepsilon < \varphi < (1 + \varepsilon)/2 < 1$ , then for every local minimum vertex  $p$  there exists  $T_{min} > 0$ , where  $T_{min}$  is a function of the triangle  $\triangle pqr$  and the parameters  $\varepsilon$  and  $\varphi$ , such that the front  $\tau_{i+1} = \text{advance}(\tau_i, p, \Delta t)$  is progressive for every  $\Delta t \in [0, T_{min}]$ .*

*Proof.* Since only the triangles of the front incident on  $P$  advance along with  $p$ , we can restrict our attention to an arbitrary triangle  $pqr$  incident on  $p$ . Let  $\tau$  and  $\tau'$  denote  $\tau_i|_{pqr}$  and  $\tau_{i+1}|_{pqr}$  respectively. Let  $\bar{p}$  be the orthogonal projection of  $p$  onto line  $qr$ .

Consider the progress constraints (Equations 4.1–4.3). Each progress constraint limits the progress  $\tau'(p) - \tau(p)$  from above. The only progress constraint for which this limit is not obviously positive is Equation 4.3 which applies when  $q$  is the apex of  $\triangle pqr$ , i.e.,

$$\tau'(p) \leq 2\tau(q) - \tau(r) + 2\tilde{w}(qrp)\sigma$$

Subtracting  $\tau(p)$  from both sides, because  $\tau(q) \geq \tau(p)$ , the above constraint is satisfied if

$$\tau(r) - \tau(q) \leq 2\tilde{w}(qrp)\sigma$$

Since  $\triangle PQR$  is progressive, we have

$$\tau(r) - \tau(q) \leq 2\tilde{w}(upq)\sigma$$

Therefore, it suffices to show that  $\tilde{w}(qrp) - \tilde{w}(upq)$  is positive and bounded away from zero. Expanding the definition of diminished width, we rewrite  $X = \tilde{w}(qrp) - \tilde{w}(upq)$  as  $X = \min\{A, B, C\}$  where

$$\begin{aligned} A &= (1 - \varepsilon)\text{dist}(q, \text{aff } pr) - \min \left\{ \begin{array}{l} (1 - \varepsilon)\text{dist}(u, \text{aff } pq), \\ (1 - \varphi)\text{dist}(p, \text{aff } qu), \\ (1 - \varphi)\text{dist}(q, \text{aff } up) \end{array} \right\} \\ &\geq (1 - \varepsilon)\text{dist}(q, \text{aff } pr) - (1 - \varphi)\text{dist}(q, \text{aff } up) \\ &= (\varphi - \varepsilon)\text{dist}(q, \text{aff } pr); \end{aligned}$$

$$\begin{aligned} B &= (1 - \varphi)\text{dist}(r, \text{aff } pq) - \min \left\{ \begin{array}{l} (1 - \varepsilon)\text{dist}(u, \text{aff } pq), \\ (1 - \varphi)\text{dist}(p, \text{aff } qu), \\ (1 - \varphi)\text{dist}(q, \text{aff } up) \end{array} \right\} \\ &\geq (1 - \varphi)\text{dist}(r, \text{aff } pq) - (1 - \varepsilon)\text{dist}(u, \text{aff } pq) \\ &= 2(1 - \varphi)\text{dist}(u, \text{aff } pq) - (1 - \varepsilon)\text{dist}(u, \text{aff } pq) \\ &= (1 + \varepsilon - 2\varphi)\text{dist}(u, \text{aff } pq); \end{aligned}$$

$$\begin{aligned} C &= (1 - \varphi)\text{dist}(p, \text{aff } qr) - \min \left\{ \begin{array}{l} (1 - \varepsilon)\text{dist}(u, \text{aff } pq), \\ (1 - \varphi)\text{dist}(p, \text{aff } qu), \\ (1 - \varphi)\text{dist}(q, \text{aff } up) \end{array} \right\} \\ &\geq (1 - \varphi)(\text{dist}(p, \text{aff } qr) - \min\{\text{dist}(p, \text{aff } qu), \text{dist}(q, \text{aff } up)\}). \end{aligned}$$

Since  $\varepsilon < \varphi < (1 + \varepsilon)/2$ , we have  $A > 0$  and  $B > 0$ . See Figure 4.19(iii) or Figure 4.20(iii); we also have

$$\begin{aligned} \text{dist}(p, \text{aff } qr) &= \frac{2\text{area}(\triangle pqr)}{|qr|} \\ &= \frac{2\text{area}(\triangle upq)}{|uv|} \\ &> \frac{2\text{area}(\triangle upq)}{\max\{|up|, |uq|\}} \end{aligned}$$

The inequality above follows because the bisector segment  $uv$  must be shorter than at least one of the two sides  $up$  and  $uq$ . Now,  $2\text{area}(\triangle upq)/|up| = \text{dist}(q, \text{aff } pr) = \text{dist}(q, \text{aff } up)$  and  $2\text{area}(\triangle upq)/|uq| = \text{dist}(p, \text{aff } qu)$ . Hence, it follows that  $C > 0$ .  $\square$

## 4.2.5 Changing the apex

Sometimes it may be advantageous to change the apex (newest vertex) of a triangle. For instance, if we wish to bisect a given edge without causing the refinement to propagate to neighboring triangles, we can make the edge a terminal edge by choosing the apexes of incident triangles appropriately. In Chapter 7, when we discuss pitching inclined tentpoles to account for boundary motion or to perform smoothing, the apex of a triangle may no longer correspond to the largest angle of the triangle. It is useful to subdivide the largest angle, or equivalently to bisect the longest edge, to guarantee sufficient progress in the next step. We therefore require some mechanism to change the apex or newest vertex of a given triangle.

The adaptive progress constraint can be strengthened to allow for changing the apex of any triangle. Specifically, for each triangle  $pqr$ , we impose all three types of progress constraints on  $\triangle pqr$  when  $p$  is the apex, when  $q$  is the apex, and when  $r$  is the apex simultaneously. Thus, we say that a causal triangle  $ABC$  is progressive if and it satisfies the adaptive progress constraint of Definition 4.6 for every choice of apex of the triangle.

Hence, when pitching a vertex  $p$  of  $\triangle pqr$  we impose all the following constraints simultaneously on the new time value  $\tau'(p)$ :

$$\tau'(p) \leq \min \left\{ \begin{array}{lll} \tau(q) + 2\tilde{w}(rpw)\sigma, & \tau(s) + \tilde{w}(pqr)\sigma, & \tau(r) + 2\tilde{w}(wpq)\sigma, \\ \tau(q) + 4\tilde{w}(uvr)\sigma, & \tau(r) + 2\tilde{w}(vqr)\sigma, & 2\tau(r) - \tau(q) + 2\tilde{w}(rpq)\sigma, \\ \tau(q) + 2\tilde{w}(uqr)\sigma, & \tau(r) + 4\tilde{w}(wuq)\sigma, & \tau(q) - \tau(r) + 2\tilde{w}(rpq)\sigma \end{array} \right\} \quad (4.6)$$

Since the new progress constraint is stronger, Lemma 2.4 still holds.

**Lemma 4.5.** *If a front  $\tau$  is progressive and if  $0 < \varepsilon < \varphi < (1 + \varepsilon)/2 < 1$ , then for any local minimum vertex  $p$  there exists  $\Delta > 0$ , where  $\Delta$  is a function of the triangle  $\triangle pqr$  and the parameters  $\varepsilon$  and  $\varphi$ , such that the front  $\tau' = \text{advance}(\tau, p, \Delta t)$  is progressive for every  $\Delta t \in [0, \Delta]$ .*

*Proof.* The proof is almost identical to that of Lemma 4.5, which does not rely on the fact that the three cases, depending on which vertex of triangle  $pqr$  is the apex, are mutually exclusive.  $\square$

## 4.2.6 Another look at the adaptive progress constraint

The progress constraint of Abedi *et al.* is equivalent to the following constraint for every descendant triangle by newest vertex bisection. Abusing notation slightly, we refer to an arbitrary descendant as  $\triangle abc$  with apex  $a$  as in Figure 4.17. Then, the bisector  $ad$  of  $\triangle abc$  must have gradient bounded by

$$|\tau(a) - \tau(d)| \leq \tilde{w}(abc)\sigma.$$

Expanding the definition of diminished width and dividing both sides by  $|ad|$ , we obtain an equivalent progress constraint:

$$\frac{|\tau(a) - \tau(d)|}{\text{len}(ad)} \leq \min \left\{ (1 - \varepsilon) \frac{\text{dist}(a, \text{aff } bc)}{\text{len}(ad)}, (1 - \varphi) \frac{\text{dist}(b, \text{aff } ac)}{\text{len}(ad)}, (1 - \varphi) \frac{\text{dist}(c, \text{aff } ab)}{\text{len}(ad)} \right\} \sigma$$

Observe the following identities:  $\text{dist}(b, \text{aff } ac) = 2 \text{dist}(d, \text{aff } ac)$ ;  $\text{dist}(c, \text{aff } ab) = 2 \text{dist}(d, \text{aff } ab)$ ; and  $\sin \angle adb = \sin \angle adc$ . Hence, we can rewrite the last inequality as

$$\|\nabla \tau|_{ad}\| \leq \min \{ (1 - \varepsilon) \sin \angle adc, 2(1 - \varphi) \sin \angle dac, 2(1 - \varphi) \sin \angle dab \} \sigma$$

Therefore, the adaptive progress constraint  $\sigma$  due to Abedi *et al.* that limits the gradient of  $\triangle abc$  along each of the four edges in the subdivided triangle can be rewritten equivalently as follows:

Triangle  $ABC$  satisfies *progress constraint*  $\sigma$  if and only if each of the following conditions is satisfied:

1.  $\|\nabla \tau|_{ab}\| \equiv \|\nabla \tau|_{de}\| \leq \min \{ (1 - \varepsilon) \sin \angle dea, 2(1 - \varphi) \sin \angle eda, 2(1 - \varphi) \sin \angle edc \} \sigma$
2.  $\|\nabla \tau|_{ad}\| \leq \min \{ (1 - \varepsilon) \sin \angle adc, 2(1 - \varphi) \sin \angle dac, 2(1 - \varphi) \sin \angle dab \} \sigma$
3.  $\|\nabla \tau|_{ac}\| \equiv \|\nabla \tau|_{df}\| \leq \min \{ (1 - \varepsilon) \sin \angle dfb, 2(1 - \varphi) \sin \angle fdb, 2(1 - \varphi) \sin \angle fda \} \sigma$
4.  $\|\nabla \tau|_{bc}\| \equiv \|\nabla \tau|_{fg}\| \leq \min \{ (1 - \varepsilon) \sin \angle fga, 2(1 - \varphi) \sin \angle gfd, 2(1 - \varphi) \sin \angle gfa \} \sigma$

Observing similarity and supplementarity of angles in Figure 4.17, we can rewrite the above constraints to refer only to angles in  $\triangle abc$  and its two children.

**Definition 4.6** (Restatement of adaptive progress constraint). *Triangle  $ABC$  with apex  $a$  satisfies the adaptive progress constraint if and only if each of the following conditions is satisfied:*

$$\begin{aligned} \|\nabla \tau|_{ab}\| &\leq \min \{ (1 - \varepsilon) \sin \angle bac, 2(1 - \varphi) \sin \angle bad, 2(1 - \varphi) \sin \angle abc \} \sigma \\ \|\nabla \tau|_{ad}\| &\leq \min \{ (1 - \varepsilon) \sin \angle adc, 2(1 - \varphi) \sin \angle dac, 2(1 - \varphi) \sin \angle dab \} \sigma \\ \|\nabla \tau|_{ac}\| &\leq \min \{ (1 - \varepsilon) \sin \angle bac, 2(1 - \varphi) \sin \angle acb, 2(1 - \varphi) \sin \angle dac \} \sigma \\ \|\nabla \tau|_{bc}\| &\leq \min \{ (1 - \varepsilon) \sin \angle bda, 2(1 - \varphi) \sin \angle acb, 2(1 - \varphi) \sin \angle abc \} \sigma \end{aligned}$$

**Lemma 4.7.** *Triangle  $\triangle PQR$  satisfies the progress constraint if and only if its every ancestor and every descendant also satisfies the progress constraint.*

*Proof.* Since  $\varphi \leq (1 + \varepsilon)/2$ , we have  $2(1 - \varphi) \geq (1 - \varepsilon)$ . Therefore, because of the correspondence between the angles of  $\triangle pqr$  and those of an ancestor or a descendant,  $\triangle abc$  satisfies the progress constraint (Definition 4.6) if and only if every ancestor and every descendant of  $\triangle pqr$  by newest vertex bisection also satisfies the progress constraint.  $\square$

### 4.3 Mesh adaptivity in higher dimensions

Generalizations of newest vertex bisection to higher dimensions exist and are well-known. For instance, the refinement method of Maubach (Mau95; Mau96) generates a bounded number of similarity classes of simplices, independent of the amount of refinement due to repeated bisection. The main challenge we confront is to extend our progress constraints in  $3D \times \text{Time}$  to account for adaptive refinement and coarsening. We anticipate more complications than the interplay of primary and secondary forbidden zones which we encountered in  $2D \times \text{Time}$ .

Our progress constraint still allows us to perform limited smoothing and retriangulation of the front at each step.

Under admittedly very strong constraints on the gradient of the front, it is possible to adapt the front to improve the mesh resolution and temporal aspect ratio of future spacetime elements.

**Lemma 4.8.** *If every angle  $\theta$  in the spatial projection of a front  $\tau$  satisfies  $\sin \theta \geq \phi_{\min}$ , and if  $\|\nabla \tau\| \leq (1 - \varepsilon)\phi_{\min}\sigma_{\min}$ , then any front  $\tau'$  obtained by retriangulating  $\tau$  is causal and satisfies progress constraint  $\sigma_{\min}$  of Definition 2.13.*

*Proof.* Since  $\sigma_{\min}$  is a lower bound on the reciprocal of the fastest wavespeed anywhere in spacetime,  $\tau$  is clearly causal.

Since  $\|\nabla \tau\| \leq (1 - \varepsilon)\phi_{\min}\sigma_{\min}$ , for any spatial direction vector  $\mathbf{n}$  we have  $(\nabla \tau) \cdot \mathbf{n} \leq \|\nabla \tau\| \leq (1 - \varepsilon)\phi_{\min}\sigma_{\min}$ . Therefore, for any face  $F$  in the spatial projection of  $\tau'$ , we obtain  $\|\nabla \tau|_F\| \leq (1 - \varepsilon)\phi_{\min}\sigma_{\min}$ .  $\square$

Thus, when the gradient of the front  $\tau$  is bounded, essentially any arbitrary front modification is permitted as long as the weak simplicial complex property is maintained; in other words, a retriangulation  $\tau \rightarrow \tau'$  is permitted only if  $\tau'$  conforms to  $\tau$  or if the operation can be achieved by adding new non-degenerate tetrahedra each of which has a causal outflow facet.

### Chapter summary

Adaptive meshing is crucial for efficient simulations. Unless the size of mesh elements adapts to changing requirements, an extremely fine mesh would be required throughout the domain. The number of elements required to be solved in such a fine mesh would render the problem intractable. In this chapter, we presented an adaptive meshing algorithm that incorporates refinement and coarsening into our advancing front framework. Our algorithm adjusts, as soon as required, the size of future spacetime elements to *a posteriori* estimates of the energy dissipation after solving each patch.

For the purposes of the meshing algorithm, we interpret the dissipation-based error indicator as a black box, specifically, a binary valued function  $\mu$  that given a spacetime element  $E$  either accepts or rejects  $E$ . To allow the algorithm to coarsen the mesh, the lower and upper thresholds on either side of the target dissipation should be sufficiently well-separated by a hysteresis zone.

Our algorithm strives for an acceptable balance between accuracy and efficiency. Aggressive coarsening, for the purpose of minimizing the number of spacetime elements, must be balanced with the minimum acceptable element quality needed for accurate numerical analysis.

We refer the reader to the paper by Abedi *et al.* (ACE<sup>+</sup>04) for a sample application to a scientific problem of practical complexity: the phenomenon of crack-tip wave scattering within an elastic solid subjected to shock loading. As expected, our experimental results show a significant improvement in the quality of the solution as a result of adaptivity, especially near discontinuities in the solution or its derivative. Also, we were able to achieve a better solution without using a fine mesh everywhere, which would have resulted in a massive increase in computation time.

We would like to extend all the current results to higher dimensions, specifically to  $3D \times \text{Time}$ . For the actual mesh refinement, we can directly use the generalization of newest vertex bisection to three dimensions by Bänsch (Bän91) and others. The main theoretical hurdle in higher dimensions is deriving minimal progress constraints that guarantee that the front can always advance. Another concern is to be able to describe the constraints in such a fashion that they are easy to implement. It seems likely that analytic constraints should suffice in higher dimensions, so the algorithm to maximize progress at each step can be solved exactly.



## Chapter 5

# Adaptive Meshing with Nonlocal Cone Constraints

In Chapter 4, we gave a meshing algorithm for  $2D \times \text{Time}$  that refines and coarsens the front to adapt the size of future spacetime tetrahedra in response to numerical error estimates. The algorithm of Chapter 4 assumed a fixed worst-case estimate of the causal slope at each step. In Chapter 3, we relaxed this conservative estimate. The result was an algorithm that adapted the duration of spacetime tetrahedra to changing wavespeeds. In this chapter, we give an algorithm to simultaneously adapt the mesh resolution to error estimates and anticipate changing wavespeeds due to nonlinear response.

We now consider the problem of supporting adaptive refinement and coarsening in  $2D \times \text{Time}$  via newest vertex bisection in the presence of changing wavespeeds. As noted in Chapter 4, devising necessary and sufficient progress constraints to support refinement and coarsening via higher-dimensional analogues of newest vertex bisection remains an open problem. The progress constraint at the  $i$ th step depends on the geometry of the front, which may change in step  $i + 1$  due to refinement and coarsening. The amount of progress going from  $\tau_i$  to  $\tau_{i+1}$  is constrained by the fastest wavespeed on the *new* front  $\tau_{i+1}$ . As before, we would like to characterize the front  $\tau_i$  as *valid* if and only if it is guaranteed to make finite progress to  $\tau_{i+1}$  such that the new front  $\tau_{i+1}$  is also valid. The problem is to anticipate a fast wavespeed in the future simultaneously with changes in the front due to refinement and coarsening. Our contribution is to combine the progress constraints of Chapters 2 and 4 with the lookahead algorithm of Chapter 3. We define a new notion of *progressive* fronts and prove that every progressive front is *valid*.

The front is refined in response to numerical error estimates. There is another reason for the meshing algorithm to refine the front. A spacetime element created by pitching a vertex of a front  $\tau$  may encounter vastly different wavespeeds. Note that the corresponding triangle of  $\tau$  must satisfy a progress constraint that depends on the wavespeed encountered after pitching. Hence, if the maximum wavespeed on any outflow facet of the element is much larger than the maximum wavespeed on any inflow facet, then the temporal aspect ratio of the tetrahedron is small. The height of the element is proportional to the ratio of maximum to minimum wavespeed anywhere in the element. If the temporal aspect ratio is too small, the element may be unsuitable for computing the numerical solution. A spacetime element with very small temporal aspect ratio may have a singular stiffness matrix, which may make it impossible to solve, or may require too many iterations for the solution to converge. If the solution does converge, the element will likely accumulate a large error and will therefore be rejected; the cost of solving the element will be incurred without any advancement of the front. There is empirical evidence that the accuracy of the solution within an element is positively correlated with the quality of the element, defined as the ratio of its inradius to its circumradius; a small decrease in the height of the spacetime element may imply a much larger decrease in its quality.

The computational cost of solving an element is significantly higher than the amortized per-element cost of mesh generation. DG solvers for nonlinear PDEs may take several iterations for the approximate solution to converge. If the accuracy of the solution and its efficiency can be improved by a better quality mesh with fewer elements, the additional

cost of mesh generation is expected to be easily compensated by the reduced total computation time.

Therefore, for correctness as well as efficiency, it is important for the meshing algorithm to avoid creating space-time elements with small temporal aspect ratio whenever possible.

In this chapter, we give a meshing algorithm that refines the front in response to a large increase in causal wavespeed, independent of and in addition to any error-driven refinement demanded by the solver. While simulating the next few tent pitching steps to estimate future wavespeed, if the algorithm predicts a bad quality element due to increasing wavespeed, then it can preemptively refine the front in the current step. Refining a triangle improves or maintains up to a constant factor the temporal aspect ratio of the tetrahedron created by pitching the triangle. Also, more progress can be made in the current step if the algorithm prepares for future refinement

In practice, especially for examples where the *Mach factor*—the ratio of global maximum to minimum wavespeeds—is not too large, it may be acceptable to allow the solver alone to guide front refinement. We cannot yet claim an improvement in temporal aspect ratio for arbitrary wavespeed distributions, as a result of the algorithm in this chapter. Regardless, we believe that this algorithm is of theoretical interest. The algorithm solves a two-parameter greedy optimization problem and illustrates the tradeoff between the two parameters—one a horizon parameter that measures future wavespeeds and the other an adaptive lookahead parameter that estimates the need to refine the front in the future. Thus, the meshing algorithm presented in this chapter attempts, in practice, to reduce the number of tetrahedra and improve their worst-case quality. Experiments are needed to determine whether the complexity of a more complicated algorithm is outweighed by a better quality and/or more efficient solution.

Recall from Chapter 3 that the algorithm maintains a bounding cone hierarchy to speed up the computation of the most restrictive cone constraint at each step. Whenever the front is refined or coarsened, we update the hierarchical decomposition by recomputing the hierarchy for a subset of the front. For the sake of efficiency, we rebalance the hierarchy after a significant refinement or coarsening of any subset of the front. Instead of updating the slope and number of cones in the hierarchy immediately after each step, we can update in a lazy fashion because the old cone constraints are still valid conservative estimates of new constraints. Lazy updates are likely to be efficient in a parallel setting by reducing interprocessor communication.

## 5.1 Adaptive meshing in $1D \times \text{Time}$ with nonlocal cone constraints

We note that it is trivial to perform adaptive refinement and coarsening of the front in  $1D \times \text{Time}$  in the presence of nonlocal (possibly anisotropic) cone constraints. We maximize the height of each tentpole subject only to the constraint that each front is causal, as described in Chapter 3.

The proof of the following theorem is almost identical to that of Theorem 2.2.

**Theorem 5.1.** *Let  $\tau$  be a causal front and let  $p$  be an arbitrary local minimum of  $\tau$ . Then, for every  $\Delta t$  such that  $0 \leq \Delta t < w_p \sigma_{\min}$ , the front  $\tau' = \text{advance}(\tau, p, \Delta t)$  is causal.*

*Proof of Theorem 5.1.* Only the segments of the front incident on  $P = (p, \tau(p))$  advance along with  $p$ . Consider an arbitrary segment  $pq$  incident on  $p$ . Since  $p$  is a local minimum, we have  $\tau(q) \geq \tau(p)$ . We have

$$\begin{aligned} \tau'(p) &\leq \tau(p) + \Delta t \\ &< \tau(p) + w_p \sigma_{\min} \\ &\leq \tau(q) + (1 - \delta) |pq| \sigma(P'Q) \end{aligned}$$

Hence,

$$\|\nabla \tau'|_{pq}\| := \frac{\tau'(p) - \tau'(q)}{|pq|} < \sigma(P'Q).$$

Therefore,  $P'Q$  is causal. □

Note that when pitching a local minimum vertex  $P$ , an interior vertex, the smaller of the temporal aspect ratios of the resulting two spacetime triangles is maximized if the two edges incident on  $P$  have comparable spatial lengths. Therefore, our adaptive strategy is guided by the desire to keep the spatial lengths of adjacent front segments roughly equal.

Because of Theorem 5.1, we obtain a lower bound on the worst case height of any tentpole. Thus, we have proved Theorem 2.3 in the situation where the wavespeed is not constant throughout spacetime.

## 5.2 Adapting the progress constraint to the level of refinement in $2D \times \text{Time}$

In this section, we consider the adaptive meshing problem in  $2D \times \text{Time}$  in the presence of changing wavespeeds. We restrict ourselves to mesh adaptivity by newest vertex bisection of front triangles and the reverse operation. See Chapter 4 for a discussion of newest vertex bisection.

The key property of newest vertex bisection is that each descendant of a triangle  $PQR$  has its edges parallel to three of the four directions defined by  $\triangle PQR$  and its apex—the three edges  $PQ$ ,  $QR$ , and  $PR$  plus the bisector  $PS$  through the midpoint  $s$  of the base  $qr$ .

Recall from the statement of Lemmas 2.4 and 2.7 that the front at each step must satisfy a progress constraint that depends on the wavespeed in the next step. When the wavespeed is not constant,  $\sigma_{\min}$  may not be a good estimate of the future wavespeed. We have improved the situation somewhat by giving an algorithm to compute an estimate  $\tilde{\sigma}_h(PQR)$  of the wavespeed encountered in the next step by  $\triangle PQR$  of the current front, by looking ahead  $h$  steps for some horizon parameter  $h$ . Thus, we can use the estimated slope  $\tilde{\sigma}_h(PQR)$  as the radius of the disc in Figure 2.2 when imposing adaptive progress constraints on  $\triangle PQR$ . However, this choice of  $\tilde{\sigma}_h(PQR)$  may be too conservative because it uses the same wavespeed  $\tilde{\sigma}_h(PQR)$  in the progress constraint on  $\triangle PQR$  as on each of its descendants after bisection.

A key property we use in deriving the new algorithm in this chapter is that the boundary of a cone is a *ruled surface*. Recall from Chapter 3 that we partition the cone constraints while pitching  $A$  into local and nonlocal constraints. Therefore, if any triangle  $\triangle ABC$  intersects a given nonlocal cone, then this intersection is a line segment in the plane of  $\triangle ABC$ . Therefore, if the bisector edge  $AD$  intersects a cone of influence, then so do at least two of the edges of  $\triangle ABC$  (Figure 4.17). Therefore, if a fast wavespeed in the future intersects  $AD$  but does not intersect both edges  $AB$  and  $AC$  of  $\triangle ABC$ , then it can do so only if  $\triangle ABC$  has been bisected at least once.

Thus, our contribution is to make the progress constraint imposed on a given triangle due to the shape of its descendants adaptive to the level of refinement of the descendant triangles.

The progress constraint that we impose on a given triangle  $PQR$  of a front  $\tau$  depends on two parameters,  $h$  and  $l$ . The parameter  $h$  is the horizon, as in Definition 3.2. For each descendant  $\triangle ABC$  of  $\triangle PQR$  by  $l$  newest vertex bisections, we enforce a progress constraint on  $\triangle PQR$  that depends on the shape of  $\triangle ABC$ , the level of refinement  $l$ , and the horizon parameter  $h$ . The greater the level of refinement of a triangle  $\triangle$ , the greater is likely to be the estimated slope  $\tilde{\sigma}_h(\triangle)$  for a fixed  $h$ , i.e., if  $\triangle_2$  is a descendant of  $\triangle_1$  by newest vertex bisection, then  $\tilde{\sigma}_h(\triangle_2) \geq \tilde{\sigma}_h(\triangle_1)$ . Therefore, we anticipate up to  $l$  levels of refinement where  $l \geq 0$  is another parameter. For a triangle  $\triangle_1$  at refinement level greater than  $l$ , we impose a progress constraint that depends on its ancestor  $\triangle_2$  at level  $l$ ; in other words, we

draw a figure similar to Figure 2.2 except with a disc of radius  $\tilde{\sigma}_h(\Delta_2)$ . If  $l = 0$ , then  $\Delta_2 = \triangle PQR$ ; the advantage of choosing  $l > 0$  is that in practice we expect  $\tilde{\sigma}_h(\Delta_2) \gg \tilde{\sigma}_h(PQR)$  because  $\Delta_2$  is smaller than  $\triangle PQR$ . In other words, for the same horizon parameter  $h$ , the smaller triangle  $\Delta_2$  will encounter a subset of the cone constraints in the next  $h$  steps of pitching vertices of  $\Delta_2$  as the larger triangle  $\triangle PQR$ . For the same number of lookahead steps  $h$ , a smaller triangle is likely to advance through more tent pitching steps than its larger ancestor because each tent pitching step makes progress in time proportional to the size of the triangle.

To support adaptive refinement and coarsening by newest vertex bisection, we have to enforce the adaptive progress constraint of Definition 4.2. We therefore define *adaptively  $h$ -progressive fronts* (Definition 3.2), to refer to this stronger adaptive progress constraint, as follows.

**Definition 5.2** (Adaptively  $h$ -progressive). *Let  $h$  be a nonnegative integer, called the horizon.*

*Let  $PQR$  be a given triangle. We inductively define  $\triangle PQR$  as adaptively  $h$ -progressive as follows.*

**Base case  $h = 0$ :** *Triangle  $PQR$  is adaptively 0-progressive if and only if it is causal and satisfies the adaptive progress constraint  $\sigma_{\min}$  (Definition 4.2).*

**Case  $h > 0$ :** *Triangle  $PQR$  is adaptively  $h$ -progressive if and only if all the following conditions are satisfied:*

1.  *$PQR$  is causal;*
2. *Let  $P$  be an arbitrary local minimum vertex of  $\triangle PQR$ . Let  $d_p$  denote  $\text{dist}(p, \text{aff } qr)$  and let  $T_{\min} = \min\{\varepsilon, 1 - \varepsilon\} \sigma_{\min} d_p$ . Let  $P'QR = \text{advance}(PQR, p, T_{\min})$  be the triangle obtained by advancing  $P$  by  $T_{\min}$ . Then,  $PQR$  must satisfy the adaptive progress constraint  $\sigma(P'QR)$  and  $P'QR$  must be  $\max\{h - 1, 0\}$ -progressive.*

We say that a front  $\tau$  is *adaptively  $h$ -progressive* if every facet of  $\tau$  is adaptively  $h$ -progressive (Definition 5.2).

The following two lemmas are analogous to Lemmas 3.3 and 3.4.

**Lemma 5.3.** *For every  $h \geq 0$ , if  $\triangle PQR$  is adaptively  $h$ -progressive, then  $\triangle PQR$  is adaptively  $(h + 1)$ -progressive.*

*Proof of Lemma 5.3.* If a triangle  $PQR$  satisfies adaptive progress constraint  $\sigma$  (Definition 4.2), then  $\triangle PQR$  satisfies progress constraint  $\sigma'$  for every  $\sigma' \geq \sigma$ . By Theorems 4.3 and 4.4, if  $\triangle PQR$  satisfies the adaptive progress constraint  $\sigma_{\min}$ , then there exists  $T_{\min} > 0$  such that the triangle  $P'QR$  after pitching a local minimum  $P$  by  $T_{\min}$  is causal and satisfies the adaptive progress constraint  $\sigma_{\min}$ . Since  $\sigma_{\min}$  is a lower bound on the causal slope anywhere in space-time, we conclude that triangle  $P'QR$  is adaptively 0-progressive. Therefore, by Definition 5.2, if  $\triangle PQR$  is adaptively 0-progressive, then it is adaptively  $h$ -progressive for every  $h \geq 0$ . Hence, if  $\triangle PQR$  is adaptively  $h$ -progressive, then it is adaptively  $h'$ -progressive for every  $h' \geq h$ .  $\square$

**Lemma 5.4.** *Suppose  $PQR$  is a triangle of an adaptively  $h$ -progressive front  $\tau$  for some  $h \geq 0$ . Let  $P$  be an arbitrary local minimum vertex of  $\triangle PQR$ . Let  $d_p$  denote  $\text{dist}(p, \text{aff } qr)$ .*

*Then, there exists  $T_{\min} > 0$  such that  $\triangle P'QR$  where  $P' = (p, \tau(p) + \Delta t)$  for an arbitrary  $\Delta t \in [0, T_{\min}]$  is adaptively  $h$ -progressive.*

*Proof of Lemma 5.4.* By Definition 5.2, triangle  $P'QR$  is adaptively  $(h - 1)$ -progressive. By Lemma 5.3, triangle  $P'QR$  is also adaptively  $h$ -progressive.  $\square$

**Definition 5.5** ( $(h, l)$ -progressive). *We inductively define a triangle  $\triangle PQR$  as  $(h, l)$ -progressive if it is  $h$ -progressive (Definition 3.2) and each of the two children obtained by newest vertex bisection of  $\triangle PQR$  is  $(h, \max\{l - 1, 0\})$ -progressive.*

**Base case  $l = 0$ :**  *$\triangle PQR$  is  $(h, 0)$ -progressive if it is adaptively  $h$ -progressive (Definition 5.2).*

We say that a front is  $(h, l)$ -progressive if every triangle on the front is  $(h, l)$ -progressive. We say that a front is progressive if it is  $(h, l)$ -progressive for some fixed  $h$  and  $l$ .

A progressive front is guaranteed to make sufficient positive progress after at most a finite number of refinements by newest vertex bisection of its facets.

**Lemma 5.6.** *If a front  $\tau$  is  $(h, 0)$ -progressive, then for every local minimum  $p$  of  $\tau$  there exists a  $T_{\min} > 0$ , such that the front  $\tau' = \text{advance}(\tau, p, \Delta t)$  is  $(h, 0)$ -progressive for every  $\Delta t \in [0, T_{\min}]$ .*

*Proof of Lemma 5.6.* By definition, every triangle  $PQR$  of the front  $\tau$  is adaptively  $h$ -progressive. By Lemma 5.4, the triangle  $P'QR$  obtained by advancing local minimum vertex  $P$  to  $P'$  by  $T_{\min}$  is also adaptively  $h$ -progressive. Hence, there exists a  $T_{\min} > 0$  such that the front  $\tau' = \text{advance}(\tau, p, \Delta t)$  is  $(h, 0)$ -progressive for arbitrary  $\Delta t \in [0, T_{\min}]$ .  $\square$

By Definition 5.5, if a triangle  $PQR$  is  $(h, l)$ -progressive, then any triangle obtained by a single newest vertex bisection of  $PQR$  is  $(h, l')$ -progressive for  $l' = \max\{l - 1, 0\}$ .

We relax the definition of a valid front (Definition 2.1) to permit refinement of the front one or more times at each step without advancing the front.

**Definition 5.7** (Valid front). *We say that a front  $\tau$  is valid if there exists a positive real  $\Delta t$  bounded away from zero such that for every  $T \in \mathfrak{R}^{\geq 0}$  there exists a finite sequence of fronts  $\tau, \tau_1, \tau_2, \dots, \tau_k$  where  $\tau_k \geq T$ , each new front  $\tau_{i+1}$  in the sequence obtained from the previous front  $\tau_i$  by one of two operations: either (i) advancing some local neighborhood of  $\tau_i$  by  $\Delta t$ , or (ii) newest vertex bisection of some triangle of  $\tau_i$ .*

Therefore, we conclude the following theorem.

**Theorem 5.8.** *If a triangle  $PQR$  is  $(h, l)$ -progressive, then  $\triangle PQR$  is valid.*

*Proof of Theorem 5.8.* The proof is by a very simple induction on the parameter  $l$ . If  $l = 0$ , then the theorem follows from Lemma 5.6. Otherwise, if  $l > 0$ , then by the induction hypothesis, the child triangle  $ABC$  of  $\triangle PQR$ , which is  $(h, l - 1)$ -progressive, is valid. Hence, by Definition 5.7, the theorem follows for the case  $l > 0$  also.  $\square$

### 5.2.1 A unified adaptive algorithm in $2D \times \text{Time}$

Our unified algorithm greedily maximizes the progress such that each front is  $(h, l)$ -progressive for some choice of  $h$  and  $l$ . The algorithm can be as complicated as desired. Definition 5.5 stresses the fact that our algorithm can optimize the choice of  $h$  and  $l$ , likely doing better than the theoretical guarantee obtained by setting  $h = l = 0$ ; however, a simple choice of  $h = l = 1$  may perform sufficiently well in practice.

### 5.2.2 A simpler algorithm in $2D \times \text{Time}$

Arguably, the algorithm presented in the previous sections is very complicated to implement for general  $h$  and  $l$ . Is this complication really necessary? In the case of discontinuities in wavespeeds due to shocks, we think the complication is unavoidable. However, in the case that the wavespeed function is smooth, we present a simpler algorithm that is guaranteed to terminate. For each triangle  $\triangle$  on the front, estimate the maximum and minimum wavespeed at any point of  $\triangle$ . If the ratio of the maximum to minimum wavespeeds is too large, say greater than 4, then refine the triangle; otherwise, if this ratio is too small, say less than 2, then mark the triangle as coarsenable. Since the wavespeed is continuous, this refinement will stop after a bounded number of steps. If the wavespeed function is discontinuous, we would need to impose a lower bound on the element size to limit refinement.

**Input:** A triangulated space domain  $M \subset \mathbb{E}^2$

**Output:** A tetrahedral mesh of  $M \times [0, \infty)$

Initial front  $\tau_0$  is the space mesh at time  $t = 0$

Fix  $h, l$ .

Repeat for  $i = 0, 1, 2, \dots$ :

1. Advance in time an arbitrary local minimum vertex  $P = (p, \tau_i(p))$  of the current front  $\tau_i$  to  $P' = (p, \tau_{i+1}(p))$  such that  $\tau_{i+1}$  is  $(h, l)$ -progressive, and  $\tau_{i+1}(p)$  is maximized.
2. Partition the spacetime volume between  $\tau_i$  and  $\tau_{i+1}$  into a patch of tetrahedra, each sharing the tentpole edge  $PP'$ .
3. Solve the resulting patch.
4. If the patch is accepted, then some outflow triangles on the new front  $\tau_{i+1}$  are marked coarsenable. Coarsen any pair of coarsenable sibling triangles if they are coplanar on the new front  $\tau_{i+1}$ , as long as the resulting coarser front is also  $(h, l)$ -progressive.
5. If the patch is rejected, then one or more triangles on the front  $\tau_i$  are marked for refinement. Perform newest vertex bisection of every triangle marked for refinement, propagating the bisection to neighboring triangles to maintain a triangulated front.

---

Figure 5.1: Unified adaptive algorithm in  $2D \times \text{Time}$ .

## Chapter summary

Refinement of a triangle on the front is easy to incorporate into the advancing front meshing algorithm with nonlocal cone constraints because any faster cone of influence that intersects a smaller triangle also intersects its parent and is accounted for in the progress constraint that must be satisfied by the parent.

Coarsening presents a challenge when the wavespeed is not constant everywhere. When two smaller triangles are coarsened, the maximum wavespeed on the larger triangle is the maximum of the wavespeeds of the original smaller triangles. Therefore, both triangles being coarsened must satisfy the same progress constraint before they can be coarsened, i.e., we can merge two triangles into one if and only if the new triangle is  $h$ -progressive. When coarsening is possible only under such constraints, we need to carefully prioritize each coarsening step so that the front is only as refined as necessary and not much more. Prioritizing the various coarsening requests remains an open problem.

## Chapter 6

# Target time conformity

For comparing the accuracy of the numerical results with those obtained by other techniques, such as for convergence studies, we sometimes need a spacetime mesh of the bounded volume from time  $t = 0$  to  $t = T$  for some target time  $T > 0$ . Also, some modifications of the front, such as coarsening by derefinement, are permitted only when the gradient of the front everywhere is small. In particular, if the entire front corresponds to a constant time function, then the algorithm can continue exactly as if this constant-time front were the initial input. To make the entire front or some subset of the front coplanar, the algorithm may have to limit the amount of progress at each step so that the vertex being pitched is coplanar with some or all of its neighbors. This coplanarity constraint, in addition to causality and progress constraints, further reduces the temporal aspect ratio of resulting tetrahedra and may create near-degenerate elements. Therefore, it is important to anticipate coplanarity constraints by limiting the amount of progress in the current step and thus ensure that both current and future tentpole heights can still be provably bounded from below.

In this chapter, we show how to make tent pitching less greedy about maximizing the progress at each step so that a subset of the front can be made coplanar in the next step. The central idea of the algorithm in this chapter is to trade off the amount of progress, i.e., tentpole height, achieved in the current step and that achieved in the next step. This algorithm can be used in arbitrary dimensions to make the entire front conform to a target time  $T \geq 0$ . The algorithm can also be used to coarsen the front and to retriangulate it by edge contraction or edge dilation by first making a subset of the front conform to a local target time. The main feature of the algorithm in this chapter is that it retains the progress guarantee up to a constant factor proved for the algorithms in earlier chapters. Thus, we are able to achieve target time conformity without significantly sacrificing the worst-case temporal aspect ratio of spacetime elements. We believe that the central idea of the algorithm in this chapter will be useful for other purposes such as when the spacetime mesh is required to conform to a singular spacetime surface, not necessarily a constant-time plane.

### 6.1 Conforming to a target time

We say that a spacetime mesh  $\Omega$  *conforms* to a target time  $T$  (or in general to any front  $\Phi$ ) if the portion  $M \times T$  of the constant time plane  $t = T$  is equal to the union of causal facets of  $\Omega$ .

In the context of pitching tents, conforming to a target time  $T$  means that the height of a tentpole is further constrained so that the top of the tentpole does not exceed time  $T$ . This additional constraint creates a problem when a vertex  $P = (p, \tau(p))$  has almost achieved the target time but not quite, i.e., when  $\tau(p) < T$  and  $T - \tau(p)$  is very small. In this case, advancing  $p$  from  $\tau(p)$  to  $T$  will create a tentpole of height  $T - \tau(p)$  which is unacceptably small and results in degenerate or poor quality elements. In this section, we show how to incorporate additional constraints into our algorithm so that the advancing front conforms to the specified target time  $T$  while still proving a lower bound on the height of each tentpole. Thus, we retain the quality guarantee of the algorithm within a constant factor.

Let  $\gamma \in (0, \frac{1}{2}]$  be an additional parameter to our advancing front algorithm.

The key idea we use is that whenever the front attempts to get too close to the target time  $T$  during a single step of pitching a local minimum  $p$ , we reduce the height of the current tentpole so that in the next step the vertex  $p$  will achieve the target time  $T$ . We call the current step the “penultimate” tent pitching step because the next step is the last step in which vertex  $p$  is pitched. The tradeoff we need to make is between the height of the tentpoles in the current (penultimate) step and in the next (final) step. We do it in a way that in both cases the tentpole height is at least  $\gamma$  times the worst-case guarantee on the height of *any* tentpole at  $p$ .

Let  $\tau$  denote the front at the current iteration. Let  $P$  be a local minimum of  $\tau$  such that  $\tau(p) < T$ . Such a local minimum vertex  $p$  must exist unless the entire front  $\tau$  has achieved the target time  $T$ ; in particular, the global minimum vertex is a candidate vertex.

Denote by  $w_p$  the minimum distance of  $p$  from  $\text{aff } \Delta$  for every simplex  $\Delta$  in (the spatial projection of) the front  $\tau$  incident on  $p$ .

$$w_p := \min_{\Delta \in \text{link}(p)} \{ \text{dist}(p, \text{aff } \Delta) \}$$

Let  $\sigma \equiv \sigma_{\min}$  denote the reciprocal of the global fastest wavespeed. For any vertex  $p$ , let  $h_p$  denote a lower bound on the height of the tentpole at  $p$  whenever  $p$  is pitched. Note that we require  $h_p$  to be small enough to be independent of the front during the step in which  $p$  is pitched, i.e.,  $h_p$  can be a function of only the spatial projection of any front. Depending on which progress constraint the algorithm uses, i.e., depending on the specific meshing algorithm,  $h_p$  may be a different lower bound; thus, for instance, the algorithm of Chapter 2 guarantees a worst-case tentpole height of

$$h_p := \min\{\varepsilon, 1 - \varepsilon\} w_p \sigma.$$

The algorithm at each step enforces the following invariant on the front  $\tau$  at the beginning of step  $i$ : for every vertex  $p$  of  $\tau$  we have:

$$\text{either } \tau(p) = T \quad \text{or} \quad \tau(p) \leq T - \gamma h_p \tag{6.1}$$

We assume, of course, that the initial front  $\tau_0$  satisfies this invariant, i.e., either the space mesh  $M$  is refined enough or the target time  $T$  is large enough to satisfy Equation 6.1.

Suppose the algorithm is currently pitching such a local minimum vertex  $p$  of  $\tau$  such that  $\tau(p) < T$ . Such a candidate vertex must exist because a global minimum of the front is always a candidate unless the entire front is at time  $T$ .

Let  $\tau'(p)$  denote the time value of the top of the tentpole at  $p$ , maximized to satisfy all causality and progress constraints. The new algorithm is allowed to lower the top by choosing a different time value  $\tau''(p)$  for the top of the tentpole such that  $\tau(p) \leq \tau''(p) \leq \tau'(p)$ .

Let  $\gamma$  be a fixed constant in the range  $0 < \gamma \leq \frac{1}{2}$ , a parameter to the algorithm. For the reasons below,  $\gamma = \frac{1}{2}$  may be a good choice in practice.

Apply the following rule at each tent pitching step.

1. **Case 1:** If  $\tau'(p) \geq T$ , then choose  $\tau''(p) := T$  as the new top of the tentpole at  $p$ .
2. **Case 2:** Otherwise, if  $\tau'(p) \geq T - \gamma h_p$ , then choose  $\tau''(p) := T - (1 - \gamma)h_p$  as the new top of the tentpole at  $p$ .
3. **Case 3:** Otherwise, we must have  $\tau'(p) < T - \gamma h_p$ ; then choose  $\tau''(p) := \tau'(p)$  as the top of the tentpole at  $p$ .



We prove that the height of the tentpole in the current step is possibly reduced to  $\gamma h_p$  instead of  $h_p$ ; however, the height of the tentpole the next time  $p$  is pitched is guaranteed to be at least  $(1 - \gamma)h_p$ . The choice of parameter  $\gamma$  represents a tradeoff between the current step and the next step.

As a corollary, the entire front will achieve the specified target time  $T$  in a finite number of steps.

It is easy to see that the algorithm must eventually advance every vertex that has not yet achieved the target time value  $T$ . We prove next that whenever a vertex  $p$  is advanced, then the height of the resulting tentpole at  $p$  is at least  $\gamma h_p > 0$ .

First, we prove by induction on the number of tent pitching steps that the invariant of Equation 6.1 is always maintained. Let  $\tau_i$  denote the front at the beginning of iteration  $i$ . We assume that the initial front  $\tau_0$  automatically satisfies the invariant. Whenever case 1 applies at step  $i$ , we have  $\tau_{i+1}(p) = T$ ; therefore, the first part of Equation 6.1 is satisfied by the new front. Otherwise, if case 2 applies, then  $\tau_{i+1}(p) := T - (1 - \gamma)h_p \leq T - \gamma h_p$  because  $\gamma \leq 1 - \gamma$ . Finally, if case 3 applies, then we have  $\tau_{i+1}(p) := \tau'(p) < T - \gamma h_p$ , so the second part of Equation 6.1 is satisfied by the new front.

**Theorem 6.1.** *Let  $\tau$  be a progressive front. Let  $\gamma$  be a parameter in the range  $(0, \frac{1}{2}]$ . Let  $T$  be a target time such that  $T \geq \tau(p) + \gamma h_p$  for every vertex  $p$ . Then, whenever our new algorithm advances a local minimum vertex  $p$  of  $\tau$ , it constructs a tentpole at  $p$  with height at least  $\gamma h_p$ .*

*Proof.* We prove that  $\tau(p) \leq \tau''(p) \leq \tau'(p)$  and that  $\tau''(p) - \tau(p) \geq \gamma h_p$ .

Note that  $\tau''(p) = T - (1 - \gamma)h_p \leq T - \gamma h_p \leq \tau'(p)$  because  $\gamma \leq \frac{1}{2}$ .

We show that lowering the top of the tentpole at  $p$  from  $\tau'(p)$  to  $\tau''(p)$  does not create degenerate elements in the current step.

There are three mutually exclusive possibilities that cover all eventual outcomes.

- (a) Suppose case 1 applies in the current step, i.e.,  $\tau''(p) = T$ . Since  $\tau(p) < T$ , it must be the case that either case 2 or case 3 must have applied in the *previous* step. If case 2 applied in the previous step, then  $\tau(p) = T - (1 - \gamma)h_p$ , so the height of the current tentpole is  $(1 - \gamma)h_p \geq \gamma h_p$  because  $\gamma \leq \frac{1}{2}$ .

This is the only (sub)case for which the claim is tight.

On the other hand, if case 3 applied in the previous step, then  $\tau(p) < T - \gamma h_p$ , so the current tentpole height is  $T - \tau(p) > \gamma h_p$ .

- (b) Suppose case 2 applies in the current step, i.e.,  $\tau''(p) = T - (1 - \gamma)h_p$ . Then, the current tentpole height is  $\tau''(p) - \tau(p)$  and we have  $\tau''(p) - \tau(p) = (T - (1 - \gamma)h_p) - \tau(p) = (T - \tau(p)) - (1 - \gamma)h_p$ .

But from the tent pitcher progress guarantee, we know that  $\tau'(p) \geq \tau(p) + h_p$ .

Hence,  $T - \tau(p) \geq (T - \tau'(p)) + h_p$ .

We also know that  $\tau'(p) < T$  because case 2 applied instead of case 1. Hence,  $T - \tau(p) > h_p$ .

Therefore,  $\tau''(p) - \tau(p) > h_p - (1 - \gamma)h_p = \gamma h_p$ .

- (c) Suppose case 3 applies in the current step, i.e.,  $\tau''(p) = \tau'(p)$ . Then, from the tent pitcher progress guarantee, we know that  $\tau'(p) = \tau''(p) \geq \tau(p) + h_p$ .

□

As an interesting corollary, we obtain the following result for the linear non-adaptive case. We can construct a spacetime mesh with the same progress guarantee that conforms to any progressive front  $\Phi$ . We can do this by running our algorithm *backwards* in time, starting from  $\Phi$  as the “initial” front and choosing to conform to the constant time plane  $t = 0$ . (Conceptually, we can imagine this as meshing the spacetime volume  $M \times [-\Phi, 0]$ .) It is possible to run the algorithm backwards in time with the same progress guarantee because the gradient constraints on the front at each step are unchanged if all time values are replaced by their negatives.

Further, we can mesh the spacetime volume between any two progressive fronts  $\Phi_1$  and  $\Phi_2$  over the same space domain  $M$ , as long as there exists a constant time plane  $t = T$  between  $\Phi_1$  and  $\Phi_2$  that has a margin of at least  $\gamma T_{\min}$  from either of the two fronts. We do this by running the algorithm in two phases: once we run the algorithm starting from the front  $\Phi_1$  and conforming to time  $t = T$ ; then, we run the algorithm starting from the front  $\Phi_2$  and conforming to time  $t = T$ . By adjoining the resulting two spacetime meshes, we obtain a spacetime mesh of the volume between  $\Phi_1$  and  $\Phi_2$ . The final spacetime mesh is a weak simplicial complex if the spatial projections of the given two fronts  $\Phi_1$  and  $\Phi_2$  are conforming, i.e., each triangle in one triangulation is the union of one or more triangles of the other triangulation.

**ANTICIPATING CHANGES DUE TO ADAPTIVE REFINEMENT AND COARSENING** For a vertex  $p$ , the local spatial geometry of the front can change due to adaptive refinement and coarsening or due to some other retriangulation of the front; thus,  $w_p$  can change and therefore a fixed  $h_p$  no longer suffices as an adequate lower bound on the tentpole height at  $p$ . However, we can interpret the invariant of Equation 6.1 as a constraint (an upper bound) on the spatial size of the triangulation in the local neighborhood,  $\text{star}(p)$ , of  $p$ , rather than as a lower bound on  $T$ . If the initial front  $\tau_0$  does not satisfy the invariant, then we refine the front until it does. If coarsening a pair of triangles would violate the invariant, then this coarsening is not permitted. Any other retriangulation that would violate the invariant is also not permitted. However, since refining the front is a requirement for numerical accuracy, we anticipate all possible changes in shape of the front due to refinement in advance and alter the definition of  $w_p$  appropriately. This is easy because newest vertex bisection generates only a small number of homothetic triangle shapes on the front.

## 6.2 Conforming to a target time: a simpler heuristic

The following is another algorithm for making a vertex  $p$  conform to its target time  $T_p$  while still guaranteeing a lower bound on the height of each tentpole height. The following logic is easier to implement than the previous one, because it does not involve the progress guarantee computation and does not involve the additional parameter  $\gamma$  (even though it can be modified to depend on such a parameter).

Let  $p$  be a local minimum of the front  $\tau$ ; let  $\tau(p)$  denote its time coordinate before lifting and let  $\tau'(p)$  denote the time coordinate of the proposed tentpole at  $p$ , maximized subject to causality and progress constraints only. Thus,  $h := \tau'(p) - \tau(p)$  denotes the proposed height of the tentpole at  $p$  before imposing any target time constraint.

Let  $T_p$  denote the target time for  $p$ . We will compute a new time value  $\tau''(p)$  for the tentpole top, instead of  $\tau'(p)$ . Apply the following rules at each tent pitching step:

1. **Case 1:**  $\tau'(p) \geq T_p$ . Choose  $\tau''(p) := T_p$ .
2. **Case 2:**  $\tau'(p) < T_p$ . If  $T - \tau'(p) < h$ , then  $T_p < 2\tau'(p) - \tau(p)$ ; in this case, choose  $\tau''(p) := (T_p + \tau(p))/2$ . Otherwise, we have  $\tau'(p) \leq T - h$ ; in this case, let  $\tau''(p) := \tau'(p)$  remain.

First, we prove that lowering the tentpole top is acceptable in the current step. We have  $t''(p) = (T - t(p))/2$ ; at the same time, we are given  $0 < T - t'(p) < h$  which means

$$T - t(p) = T - t'(p) + t'(p) - t(p) = T - t'(p) + h > h$$

Hence, we conclude  $t''(p) = (T - t(p))/2 > h/2$ .

Finally, we prove that lowering the tentpole top is acceptable in future steps. We have  $T - t''(p) = T - (T - t(p))/2$ ; we also know that  $T - t'(p) < h$ , so  $T - t(p) = T - t'(p) + t'(p) - t(p) = T - t'(p) + h < 2h$ . Hence, we conclude that  $T - t''(p) < T - 2h/2 = T - h$ .

### 6.3 Smoothing out large variations in tentpole heights

We would like to smooth out large variations in the heights of the tentpoles erected at any given vertex  $p$  in any two consecutive steps.

Let  $p$  be a local minimum of the front  $\tau$ ; let  $\tau(p)$  denote its time coordinate before lifting and let  $\tau'(p)$  denote the time coordinate of the proposed tentpole at  $p$ , maximized subject to causality and progress constraints only. Thus,  $h := \tau'(p) - \tau(p)$  denotes the proposed height of the tentpole at  $p$  before imposing any target time constraint.

Let  $\gamma > 0$  be a parameter. Let  $h_p$  denote a lower bound on the height of the tentpole at  $p$ ; thus,

$$h_p := \min\{\varepsilon, 1 - \varepsilon\}w_p\sigma.$$

If  $h > (1 + \gamma)h_p$ , then choose  $h' = (h + h_p)/2$  as the new tentpole height; otherwise, let  $h' = h$  remain the chosen tentpole height. Clearly, this choice still retains the progress guarantee of  $h_p$ .

In the context of a target time constraint, we apply the above rule only in the last case when the original tentpole height is accepted by the logic that aims to achieve the target time  $T_p$ . If the tentpole height has already been curtailed by a target time constraint, then we do not reduce it any further.

### 6.4 Coarsening

Coarsening is always stated as a request while refinement is a necessity. However, for the purpose of efficiency, it is important to coarsen aggressively any parts of the front that are marked as coarsenable so that the number of spacetime elements, and thus the total computation time, is reduced.

Coarsening the front by merging adjacent triangles requires the triangles to be coplanar in spacetime. In the previous sections, we gave algorithms to make the entire front conform to a global target time  $T$ . We use a similar approach to give a new reliable coarsening algorithm. Our new algorithm guarantees that any part of the front that is marked as coarsenable will eventually be coarsened. This requires that coarsenable pairs of triangles be made coplanar after a finite number of tent pitching steps. Often, this requires that the actual tentpole height at a vertex of the two triangles being merged be reduced to achieve the coplanarity constraint. Our new algorithm guarantees that, even with the additional coplanarity constraints, the worst-case tentpole height, and hence the minimum temporal aspect ratio of elements, is bounded from below. In fact, the minimum tentpole height at a given vertex is guaranteed to be at least  $\gamma$  times the minimum height in the absence of any coplanarity constraints, where  $\gamma \in (0, \frac{1}{2}]$  is a parameter to the coarsening algorithm.

Suppose  $S$  is a subset of triangles that are scheduled for coarsening. Choose a synchronization time  $T$  and assign it to each vertex incident on a triangle of  $S$ . Now, use the algorithm from the previous section to ensure that each of these vertices achieves their target time  $T$ . When all of them are coplanar with the constant time plane  $t = T$ , then perform the scheduled coarsening and then remove the scheduling constraint  $T$  from all vertices. Recompute a new target time for all vertices of the coarser triangles if the coarser triangles are also coarsenable. In fact, we also recompute the target time for every vertex of a triangle that gets refined.

What if multiple coarsenings are scheduled at the same time? In that case, it is possible that some vertex  $p$  has achieved its scheduled time  $T_2$  and is waiting for another vertex  $s$  of a sibling triangle to also achieve time  $T_2$ . Note that  $s$  need not be a neighbor of  $p$ , but  $s$  must be a neighbor of an immediate neighbor of  $p$ . In such a situation,  $p$  cannot be pitched even though it is a local minimum because  $p$  is waiting for  $s$ . However, this is not a problem because we can prove that  $s$  must eventually achieve time  $T_2$ .

If  $s$  has no scheduling constraint, then it will eventually be pitched because it will eventually become a local minimum vertex. Since  $s$  is lower than time  $T_2$ , it will be pitched to time  $T_2$ . On the other hand, if  $s$  has been scheduled to achieve a target time  $T_1$  because some other triangle incident on  $s$  is being coarsened, then it must be that  $T_1 < T_2$ . Hence, by induction, eventually  $s$  will achieve time  $T_1$  at which step the algorithm is free to pitch  $s$  further until it eventually achieves time  $T_2$ .

Formally, the new algorithm with coarsening constraints is given next.

### 6.4.1 New algorithm

Let  $\sigma \equiv \sigma_{\min}$  denote the reciprocal of the global fastest wavespeed.

Given a front  $\tau_i$  and a vertex  $p$  of the spatial projection of  $\tau$ , denote by  $w_p^i$  the minimum distance of  $p$  from line  $qr$  for every triangle  $pqr$  incident on  $p$ .

$$w_p^i := \min_{\Delta pqr \ni p} \{ \text{dist}(p, \text{aff } qr) \}$$

Let  $\tilde{\varepsilon}$  denote  $\min\{\varepsilon, 1 - \varepsilon\}$ . Since  $0 < \varepsilon < 1$ , we have  $0 < \tilde{\varepsilon} \leq \frac{1}{2}$ . Let  $h_p^i$  denote  $\tilde{\varepsilon} w_p^i \sigma$ . Note that  $w_p^i$  and  $h_p^i$  depend on the current front  $\tau_i$ .

Call a vertex  $v$  a *leaf vertex* if  $v$  is an interior vertex incident on four triangles, or  $v$  is a boundary vertex incident on two triangles, and if every triangle incident on  $v$  is a leaf in the refinement hierarchy. Call a leaf vertex  $v$  *coarsenable* if  $\text{level}(v) > 0$  and if all triangles incident on  $v$  are marked coarsenable by the numerical analysis.

#### Initialize

Fix the value of parameter  $\gamma$  such that  $0 < \gamma \leq \frac{1}{2}$ , e.g.,  $\gamma = \frac{1}{2}$ . Initialize the front  $\tau_0$ . Every vertex of  $\tau_0$  is assigned level zero. Every triangle of  $\tau_0$  is assigned a level number of zero.

Every vertex  $p$  of  $\tau$  (not just a local minimum) is assigned a target time  $T_p$ . We maintain the invariant that for every front  $\tau$ , for every vertex  $p$  of  $\tau$  we have  $\tau(p) \leq T_p$ .

If the problem requires a finite global target time, then let  $T$  denote this target time, otherwise let  $T \leftarrow \infty$ . Initially, every vertex  $p$  of  $\tau$  (not just a local minimum) is assigned a target time  $T_p \leftarrow T$ .

Refine the current front  $\tau$  as many times as needed until the following inequality is satisfied for each vertex  $p$ :

$$T_p \geq \tau(p) + \gamma h_p$$

Note that  $h_p$  is halved after every two levels of newest vertex bisection; hence, for a fixed  $T_p$  the refinement process will terminate. The refinement process does not change  $\tau(p)$ , hence the above inequality gives an upper bound on  $h_p$ .

### Tent pitching

At the current iteration of the algorithm, let  $\tau_i$  denote the current front at the beginning of iteration  $i$ .

**STEP 1: ASSIGN A TARGET TIME TO EACH VERTEX (NOT JUST LOCAL MINIMA).** The general idea is that if a set of triangles of  $\tau$  is marked as coarsenable by the numerical analysis, then we bring all the five vertices involved to a common target time value; then, the triangles are coplanar and the front can be coarsened immediately.

There are three steps to computing a target time  $T_p$  for each vertex  $p$ .

(1) For each vertex  $p$ , there is a lower bound  $l_p$  on the target time  $T_p$ . (The target time  $T_p$  is computed in step 3.) A lower bound is necessitated in order to maintain the invariant of Equation 6.1. This lower bound  $l_p$  depends on all the triangles on the current front incident on  $p$ .

The lower bound  $l_p$  on the target time  $T_p$  is computed as follows:  $l_p = \tau_i(p) + \gamma h_p^i$ .

(2) We can coarsen a set of four triangles at once (as long as they are marked for coarsening by the numerical analysis). Call this a coarsenable cluster  $C$ . Compute a target time  $T_C$  for the cluster as the *maximum* of  $l_p$  for each vertex  $p$  in the cluster. (There will be exactly five vertices incident on the four triangles.)

If  $s$  denotes the degree-4 vertex of the cluster  $C$  that will be removed as a result of coarsening cluster  $C$ , then the vertex  $s$  participates in only one coarsenable cluster, the cluster  $C$ . Therefore, the target time  $T_C$  is also the target time  $T_s$  assigned to vertex  $s$  in step 3.

(3) For each vertex  $v$ , compute the target time  $T_v$  as the *minimum* of the cluster times  $T_C$  for each coarsenable cluster  $C$  to which the vertex  $v$  belongs. Since  $T_C \geq l_v$  for each cluster  $C$ , we conclude that  $T_v \geq l_v$  and, hence, the invariant of Equation 6.1 is satisfied.

Note that a cluster of triangles is coarsenable only if each of the four triangles in the cluster is a leaf, i.e., has not been subdivided any further. If  $v$  does not belong to any coarsenable cluster, then the target time  $T_v$  is the global target time  $T$  (which may be  $+\infty$ ). Note that step (1) looks at *all* triangles incident on  $p$  in order to compute  $l_p$ , but step (3) looks at only *coarsenable* triangles incident on  $p$  in order to compute  $T_p$ .

After a coarsening takes place, a new lower bound  $l_p$  is computed for each vertex  $p$  of the two coarser triangles that violates the invariant, and a new target time is computed for each coarsenable cluster to which  $p$  belongs.

Let  $s$  be a coarsenable vertex (see Figure 6.1) and let  $C$  denote the set of four coarsenable triangles incident on  $s$ . (See figure.) Let  $V$  be the set of five vertices of the triangles in  $S$ . (In Figure 6.1, the set  $V$  is  $\{p, q, r, s, u\}$ .)

For each vertex  $v \in V$ , compute  $l_v$  such that

$$l_v = \tau_i(v) + \gamma h_v^i$$

Next, assign a target time  $T_s$  to the coarsenable vertex  $s$  (and thus to  $C$ ) such that  $T_s := \max_{v \in V} l_v$ .

Mark each vertex  $p$  such that  $\tau(p) < T_p$  as *not ready*.

**STEP 2: PITCH A TENT AT A LOCAL MINIMUM.** Let  $p$  be an arbitrary local minimum of  $\tau$  such that  $\tau(p) < T_p$ . In other words, select as a candidate for tent pitching only those local minima that have not yet achieved their respective target times. At least one candidate vertex must exist; in particular, a global minimum vertex must be a candidate vertex unless the entire front has achieved the global target time  $T$ .

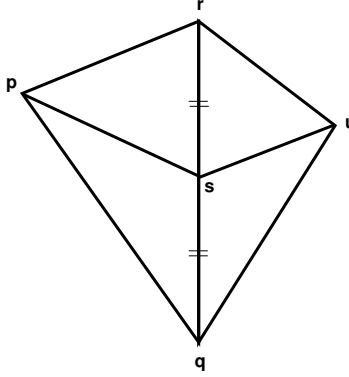


Figure 6.1: Coarsening a set of four triangles in one step.

Let  $\tau'(p)$  denote the time value of the top of the tentpole at  $p$ , maximized to satisfy all causality and progress constraints. The new algorithm chooses a possibly different time value  $\tau''(p)$  for the top of the tentpole such that  $\tau(p) \leq \tau''(p) \leq \tau'(p)$ .

Apply the following rule at each tent pitching step.

1. **Case 1:** If  $\tau'(p) \geq T_p$ , then choose  $\tau''(p) := T_p$  as the new top of the tentpole at  $p$ . After pitching  $p$ , mark  $p$  as *ready*.

After pitching  $p$ , some cluster  $C$  of triangles participating in a single coarsening step may become coplanar with the corresponding target time  $T_C$ . For each coarsenable vertex  $q$  neighboring  $p$ , if all neighbors of  $q$  are ready, then all triangles incident on  $q$  are coarsened immediately. Note that  $q$  is deleted as a result of this coarsening step. For each neighbor of  $q$ , compute a new target time as described in Step 1.

2. **Case 2:** Otherwise, if  $\tau'(p) \geq T_p - \gamma h_p$ , then choose  $\tau''(p) := T_p - (1 - \gamma)h_p$  as the new top of the tentpole at  $p$ .
3. **Case 3:** Otherwise, we must have  $\tau'(p) < T_p - \gamma h_p$ ; then choose  $\tau''(p) := \tau'(p)$  as the top of the tentpole at  $p$ .

If a patch is rejected, causing refinement of the front, then each new triangle is marked *not* coarsenable. Whenever an edge is bisected as a result of newest vertex bisection, then assign the new vertex (the interior point of the bisected edge) a target time equal to the global target time  $T$ .

### A cycle in the propagation pattern

If the pattern of marked vertices is such that it causes a cycle in the propagation pattern (see Figure 6.2), then the only reliable way to coarsen any pair of triangles in the set is to coarsen them all simultaneously. Fortunately, if the largest edge of each triangle is chosen as the base, then a cyclic marking is very unlikely to occur because it would require a cycle of isosceles triangles. If ties between two edges of equal length are broken consistently, for instance using lexicographic order, then such a cycle will *never* occur.

### 6.4.2 Proof of correctness

It remains only to prove that the minimum height of each tentpole is bounded. In the previous section, we showed that for every vertex  $p$  of the front  $\tau_i$  the minimum height of every tentpole was at least  $\gamma h_p^i$ . Since there is a minimum

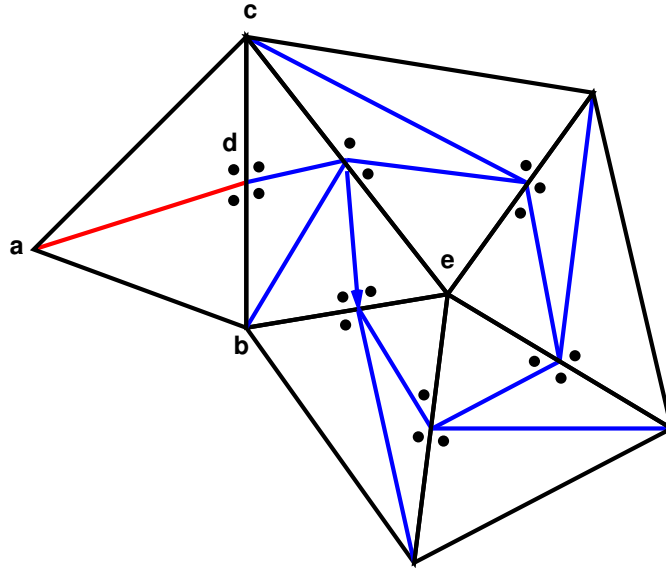


Figure 6.2: Coarsening a set of several triangles in one step.

element size that is always numerically acceptable, there is a global minimum  $h_p$  that implies a corresponding positive lower bound on the minimum height of each element.

## Chapter summary

Guaranteed coarsening has been an open problem ever since our adaptive meshing result was published (ACE<sup>+</sup>04). We need to strike the right balance between efficiency and accuracy—the former achieved by adaptive refinement and aggressive coarsening, the latter achieved by theoretical guarantees on worst-case element quality. The coarsening algorithm in this chapter retains the lower bounds on element temporal aspect ratios proved in the absence of coarsening, and this represents a big step forward. However, the heuristic of Section 6.2 seems to perform a little better in practice. We can imagine a few other heuristics that would attempt to improve element quality and solution accuracy in practice, but it seems hard to prove that they will be efficient in terms of guaranteed coarsening of coarsenable regions.

A new coarsening operation proposed by Jeff Erickson is to delete an interior vertex  $U$  of degree-4 with neighbors  $P$ ,  $Q$ ,  $R$ , and  $S$  by constructing a patch consisting of two tetrahedra: either the two tetrahedra  $PQRU$  and  $PRSU$ , or the two tetrahedra  $PQSU$  and  $QRSU$ ; the first choice creates two new triangles  $PQR$  and  $PRS$  on the new front while the second choice creates the triangles  $PQS$  and  $QRS$ . The coarsening operation is performed only when the quality of each tetrahedron in the patch exceeds an acceptable threshold. The same idea is used to coarsen the boundary by deleting a degree-3 boundary vertex and creating a single-tetrahedron patch. The algorithm extends naturally to deleting a vertex  $u$  of arbitrary degree; the triangulation after deleting  $u$  is obtained, for instance, by contracting the edge  $up$  for some neighbor  $p$  of  $u$ . We could prefer contracting the shortest contractible edge incident on  $u$ . The alternative coarsening algorithm is to pitch possibly inclined tentpoles at  $u$  and/or any of its four neighbors, to make triangles  $PQU$  and  $UQR$  coplanar and the triangles  $PUS$  and  $SUR$  coplanar before merging them pairwise. The former coarsening method does not guarantee non-degeneracy of the spacetime elements but uses fewer tetrahedra (two instead of four) and does not require that pairs of triangles be coplanar.

# Chapter 7

## Extensions

In this chapter, we describe extensions to our algorithms, in the form of newer advancing front operations. We show how to incorporate operations that simultaneously advance the front in time as well as smooth the spatial projection of the front to improve the spatial aspect ratio of front simplices. Front smoothing will likely increase the amount of progress in subsequent tent pitching steps and potentially improve the quality of future spacetime elements. These more general operations are potentially useful for tracking moving boundaries. We give a framework that employs the new advancing front operations to make local modifications to the front in response to changes in the geometry of the domain. We describe our recent work and initial progress on tracking moving domain boundaries.

Next, we discuss details of implementing our algorithms, such as the choice of various parameters. Our advancing front algorithms can be tuned to perform much better in practice than the theoretical performance guarantee by a suitable choice of parameters and heuristics.

### 7.1 Extensions and heuristics

In this section, we describe extensions to our advancing front algorithm and propose heuristics to improve the performance in practice.

#### 7.1.1 Asymmetric cone constraints

In the presence of anisotropy, waves travel with different speeds in different directions. Therefore, a cone of influence whose slope in spatial direction  $\mathbf{n}$  is equal to the wavespeed in that direction must necessarily be non-circular. The resulting cone constraint is asymmetric because it enforces a different gradient constraint in different spatial directions in order to satisfy causality.

Our algorithm can be easily extended to handle asymmetric cone constraints by enforcing the causality constraint separately for each spatial direction. Thus, we enforce a constraint on the gradient of every front in every spatial direction  $\mathbf{n}$  to satisfy the causality constraint in the direction  $\mathbf{n}$ . This will be our approach in higher dimensions as well. In the presence of asymmetric cones of influence, we assume implicitly that each slope  $\sigma$  is quantified universally for every spatial direction  $\mathbf{n}$ . Causality and progress constraints are interpreted as gradient constraints in each spatial direction  $\mathbf{n}$ .

We can re-interpret each theorem in the anisotropic setting. We understand every statement to be implicitly quantified over every spatial direction  $\mathbf{n}$ .

For instance, we can restate our theorems for  $2D \times \text{Time}$  in the anisotropic setting as follows. Let  $\triangle PQR$  be a triangle of the front  $\tau$  with  $P$  as one of its lowest vertices. Without loss of generality, assume  $\tau(p) \leq \tau(q) \leq \tau(r)$ .



Let  $\varepsilon$  be any real number in the range  $0 < \varepsilon < 1$ . Let  $\sigma_{\min}$  denote the global minimum causal slope in any spatial direction. Let  $\sigma_{\mathbf{n}}(\Delta)$  denote the minimum causal slope in spatial direction  $\mathbf{n}$  over every point of  $\Delta$ , i.e.,

$$\sigma_{\mathbf{n}}(\Delta) := \min_{P \in \Delta} \{\sigma_{\mathbf{n}}(P)\}$$

1. Let  $\Delta P'QR$  denote the triangle of the front  $\tau'$ , obtained by pitching the local minimum  $P$ , for arbitrary  $\tau'(p)$  in the range  $\tau(q) \leq \tau'(p) \leq \tau(q) + \varepsilon \sigma_{\min} \text{dist}(p, \text{aff } qr)$ .

For every spatial direction  $\mathbf{n} \in \mathbb{R}^2$ , if  $\|\nabla \tau|_{qr}\| \leq (1 - \varepsilon) \phi_{qr} \sigma_{\mathbf{n}}(P'QR)$ , then  $\Delta P'QR$  satisfies  $\|\nabla \tau'\| < \sigma_{\mathbf{n}}(P'QR)$ .

2. Let  $\Delta P'QR$  denote the triangle of the front  $\tau'$ , obtained by pitching the local minimum  $P$ , for arbitrary  $\tau'(p)$  in the range  $\tau(q) \leq \tau'(p) \leq \tau(q) + (1 - \varepsilon) \sigma_{\min} \min\{|pq|, |pr|\}$ .

For every spatial direction  $\mathbf{n} \in \mathbb{R}^2$ ,  $\Delta P'QR$  satisfies

$$\|\nabla \tau'|_{pq}\| \leq (1 - \varepsilon) \phi_{pq} \sigma_{\mathbf{n}}(P'QR) \quad \text{and} \quad \|\nabla \tau'|_{pr}\| \leq (1 - \varepsilon) \phi_{pr} \sigma_{\mathbf{n}}(P'QR)$$

Our algorithm is modified to enforce gradient constraints simultaneously in every spatial direction. In other words, we require that for every triangle  $PQR$  with local minimum vertex  $P$ , the slope of the edge  $QR$  is less than or equal to  $(1 - \varepsilon) \phi_{qr} \sigma_{\mathbf{n}}(PQR)$ . If the wavespeed is increasing in the future, then the lookahead process will enforce a stronger gradient constraint parameterized by the future wavespeed  $\sigma'_{\mathbf{n}}$ . All previous theorems assure positive progress at each step when the appropriate gradient constraint is enforced for each spatial direction. The correctness of our algorithm requires the anisotropic no-focusing axiom, Axiom 1.3, which is also sufficient.

The asymmetric nature of cones of influence complicates the data structures, specifically the bounding cone hierarchy. While constructing the hierarchy, at each step we need to compute a tight, possibly asymmetric, cone that contains two given cones of influence. We have several choice for representing asymmetric cones, such as polyhedral cones (the convex hull of vectors in spacetime with the same origin) or cones with elliptical cross-sections. For the sake of efficiency, we require each cone to have constant complexity.

However, a noncircular cone is still a ruled surface. Therefore, both our earlier algorithms, exact and approximate, to maximize the progress at each step subject to causality continue to apply without any changes.

Anisotropic response means that waves propagate faster in one direction than another. This can lead to nonlocal cone constraints. However, our algorithm already handles nonlocal constraints.

### 7.1.2 Non-manifold domains

So far, we have assumed implicitly that the space domain at time  $t$  is a  $d$ -dimensional manifold. However, our algorithms and all discussions in this thesis extend to non-manifold domains. An example of a non-manifold domain in practice would be three thin metal sheets intersecting in a T-junction, or a mechanical assembly consisting of parts with complicated intersections.

Let  $M_t$  denote the space domain at time  $t$ . The space domain  $M_t$  is a subset of Euclidean space of appropriate dimensionality such that  $M_t$  has a  $d$ -dimensional simplicial complex. In this case,  $M_t$  could be a collection of triangles, edges, and vertices forming a 2-dimensional simplicial complex embedded in  $\mathbb{E}^3$ . However,  $M_t$  need not be a surface; for instance,  $M_t$  could consist of three triangles sharing a common edge. In this case, we say that the space domain has dimension  $d = 2$ . We measure distances between points in  $M_t$  by taking the corresponding distances in the ambient

Euclidean space which by the nature of the embedding is a lower bound on the geodesic distance between the same points.

### 7.1.3 Front smoothing

The progress constraint at the  $i$ th step also depends on the geometry of the front in step  $i + 1$ . As in the previous section, our aim is also to ensure that the progress guarantee at the  $i$ th step is proportional to local geometry of the spatial projection of the front  $\tau_i$ . The discussion in this section applies to arbitrary dimensions  $d \geq 2$ .

The amount of progress made by a local minimum  $p$  of  $\tau_i$  is proportional to

$$w_p := \min_{\Delta \in \text{link}(p)} \text{dist}(p, \text{aff } \Delta).$$

If we can increase  $w_p$ , then we would get taller tentpoles and therefore fewer spacetime elements overall. In this section, we give an algorithm that allows more general operations such as pitching inclined tentpoles and performing edge flips as long as causality and all progress constraints are satisfied. Each such operation is desirable if it improves the front locally in the sense of increasing the minimum  $w_p$  for any vertex  $p$  in the local neighborhood.

#### Inclined tentpoles

Mesh smoothing in the neighborhood of a vertex  $p$  is achieved by pitching an inclined tentpole at  $p$  from  $P = (p, \tau(p))$  to  $P'' = (p', \tau'(p'))$ . Advancing  $p$  in time as well as moving it in space can be thought of as a combination of two successive operations: (i) move  $p$  in space to  $p'$ , and then (ii) advance  $p'$  in time from  $P' = (p', \tau(p'))$  to  $P'' = (p', \tau'(p'))$ . Each of the spacetime elements in the resulting patch shares the tentpole  $PP''$  and has both a causal inflow facet on the old front  $\tau$  as well as a causal outflow facet on the new front  $\tau'$ .

We assume that the direction of the inclined tentpole  $PP''$  is fixed, for instance in an earlier iteration of the algorithm. To perform Laplacian smoothing, the direction of  $PP''$  could be chosen to move  $p$  closer to the centroid of its neighbors in the spatial projection of  $\tau_i$ .

Let  $\tilde{\tau}$  denote the intermediate front obtained from  $\tau$  after the first step. If  $\tilde{\tau}$  is progressive and if  $P'$  is a local minimum of  $\tilde{\tau}$ , then the final front  $\tau_{i+1} = \text{advance}(\tilde{\tau}, p', \Delta t)$  after pitching  $P' = (p', \tilde{\tau}(p'))$  to  $P'' = (p', \tau_{i+1}(p'))$  is progressive, for some  $\Delta t > 0$ . It follows by induction on the number of tent pitching steps that every front constructed by the algorithm is valid.

The length of the inclined tentpole  $PP''$  is constrained so that every triangle  $P''Q'fr$  is causal, i.e., not too steep. See Figure 7.1.

#### Anticipating changing geometry

The primary challenge we face is how to modify the progress constraints in response to changing geometry of the spatial projection of the front. The need to strengthen the progress constraint is clear from Lemma 2.4—if  $\phi(pqr)$  decreases because the obtuse angle of  $\triangle pqr$  becomes more obtuse (Figure 7.2), then positive progress cannot be guaranteed. The factor  $\phi(pqr)$  that appears in the progress constraint of Definition 2.6 must be changed to anticipate any potential increase in the largest obtuse angle of any triangle of the front.

We enforce a lower bound on the smallest acute angle and on the largest obtuse angle in the spatial projection of any front. Fix  $\phi_{\min} > 0$  such that  $\phi_{\min}$  is less than  $\phi(pqr)$  for any triangle  $pqr$  of the front  $\tau$ . (Recall Definition 2.5.)

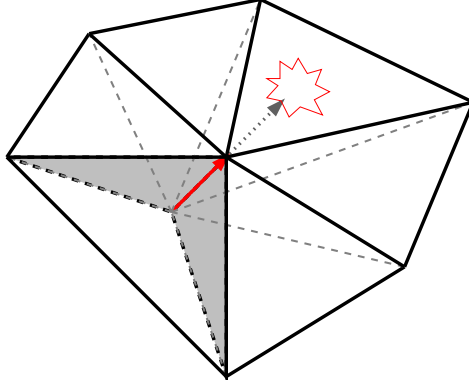


Figure 7.1: The length of an inclined tentpole is limited so that new front triangles are causal.

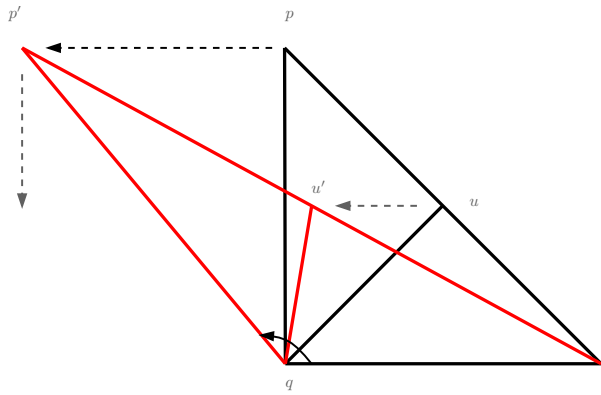


Figure 7.2: Moving a vertex can introduce or increase an obtuse angle on the front.

We will enforce that  $\sin \theta \geq \phi_{\min}$  for every angle of every triangle on the front constructed at each step. We are now able to strengthen the progress constraint to anticipate the changing geometry of the front as long as the front does not violate the following angle bound.

**Definition 7.1** (Angle bound  $\phi_{\min}$ ). *We say that a triangle  $\triangle abc$  satisfies the angle bound  $\phi_{\min}$  if the minimum sine of any angle of  $\triangle abc$  is at least  $\phi_{\min}$ .*

In many ways, the choice of  $\phi_{\min}$  is like the estimate of the global maximum wavespeed. We will exert a lot of effort in Chapter 3 to obtain better estimates of future wavespeed than the global maximum. However, for arbitrary changes to the front due to spatial motion, we do not know yet how to adaptively obtain a better estimate of how  $\phi(pqr)$  changes. For now, we have to be content with a global bound on the smallest acute angle as well as the largest obtuse angle allowed in the spatial projection of any front. Techniques similar to those in Chapter 3 may prove useful to adaptively estimate the changing geometry due to motion.

Currently, we do not know how to exploit the fact that the algorithm may freely choose the tentpole direction.

We strengthen the progress constraint by replacing, in Definition 2.6, every occurrence of  $\phi$  by  $\phi_{\min}$ , where  $\phi_{\min}$  is a parameter. Since our new progress constraint is stronger, Lemma 2.4 still holds. The price we pay for strengthening the progress constraint is a smaller worst-case progress guarantee, smaller by a factor of  $\phi_{\min}$ , due to the fact that the front in the *next* step has to satisfy a stronger gradient constraint.

**Definition 7.2** (Progress constraint  $\sigma$ ). *Let  $PQR$  be an arbitrary triangle of a front  $\tau$ . We say that the triangle  $PQR$  satisfies progress constraint  $\sigma$  if and only if for every edge, say  $qr$ , we have*

$$\|\nabla \tau|_{qr}\| := \frac{|\tau(r) - \tau(q)|}{|qr|} \leq (1 - \varepsilon)\sigma\phi_{\min}$$

In arbitrary dimensions, fix  $\phi_{\min} > 0$  such that  $\phi_{\min}$  is less than  $\phi(p_0p_1p_2\dots p_k)$  for any  $k$ -dimensional simplex  $p_0p_1p_2\dots p_k$  of the front  $\tau$ . (Recall Definition 2.11.)

Consider an arbitrary  $k$ -dimensional face  $p_0p_1p_2\dots p_k$  incident on  $p_0$ .

**Definition 7.3** (Progress constraint). *We say that a simplex  $P_0P_1P_2\dots P_k$  of the front  $\tau$  satisfies the progress constraint  $\sigma$  if and only if for every facet  $\Delta_i$  where  $0 \leq i \leq k$  we have  $\|\nabla \tau|_{\Delta_i}\| \leq (1 - \varepsilon)\sigma\phi_{\min}$ .*

Note that the progress constraints of Definition 7.2 and Definition 7.3 limit the gradient of every facet of a front simplex uniformly, unlike Definition 2.6 and Definition 2.13 which limits the gradient of only highest facets of each front simplex.

Let  $p$  be a local minimum of  $\tau$ . Suppose we advance  $p$  in time from  $\tau(p)$  to  $\tilde{\tau}(p)$  but no higher than its lowest neighbor, i.e.,  $\tilde{\tau}(p) \leq \tau(q)$  for every neighbor  $q$  of  $p$ . Additionally, we move  $p$  in space to  $p'$  but only so far that  $\Delta p'qr$  also satisfies the angle bound  $\phi_{\min}$ . By the monotonicity of the progress constraint, we know that the new triangle  $P'QR$  where  $P' = (p', \tilde{\tau}(p))$  satisfies the new progress constraint  $\sigma$  as long as  $\Delta PQR$  also satisfies the new progress constraint  $\sigma$ . We have thus proved the following lemma.

**Lemma 7.4.** *If a front  $\tau$  satisfies the progress constraint  $\sigma$  of Definition 7.2 and if  $p$  is a local minimum of  $\tau$ , then the new front  $\tilde{\tau}$  satisfies the progress constraint  $\sigma$  of Definition 2.6 where  $\tilde{\tau}$  is obtained by moving  $P = (p, \tau(p))$  to  $P' = (p', \tilde{\tau}(p))$  such that  $P'$  is also a local minimum of  $\tilde{\tau}$ ,  $p'$  is in the kernel of  $\text{star}(p)$ , and  $\tilde{\tau}$  satisfies angle bound  $\phi_{\min}$ .*

We restrict the motion of  $p$  so that for every triangle  $pqr$  incident on  $p$ , the smallest angle of  $\Delta p'qr$  is bounded from below. To build on earlier work which guarantees that  $p'$  can make finite positive progress if  $p'$  is a local minimum, we also need to guarantee that  $\tilde{\tau}$  is progressive and that  $p'$  is a local minimum of the front  $\tilde{\tau}$ . It is easy to see that, as long as  $p'$  stays a local minimum, the front  $\tilde{\tau}$  is progressive if  $\tau$  is progressive; this is because as long as  $p'$  is a local minimum of  $\tilde{\tau}$  we have  $\|\nabla \tilde{\tau}|_{\Delta}\| \leq \|\nabla \tau|_{\Delta}\|$  for every simplex  $\Delta$ . Therefore,  $p'$  must satisfy  $\tau(p') \leq \tau(q)$  for every neighbor  $q$  of  $p$ , where  $p$  is a local minimum of  $\tau$ .

The allowed region for  $p'$  such that  $\Delta p'qr$  satisfies the angle bound  $\phi_{\min}$  is shown in Figure 7.3 when a single triangle  $pqr$  is considered in isolation where  $\tau(p) \leq \tau(q) \leq \tau(r)$ . When all triangles incident on  $p$  are taken together and we know that the intersection of their allowed regions is nonempty because it contains at least  $p$ .

**Lemma 7.5.** *If  $\Delta PQR$  of the front  $\tau$  with  $\tau(p) \leq \tau(q) \leq \tau(r)$  satisfies  $\|\nabla \tau|_{qr}\| \leq (1 - \varepsilon)\phi_{\min}\sigma$ , then for every  $\Delta t \in [0, (1 - \varepsilon)\phi_{\min}\text{dist}(p, \text{aff } qr)\sigma]$  the front  $\tau' = \text{advance}(\tau, p, \Delta t)$  satisfies  $\|\nabla \tau'|_{rp}\| \leq (1 - \varepsilon)\phi_{\min}\sigma$ .*

*Proof of Lemma 7.5.* By Definition 2.6, the front  $\tau'$  satisfies progress constraint  $\sigma$  if and only if

$$\max\{\|\nabla \tau'|_{pq}\|, \|\nabla \tau'|_{qr}\|, \|\nabla \tau'|_{rp}\|\} \leq (1 - \varepsilon)\phi_{\min}\sigma$$

Since advancing  $p$  in time does not change the time function along  $qr$ , we have  $\|\nabla \tau'|_{qr}\| = \|\nabla \tau|_{qr}\| \leq (1 - \varepsilon)\phi_{\min}\sigma$ .

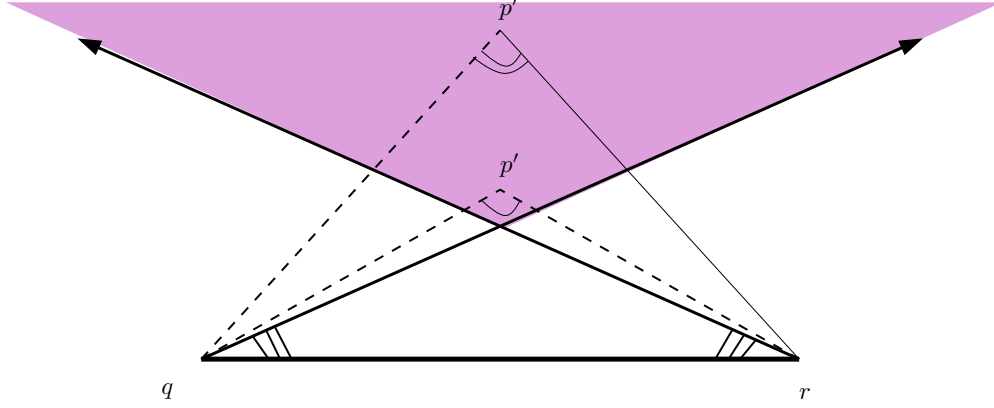


Figure 7.3: The allowed region for  $p'$  is the shaded region in the top:  $p'$  is restricted to the allowed region to ensure that  $\min\{\sin \angle p'qr, \sin \angle p'rq, \sin \angle rp'q\} \geq \phi_{\min}$ .

Since  $\triangle PQR$  satisfies progress constraint  $\sigma$ , we have

$$\max\{\|\nabla \tau|_{pq}\|, \|\nabla \tau|_{qr}\|, \|\nabla \tau|_{rp}\|\} \leq (1 - \varepsilon)\phi_{\min}\sigma$$

Also,  $p$  is a lowest vertex of  $\tau$ ; so  $\tau(p) \leq \min\{\tau(q), \tau(r)\}$ .

Consider the constraint  $\|\nabla \tau'|_{pq}\| \leq (1 - \varepsilon)\phi_{\min}\sigma$ . As long as  $\tau'(p) \leq \tau(q)$ , we have  $\|\nabla \tau'|_{pq}\| \leq \|\nabla \tau|_{pq}\| \leq (1 - \varepsilon)\phi_{\min}\sigma$ . Similarly, as long as  $\tau'(p) \leq \tau(r)$ , the constraint  $\|\nabla \tau'|_{rp}\| \leq (1 - \varepsilon)\phi_{\min}\sigma$  is automatically satisfied because  $\|\nabla \tau'|_{rp}\| \leq \|\nabla \tau|_{rp}\| \leq (1 - \varepsilon)\phi_{\min}\sigma$ .

When  $\tau'(p) > \tau(q)$ , the constraint  $\|\nabla \tau'|_{pq}\| \leq (1 - \varepsilon)\phi_{\min}\sigma$  is equivalent to  $\tau'(p) \leq \tau(q) + (1 - \varepsilon)\phi_{\min}\sigma|pq|$ . We have

$$\begin{aligned} \tau'(p) &\leq \tau(p) + (1 - \varepsilon)\phi_{\min}\sigma d_p \\ &\leq \tau(q) + (1 - \varepsilon)\phi_{\min}\sigma d_p \\ &\leq \tau(q) + (1 - \varepsilon)\phi_{\min}\sigma|pq| \end{aligned}$$

where the last inequality follows because  $d_p = \text{dist}(p, \text{aff } qr) \leq |pq|$ .

Similarly, when  $\tau'(p) > \tau(r)$ , the constraint  $\|\nabla \tau'|_{rp}\| \leq (1 - \varepsilon)\phi_{\min}\sigma$  is equivalent to  $\tau'(p) \leq \tau(r) + (1 - \varepsilon)\phi_{\min}\sigma|pr|$ . We have

$$\begin{aligned} \tau'(p) &\leq \tau(p) + (1 - \varepsilon)\phi_{\min}\sigma d_p \\ &\leq \tau(r) + (1 - \varepsilon)\phi_{\min}\sigma d_p \\ &\leq \tau(r) + (1 - \varepsilon)\phi_{\min}\sigma|pr| \end{aligned}$$

where the last inequality follows because  $d_p = \text{dist}(p, \text{aff } qr) \leq |pr|$ . □

We have thus shown that as long as the motion of  $p$  to  $p'$  is constrained to the allowed region at each step, the progress made by pitching  $p$  is positive and bounded away from zero.

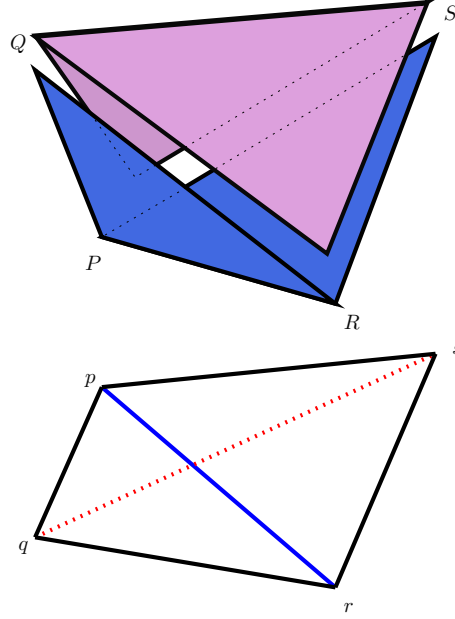


Figure 7.4: An edge is flipped by inserting a single tetrahedron.

### Edge flips

Another front advancing operation is to insert a single tetrahedron  $PQRS$  with inflow facets  $\triangle PQR$  and  $\triangle PRS$  and outflow facets  $\triangle PQS$  and  $\triangle QRS$ ; see Figure 7.4. If the volume of the tetrahedron  $PQRS$  is positive, this operation advances the front. If the solution within  $PQRS$  is sufficiently accurate, the single-element patch is accepted.

Let  $\tau$  and  $\tau'$  denote the fronts before and after this operation. We require that the front  $\tau'$  be causal and progressive to guarantee sufficient progress when a tent is pitched in the next step.

Triangles  $pqr$  and  $prs$  belong to the spatial projection of  $\tau$ , and triangles  $pqs$  and  $qrs$  belong to the spatial projection of  $\tau'$ . Therefore, the operation results in an edge flip, replacing the diagonal  $pr$  of the quadrilateral  $pqrs$  with the diagonal  $qs$ ; of course, quadrilateral  $pqrs$  must be convex.

Thus, the edge flip replacing  $pr$  by  $qs$  is allowed only if  $pqrs$  are in convex position in the spatial projection, tetrahedron  $PQRS$  has positive volume, and all four facets of the tetrahedron are causal and progressive.

The edge flip is desirable only if the resulting tetrahedron is non-degenerate and has acceptable quality, and if it improves or does not worsen the spatial aspect ratio of front triangles, i.e.,

$$\min \{ \phi(pqs), \phi(qrs) \} \geq \min \{ \phi(pqr), \phi(prs) \}$$

A similar flip operation could be defined in higher dimensions. It is not clear whether the resulting patch, which must sometimes consist of more than one spacetime element, satisfies all the objectives such as, for instance, the requirement that every element have a causal outflow facet.

### 7.1.4 Heuristics

In this section, we describe more general meshing operations, in addition to tent pitching, performed as long as each operation alters the front only in ways such that the new front is  $(h, l)$ -progressive for the chosen parameters  $h$  and  $l$ . We label these new operations *heuristics* because we cannot yet provide a guarantee that each such operation will be possible when it becomes necessary or even when it is desirable. These enhancements represent a step towards an adaptive advancing front algorithm for tracking spacetime features, such as moving boundaries, by aligning mesh facets along these features. Developing such a boundary-tracking meshing algorithm is still work in progress. We cannot yet guarantee that any of the operations mentioned can always be performed in response to an urgent need to improve the quality of the front or to guarantee progress at all. However, we are able to give sufficient and admittedly strong gradient constraints under which any front can be retriangulated, subject to the angle bound, so as to achieve the generalized front modification operations of this section.

Note that newest vertex bisection does not improve the quality of front triangles beyond a very limited amount. For instance, the largest obtuse angle in a triangle also occurs in its grandchildren. The more general operations on the other hand can improve the quality of front triangles, and therefore the worst-case progress guarantee. Our stronger progress constraints are sufficient gradient constraints under which a limited amount of improvement of the front can be performed whenever permitted by the constraints.

Our earlier work on adaptivity was restricted to adapting the mesh resolution to an error indicator; now, we are concerned also with adapting the mesh quality, in terms of worst-case temporal aspect ratio of spacetime tetrahedra.

1. **Generalized bisection** Our algorithm refines a triangle on the front by bisecting an edge the triangle at a point other than its midpoint, as long as the resulting smaller triangles satisfy the so-called *angle bound*.

The bisection direction for each triangle must be chosen so that repeated bisection retains the key property that each descendant of a triangle  $PQR$  has its edges parallel to three of the four directions defined by  $\triangle PQR$  and its apex—the three edges  $PQ$ ,  $QR$ , and  $PR$  plus the bisector  $PS$  for the appropriately chosen interior point  $s$  on the base  $qr$ .

Adjacent triangles must be bisected *compatibly*, i.e., adjacent triangle must agree on how to bisect their common edge so that refinement maintains a triangulated front.

The front is coarsened by undoing previous refinement.

The new bisection method means, for instance, that the largest angle in any triangle on each front can be bisected.

To ensure that the front can be advanced successfully after the bisection, each bisection is permitted only if the front after bisection is progressive. Note that this condition also limits the choice of direction along which to bisect a given triangle.

2. **Mesh smoothing:** Advancing a vertex  $p$  in time takes  $P = (p, \tau)$  to  $P' = (p, \tau')$  where  $\tau' > \tau$ . Pitching an inclined tentpole at  $p$  takes  $P = (p, \tau)$  to  $P' = (p', \tau')$  which simultaneously changes the spatial projection of the front, taking  $p$  to  $p'$  such that  $p'$  is in the kernel of  $\text{star}(p)$ . This achieves a limited amount of smoothing of the front, also known as  $r$ -refinement.

With the stronger progress constraints, we are able to allow inclined tentpoles subject to the angle bound. As long as the slope of each tentpole is *subsonic*, i.e., greater than the local causal slope, we are still able to prove a positive lower bound on the temporal aspect ratio of each spacetime tetrahedron.

3. **Flipping an edge:** We relax the assumption that the spatial projection of each front is a hierarchical refinement of the initial space mesh. Flipping an interior edge  $e = (p, q)$  replaces the diagonal  $e$  of a convex quadrilateral with the other diagonal  $e' = (r, s)$ . An edge flip in the spatial projection of a front  $\tau$  corresponds to adding a single tetrahedron  $PRQS$  to the spacetime mesh; this edge flip can be performed only if the resulting tetrahedron has bounded positive volume.

With the stronger progress constraints, we are able to allow flipping of interior edges as long as all triangles of every front satisfy the angle bound. An edge flip is desirable only if the resulting tetrahedron has bounded temporal aspect ratio. The algorithm is free to choose the marked vertex of each new front triangle created as a result of an edge flip.

By construction, since each of the above operations is performed only when permitted by the progress constraints, the new front  $\tau'$  after the operation satisfies the angle bound and is  $(h, l)$ -progressive. See Lemma 4.8.

Another operation that changes both the spatial projection of a front  $\tau$  as well as the time function is the following. Let  $p$  be a local minimum of  $\tau$ . The new progress constraint limits the gradient of each triangle  $\triangle PQR$  in  $\text{star}(p)$  in four different directions. Suppose we advance  $p$  in time from  $\tau(p)$  to  $\tilde{\tau}(p)$  but no higher than its lowest neighbor, i.e.,  $\tilde{\tau}(p) \leq \tau(q)$  for every neighbor  $q$  of  $p$ . Additionally, we move  $p$  in space to  $p'$  but only so far that  $\triangle p'qr$  also satisfies the angle bound  $\phi_{\min}$ . Then, by Lemma 7.4, we know that the new front  $\tilde{\tau}$  also satisfies the new progress constraint  $\sigma$ . Therefore, the algorithm is guaranteed to be able to pitch  $\tilde{P}$ , a local minimum of the front  $\tilde{\tau}$ , by a positive amount to make progress in time to get the new front  $\tau'$  with  $P' = (p', \tau'(p'))$ .

## 7.2 Tracking moving boundaries

In many applications, the geometry or even the topology of the domain changes over time. For instance, combustion of solid rocket fuel eats away at the boundary where the fuel burns. The mesh must adapt by changing the size of mesh elements, or by varying the placement of mesh features, or both. How to dynamically re-mesh in response to evolving geometry is a well-studied problem (ABG<sup>+</sup>00). With other dynamic meshing algorithm, global remeshing of the domain is performed whenever the mesh gets too distorted due to motion; at intermediate steps, smoothing or other incremental changes are interleaved with the solution.

In this section, we restrict our attention to meshing in response to changes in the geometry of the domain due to boundary motion. We assume that the topology of the domain does not change, which means it is sufficient to consider each connected component of the original space mesh separately. In our context, we always remesh locally by anticipating and adapting to changes in the shapes of front triangles. An external or an internal boundary (such as a material interface) moving with time describes a surface in spacetime. Similarly, shocks describe singular surfaces in spacetime. The solution jumps discontinuously across the shock surface. *Tracking* the boundary means aligning vertices, edges, and facets of our tetrahedral mesh with the corresponding surface (approximately). Boundary tracking combined with SDG methods implies a highly accurate resolution of discontinuities in the solution field.

We incorporate spatial motion over time in our advancing front framework by assuming either a spatial velocity vector or a direction in spacetime for every vertex of every front. The tentpole direction can be inferred from either input. Boundary vertices have the tentpole direction assigned to them by the numerical analysis, which is aware of the evolving nature of the domain. For all other vertices, the meshing algorithm is free to choose any subsonic tentpole direction. For instance, for the purpose of Laplacian smoothing, we choose for every interior vertex  $p$  a direction



vector in space pointing towards the centroid of the neighbors of  $p$ . The slope of the tentpole at  $p$  is chosen to be at least a constant factor greater than the reciprocal of the maximum wavespeed anywhere in  $\text{star}(p)$ .

We modify the basic framework of our interleaved mesh construction and solution procedure to recompute vertex velocities along with or as part of the solution.

Our motion model is sufficient to capture boundary motion that does not alter the topology of the underlying space domain over time—boundary vertices remain boundary vertices and interior vertices remain interior vertices throughout. This model therefore seems insufficient to capture splitting apart of the domain into more components, creation of tunnels, and other ways that increase the topological complexity of the domain such as creation of new non-manifold features by folding.

In previous chapters, we were meshing the spacetime domain, a prefix of  $M \times [0, \infty)$ , for the space domain  $M$  that did not change over time. In this section, our spacetime domain of interest,  $\Omega$ , is the volume swept through time by the space domain  $M_t$  at time  $t$ . Since different parts of a front  $\tau$  may have different time coordinates, the spatial projection of  $\tau$  need not correspond to the space domain at any time  $t$ .

## 7.2.1 Tracking boundaries in 1D×Time

Meshing in 1D×Time presents fewer challenges because the front at each step is constrained only by causality. We are free to modify the front at each step, such as by refinement or by smoothing, as long as the new front is causal.

### Front advancing operations

*Boundary vertices* are those that have velocities prescribed by the numerical analysis. We assume that all prescribed velocities are subsonic. All other vertices are *interior vertices*. The velocity of an interior vertex is computed as the average of the velocity vectors of its neighbors.

Our algorithm in 1D×Time only performs tent pitching operations, advancing a local minimum vertex at each step. The major challenge is prioritizing which vertex to pitch at each step. Since boundary vertices have prescribed motion, we have to adapt the geometry of the rest of the front, especially near the boundary, to anticipate the necessary change of geometry on the boundary.

As a first approximation, we choose in our new algorithm to prefer pitching an interior vertex over a boundary vertex.

The goal of our algorithm is to ensure a lower bound on the temporal aspect ratio of spacetime triangles while simultaneously satisfying a prescribed global lower bound  $l_{\min}$  on the length of the spatial projection of all spacetime triangles.

Let  $p$  be a local minimum vertex chosen by the algorithm to pitch next. Let  $q$  be a neighboring vertex and let  $r$  be the neighbor of  $q$  other than  $p$  if it exists. The tentpole at  $p$  is inclined and its slope with respect to the space domain is equal to the reciprocal of the speed of  $p$ .

The height of the tentpole at  $p$  is constrained in three different ways. Let  $h_c$  denote the supremum of the height of the tentpole  $PP'$  such that  $P'Q$  is causal. Let  $h_l$  denote the height of the tentpole  $PP'$  such that  $P'QR$  are collinear in spacetime. Let  $h_w$  denote the height of the tentpole  $PP'$  such that the length of the spatial projection of  $P'Q$  is equal to  $l_{\min}$  where  $l_{\min}$  is the minimum allowed length of the spatial projection of any segment of any front.

The algorithm chooses the final height of the tentpole depending on the following cases. The algorithm always satisfies the causality constraint; hence, the final height  $h$  of the tentpole is always less than  $h_c$ .

Let  $\delta$  be a positive quantity,  $0 < \delta < 1$ , large enough to avoid numerical difficulties. Hence,  $(1 - \delta)h_c < h_c$ .

Note that  $h_l \leq h_c$  always because  $h_l > h_c$  contradicts the causality of  $QR$ .

First, consider the situation  $h_w \leq (1 - \delta)h_c$ .

**CASE 1** Consider first the case  $h_l, h_w \leq (1 - \delta)h_c < h_c$ .

1.1. **Case  $h_l \leq h_w \leq (1 - \delta)h_c$ :** Choose  $h := h_w$ . If the resulting patch is rejected, then bisect  $pq$ .

1.2. **Case  $h_w \leq h_l \leq (1 - \delta)h_c$ :** We have no choice but to choose  $h := h_w$ . If the resulting patch is rejected, then bisect  $pq$ .

**CASE 2** Next, consider the case  $h_w \leq (1 - \delta)h_c < h_l \leq h_c$ .

2.1. **Case  $h_w \leq (1 - \delta)h_c < h_l$ :** We have no choice but to choose  $h := h_w$ . If the resulting patch is rejected, then choose  $h := \frac{1}{2}h_c$  if  $\frac{1}{2}h_c \leq h_w$ , otherwise bisect  $pq$ .

Next, consider the situation  $h_w > (1 - \delta)h_c$ .

**CASE 3** Thirdly, consider the case  $h_l \leq (1 - \delta)h_c < h_w$ . We do not distinguish between the two subcases (i)  $h_w \leq h_c$ , and (ii)  $h_c \leq h_w$ .

3.1. **Case  $h_l \leq (1 - \delta)h_c < h_w$ :** Choose  $h := h_c$  if  $h_w - h_c$  is sufficiently large, otherwise choose  $h := \frac{1}{2}h_c$ .

**CASE 4** Finally, consider the case  $(1 - \delta)h_c < h_w, h_l$ .

4.1. **Case  $(1 - \delta)h_c < h_l \leq h_w$ :** We do not distinguish between the two subcases (i)  $h_l \leq h_w \leq h_c$ , and (ii)  $h_l \leq h_c \leq h_w$ .

We have no choice but to choose  $h := (1 - \delta)h_c$ ; however, if  $h_w - h_c$  is too small, then choose  $h := \frac{1}{2}h_c$ .

4.2. **Case  $(1 - \delta)h_c < h_w < h_l$ :** We do not distinguish between the two subcases (i)  $h_w < h_l \leq h_c$ , and (ii)  $h_w \leq h_c \leq h_l$ .

We have no choice but to choose  $h := (1 - \delta)h_c$ ; however, if  $h_w - h_c$  is too small, then choose  $h := \frac{1}{2}h_c$ .

## Proofs

We would like to prove that the algorithm makes positive progress at each step while still guaranteeing causality and a lower bound of  $l_{\min}$  spatial projection length. In cases 3 and 4, the height of the tentpole is at least a constant fraction of  $h_c$ . We claim that in any sequence of tent pitching steps, cases 1 and 2 apply only a finite number of times before either case 3 or case 4 applies in the next step. Clearly, causality is always maintained because the final height  $h$  always satisfies  $h \leq (1 - \delta)h_c < h_c$ . It is easy to see that all four cases together ensure that the spatial projection of every segment on each front has length at least  $l_{\min}$ . Hence, all requirements are satisfied.

Note that cases 1 and 2 deal with the situation  $h_w \leq (1 - \delta)h_c$ . If the resulting patch is rejected, then the segment  $pq$  is bisected which means that the causality constraint  $h'_c$  that applies in the next step is smaller than  $h_c$  by a finite amount. Specifically,  $h'_c - h_c = \frac{1}{2}\text{len}(pq)\sigma$ . On the other hand, the constraint  $h_w$  also decreases to  $h'_w$  where  $h'_w - h_w = l_{\min}\sigma$ . Therefore, if  $l_{\min} < \text{len}(pq)/2$ , then the constraint  $h_c$  decreases faster than the constraint  $h_w$  with repeated applications of either case 1 or case 2. Note that  $\text{len}(pq)$  also halves with each iteration. Therefore, that after a bounded number of applications of cases 1 or 2, it must be the case that either case 3 or case 4 applies.

Thus, we can show that the front advances after a finite number of steps; however, we haven't shown yet that the front achieves a target time  $T$  in a finite number of steps, unless we also show that the front is refined only a finite number of times before being coarsened because  $h := h_l$  is chosen at some step.

## Coarsening

Let  $P$  be an arbitrary local minimum of a causal front  $\tau$ . Let  $Q$  and  $R$  be neighbors of  $P$ . We claim that in the next step in which  $P$  is pitched to create the new causal front  $\tau'$ , it is possible to coarsen and delete at least one of the segments  $PQ$  or  $PR$  or both, without creating degenerate spacetime triangles.

Without loss of generality, assume  $\tau(r) \geq \tau(q)$ . First, consider the case that  $\tau(r) \geq \tau(p) + \Delta$  for some sufficiently large  $\Delta > 0$ . Then, in the next step,  $P$  can be pitched to  $P'$  such that  $Q - P' - R$  are collinear in spacetime and  $\tau'(p) \geq \tau(p) + \Delta t$  where  $\Delta t \geq \frac{\text{len}(pq)}{\text{len}(qr)} \Delta$ .

This suggests that we need to bound the ratio of the spatial lengths of any two adjacent segments on the front. For instance, if  $\frac{\text{len}(pq)}{\text{len}(pr)} > \frac{2}{3}$ , then bisect  $pq$ . Equivalently, if we start with an initial front that satisfies this balance condition then the balance can be maintained by propagating refinement of a segment to neighboring segments.

Next, consider the remaining case that  $\tau(q), \tau(r) \cong \tau(p)$ . Then,  $P$  can be pitched to  $P'$  such that either  $P'Q$  or  $P'R$  is tight against the causality constraint, i.e., has slope equal to  $(1 - \varepsilon)\sigma$ . This reduces the number of non-strict local minima. Specifically, it reduces the number of local minima for which both the incident edges are not tight against the causality constraint. By induction on the number of such minima, it follows that eventually there will be a local minimum vertex such that at least one of its incident edges has slope equal to  $(1 - \varepsilon)\sigma$ . (Such a local minimum may be a boundary vertex and therefore also a strict local minimum.) In this situation, the first case above will apply and it will result in coarsening.

**GUARANTEED COARSENING** In Chapter 6 we give an algorithm that will guarantee coarsening while still maintaining lower bounds on the minimum tentpole height. Coarsening a portion of the front takes some time before that portion can be made coplanar and coarsenable. As long as the motion of the boundary permits the additional time taken to coarsen reliably, for instance if the boundary moves very slowly, we can guarantee that the segments near the front will also satisfy the lower bound on the size of their spatial projections.

## 7.2.2 Tracking boundaries in $2D \times \text{Time}$

In this section, we describe an algorithm in  $2D \times \text{Time}$  that uses the following advancing front operations to track moving domain boundaries—tent pitching, smoothing, edge bisection, vertex deletion, and edge flips. Our algorithm does not create inverted elements (i.e., tetrahedra with negative volume). We cannot yet guarantee that the algorithm will always make progress by creating non-degenerate elements. In the future, we could use a similar algorithm for tracking shock fronts. Each operation changes the triangulation of the front. Most operations also advance the front and the solution.

Meshing in  $2D \times \text{Time}$  to track spacetime features is challenging because of the need to satisfy not only causality but also progress constraints at each step. The general framework of our algorithm in  $2D \times \text{Time}$  is to prefer operations that increase the spatial quality of front triangles without introducing refinement whenever possible. We devised a policy to assign priorities to various front advancing operations with the aim of proving correctness as done for Delaunay refinement algorithms (Ede01; CD03; CP03).

First, we outline the various meshing operations, in addition to the usual tent pitching operation which advances a single vertex in time.

**PITCHING INCLINED TENTPOLES** We advance  $P$  to  $P'$  along the given tentpole direction in spacetime, creating a tentpole  $PP'$ . The tentpole direction is the one computed by the solver; when the boundary is moving the tentpole

is inclined with respect to the vertical time axis. The amount of progress, i.e., the length of the inclined tentpole, is constrained to prevent inverted elements and is limited by causality. See Figure 7.1.

**SMOOTHING** The meshing algorithm can freely choose the tentpole direction for other vertices such as those created by refinement in the interior. We choose the tentpole  $PP'$  to smooth the front and improve the spatial aspect ratio of front triangles. Alternatively, we choose the tentpole  $PP'$  to align some implicit facets with a spacetime surface.

**EDGE BISECTION** Edge bisection is the same operation as the newest vertex refinement described in Chapter 4. Bisecting triangles on the current front decreases the size of future spacetime elements. As long as the vertex incident on the largest angle is chosen as the apex of the triangle, newest vertex refinement also decreases the largest angle which increases the likely progress in the next step.

**VERTEX DELETION** The front is coarsened by deleting a vertex when permitted by the numerical error estimate. Vertex deletion is achieved by inserting a patch of one or more tetrahedra and simultaneously advancing the front.

**EDGE FLIPS** Flipping an edge of the front triangulation can increase the aspect ratio of front triangles and improve the quality of future spacetime tetrahedra. An edge flip of the edge  $pr$ , a diagonal of the convex quadrilateral  $pqrs$ , is achieved by inserting a single tetrahedron  $PQRS$  as long as the tetrahedron has positive volume and sufficient quality. See Figure 7.4.

### **A framework in $2D \times Time$**

Choose the applicable operation that is first in the sequence listed below. If a patch created by one of the operations is rejected, then proceed to the next operation in the sequence to try to create an acceptable patch. If there are several candidates for where to perform a given operation, choose a candidate that makes it most likely that in the next step an operation earlier in the sequence will become possible. If there is more than one candidate operation, then perform these independent operations simultaneously in parallel whenever possible.

1. Coarsen the front by deleting a vertex  $u$
2. Flip an edge of the front if it improves the spatial aspect ratio
3. Pitch an interior vertex to smooth local triangulation
4. Pitch a boundary vertex in prescribed direction

In general, coarsening operations, or operations that decrease the number of triangles on the front, are preferred over those that refine the front because coarsening is harder to achieve in practice and to guarantee in theory. The front will still be at least as refined as required by the numerical error indicator.

Additional heuristics include preferring to pitch local minima in the interior of the domain over those on a moving boundary. For an interior vertex, we choose a tentpole direction that is the average of the tentpole directions computed for its neighbors. If an obtuse angle gets too big, we flip or bisect the opposite edge. We bisect an edge if its endpoints have very different velocities; we choose an average velocity for the new midpoint.

Each operation is performed only when allowed by the DG solver. We adapt the mesh in response to numerical error estimates as before; in addition, we allow the algorithm to refine and coarsen the front in response to changing local feature size.

We speculate that the above policy for choosing the various front advancing operations and prioritizing among them is an acceptable first approximation for very simple classes of motion. However, a more sophisticated policy needs to be devised. Note that the algorithm incurs the additional complexity of choosing which operation to perform at each step. Also, the more complicated the policy, the harder it is to parallelize the meshing algorithm.

We described a framework using a wider vocabulary of advancing front operations to mesh in spacetime. Even without motion, we could use our algorithm to mesh static curved features adaptively. Theorems are lacking, except in very restricted cases, such as  $1D \times \text{Time}$ , and uniform translation of the entire domain. It remains a very interesting and challenging open problem to devise a provably correct algorithm even for a restricted but still useful class of motion.

### 7.3 Practical issues

There are several choices to be made in practice when implementing our meshing algorithms.

**CHOICE OF PARAMETER  $\varepsilon$**  The value of the parameter  $\varepsilon$  in the range  $0 < \varepsilon < 1$  controls how greedy the algorithm is. Values of  $\varepsilon$  close to 1 strengthen the progress constraint and therefore potentially limit the height of tentpoles. Choosing a very small values of  $\varepsilon$  weakens the progress constraint. It is reasonable to expect that in practice smaller values of  $\varepsilon$  mean that most tentpole heights are limited by causality and therefore the average tentpole height is larger. However, the *theoretical guarantee* on tentpole height due to the causality constraint is proportional to  $\varepsilon$ . It is therefore important to choose an appropriate value of  $\varepsilon$ , perhaps specific to each problem instance, that achieves both adequate minimum tentpole height while maximizing the average tentpole height. A value of  $\varepsilon$  around the middle of its allowed range, i.e.,  $\varepsilon \approx \frac{1}{2}$ , is likely to be a good choice in practice.

**CHOICE OF LOOKAHEAD PARAMETERS** The horizon parameter  $h$  and the adaptive lookahead parameter  $l$  (Chapter 5) can be fixed *a priori* or can be increased adaptively if greater progress is desired. Arguably, the algorithm for general  $(h, l)$  is complicated to implement. In practice, depending on the underlying physics, it may suffice to fix the parameters at a small value, say  $h = l = 1$ .

**CHOICE OF HEURISTIC** Tent Pitcher is not restricted to pitching only local minima, even though the theoretical progress guarantee applies only to the minimum progress made by advancing an arbitrary local minimum. To increase the degree of parallelism of the algorithm, it is beneficial to pitch any vertex where some positive progress is guaranteed even though it might not be the choice that guarantees the most progress at the current step.

Preliminary experiments suggest that the quality and overall efficiency of the solution strategy depend on the choice of which local minimum vertex to advance at each step, whenever more than one candidate is available or whenever other operations are also available. All algorithms so far leave this as a free choice to be decided heuristically. We strongly recommend making empirical studies of how to exploit different heuristics to generate better quality and more efficient meshes.

**DATA STRUCTURES FOR THE FRONT** A significant advantage of the advancing front approach is that we need to store only the front and a collection of unsolved patches. The front is  $d$ -dimensional, the same as the space domain. The

unsolved patches are transient and can be discarded as soon as they are solved and accepted. We recommend separate representations of solved elements and unsolved patches because this would allow the solver to be oblivious of how the inflow information for a unsolved patch was computed—whether by a previous iteration of the same algorithm, by initial and boundary conditions, or by some entirely different solution procedure. Standard data structures (Wei85) are available to represent the front in  $2D \times \text{Time}$ . The adjacency information between facets of the front and facets of the spacetime elements stores either a many-one or a one-many relation, because of the weak simplicial complex property, which can be represented by pointers or arrays. Thus, our algorithms truly require only very basic data structures capable of representing a weakly conforming unstructured simplicial mesh.

**MAINTAINING A TRIANGULATION** When we refine one triangle on a 2D front, we may be forced to refine other nearby triangles in order to maintain a conforming triangulation of the front. See Figure 4.3. The propagation path touches every triangle in the worst case, but in practice, the propagation path usually has small constant length and does not involve loops. This is especially the case if the largest angle in each triangle is used to choose the marked vertex.

The algorithm need not wait for the entire propagation path to be executed before proceeding with the next advancing step. In fact, only the initial bisection was required by the numerical error indicator; all further bisections are merely artifacts of the algorithm because the algorithm requires the front to be conforming. Therefore, we employ a lazy propagation scheme that delays propagating refinement to adjacent triangles unless absolutely necessary. This also reduces the need to synchronize and communicate across processors in the parallel setting.

Lazy propagation splits the adjacent triangle but does not propagate further immediately. Instead, the propagation is delayed until the adjacent triangle needs to be refined or pitched. In the interim, the triangulation may consist of transient triangles. Eventually, the final result is exactly the same as if the entire propagation path was executed in one step.

**Coarsening:** A coarsening step that nullifies the last refinement in a refinement propagation path usually does so by deleting a degree-4 vertex. An exception to this rule is shown in Figure 4.3, where the last refinement cannot be nullified by deleting a degree-4 vertex because all vertices have degree greater than 4. However, a simple edge flip of one of the edges involved in the penultimate bisection produces a degree-4 vertex that can be deleted to remove the last refinement. Thus, five triangles are involved in the coarsening step instead of just four. Note that this case occurs only when a refinement propagation contains a loop. This is not the case when the largest angle of each triangle is marked and ties are broken suitably.

**BOUNDING CONE HIERARCHY** Non-constant wavespeed due to nonlinear response means that the strictest cone constraint that limits the height of a tentpole can belong to a point of the front arbitrarily far away. It is expensive to examine all cone constraints, one for each triangle of the front, to determine the most limiting cone. We adopt standard techniques used in computational geometry and collision detection in robot motion planning (Lat91). At each step, we wish to solve the following optimization problem: maximize the height of the tentpole subject to all cone constraints. We group all cone constraints into a hierarchy. Specifically, we use a bounding cone hierarchy to efficiently compute a hierarchical approximation of the actual wavespeed at a point in the future. In practice, we expect that only a few constraints in the hierarchy need to be examined on average.

We compute a hierarchical decomposition of the front, say using METIS (Kar; KK98) as a mesh partitioning tool or using a *kd-tree* (dBSvK00). We build the cone hierarchy bottom-up, combining pairs of bounding cones by

computing a tight bounding cone for them. Each node in the hierarchy (a binary tree) stores a cone tightly containing the cones of its children.

The cone hierarchy is traversed top-down. Starting at the root, we maintain a priority queue of cone constraints. At each step, we query the strictest constraint from the queue. If the current strictest cone is a leaf in the hierarchy or if it guarantees sufficient progress (say a constant fraction of the amount of progress when limited by the causality constraint alone), then we accept the resulting tentpole height. Otherwise, we replace the strictest cone by its children and repeat.

Refinement and coarsening of the front induce a corresponding refinement and coarsening of the cone hierarchy. Since the front adaptivity in response to the error indicator can be non-uniform, the cone hierarchy can get heavily unbalanced. To maintain efficiency, the cone hierarchy needs to be periodically rebalanced or recomputed.

**NONCIRCULAR BOUNDING CONES** Anisotropic cone constraints, i.e., cones with noncircular cross sections, complicate the data structures used for the cone hierarchy but do not introduce substantial algorithmic difficulties. For instance, if cones of influence are elliptical, then at each step while constructing the hierarchy we need to compute an elliptical cone that contains as tightly as possible the two elliptical cones of its children. Likewise, queries of the cone hierarchy are a little different—each requires checking whether a triangle or  $d$ -simplex of the front intersects an elliptical cone. We are able to exploit the facet that a cone of any cross-section is a ruled surface to reduce the dimensionality of the simplex involved in checking for intersections.

**PARALLEL DATA STRUCTURES** The Tent Pitcher algorithm and all algorithms in this thesis are inherently parallel—patches created by pitching non-adjacent local minima of the same front can be solved simultaneously and independently of each other because patch boundaries are causal.

The front is decomposed into subdomains by a hierarchical partition. Within each subdomain, a local neighborhood  $N$  can be advanced independently of other subdomains unless  $N$  is at the boundary of its subdomain in which case interprocessor communication is required to ensure mutual exclusion. The bounding cone hierarchy within the subdomain assigned to a single processor is a local sequential data structure. We need a parallel tree data structure to query bounding cones stored on other processors.

Load balancing means repartitioning of the domain. The bounding cone hierarchy must also be recomputed.

**LAZY UPDATES TO REDUCE INTERPROCESSOR COMMUNICATION** At every step, the wavespeed is computed as part of the solution and the bounding cone hierarchy needs to be updated to reflect this change. An increase in the wavespeed somewhere may impact the progress at a remote location. Therefore, this change propagates potentially to every other subdomain, requiring communication and synchronization between processors.

We can reduce interprocessor communication by performing lazy updates of the bounding cone hierarchy to reflect changes in the wavespeed. Because of the no-focusing assumption, current estimates of the wavespeed are always conservative and therefore acceptable approximations of future wavespeed. If sufficient progress is guaranteed even with these conservative approximations, then there is no immediate need to compute the new wavespeed. Therefore, we can queue the updates of the cone hierarchy and perform the actual update later.

## Chapter summary

We have been able to use the new operations in our arsenal, such as pitching inclined tentpoles and performing edge flips, to give advancing front meshing algorithms in 1D- and 2D×Time. Extending the heuristics of this chapter to higher dimensions, say 3D×Time would be very interesting. These newer algorithms remain heuristics in the sense that we are not able to prove yet that we will be able to successfully mesh the spacetime domain of interest with nondegenerate elements for a general class of motion of the boundary or for tracking a fairly diverse class of spacetime features. For instance, it remains an open question whether we can align causal and implicit facets of the mesh with an arbitrary set of piecewise linear constraints in spacetime. The main challenge remains to prove nontrivial worst-case lower bounds on the temporal aspect ratio of spacetime elements under these additional constraints.



# Chapter 8

## Conclusion and open problems

We extended Tent Pitcher, the advancing front algorithm due to Üngör and Sheffer (ÜS00) and Erickson *et al.* (EGSÜ02), to adaptively compute efficient, near-size-optimal spacetime meshes suitable for DG solutions that adapt to *a posteriori* spacetime error indicators as well as to nonlinear and anisotropic physics. Our primary motivation was to prove that such an algorithm was at all possible with provable theoretical guarantees. In addition to our theoretical results, an important contribution of our work is that the algorithms are currently being fruitfully implemented and tested on problems of practical complexity. We were able to unify earlier results that considered nonlocal cone constraints (Thi04) and mesh adaptivity (ACE<sup>+</sup>04) separately. Our extensions to Tent Pitcher retain the benefits of earlier algorithms such as ease of implementation and inherent high degree of parallelism. Additionally, we aim to solve robustness issues and generate even better quality meshes in practice than those guaranteed in theory.

Several theoretical problems remain open and are actively being researched by this author and others. We discuss them in the next and final section.

### 8.1 Open problems

There are many exciting avenues to explore and many more problems are likely to be discovered as our algorithm are used to solve increasingly realistic problems. In this section, we highlight some promising directions for future research.

**ADAPTIVITY IN ARBITRARY DIMENSIONS** An important open problem is extending adaptive refinement and coarsening to spatial dimensions  $d \geq 3$ . Extensions of newest-vertex bisection to higher dimensions are known (AMP00; B91). However, it is challenging to devise necessary and sufficient progress constraints that guarantee positive progress. It is also important that the constraints be easy to implement. We consider the problem of incorporating adaptive refinement and coarsening in 3D×Time into our meshing algorithm to be the most interesting and practically relevant open problem.

**ELEMENT QUALITY** Consider another measure of element quality: the ratio of inradius to circumradius. The circumradius to inradius ratio of an element is defined after scaling the time axis by the wavespeed. A larger inradius:circumradius ratio means a “better” element. Experiments suggest that the inradius to circumradius ratio is a useful measure of element quality. Our algorithms guarantee a lower bound on the worst-case ratio as a result of causality and progress constraints, but this bound is not very good. At the same time, some elements with small inradius to circumradius ratio also seem to have small temporal aspect ratio. It is an important research question to devise an algorithm to explicitly maximize the smallest inradius to circumradius ratio.

Scale the time axis relative to space by the local wavespeed. Now, the spacetime domain, at least locally within each patch is identical to  $(d + 1)$ -dimensional Euclidean space. After this scaling, define the *quality* of a spacetime element as the ratio of its inradius to its circumradius—a larger ratio means a better quality element.

It is clear that maximizing the tentpole height is not likely to maximize the worst-case quality of spacetime elements. The following is an attempt to describe another choice of location for the top of the tentpole so as to guarantee element quality.

Let  $\tau$  be a front. Let  $P$  be a local minimum of  $\tau$ . Let  $PQR$  be an arbitrary triangle incident on  $P$ . Let  $\rho$  denote the circumradius of  $\triangle PQR$ . Any tetrahedron with  $PQR$  as a facet must have circumradius at least  $\rho$ . Attempt to create a spacetime tetrahedron over  $PQR$  with circumradius not much larger than  $\rho$  but with a guaranteed lower bound on its inradius.

For each triangle  $PQR$ , consider its diametral circumball but with radius scaled by  $(1 + \delta)$  for some  $\delta \geq 0$ . We wish to place the top  $P'$  of the tentpole inside the intersection of all such circumballs so as not to increase the circumradii of resulting tetrahedra by more than  $(1 + \delta)$ .

In addition, we wish to ensure that the volume of each tetrahedron is bounded from below. We do this by ensuring that the distance of  $P'$  from the plane of  $\triangle PQR$  is bounded from below. Thus, we place  $P'$  above the plane at an orthogonal distance of  $\gamma$  times the width of  $\triangle PQR$ .

Overall, we need to ensure that the intersection of all the circumballs and all halfspaces is nonempty so that we have at least one candidate placement of  $P'$ , the top of the tentpole at  $P$ . Note that the final tentpole need not be vertical.

**EMPIRICAL STUDY OF HEURISTICS** Even for the basic linear nonadaptive algorithm of Chapter 2, an experimental study is needed to try several heuristics for which portion of the front to advance in each step, i.e., which local minimum vertex to pitch next when several candidates are available. Different heuristics have been observed to affect the mesh quality differently in  $1D \times \text{Time}$ . With the more general advancing front operations of Chapter 7, it is important to prioritize various operations that modify the front to ensure that the quality and efficiency of the mesh is improved in practice.

**PROVABLY CORRECT BOUNDARY TRACKING** We would like to devise a provably correct and complete boundary tracking algorithm for interesting classes of motion. In many practical situations, the topology of the domain also changes with time (fPCS99). For instance, a rocket fuel grain may split into multiple components due to combustion. We would be interested in an advancing front algorithm, initially in  $2D \times \text{Time}$ , that handles changes in the topology of the domain over time. In higher dimensions, a wider array of front operations is possible and necessary for boundary tracking. For instance, edge flips in  $2D \times \text{Time}$  generalize to  $2 - 3$  flips that replace two adjacent tetrahedra by three tetrahedra sharing an edge, and vice versa. The problem of devising a boundary tracking algorithm in arbitrary dimensions remains open and of a great deal of interest even in  $3D \times \text{Time}$ .

**NON-GREEDY ALGORITHMS** It should be clear that the progress constraints can be modified in different ways to meet different mesh generation objectives. Research so far has focused on worst-case guarantees for temporal aspect ratio. Much more research is needed to guarantee worst-case quality in the sense of inradius to circumradius ratio. Even more desirable is to guarantee a certain distribution of elements by quality measure. We believe that greedy algorithms will not suffice to guarantee worst-case inradius to circumradius ratio in theory and will not perform well, without additional heuristics, in practice.

Another context in which greedy algorithms are unlikely to fare better than current work is in the case of tracking moving boundaries. Intuition suggests that we need an algorithm that constructs only “robustly progressive” fronts. We say that a front  $\tau$  is *robustly progressive* if  $\tau$  is progressive and if  $\tau$  has a local minimum  $p$  such that for every sufficiently small but finite motion of  $p$  with finite velocity the resulting front  $\tilde{\tau}$  is also progressive. For a front  $\tau$  to be robustly progressive, it suffices that  $\tau$  has a local minimum  $p$  such that (i) for every neighbor  $q$  of  $p$ , we have  $\tau(q) - \tau(p)$  is bounded away from zero, and (ii) the kernel of  $\text{link}(p)$  contains a disk of finite radius centered at  $p$ . Deriving such an algorithm is an open question.

**NON-SIMPLICIAL ELEMENTS** To perform more general front advancing operations, those that change the combinatorics of the spatial projection as well as advance the front in time, it seems necessary to allow more general spacetime elements in the near future. Satisfying the two requirements that the spacetime mesh be a weak simplicial complex and that every element have at least one causal outflow facet will be harder with the incorporation of more general operations. The numerical techniques can be extended to other linear elements like hexahedra, prisms, and pyramids with very little difficulty. The data structures used to represent a patch (admittedly, only a transient object) would be a little more complicated because incidences between elements and their facets, and adjacencies between elements will be a little more complicated. I anticipate no significant difficulties in extending the advancing front framework to create and solve patches of mixed types of linear elements.

**MORE COMPLICATED PATCHES** Our current algorithms advance a local neighborhood  $N$  of the front  $\tau$  to a new neighborhood  $N'$  of the new front  $\tau'$ . How complicated can the neighborhoods  $N$  and  $N'$  be? Can we triangulate the spacetime volume between  $N$  and  $N'$  with a small number of spacetime elements? Given the spacetime volume, can we decompose it into a minimum number of good quality spacetime elements? There is a tradeoff between the time to solve a single patch versus the number of patches in the mesh for a given spacetime volume. On the one hand, we would like patches of small complexity so that the time to solve one patch, even for high polynomial order, is not large. This is especially important for an incremental solution strategy where the physical parameters that govern the solution are changing rapidly. On the other hand, we would like to minimize the total number of patches for a given accuracy to reduce the total computation time.

The number of elements in a patch created by pitching a vertex  $p$  is equal to the number of simplices in  $\text{star}(p)$ . We are already considering operations, such as edge dilation and edge contraction, where the number of elements in a patch could be twice as much. The larger is the neighborhood advanced in a single step, the less is the degree of parallelism of the meshing algorithm.

# References

- [ABE99] A. B. Amenta, M. W. Bern, and D. Eppstein. Optimal point placement for mesh smoothing. *J. Algorithms*, 30(2):302–322, February 1999.
- [ABG<sup>+</sup>00] J. F. Antaki, G. E. Belloch, O. Ghattas, I. Malcevic, G. L. Miller, and N. J. Walkington. A parallel dynamic-mesh lagrangian method for simulation of flows with dynamic interfaces. In *Proc. Supercomputing (SC2000)*, 2000.
- [ACE<sup>+</sup>04] R. Abedi, S.-H. Chung, J. Erickson, Y. Fan, M. Garland, D. Guoy, R. Haber, J. M. Sullivan, S. Thite, and Y. Zhou. Spacetime meshing with adaptive refinement and coarsening. In *Proc. 20th Symp. Computational Geometry*, pages 300–309, June 2004.
- [ACF<sup>+</sup>04] R. Abedi, S.-H. Chung, Y. Fan, S. Thite, J. Erickson, and R. B. Haber. Adaptive discontinuous galerkin method for elastodynamics on unstructured spacetime grids. In *Proc. XXI International Congress of Theoretical and Applied Mechanics (ICTAM)*, August 2004. To appear.
- [AGR00] N. M. Amato, M. T. Goodrich, and E. A. Ramos. Linear-time triangulation of a simple polygon made easier via randomization. In *Proc. 16th Symp. Computational Geometry*, pages 201–212, 2000.
- [AHP05] R. Abedi, R. B. Haber, and B. Petracovici. A spacetime discontinuous galerkin method for elastodynamics with element-level balance of linear momentum. *Computer Methods in Applied Mechanics and Engineering*, 2005. In press.
- [AHTE05] R. Abedi, R. Haber, S. Thite, and J. Erickson. An  $h$ -adaptive spacetime-discontinuous galerkin method for linearized elastodynamics. *Revue Européenne des Éléments Finis*, 2005. Submitted.
- [AMP00] D. N. Arnold, A. Mukherjee, and L. Pouly. Locally adaptive tetrahedral meshes using bisection. *SIAM J. Sci. Comput.*, 22(2):431–448, 2000.
- [Bö91] E. Bänsch. Local mesh refinement in 2 and 3 dimensions. *Impact of Computing in Science and Engineering*, 3:181–191, 1991.
- [Bän91] E. Bänsch. Local mesh refinement in 2 and 3 dimensions. *Impact of Computing in Science and Engineering*, 3:181–191, 1991.
- [BEG94] M. Bern, D. Eppstein, and J. Gilbert. Provably good mesh generation. *J. Comp. Sys. Sci.*, 48:384–409, 1994. Special issue for FOCS’90.
- [Bey95] J. Bey. Tetrahedral grid refinement. *Computing*, 55(4):355–378, 1995.
- [Bey00] J. Bey. Simplicial grid refinement: On Freudenthal’s algorithm and the optimal number of congruence classes. *Numer. Math.*, 85(1):1–29, 2000.
- [BH86] J. E. Barnes and P. Hut. A hierarchical  $o(n \log n)$  force calculation algorithm. *Nature*, 324(4):446–449, December 1986.

- [BSW83] R. E. Bank, A. H. Sherman, and H. Weiser. Refinement algorithm and data structures for regular local mesh refinement. In R. Stepleman et al., editors, *Scientific Computing*, pages 3–17. IMACS/North-Holland, Amsterdam, 1983.
- [CD03] S.-W. Cheng and T. K. Dey. Quality meshing with weighted Delaunay refinement. *SIAM J. Computing*, 33:69–93, 2003.
- [CDE<sup>+</sup>00] S.-W. Cheng, T. K. Dey, H. Edelsbrunner, M. A. Facello, and S.-H. Teng. Sliver exudation. *J. ACM*, 47:883–904, 2000.
- [Cen03] C. F. E. Center. Online at <http://www.md.chalmers.se/Centres/Phi/>, 2003.
- [Cha91] B. Chazelle. Triangulating a simple polygon in linear time. *Discrete and Computational Geometry*, 6(5):485–524, 1991.
- [Che89] L. P. Chew. Guaranteed-quality triangular meshes. Technical Report TR-89-983, Department of Computer Science, Cornell University, 1989.
- [CKS00] B. Cockburn, G. Karniadakis, and C. Shu. *Discontinuous Galerkin methods: theory, computation and applications*, volume 11 of *Lecture Notes in Computational Science and Engineering*. Springer, 2000.
- [Coo98] J. Cooper. *Introduction to Partial Differential Equations with MATLAB*. Birkhauser, 1998.
- [CP03] S.-W. Cheng and S.-H. Poon. Graded conforming Delaunay tetrahedralization with bounded radius-edge ratio. In *SODA*, pages 295–304, 2003. Version dated July 9, 2002.
- [CRMS03] P. Cignoni, C. Rocchini, C. Montani, and R. Scopigno. External memory management and simplification of huge meshes. *IEEE Trans. on Visualization and Computer Graphics*, 9(4):525–537, 2003.
- [dBSvKO00] M. de Berg, O. Schwarzkopf, M. van Kreveld, and M. Overmars. *Computational Geometry: Algorithms and Applications*. Springer-Verlag, 2nd ed. edition, 2000.
- [Ede01] H. Edelsbrunner. *Geometry and Topology for Mesh Generation*. Cambridge Monographs on Applied and Computational Mathematics. Cambridge University Press, 2001.
- [EG00] H. Edelsbrunner and D. R. Grayson. Edgewise subdivision of a simplex. *Discrete Comput. Geom.*, 24(4):707–719, 2000.
- [EG01] H. Edelsbrunner and D. Guoy. Sink-insertion for mesh improvement. In *Proc. 17th Annual Symposium on Computational Geometry*, pages 115–123, 2001.
- [EGSÜ02] J. Erickson, D. Guoy, J. M. Sullivan, and A. Üngör. Building space-time meshes over arbitrary spatial domains. In *Proc. 11th Int'l. Meshing Roundtable*, pages 391–402, 2002.
- [EGSÜ05] J. Erickson, D. Guoy, J. M. Sullivan, and A. Üngör. Building spacetime meshes over arbitrary spatial domains. *Engineering with Computers*, 20:342–353, 2005. Online at <http://dx.doi.org/10.1007/s00366-005-0303-0>.
- [EJL03] K. Eriksson, C. Johnson, and A. Logg. Explicit time-stepping for stiff ODEs. *SIAM Journal on Scientific Computing*, 25(4):1142–1157, 2003.
- [Fol95] G. B. Folland. *Introduction to Partial Differential Equations*. Princeton University Press, 2nd ed edition, 1995.
- [fPCS99] T. M. from Planar Cross Sections. Chandrajit bajaj and edward j. coyle and kwun-nan lin. *Computer Methods in Applied Mechanics and Engineering*, 179:31–52, 1999.
- [GJPT78] M. R. Garey, D. S. Johnson, F. P. Preparata, and R. E. Tarjan. Triangulating a simple polygon. *Information Processing Letters*, 7(4):175–179, June 1978.

- [Gut84] A. Guttman. A dynamic index structure for spatial searching. In *Proc. ACM SIGMOD Conf. Principles Database Systems*, pages 47–57, 1984.
- [Hea02] M. T. Heath. *Scientific Computing: An Introductory Survey*. McGraw-Hill, New York, 2d edition, 2002.
- [Her04] J. Herod. Partial differential equations. Online at <http://www.math.gatech.edu/~herod/conted/Async.html>, 2004. Accompanying notes at <http://www.mapleapps.com/power/tools/pdes/pdes.shtm>.
- [JJ04] K. Jegdic and R. L. Jerrard. Convergence of a spacetime discontinuous Galerkin finite element method for a class of hyperbolic systems. Preprint, August 2004.
- [JP97] M. T. Jones and P. E. Plassmann. Adaptive refinement of unstructured finite-element meshes. *Finite Elements in Analysis and Design*, 25:41–60, 1997.
- [Kar] G. Karypis. METIS: Family of multilevel partitioning algorithms. Online at <http://www-users.cs.umn.edu/~karypis/metis/>.
- [KK98] G. Karypis and V. Kumar. Multilevel algorithms for multi-constraint graph partitioning. Technical Report 98-019, Department of Computer Science, University of Minnesota, May 1998.
- [Lat91] J.-C. Latombe. *Robot Motion Planning*. Kluwer Academic Publishers, 1991.
- [LJ94] A. Liu and B. Joe. On the shape of tetrahedra from bisection. *Math. Comp.*, 63(207):141–154, 1994.
- [LJ95] A. Liu and B. Joe. Quality local refinement of tetrahedral meshes based on bisection. *SIAM J. Sci. Comput.*, 16:1269–1291, 1995.
- [LMCG96] M. Lin, D. Manocha, J. Cohen, and S. Gottschalk. *Algorithms for Robotics Motion and Manipulation*, chapter Collision Detection: Algorithms and Applications, pages 129–142. A.K. Peters, 1996.
- [LS03] F. Labelle and J. R. Shewchuk. Anisotropic Voronoi diagrams and guaranteed-quality anisotropic mesh generation. In *Proc. 19th ACM Symp. Computational Geometry*, pages 191–200, 2003.
- [Mau95] J. M. L. Maubach. Local bisection refinement for  $n$ -simplicial grids generated by reflection. *SIAM J. Sci. Comput.*, 16:210–227, 1995.
- [Mau96] J. M. L. Maubach. The efficient location of neighbors of locally refined  $n$ -simplicial grids. In *Proc. 5th International Meshing Roundtable*, pages 137–156, October 1996.
- [Mit88] W. F. Mitchell. *Unified multilevel adaptive finite element methods for elliptic problems*. Ph. D. thesis, Computer Science Department, University of Illinois, Urbana, IL, 1988. Tech. Rep. UIUCDCS-R-88-1436.
- [Mit89] W. F. Mitchell. A comparison of adaptive refinement techniques for elliptic problems. *ACM Trans. Math. Soft.*, 15:326–347, 1989.
- [Mit91] W. F. Mitchell. Adaptive refinement for arbitrary finite-element spaces with hierarchical bases. *J. Comp. Appl. Math.*, 36:65–78, 1991.
- [MV00] S. Mitchell and S. Vavasis. Quality mesh generation in higher dimensions. *SIAM J. Comput.*, 29:1334–1370, 2000.
- [Owe99] S. J. Owen. *Non-Simplicial Unstructured Mesh Generation*. PhD thesis, Department of Civil and Environmental Engineering, Carnegie Mellon University, April 1999.
- [Ric94] G. R. Richter. An explicit finite element method for the wave equation. *Applied Numerical Mathematics*, 16:65–80, 1994.

- [Riv84] M.-C. Rivara. Algorithms for refining triangular grids suitable for adaptive and multigrid techniques. *Int. J. Numer. Meth. Eng.*, 20:745–756, 1984.
- [Riv96] M. C. Rivara. New mathematical tools and techniques for the refinement and/or improvement of unstructured triangulations. In *Proc. 5th Int’l. Meshing Roundtable*, pages 77–86, 1996.
- [Riv97] M.-C. Rivara. New longest-edge algorithms for the refinement and/or improvement of unstructured triangulations. *International Journal for Numerical Methods in Engineering*, 40:3313–3324, 1997.
- [RS75] I. G. Rosenberg and F. Stenger. A lower bound on the angles of triangles constructed by bisecting the longest side. *Math. Comput.*, 29:390–395, 1975.
- [RS92] J. Ruppert and R. Seidel. On the difficulty of triangulating three-dimensional nonconvex polyhedra. *Discrete and Computational Geometry*, 7(3):227–253, 1992.
- [Rup95] J. Ruppert. A Delaunay refinement algorithm for quality 2-dimensional mesh generation. *J. Algorithms*, 18(3):548–585, May 1995.
- [Sev97] E. Seveno. Towards an adaptive advancing front method. In *Proc. 6th International Meshing Roundtable*, pages 349–360, 1997.
- [Sew72] E. G. Sewell. *Automatic generation of triangulations for piecewise polynomial approximation*. Ph. D. thesis, Department of Mathematics, Purdue University, West Lafayette, IN, 1972.
- [She02] J. R. Shewchuk. What is a good linear element? interpolation, conditioning, and quality measures. In *Proc. 11th International Meshing Roundtable*, pages 115–126. Sandia National Laboratory, September 2002.
- [SPC03] J. P. Suárez, A. Plaza, and G. F. Carey. Propagation path properties in iterative longest-edge refinement. In *Proc. 12th Internat. Meshing Roundtable*, pages 79–90, 2003.
- [Str86] G. Strang. *Introduction to Applied Mathematics*. Wellesley College, 1986.
- [STÜ04] D. Spielman, S.-H. Teng, and A. Üngör. Time complexity of practical parallel steiner point insertion algorithms. In *Proceedings of ACM-SPAA*, 2004. Extended abstract.
- [Thi04] S. Thite. Efficient spacetime meshing with nonlocal cone constraints. In *Proc. 13th International Meshing Roundtable*, pages 47–58, September 2004.
- [Tho99] J. W. Thomas. *Numerical Partial Differential Equations: Conservation Laws and Elliptic Equations*. Springer, 1999.
- [TW98] A. Tveito and R. Winther. *Introduction to Partial Differential Equations: A Computational Approach*. Springer-Verlag, 1998.
- [Ü02] A. Üngör. *Parallel Delaunay Refinement and Space-Time Meshing*. PhD thesis, University of Illinois at Urbana-Champaign, October 2002.
- [Üng04] A. Üngör. Off-centers: A new type of steiner points for computing size-optimal guaranteed-quality Delaunay triangulations. In *Proceedings of LATIN 2004*, pages 152–161, April 2004.
- [ÜS00] A. Üngör and A. Sheffer. Tent-Pitcher: A meshing algorithm for space-time discontinuous Galerkin methods. In *Proc. 9th Int’l. Meshing Roundtable*, pages 111–122, 2000.
- [ÜS02] A. Üngör and A. Sheffer. Pitching tents in space-time: Mesh generation for discontinuous Galerkin method. *Int. J. Foundations of Computer Science*, 13(2):201–221, 2002.
- [Wei85] K. Weiler. Edge-based data structures for solid modeling in curved-surface environments. *IEEE Computer Graphics and Applications*, 5(1):21–40, January 1985.

- [Wei99a] E. W. Weisstein. Galerkin method. Online at <http://mathworld.wolfram.com/GalerkinMethod.html>, 1999.
- [Wei99b] E. W. Weisstein. Partial differential equation. Online at <http://mathworld.wolfram.com/PartialDifferentialEquation.html>, 1999.
- [Whi74] G. B. Whitham. *Linear and Nonlinear Waves*. Wiley, New York, 1974.
- [YAS<sup>+</sup>99] L. Yin, A. Acharya, N. Sobh, R. B. Haber, and D. A. Tortorelli. A space-time discontinuous Galerkin method for elastodynamic analysis. *Proc. of Int. Symp. on Discontinuous Galerkin Methods, Salve Regina University, Newport, RI*, 1999.
- [YAS<sup>+</sup>00] L. Yin, A. Acharya, N. Sobh, R. Haber, and D. A. Tortorelli. A space-time discontinuous Galerkin method for elastodynamic analysis. In B. Cockburn, G. Karniadakis, and C. Shu, editors, *Lecture Notes in Computational Science and Engineering*, volume 11, pages 459–464. Springer, 2000.
- [Yin02] L. Yin. *A New Spacetime Discontinuous Galerkin Finite Element Method for Elastodynamic Analysis*. PhD thesis, Department of Theoretical and Applied Mechanics, University of Illinois at Urbana-Champaign, 2002.
- [YLPM05] S.-E. Yoon, P. Lindstrom, V. Pascucci, and D. Manocha. Cache-oblivious mesh layouts. In *Proc. ACM SIGGRAPH*, 2005. Available as Lawrence Livermore National Laboratory Technical Report UCRL-JRNL-211774.
- [Zie95] G. M. Ziegler. *Lectures on Polytopes*. Springer, 1995.



# Curriculum Vitæ

## SHRIPAD THITE

Department of Computer Science  
University of Illinois at Urbana-Champaign

### Research interests

Computational geometry	Mesh generation for finite element methods; Spacetime meshing; Optimal triangulations; Delaunay triangulations; Combinatorial problems in geometry; Lower bounds.
Robotics	Capturing and motion planning.
Graph algorithms	Strong edge coloring and matching; Optimization problems on graphs.
External memory	Data structures on nonuniform memory models of computation.
Economic simulation	Computer simulations of Vickrey auctions in deregulated electrical power markets.

### Education

2001	M.S., Computer Science <i>Advisor:</i> Prof. Michael Loui University of Illinois at Urbana-Champaign, IL, USA
1997	B.E., Computer Engineering University of Pune, India (Government College of Engineering, Pune)

### Awards and honors

1997	Graduated with first rank in the University of Pune, Pune, India, among a graduating class of approximately 800. Awarded Dr. D. Y. Patil Gold Medal by the University of Pune.
1991	Among 750 students selected all over India for award of the National Talent Search (NTS) Scholarship by the National Council for Educational Research and Training (NCERT), New Delhi, after a three-tier selection process.

## Theses

M.S. thesis

### **Optimum Binary Search Trees on the Hierarchical Memory Model**

Modern computer architectures are modeled realistically as having several different types of memory organized in a memory hierarchy from fast but small caches to slow but large external storage. On the abstract model with memory organized in a hierarchy with an arbitrary number of levels and with arbitrary access costs at each level, we develop algorithms for computing a minimum-cost binary search tree (BST); these algorithms are efficient under constraints on the parameters of the memory hierarchy. A BST is a widely used data structure for indexing and retrieving data that is very well-studied on the uniform memory (RAM) model of computation.

## Research experience

1999–

*Research Assistant*

Department of Computer Science, University of Illinois at Urbana-Champaign

Research in computational geometry, mesh generation for finite element methods; Prof. Jeff Erickson, Advisor.

2001

M.S. Thesis with Prof. Michael Loui, Advisor.

2001, 2002

*Graduate Research Assistant*

D-2, Los Alamos National Laboratory, Los Alamos, NM

Dr. Madhav Marathe, mentor

Designed and implemented a computer program for the simulation of a deregulated electrical power market. The project includes being able to simulate power demand and consumption, market forces, external regulatory policies, and physical constraints of the power grid. The project is ongoing and program code is currently being written and tested.

Research on theoretical and practical problems associated with wireless radio networks. This work intersects the areas of graph theory, computational geometry, and networking. The results of this research are being submitted for publication.

1998

*Graduate Research Assistant*

CIC-3, Los Alamos National Laboratory, Los Alamos, NM

Dr. Madhav Marathe, mentor

Extended blocking algorithms for matrices to improve memory-efficiency of matrix operations. Implemented and simulated the same on an SGI Origin multiprocessor system, and empirically demonstrated a significant improvement in performance. Implemented a blocking algorithm for graphs, as proposed by Awerbuch *et al.*

1996–1997

*Student Intern*

Centre for Development of Advanced Computing (C-DAC), Pune, India

Constructed a model in VHDL for a Fast Ethernet switch and performed system-level simulation and analysis using VHDL tools.

## Publications

- 2005      **A Unified Algorithm for Adaptive Spacetime Meshing with Nonlocal Cone Constraints.** Shripad Thite. In *Proc. 21st European Workshop on Computational Geometry (EWCG)*, pages 1–4, March 9–11, 2005 (Eindhoven, the Netherlands). Invited and submitted to special issue of *Computational Geometry: Theory and Applications (CGTA)*; journal version in review.
- 2004      **Efficient Spacetime Meshing with Nonlocal Cone Constraints.** Shripad Thite. In *Proc. 13th International Meshing Roundtable (IMR)*, pages 47–58, September 19–22, 2004 (Williamsburg, Virginia). Invited to special issue of *International Journal of Computational Geometry and Applications (IJCGA)*; journal special issue cancelled.
- Spacetime Meshing with Adaptive Refinement and Coarsening.** Reza Abedi, Shuo-Heng Chung, Jeff Erickson, Yong Fan, Michael Garland, Damrong Guoy, Robert Haber, John M. Sullivan, Shripad Thite, and Yuan Zhou. In *Proc. ACM Symp. on Computational Geometry (SoCG)*, pages 300–309, June 8–11, 2004 (New York, NY); (33% acceptance rate: SoCG is considered the premier computational geometry conference.)
- The Distance-2 Matching Problem and its Relationship to the MAC-layer Capacity of Ad hoc Wireless Networks.** Hari Balakrishnan, Christopher L. Barrett, V. S. Anil Kumar, Madhav V. Marathe, and Shripad Thite. *IEEE Journal on Selected Areas in Communications* issue on Fundamental Performance Limits of Wireless Sensor Networks, Volume 22, Number 6, pages 1069–1079, August 2004.
- Marketecture: A Simulation-Based Framework for Studying Experimental Deregulated Power Markets.** Karla Atkins, Chris Barrett, Christopher M. Homan, Achla Marathe, Madhav Marathe, and Shripad Thite. *6th IAEE European Energy Conference*, September 2–3, 2004 (Zurich, Switzerland). (Journal version submitted to *Computational Economics*)
- 2003      **Capturing a Convex Object with Three Discs.** Jeff Erickson, Shripad Thite, Fred Rothganger, and Jean Ponce. In *Proc. IEEE International Conference on Robotics and Automation (ICRA)*, pages 2242–2247, September 14–19, 2003 (Taipei, Taiwan); (50–60% acceptance rate: nevertheless, ICRA is considered the premier robotics conference.)
- 2000      **Optimum Binary Search Trees on the Hierarchical Memory Model.** Shripad Thite. M.S. thesis with Prof. Michael Loui, Advisor. Department of Computer Science, University of Illinois at Urbana-Champaign, CSL Technical Report UILU-ENG-00-2215 ACT-142, November 2000.
- ABSTRACTS AND MANUSCRIPTS:
- 2005      **Adaptive Spacetime Meshing in  $2D \times \text{Time}$  for Nonlinear and Anisotropic Media.** Shripad Thite, Jayandran Palaniappan, Jeff Erickson, and Robert Haber. At the *8th US National Congress on Computational Mechanics*, July 2005.
- Meshing in  $2D \times \text{Time}$  for Front-Tracking DG Methods.** Shripad Thite, Jeff Erickson, Shuo-Heng Chung, Reza Abedi, Jayandran Palaniappan, and Robert Haber. At the *8th US National Congress on Computational Mechanics*, July 2005.

- 2004 **Efficient Algorithms for Channel Assignment in Wireless Radio Networks.** Christopher L. Barrett, Gabriel Istrate, V. S. Anil Kumar, Madhav V. Marathe, Shripad Thite, and Sunil Thulasidasan. Manuscript, journal version in preparation as of October 2004.
- 2003 **Efficient Spacetime Meshing with Nonlocal Cone Constraints.** Jeff Erickson, Robert Haber, Jayandran Palaniappan, John Sullivan, and Shripad Thite. *4th Symposium on Trends in Unstructured Mesh Generation at the 7th US National Congress on Computational Mechanics*, July 27–31, 2003 (Albuquerque, NM).
- Spacetime Meshing with Adaptive Coarsening and Refinement.** Reza Abedi, Shuo-Heng Chung, Jeff Erickson, Yong Fan, Robert Haber, John Sullivan, and Shripad Thite. *4th Symposium on Trends in Unstructured Mesh Generation at the 7th US National Congress on Computational Mechanics*, July 27–31, 2003 (Albuquerque, NM).
- An Efficient Parallel Implementation of the Spacetime Discontinuous Galerkin Method Using Charm++.** L. V. Kale, Robert Haber, Jonathan Booth, Shripad Thite, and Jayandran Palaniappan. *4th Symposium on Trends in Unstructured Mesh Generation at the 7th US National Congress on Computational Mechanics*, July 27–31, 2003 (Albuquerque, NM).
- 2001 **Link Scheduling Problems in Packet Radio Networks.** Chris Barrett, Gabriel Istrate, Madhav Marathe, Shripad Thite, and V. S. Anil Kumar. Manuscript, 2001.
- Other technical reports, manuscripts; available at <http://www.uiuc.edu/~thite/pubs/> and on request.

## Conference presentations

- 2005 **Provably Good Adaptive Meshing of Spacetime.** 50th biannual Midwest Theory Day, University of Illinois at Urbana-Champaign, Urbana, IL, May 2005.
- A Unified Algorithm for Adaptive Spacetime Meshing with Nonlocal Cone Constraints.** 21st European Workshop on Computational Geometry (EWCG), Eindhoven, the Netherlands, March 2005.
- 2004 **Efficient Spacetime Meshing with Nonlocal Cone Constraints.** 13th International Meshing Roundtable (IMR), Williamsburg, VA, September 2004.
- Spacetime Meshing with Adaptive Refinement and Coarsening.** ACM Symp. on Computational Geometry (SoCG), Brooklyn, NY, June 2004.
- 2003 **Efficient Spacetime Meshing with Nonlocal Cone Constraints.** 7th US National Congress on Computational Mechanics, Albuquerque, NM, July 2003.
- Capturing a Convex Object with Three Discs.** IEEE International Conference on Robotics and Automation (ICRA), Taipei, Taiwan, September 2003.

## Professional service

- Various times Served as *anonymous technical referee* for articles submitted to ACM Symposium on Computational Geometry (SoCG), ACM Symposium on Theory of Computing (STOC), Discrete and

Computational Geometry, Journal of Information and Computation, Information Processing Letters, International Meshing Roundtable, IEEE Journal on Selected Areas in Communications, IEEE Communications Letters.

- 2002–2003 Served on the *Fellowships, Assistantships, and Admissions (FAA) Committee* of the Computer Science department. Members of this committee are faculty and senior graduate students, who evaluate entrance requirements and recommend applications for admissions, fellowships, and assistantships.
- 2001 Organized the *44th biannual Midwest Theory Day*, University of Illinois at Urbana-Champaign, December 1, 2001. (<http://www.uiuc.edu/~thite/mtd>)

## Teaching experience

- 1997–1999 Teaching Assistant  
Department of Computer Science, University of Illinois at Urbana-Champaign
- Summer 1999*  
CS 273: Introduction to the Theory of Computation  
Duties included conducting office hours, discussion sessions, and helping design and grade homework assignments and exams.
- Spring 1999*  
CS 373: Combinatorial Algorithms
- Fall 1998:*  
CS 375: Automata, Formal Languages, and Computational Complexity; and  
CS 373: Combinatorial Algorithms
- Spring 1998:*  
CS 110: C++ programming laboratory. Duties included giving lectures, assigning and grading small- and medium-scale programming projects, assigning grades.
- Fall 1997:*  
CS 110: C programming laboratory. Duties included giving lectures, assigning and grading small- and medium-scale programming projects, assigning grades.